UNIVERSITY OF BIRMINGHAM

THE DEVELOPMENT OF AN ANTI-SCARRING BURN DRESSING

By

KWANG CHEAR LEE

A thesis submitted to the University of Birmingham for the degree of

DOCTOR OF PHILOSOPHY

Institute of Inflammation and Ageing

School of Clinical and Experimental Medicine

College of Medical and Dental Sciences

University of Birmingham

October 2018

Abstract

Introduction: Scarring has a significant impact on the function and quality of life in burn patients. This thesis describes selected stages of the development of an anti-scarring burn dressing and an objective scar assessment panel.

Methods: This thesis is divided into two sections. Section 1 covers the development of an objective scar measurement tool based panel and score via a systematic review and subsequent reliability testing and validation of selected devices. Section 2 covers different aspects of dressing formulation. The cytotoxicity effects of decorin were investigated in dermal fibroblast cultures to provide guidance to safe and effective decorin dosing. Manufacturing, sterilisation and clinical use exposes decorin to elevated temperatures and the effects of this on the structure of decorin and bio-activity of decorin is investigated with circular dichroism and in-vitro cell cultures respectively. Lastly, a skin contact study in healthy volunteers was performed to establish the safety of two gellan formulations (sheet and fluid gel).

Results: Objective scar measurement tools were found to be more reliable than subjective scar scores and an objective scar score was created consisting of high frequency ultrasound and pliability measures. Decorin had no measurable cytotoxicity on dermal fibroblasts even at high concentrations. Conformational change in decorin structure was seen at relatively low temperatures however results suggest that heating may enhance its bio-activity. Both gellan formulations were found to be safe for use on intact skin.

Conclusion: The new objective scar scale can be used to accurately measure the effects of anti-scarring treatments. Decorin and gellan are safe to be used in patients but the dressings may need to be protected against high temperatures.

Acknowledgements

To my supervisors Professor Ann Logan, Professor Liam Grover and Professor Naiem Moiemen for their expert guidance, patience, help and advice without which this thesis would not have been possible.

To Mrs Amy Bamford and Ms Fay Gardiner (Queen Elizabeth Hospital, Birmingham) for their guidance and help in setting up and running the clinical studies.

To Dr. Gary Reynolds for assistance and guidance with scar biopsy histology and Dr. Jon Bishop for his assistance with the statistical analyses.

To my burns clinical fellow colleagues, Mr. Khaled al-Tarrah, Dr. Britt ter Horst and Dr. Annarita Agovino for helping me in various aspects of my PhD as well as providing encouragement and support.

To the other PhD students (especially Dr. Maryam Esmaeili) and other post-doctorates who have helped me at the University of Birmingham.

To all the burns patients as well as healthy volunteers who have sacrificed their valuable time in volunteering for my studies.

To the Scar Free Foundation and Wellcome Trust for funding this PhD.

To my friends who have always been encouraging.

To my mum and dad who have supported me through my studies as well as my siblings.

To Christabel for her love and support.

To God.

Even though I walk through the valley of the shadow of death, I will fear no evil, for you are with me; your rod and your staff, they comfort me. Psalm 23:4

Funding

The Scar Free Foundation, United Kingdom

Wellcome Trust, United Kingdom

Table of Contents

Table of Contents vi

Figures xiii

Tables xv

Abbreviations xvii

1. Introduction 2

1.1. The clinical problem: Hypertrophic scarring in burn patients 2

1.1.1 Wound healing 2

1.1.2 Scarring 4

1.2. Anti-scarring therapies in burn patients 6

1.2.1 Current therapies 6

1.2.1.1 Silicone gels and sheets 6

1.2.1.2 Pressure garments 6

1.2.1.3 Vacuum therapy 7

1.2.1.4 Intra-lesional scar therapies 8

1.2.1.4.1 Corticosteroids 8

1.2.1.4.2 Anti-neoplastic agents 8

1.2.1.5 Radiotherapy 9

1.2.2 Emerging therapies 9

1.2.2.1 Ablative CO_2 Fractional laser 9

1.2.2.2 Micro-needling 10

1.2.2.3 Botulinum toxin 11

1.2.2.4 Interferon 12

1.2.2.5 Verapamil 12

1.2.2.6 Autologous fat grafting and stem cell therapy 12

1.2.3 Novel therapies 13

1.2.3.1 Topical Salbutamol 13

1.2.3.2 Decorin 14

1.3. Development of an anti-scarring burn dressing 14

1.3.1 The molecular pathway of scarring: The roles of decorin and Transforming Growth Factor-β2 in scarring 14

1.3.1.1 Transforming Growth Factor –β 14

1.3.1.2 Decorin 15

1.3.1.3 Gellan: a polysaccharide based dressing material 19

1.3.2 Decorin delivery methods in literature 19
1.3.2.1 Injection *19*
1.3.2.2 Intravenous injection *20*
1.3.2.3 Decorin gene transfection *20*
1.3.2.4 Surface coating of implants *20*
1.3.2.5 Topical application and dressings *21*
1.3.3 Characteristics of gellan: Suitability as a dressing material 22
1.3.3.1 Gellan toxicity studies in literature *25*
1.3.3.2 Pharmaceutical use of gellan *25*
1.4 Scar assessment 26
1.5. Aims of the study and processes involved in development of a new therapeutic dressing membrane and clinical outcomes 27
SECTION 1- SCAR ASSESSMENT 30
2. Assessment of burn scar quality: A systematic review of objective burn scar measurements 32
2.1 Background 32
2.2 Aims 33
2.3 Methods 33
2.3.1 Criteria for considering articles for inclusion 33
2.3.2 Search methods 34
2.3.3 Quality assessment 36
2.4 Results 37
2.4.1 Colour 37
2.4.1.2 Reflectance spectroscopy *38*
2.4.1.3 Large area spectrophotometry *42*
2.4.1.4 Spectrophotometric intra-cutaneous analysis (SIA) *43*
2.4.1.5 Computerised analysis of digital photographs *43*
2.4.2 Laser imaging 47
2.4.3 Thermographic analysis of burn scars 50
2.4.4 Scar dimensions 50
2.4.4.1 Surface area and volume *50*
2.4.5 Thickness 57
2.4.6 Texture 62
2.4.6.1 Skin topography *62*

2.4.7 Biomechanical properties 64
2.4.7.1 Pliability, elasticity or stiffness *64*
2.4.7.2 Non-suction extension methods *64*
2.4.7.3 Suction extension methods *65*
2.4.7.4 Tonometry *68*
2.4.7.5 Torsional force and adherence measurement methods *69*
2.4.7.6 Acoustic methods *69*
2.4.7.7 Electrical of bio-impedance methods *70*
2.4.7.8 Modelling and other techniques *70*
2.4.8 Pathophysiological disturbances *74*
2.4.9 Transcutaneous oxygen tension *74*
2.4.10 Transepidermal water loss and moisture content *74*
2.4.8 Multispectral imaging systems 76
2.4.9 Non-invasive morphological imaging techniques 76
2.4.9.1 Optical coherence tomography *76*
2.4.9.2 Other in vivo tomography/microscopy techniques *77*
2.4.9.3 Spectroscopy techniques *78*
2.4.9.4 High-frequency ultrasound systems *79*
2.4.9.5 Intravital video-capillaroscopy *79*
2.4.10 Measurement of sensory change 80
2.5 Discussion 81
2.6 Conclusions 83
3. Clinical assessment of burn scar quality: Birmingham Objective Scar Scale study 86
3.1 Background 86
3.2 Aims and Objectives 89
3.2.1 Primary Objectives 89
3.2.2 Secondary Objectives 89
3.3 Methods 89
3.3.1 Location 89
3.3.2 Subjects 90
3.3.3 Study design 91
3.3.4 Scar assessment 91
3.3.4.1 Scar Selection and Measurement procedures *91*
3.3.4.2 Raters *92*

3.3.5 Measurement tools 92
3.3.5.1 Subjective measurement tools *92*
3.3.4.1.1 Modified Vancouver Scar Scale (mVSS) *92*
3.3.4.1.2 Patient and Observer Scar Assessment Scale (POSAS) *93*
3.3.4.1.3 Fitzpatrick skin type *94*
3.3.4.2 Objective measurement tools *94*
3.3.4.2.1 DSM II Colormeter *94*
3.3.4.2.2 Scanoskin camera *95*
3.3.4.2.3 Dermascan 20MHz high frequency ultrasound *96*
3.3.4.2.4 Cutometer Elasticity probe *97*
3.3.4.3 Histology *98*
3.3.4.4 Patient satisfaction with devices questionnaire *99*
3.4 Statistical analysis 100
3.4.1 Sample size 100
3.4.2 Reliability 100
3.4.3 Concurrent validity 101
3.5 Results 102
3.5.1 Demographics 102
3.5.2 Subjective Scar Scales 103
3.5.3 DSM II Colormeter: Erythema and Pigmentation 107
3.5.3.1 Erythema measurements *107*
3.5.3.2 Pigmentation measurements *109*
3.5.4 Scanoskin camera: Erythema and Pigmentation 111
3.5.5 Dermascan ultrasound: Dermal thickness and intensity 112
3.5.6 Cutometer: R0 and R2 measurements 113
3.5.7 Concurrent validity 115
3.5.8 Histological measurements 120
3.5.9 Patient Reported Outcome Measures 123
3.5.9.1 Patient Satisfaction with devices questionnaire *123*
3.5.9.2 Patient rated scar parameter importance *124*
3.5.10 Sensitivity and Specificity 125
3.11 Global Scar Scale 127
3.6 Discussion 131
3.6.1 Subjective scores 132

3.6.2 Colour 133
3.6.3 Thickness 135
3.6.4 Pliability 136
3.6.5 Global Scar Scale 136
3.7 Conclusion 138
SECTION 2- DRESSING FORMULATION 140
4. Decorin Cytotoxicity 142
4.1 Cytotoxicity of decorin 142
4.1.1 Background 142
4.1.2 Hypotheses 142
4.1.3 Aims 142
4.2 Materials and Methods 143
4.2.1 Materials 143
4.2.2 Cell culture 143
4.2.3 Cell proliferation and cytotoxicity assays 143
4.2.4 Haemocytometer calibration, and determining optimal cell counts and Calibration of the MTT with haemocytometer readings 144
4.2.5 Haemocytometer calibration 145
4.2.6 MTT assay calibration 145
4.2.7 Cell proliferation and cytotoxicity assay 146
4.3 Results 147
4.3.1 Haemocytometer calibration 147
4.3.2 MTT assay calibration results 147
4.3.3 Cell proliferation and cytotoxicity assay 148
4.4 Discussion 151
4.5 Conclusions 151
5. Effects of heat treatment on the bio-activity of decorin 153
5.1 Background 153
5.2 Hypothesis 154
5.3 Aims 154
5.4 Materials and Methods 154
5.4.1 Materials 154
5.4.1.1 Thermal stability studies 154
5.4.1.2 Cell proliferation bio-activity studies 154

5.4.1.3 Immunohistochemistry bio-activity studies *155*
5.4.1.4 Collagen assay studies *156*
5.4.2 Methods 156
5.4.2.1 Decorin heating protocol *156*
5.4.2.2 ELISA analysis of decorin post-heat treatment *157*
5.4.2.2.1 Plate preparation *157*
5.4.2.2.1 Assay procedure *157*
5.4.2.3 Circular dichroism analysis of heat treatment of Decorin *158*
5.4.2.3.1 Non-continuous heat treatment *158*
5.4.2.3.2 Continuous heating and cooling treatment *158*
5.4.4.4 Effects of heat treated decorin on ECM production *159*
5.4.4.4.1 Cell proliferation bioactivity assays *159*
5.4.4.4.2 Immunohistochemistry bioactivity assays *159*
5.4.4.4.3 Collagen assays *160*
5.5 Results 163
5.5.1 ELISA analysis of decorin post-heat treatment 163
5.5.2 Circular dichroism analysis of heat treatment of decorin 164
5.5.3 Proliferation based Bioactivity studies 168
5.5.4 Immunohistochemistry based bio-activity studies 169
5.5.5 Collagen based bio-activity studies 171
5.6 Discussion 175
5.7 Conclusions 178
6. Gellan Contact Study (GCS) 180
6.1. Background 180
6.2. Aims 180
6.3. Materials and Methods 180
6.3.1 Materials 180
6.3.2 Location 181
6.3.2 Subjects 181
6.3.3 Study design 182
6.3.3.1 Measured outcomes *182*
6.3.3.2 Randomisation *183*
6.3.3.3 Statistical analysis *184*
6.4 Results 184

6.4.1 Demographics 184
6.4.2 Erythema 185
6.4.3 Dryness 186
6.4.4 Oedema 188
6.4.5. Participant feedback 189
6.5 Skin patch test 189
6.6 Discussion 191
6.7 Conclusion 194
7. Overall Discussion and Conclusions 196
7.1 Main findings and future work 196
8. References 199
Appendix 228
Appendix A 228
Appendix B 259

Figures

Figure 1: Phases of wound healing. 3
Figure 2: Model structure of decorin, with its Carboxyl (C) and NH_2-terminals (N). 17
Figure 3: Dimeric structure of decorin. 18
Figure 4: Gellan gum structure. 23
Figure 5: The mechanism of gellation of gellan gum. 24
Figure 6: Development phase of the anti-scarring burn dressing, its work packages and the associated thesis chapters. 29
Figure 7: Preferred Reporting Items for Systematic Reviews and Meta-Analyses (PRISMA) flowchart. 36
Figure 8: Graphical illustration of the concept of reflectance spectroscopy. 39
Figure 9: Graphical representation of the L*a*b* colour measurement system. 40
Figure 10: Comparison of 2D and 3D areas. 52
Figure 11: High-frequency ultrasound image of normal and scarred skin. 58
Figure 12: Different frequencies of ultrasounds and their penetrance into the skin. 59
Figure 13: Cutometer and Dermalab probes. 65
Figure 14: Example of skin deformation curve obtained with the Cutometer. 66
Figure 15: Open chamber transepidermal water loss system. 75
Figure 16: Diagrammatic overview of study design and patient pathway for the scar assessment day. 91
Figure 17: Patient and Observer Scar Assessment Scale. 94
Figure 18: Scanoskin image processing 96
Figure 19: Dermasan ultrasound image of scar and normal skin. 97
Figure 20: Fontana-Masson staining for melanin pigmentation. 99
Figure 21: CD31 staining of the endothelial cells in blood vessels. 121
Figure 22: Receiver Operating Characteristic curves for the panel of scar measurement tools. 129
Figure 23: Haemocytometer grid used in the experiment. 145
Figure 24: The standard deviation of readings 1-6 plotted against the number of readings. 147
Figure 25 (a &b): MTT assay spectrometer optical density readings 148
Figure 26 (a-d): MTT assay of human dermatofibroblasts cultured with different concentrations of decorin. 150
Figure 27: Decorin concentration as measured using an ELISA assay during heat treatment. 164
Figure 28 (a-d): Circular dichroism analysis of decorin heated at 40°C (a), 50°C (b), 70°C (c) and 90°C (d) 165
Figure 29 (a-d): Circular dichroism of decorin 167
Figure 30 (a & b): Rat glioma C6 cell proliferation in the presence of decorin 168
Figure 31: Immuno-histochemical staining for fibronectin (red) in human dermatofibroblasts 170
Figure 32: Quantification of surface area staining positively for fibronectin after immuno-histochemical staining. 170
Figure 33: Quantification of immune-histochemical staining of fibronectin in human dermato-fibroblasts after treatment with TGF- β2, unheated decorin and heated decorin. 171
Figure 34: Quantification of collagen via the Sirius red assay in HDF's treated with TGF-β2 and various concentrations of decorin 172
Figure 35: Bar chart showing the levels of collagen as ascertained by the Sirius red assay on day 14 of HDF's treated with TGF-β2 and various concentrations of decorin 173

Figure 36: Quantification of collagen via the Sirius red assay in HDF's treated with TGF-β2 and various preparations of decorin.....174
Figure 37: Bar chart showing the levels of collagen as ascertained by the Sirius red assay on day 14 of HDF's treated with TGF-β2 and various preparations of decorin.....175
Figure 38: Distribution of participants according to Fitzpatrick score classification.....185

Tables

Table 1: Comparison of colour measurement devices in terms of parameter measured, reliability, correlation with clinical score and cost. 45
Table 2: Comparison of laser devices in terms of parameter measured, reliability, correlation with clinical score and cost. 49
Table 3: Comparison of 3D measurement devices in terms of parameter measured, reliability, correlation with clinical score and cost. 56
Table 4: Comparison of ultrasound devices in terms of parameter measured, reliability, correlation with clinical score and cost. 61
Table 5: Comparison of surface topography measuring devices in terms of parameter measured, reliability, correlation with clinical score and cost. 64
Table 6: Comparison of used and recommended parameters for the Cutometer in the literature.The most commonly recommended parameters are Ue and Uf (R0). 67
Table 7: Modified Vancouver Scar Subscales and parameters. Skin characteristics are divided into pliability, height, vascularity (erythema) and pigmentation subscales. 93
Table 8: Patient satisfaction with devices questionnaire. 99
Table 9: Demographics of participants and clinical characteristics of the scar sites chosen for evaluation. 103
Table 10: Inter-rater reliability values for the mVSS individual subscales. 105
Table 11: Inter-rater reliability values for the mVSS total score, POSAS subscale and total scores. 105
Table 12: Comparison of paired Fleiss kappa values with multiple combinations of assessors. 106
Table 13: The ICC (Average) of two assessors versus three assessors. 106
Table 14: Inter-rater reliability values for the erythema measures of the DSM II Colormeter for scar tissue and normal skin. 108
Table 15: Intra-rater reliability values for the DSM II Colormeter a* and Erythema parameters for scar tissue. 108
Table 16: Intra-rater reliability values for the DSM II Colormeter a* and Erythema parameters for normal skin. 108
Table 17: Inter-rater reliability ICC values of the pigmentation measures for the DSM II Colormeter for scar tissue and normal skin. 109
Table 18: Intra-rater reliability values for the DSM II Colormeter pigmentation measures for scar tissue. 110
Table 19: Intra-rater reliability values for the DSM II Colormeter pigmentation measures for normal skin. 110
Table 20: Inter-rater reliability values of the erythema and pigmentation measures for the Scanoskin system for scar tissue and normal skin. 111
Table 21: Intra-rater reliability values for the Scanoskin camera for scar tissue. 111
Table 22: Intra-rater reliability values for the Scanoskin camera for normal skin. 112
Table 23: Inter-rater reliability values for the Dermascan ultrasound Thickness and Intensity measurements for scar tissue and normal skin. 112
Table 24: Intra-rater reliability values for the Dermascan for scar tissue. 113
Table 25: Intra-rater reliability values for the Dermascan for normal skin. 113
Table 26: Inter-rater reliability values for the Cutometer R0 and R2 measures for scar tissue and normal skin. 114
Table 27: Intra-rater reliability values for the Cutometer for scar tissue. 114

Table 28: Intra-rater reliability values for the Cutometer for normal skin. 114
Table 29: Differences in R0 and R2 inter-rater ICC values between non-hypertrophic scars (mVSS Pliability scores of 2 or less) and hypertrophic scars (mVSS Pliability values of >2) 115
Table 30: Concurrent validity of subjective to objective scores 118
Table 31: Concurrent validity of objective vascularity parameters 119
Table 32: Spearman's rho correlations of histological thickness, blood vessel density (CD31 staining), and melanin (Fontana-Masson staining) with the corresponding subjective and objective parameters. Parameters with statistically significant correlations are shaded in grey. 122
Table 33: Ratings for the objective measurement tools used in the study and skin biopsy. 123
Table 34: Mean rank of parameters arranged according to rank. 124
Table 35: Wilcoxon signed-rank test comparison of the scar parameters. 125
Table 36: Receiver Operating Characteristic values for the Dermascan, Cutometer and DSM II parameters. 128
Table 37: Chi-square test (X^2) values for the objective parameters. 130
Table 38: Parameter combinations and the ROC Area under the curve values for predicting mVSS scores of 6 or more. 130
Table 39: Objective Scar Scale total scores and their corresponding sensitivities and specificities in predicting an mVSS score of 6 and above. 131
Table 40: Study inclusion and exclusion criteria. 181
Table 41: Scoring scale used to quantify erythema, dryness and oedema of the subject's skin. 182
Table 42: Treatment groups of the first (open cutaneous test) and second (closed cutaneous test) phases of the study. 184
Table 43: Distribution of erythema grades of participants after 1 hour of dressing application. 186
Table 44: Distribution of erythema grades of participants after 3 days of dressing application. 186
Table 45: Distribution of dryness grades of participants after 1 hour of dressing application. 187
Table 46: Distribution of dryness grades of participants after 3 days of dressing application. 187
Table 47: Distribution of oedema grades of participants after 1 hour of dressing application. 188

Abbreviations

Numbers and Symbols
α-SMA- α-Smooth Muscle Actin
β-AR- Beta β adrenergic receptors
µL- microlitre
µm- micrometre
2D- Two dimensional
3D- Three dimensional
5-FU- 5-Fluorouracil

A

A431 cells- model human cell line (epidermoid carcinoma)
AF- Auto-fluorescence
ALK- Activin-receptor-like kinase
AUC- Area under the curve

B

BASE- Bielefeld Academic Search Engine
bFGF- basic fibroblast growth factor
BSA- Bovine Serum Albumin
BTX-A- Botulinum type A
BTX-B- Botulinum type B

C

C1V1- Concentration 1 x Volume 1
CD- capillary density
cDNA- complementary DNA
CI- Confidence Interval
CIE- International Commission on Illumination
CLM- Confocal Laser Microscopy
CMYK- Cyan, Magenta, Yellow and Black
CO2- Carbon dioxide
CTGF- Connective tissue growth factor
CV- coefficient of variation

D

DAPI- 4',6-diamidino-2-phenylindole
DMEM- Dulbecco Modified Eagle's Media
DNA- Deoxyribonucleic acid
DR- Diffuse Reflectance
DSLR- Digital Single-Lens Reflex
DSM II- Dermaspectrometer II

E

E- Young's modulus
EAI- Equal Appearing Interval
ECM- Extra-Cellular Matrix
ECM2- Extra-Cellular Matrix protein 2
EDC- 1-ethyl-3-(3-dimethylaminopropyl) carbodiimide
EGFR- Epidermal Growth Factor Receptor
ELISA- enzyme-linked immunosorbent assay
EM- Electromagnetic

F

FAQ- Frequently Asked Questions
FBS- Foetal Bovine Serum
FDA- Food and Drug Administration
FEM- Finite element modelling
Fig- Figure
fMRI- Functional Magnetic Resonance Imaging

G

GAG- glycosaminoglycan
GCS- Gellan Contact Study

H

HCl- Hydrochloric acid
HDF- Human Dermato-Fibroblasts
HRBC- Human Biomaterials Resource Centre
HRP- horseradish peroxidase
HSV- Hue-Saturation-Value

I

ICC- Intra-Class Correlation coefficients
ID- Identification
IFNα2b- Interferon α-2b
IL- Interleukin
ISO- International Organization for Standardization

K

kDa- Kilodaltons
kPA- kilopascals

L

LA50- Lethal Area 50 Index
LAP- Latency Associated Peptide

LDF- Laser Doppler Flowmetry
LDI- Laser Doppler Imaging
LRR- Leucine-Rich Repeats
LSI- Laser Speckle Imaging
LSPI- Laser Speckle Perfusion Imaging
LTβP- Latent TGFβ Binding Protein

M

MeSH- Medical Subject Headings
MHz- Megahertz
mm- Milimetre
MMP- Matrix Metalloproteinases
MP- Megapixel
MPT- Multiphoton technology
MRC- Medical Council Research
MRI- Magnetic Resonance Imaging
mRNA- messenger ribonucleic acid
ms- millisecond
MSS- Manchester Scar Scale
MTT- 3-4,5-Dimethythiazol-2-yl)-2,5-diphenyltetrazolium bromide
mVSS- Modified Vancouver Scar Scale

N

NADH- Nicotinamide adenine dinucleotide (reduced form)
NADPH- Nicotinamide adenine dinucleotide phosphate (reduced form)
ng- nanogram
NGS- Normal Goat Serum
nm- nanometre
NRES- National Research Ethics Service

O

OCT- Optical Coherence Tomography

P

PBS- Phosphate buffered saline
PC- Peak Count
PCI- Percutaneous collagen induction
PCNA- Proliferating cell nuclear antigen
pg- picogram
PGT- Pressure Garments
PhD- Doctorate of Philosophy
pHEMA- poly(2-hydroxyethyl methacrylate)
PIL- Patient Information Leaflet
POSAS- Patient and Observer Scar Assessment Scale
PRIMOS- Phaseshift Rapid In Vivo Measurement Of the Skin
PRISMA- Preferred Reporting Items for Systematic Reviews and Meta-Analyses

Q

QEHB- Queen Elizabeth Hospital

R

R- residual deformation (Cutometer system)
R0- Maximum extension (Cutometer system)
R2- Ratio of final retraction and maximum deformation (R2)
R8- visco part (Cutometer system)
RGB- Red, Green and Blue
ROC- Receiving Operating Characteristic
ROI- Region of Interest
RRT- resonance running time

S

Sa- arithmetic mean of surface area roughness (PRIMOS system)
SD- Standard Deviation
SELS- Surface Evaluation for Living Skin
SEM- Standard Error of Mean
Ser- Index of skin roughness (Visioscan system)
Sesc- Index of skin scaliness (Visioscan system)
Sesm- Index of skin smoothness (Visioscan system)
Sew- Index of skin wrinkles (Visioscan system)
SHG- Second Harmonic Generation
SIA- Spectrophotometric intra-cutaneous analysis
SLRP- Small Leucine-Rich Proteoglycans
SVD- Shear Velocity Device
Sz- mean of five highest peaks and five deepest valleys form entire measurement (PRIMOS system)

T

TBSA- Total Burns Surface Area
tcpCO2- Transcutaneous carbon dioxide tension
tcpO2- Transcutaneous oxygen tension
TEWL- Transepidermal water loss
TGF-β1- Transforming Growth Factor Beta 1
TGF-β2- Transforming Growth Factor Beta 2
TGF-β3- Transforming Growth Factor Beta 3
TPEF- Two photon excited fluorescence
TPT- touch pressure threshold
TUPS- Tissue Ultrasound Palpation System

U

Ua- final detraction (Cutometer system)
Ue- immediate deformation (Cutometer system)

Uf- immediate retraction (Cutometer system)
Uf- maximal deformation (Cutometer system)
UK- United Kingdom
USA- United States of America
Uv- delayed deformation (Cutometer system)
UV- Ultra-violet
UVA- Ultraviolet A

V

VEGF- Vascular Endothelial Growth Factor
VSS- Vancouver Scar Scale

W

WP- Work packages

CHAPTER 1

GENERAL INTRODUCTION

1. Introduction

1.1. The clinical problem: Hypertrophic scarring in burn patients

Burns are injuries to the skin that are primarily caused by heat (hot solids, liquids or flames), but can also be due to electricity, chemicals, friction and radiation. These injuries constitute a global health problem which can lead to significant mortality and morbidity. Although burn injuries still lead to a high rate of mortality in low developed countries[1], burn mortality rates have been decreasing in most high and very highly developed countries e.g. in Europe[2, 3].

With the advancements seen in burn care over the last few decades, an increasing number of patients are now surviving large percentage burns (defined by the American Burn Association burn injury severity grading system as a Total Burn Surface Area, TBSA, of >25%). Klein et al (2014) showed that the 50% mortality rate for burn area (LA50) has increased from 20% TBSA in the 1940's to 90% today[4], likely due to the tremendous advancements seen in surgical interventions and critical care support. However, this effectively means that an increasing number of patients are surviving with extensive burn scars and hypertrophic scarring which is often a complication that is suffered by these patients when a thermal injury penetrates and damages the dermis. During the healing process, an excessive amount of collagen is deposited secondary to an abnormal proliferation of fibroblasts and this results in a raised, bulky, firm scar that is pruritic and erythematous. Non-fatal burn injuries therefore result in a high level of morbidity, stemming from increased hospital length of stay, disability and disfigurement resulting in difficulty for the patient to reintegrate back into society.

1.1.1 Wound healing

Wound repair is a complex process which requires the right balance and coordination of multiple cell types. Normal wound healing consists of four different phases: haemostasis, inflammation, proliferation and maturation[5] (Figure 1). These phases do not occur in isolation but overlap each other[6].

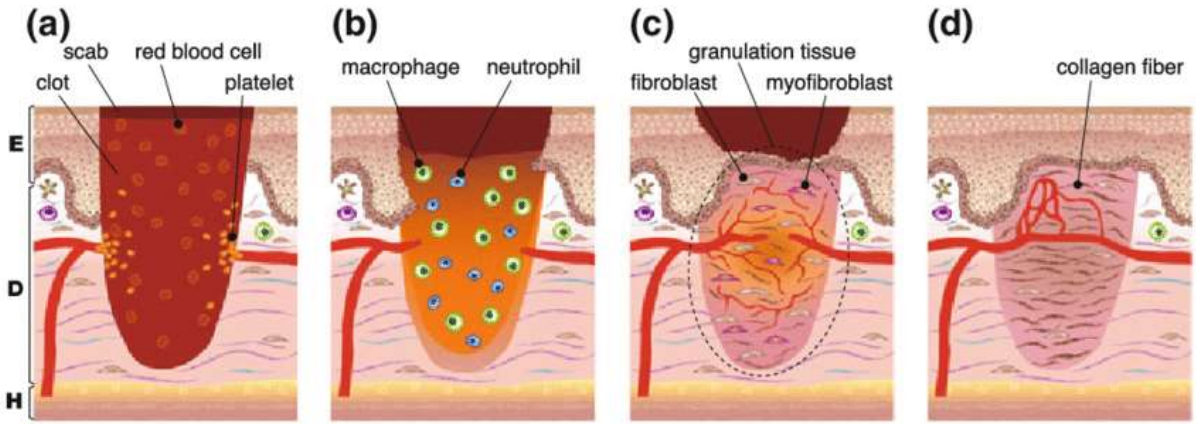

Figure 1: Phases of wound healing. (a) Haemostasis, (b) Inflammation, (c) Proliferation, (d) Maturation. E: Epidermis, D: Dermis, H: Hypodermis. (Source: Kawasumi, Aiko & Sagawa, Natsume & Hayashi, Shinichi & Yokoyama, Hitoshi & Tamura, Koji. (2012). Wound Healing in Mammals and Amphibians: Toward Limb Regeneration in Mammals. Current topics in microbiology and immunology. 367. 10.1007/82_2012_305.)

The haemostasis phase occurs after the injury is sustained and the damaged blood vessels constrict and platelets congregate to seal off the damaged vessel walls. The inflammatory phase then occurs and this causes the activation of the coagulation cascade which then causes further release of chemotactic cytokines that attract neutrophils and macrophages to the site of injury. This phase lasts for around 48 to 72 hours.

The proliferation (new tissue formation) stage of healing occurs after this, and can lasts for 3-6 weeks[7]. The proliferation of cells is necessary as migrated cells alone would not sufficiently replace damaged tissue. This stage also involves the creation of new extracellular matrix (ECM) by fibroblasts. The ECM consists of a collection of cell-secreted molecules including proteoglycans (such as heparan sulfate, chondroitin sulfate), non-proteoglycan polysaccharides such as hyaluronic acid, and proteins such as collagen and elastin. Structurally, hypertrophic scars contain a greater ratio of collagen type III over collagen type I compared to normal skin.

In addition to this re-epithelialisation, angiogenesis and wound contraction also occur[8]. Re-epithelialisation occurs within hours of injury when keratinocytes start migrating from the wound edges and also residual structures such as hair follicles and sweat glands.

Multiple factors can affect the process of wound healing[9]. These can be divided into local factors such as infection, presence of a foreign body, or circulation problems (both venous, arterial and lymphatic) and systemic factors such as age, nutrition and diseases such as diabetes. Delayed wound healing can then lead to a higher risk of hypertrophic scarring[10].

1.1.2 Scarring

The restoration of damaged skin is an important survival mechanism as it protects against infection, fluid loss and also restores function to the injured tissue. Scarring however is not inherently required for wound healing as there is evidence that wound healing in early human foetuses[11] (and other early mammalian embryos)[12] occur without scar tissue formation, and thus some have theorised that scarring is a survival adaptation that allows wounds to heal quicker[13].

The orientation and alignment of collagen during dermal wound healing is an important determinant of scar tissue formation[14]. The collagen laid down in hypertrophic scars differs from normal skin in the configuration in which it is arranged. In normal skin, collagen is organized into fibres and fibre-bundles which run parallel to the surface of the skin, which results in a phenomenon called Langer's lines. In hypertrophic scars however, collagen is bundles are disorganized and present as whorls and nodules[15]. These disorganized collagen depositions contract with time and this can result in severe problems depending on their location, for example the reduction in range of motion at joints and extremities and in some cases immobilize structures such as eyes and the constriction of orifices. The poor cosmetic appearances of these scars also causes psychological problems which can impede the reintegration of the patient back into society after the physical recovery of the injury.

Factors that influence scarring are myriad but the main factors shown in studies include race, depth of injury[16], delay in healing[17] and anatomical area (high tension areas e.g. sternum and deltoid).

Hypertrophic scars and keloids are two forms of excessive scarring that can occur after injury. Both hypertrophic and keloid scars are characterised by an increased thickness above the skin surface, redness and itch however keloids differ from hypertrophic scarring in that keloids spread beyond the boundaries of the initial injury (compared to hypertrophic scars which increase in size by pushing out the margins of the scar,) and do not regress over time[18]. Additionally, genetic predisposition also plays a role in keloid scar formation and is typically seen in higher rates in the African, Asian and Hispanic populations compared to Caucasians[19].

Both hypertrophic and keloid scars have particular histological characteristics as well as constituent differences in comparison to normal skin. In terms of collagen types, there is a higher ratio of collagen type III to type I in hypertrophic and keloid scars[20, 21]. In terms of cell types, myofibroblasts, which are differentiated fibroblasts which express α-Smooth Muscle Actin (α-SMA), are seen in both types of scares and are responsible for the production of collagen and contraction in scar tissue[22]. Hypertrophic scars however commonly exhibit nodular structures (containing fibroblastic cells, small vessels and fine randomly organised collagen fibres) which are rarely seen in keloids[22].

Pathological scarring can have a significant impact on burn survivors' quality of life even years after injury[23]. Scars are not only cosmetically disfiguring and cause emotional and psychological distress to patients but other common complications of scarring such as pain, itch and restriction of mobility can also greatly reduce the quality of life of patients[24]. A study by Wiechman et al (2018) found that pain and sleep disturbance had the biggest effect on the ability of survivors to return to work[25]. Other studies have also found that pathological scarring was found to predict post-burn itch which persists in a majority of burn survivors and affected their quality of life[26].

1.2. Anti-scarring therapies in burn patients

Despite the advances in survival of burn victims, prevention of pathological scarring is limited to early burn wound excision which remains as one of the most effective strategies to reduce time to healing and minimise severe scarring[27, 28]. A study by Chipp et al (2017) showed that the risk of hypertrophic scarring increases with every additional day taken for the burn wound to heal[10]. Other forms of treatment of pathological scarring is currently still limited to after the scar has formed and little progress has been made in the field of scar prevention.

Treatments aimed at ameliorating hypertrophic scarring can be broadly classified into mechanical based therapies, intralesional pharmaceutical agents, radiotherapy, and surgical.

1.2.1 Current therapies

1.2.1.1 Silicone gels and sheets

Silicone gels and sheets were introduced in the 1970's for scar treatment[29]. They consist of long chain silicone polymers (polysiloxanes), silicone dioxide and a volatile component[30]. The exact mechanism of how silicone gels and sheets work is not known, but various mechanisms have been suggested such as the hydration of the stratum corneum (facilitating fibroblast production and reducing collagen production)[31], alteration of environmental stimuli such as temperature[32]. Studies however have shown that the beneficial effects are not likely to be due to change in oxygenation, blood flow or silicone absorption[32-34]. Studies have shown an improvement in colour, thickness , elasticity, and itching after silicone gel/sheet use on hypertrophic and keloid scars[29]. A Cochrane database systematic review (2013) involving 20 trials however reported that the evidence for the benefit of silicone gel sheets is weak[35]. No significant side effects from its use have been reported other than skin irritation[29].

1.2.1.2 Pressure garments

Pressure garments (PGT) are a mainstay of current post-burn scar treatment and are considered in many centres as a standard of care despite there being no strong evidence of their effectiveness in preventing or treating hypertrophic scars. The mechanism of action of PGT is not clear as well, but

some studies have found alterations in the release of prostaglandins and collagenases with PGT use[36]. The popularity of PGT's is understandable as it is non-invasive and it is presumed by many clinicians to have beneficial effects and few adverse effects[37]. Studies have reported improvements in scar thickness, redness and reduced contraction[38], with better results seen with higher pressures (20-25mmHg)[37]. A meta-analysis by Anzarut et al (2009) showed that unlike studies on silicone sheets/gels, of which the majority were of low methodological quality, studies in PGT use were of high quality but showed that PGT use only led to a small improvement in scar height[39]. The burden of wearing PGTs (e.g. poor fit[40], negative public perception[41],) however can be an issue to some especially in patients with large burns, and non-compliance is a frequently encountered problem in PGT use[41, 42]. The combination use of both silicone gel sheets and PGT have been shown to provide better outcomes in terms of scar thickness[43].

1.2.1.3 Vacuum therapy

Mechano-transduction is a physiological process whereby mechanical loads and stress are sensed by cells and converted into a biochemical response[44]. Mechanical forces such as compression and stretch (e.g. vacuum therapy) are detected by two different systems[45]: by mechano-sensitive proteins and molecules (e.g. actin filaments, vinculin and talin[46]) in cells in the extra-cellular matrix (ECM, i.e. endothelial cells, fibroblasts, myofibroblasts) that lead to local re-organisation of the ECM and also nerve receptors (mechanosensitive nociceptors) that then release neuropeptides that lead to systemic modulation of scarring through the skin and alterations in the immune cell functions. A study by Yagmur et al (2011) showed that surgical denervation prevented excessive dermal scarring in a rabbit model[47], and Brown et al (2014) showed that distraction techniques which reduced pain and anxiety during dressing changes led to an improvement in burn wound re-epithelialisation[48].

Vacuum therapy is a non-invasive technique that utilises the principle of mechano-transduction through mechanical massage to treat burn scars[49], with purported benefits of improvement in scar hardness and elasticity[50]. Vacuum massage works by lifting the skin through suction and then mobilising the suctioned skin fold. Although this treatment modality has been present since the late

1970's[51] for the treatment of traumatic or burn scars, very few studies have been done to determine its effectiveness[50]. Marques et al (2011) showed that mechanical massage may up-regulate anti-inflammatory gene expression although this was in adipose tissue[52]. A study by Meirte et al (2016) showed, through ultrasound imaging, that the vacuum device (PRUS, F care systems NV, Antwerp, Belgium) was able to disrupt the epidermis and cause changes in the dermal density[49]. Majani et al (2013) showed that biweekly vacuum sessions (ranging from 8-20 sessions,) led to subjective symptom improvement (e.g. pain, paraesthesia) and scar appearance[53]. Better designed clinical studies are still needed in order to ascertain the effectiveness of vacuum therapy in burn scars and its long term effects[49].

1.2.1.4 Intra-lesional scar therapies

1.2.1.4.1 Corticosteroids

Corticosteroids are currently routinely used for the treatment of keloid and hypertrophic scars through intra-lesional injections. A literature review by Taheri et al (2014), showed that the use of corticosteroids to prevent recurrence after keloid or hypertrophic scar excision showed variable results[54], with some studies showing a 5 year response rate of only ~50%[55]. Furthermore the authors did not find any studies reporting on the use of corticosteroids after skin burns. Furthermore, intra-lesional steroid injections can also lead to a variety of side effects including hypopigmentation, telangiectasia and tissue atrophy[56].

1.2.1.4.2 Anti-neoplastic agents

5-Fluorouracil is an antineoplastic agent that works primarily as a thymidylate synthase inhibitor which causes the blockage of the synthesis of pyrimidine thymidine, a nucleoside which is required for DNA replication.

Current evidence shows that 5-Fluorouracil (5-FU) is a safe and effective treatment of pathological scarring in terms of improvement of scar appearance and the prevention of recurrence, and is best used in conjunction with corticosteroids[57, 58]. However, no randomised controlled trial with large sample sizes has yet to be done.

Another antineoplastic agent that has been used to treat keloids is Bleomycin. Bleomycin acts by inducing DNA strand breaks and inhibits the synthesis of DNA[59]. It was first introduced by Bodokh and Brun for the treatment of keloids and hypertrophic scarring in 1996 thorough intra-lesional injections[59] and studies have shown significant improvement of pathological scarring in human subjects[60].

1.2.1.5 Radiotherapy

Radiotherapy is commonly reserved for keloid scars which have not responded to other forms of therapy. Radiation functions by inhibiting the degranulation of mast cells leading to decreasing fibroblast proliferation and collagen synthesis mediated by Transforming Growth Factor β1 (TGF-β1)[61]. Several studies have shown that the recurrence rate of keloids is lower with adjunctive radiotherapy compared to just surgery and steroids alone[62-64]. Additionally, contrary to commonly held beliefs, radiotherapy is also well tolerated with few side effects when the appropriate doses are used[62, 65].

Radiation carries the risk of induction of malignant tumours and thus is often used as a last resort, however a review by Ogawa et al (2009) showed that the risk of carcinogenesis attributed to keloid radiation therapy is very low however adequate protection of the surrounding tissue are required especially in young children[66].

1.2.2 Emerging therapies

1.2.2.1 Ablative CO_2 Fractional laser

CO_2 lasers are used increasingly to treat pathological scarring in burns with several studies showing improvement in scar quality[67] and also itch and pain[68]. There are several hypotheses on how lasers work, in contrast to non-ablative lasers which are thought to work through focal heating in deeper microthermal zones leading to normalisation of the cycle of collagenesis and collagenolysis[69], ablative CO_2 lasers are theorised to work via the breaking down of disorganised collagen fibrils that are responsible for scar contracture[68]. Few studies however have actually demonstrated the histological changes that occur after laser treatment, many of which only have small sample sizes.

Several studies have shown that laser treatment leads to significant structural and composition changes in the dermal layer. Naouri et al (2011) demonstrated an increase in dermal thickness of the scar post laser treatment (via high frequency ultrasound[70]). Other studies showed the restoration of the papillary dermis layer[71] and a decrease in collagen bundle thickness and density in the upper dermis [72]. The orientation of collagen fibres is important for the strength of the tissue and its ability to withstand repeated stresses[73] which underlies the concept of Langer's lines (skin tension lines) which guides surgical incision orientation[74]. With laser treatment, collagen fibres have also been seen to reorganise to a more aligned horizontal and parallel arrangement[72] although the scars do not revert back to the native nest-like collagen orientation in normal skin. Connolly et al (2014) also showed a decrease in vascular density in upper dermis (in particular small calibre vessels) [75] which may explain the improvements in scar erythema although the relationship between clinically perceived erythema and blood vessel density and distribution is complex and multifactorial[76] . Other studies have shown a reduction in chronic inflammatory cell infiltrate[77] and reduced fibroblast proliferation[78] with laser use.

Qu et al[79] (2012) found a significant improvement in subjective scores for scars after laser treatment (after 3 treatments). Molecular analyses of these scars (after 48 hours) indicated that CO_2 laser treatment induced mature hypertrophic scar regression through the suppression of both types of I and III procollagen (mRNA levels down regulated, but ratio did not change) via the suppression of TGF-β2, 3 and bFGF (basic fibroblast growth factor) expression and upregulation of Matrix metalloproteinase-1 (MMP-1) and certain microRNAS (miR-18a and miR-19a). Ozog et al (2013) showed a significant decrease in type I collagen and increase in type III collagen after laser treatment[80]. Other laser studies (Pulsed dye laser treatment) also showed reduced levels of TGF-β1, Proliferating cell nuclear antigen (PCNA) and collagen type III (but not type I)[78] after treatment.

1.2.2.2 Micro-needling

Micro-needling or otherwise also known as Percutaneous collagen induction (PCI) or medical needling is a minimally invasive technique where controlled puncturing of the skin is performed

using miniature fine needles which range from 0.5 to 2.0mm[81]. Originally used in the cosmetic industry for skin rejuvenation, it has now been adapted for transdermal delivery of therapeutic drugs[82] as well as burn scar treatment[83]. PCI is most commonly performed using a drum-shaped roller (e.g. Dermaroller[83]) or a pen shaped device with a tip equipped with the microneedles (e.g. Dermapen[81]) . Aust et al (2010) showed that micro-needling of burn scars led to an 80% patient-rated improvement in scar appearance with histology showing increase in collagen and elastin deposition[83].

1.2.2.3 Botulinum toxin

Botulinum toxin is a neurotoxin produced by Clostridium botulinum which reduced acetylcholine release at the neuromuscular junction. Botulinum type A (BTX-A) and B (BTX-B) forms of the toxin are primarily used medically to treat muscle spasticity and disorders of nerve hyperactivity including hyperhidrosis and neuropathic pain. Botulinum toxin is hypothesised to primarily exert its effects on scars through the relief of tensile force on the healing wound but there is evidence that it may also affect scars on a cellular level[84]. Several studies have investigated its use for the treatment or prevention of hypertrophic scars.

Studies by Xiao et al (2011) showed that BTX-A inhibited proliferation of hypertrophic scar derived fibroblasts and inhibited the expression of Connective tissue growth factor (CTGF)[85]. However in-vitro studies by Haubner et al (2012 & 2014) showed that botulinum toxin A incubation of human keloid tissue did not lead to any significant changes of Interleukin-6 (IL-6), Vascular Endothelial Growth Factor (VEGF), or TGF-β[86] nor showed no effect on cell proliferation[87].

The results of clinical studies have been mixed with some showing improvement in subjective scar scores in patients[88, 89] while others such as a study by Gauglitz et al (2012) which investigated intra-lesional BTX-A injections into keloids showed no regression of keloid tissue after 2 monthly injections up to 6 months with no differences in ECM markers, collagen synthesis, or TGF-β[90].However a systematic review by Prodromidou et al (2015) concluded that the current evidence did not support

the use of botulinum toxin due to small patient numbers and reliance on subjective assessment of cosmetic improvement[91].

1.2.2.4 Interferon

Interferons are a type of signalling proteins and cytokines which are released by cells in response to pathogens including viruses, bacteria and cancer cells leading to heightened cellular defences. Interferon α-2b (IFNα2b) is a type I interferon (that binds to IFN-α/β receptor) which is produced by fibroblasts which is typically released in response to viral infection and been shown to decrease the synthesis of collagen and increase collagenase production[92]. Studies have shown that IFNα2b may reduce fibrosis by inhibiting fibroblast proliferation (but not inducing apoptosis)[92] and antagonising the effects of TGF-β and histamine[93]. Subcutaneous recombinant IFNα2b therapy for 24 weeks was found to significantly improve scar quality and volume with accompanying reduction in serum TGF-β and plasma Ntau-methylhistamine levels[94]. Interferon α therapy however is expensive and may cause adverse effects in almost every organ system including flu-like symptoms, haematological toxicity and nausea[95].

1.2.2.5 Verapamil

Verapamil is a calcium channel blocker that is normally utilised to control the heart rate. In-vitro studies have shown that verapamil decreased IL-6 and VEGF production in keloid fibroblasts as well as reducing cellular proliferation and increasing apoptosis rates[96]. Used intra-lesionally as an adjuvant treatment post-surgery, verapamil has been shown to reduce keloid scar recurrence[97] and improve scar vascularity and pliability[97].

1.2.2.6 Autologous fat grafting and stem cell therapy

Autologous fat grafting is a well-established technique, having been first described by Neuber in 1893 to fill a retracted infraorbital rim scar[98], and subsequently refined by Coleman in the late 1980's[99]. Primarily used for its volume increasing effect, it has also been shown to result in improvement of skin quality[100], pain[101, 102] and itch. This is hypothesised to be a result of the adipose-derived stem cells contained within the fat tissue which are multipotent and thus able to

differentiate into various cells types[103]. Additionally, these cells also have the capacity to secrete a broad range of cytokines, chemokines and growth factors which may contribute to their anti-scarring effects[103].

1.2.3 Novel therapies

1.2.3.1 Topical Salbutamol

The beta-adrenergic family of receptors (βARs: β1AR; β2AR; β3AR)[104] are G-protein receptors for catecholamines that are released primarily by the adrenal medulla, and the sympathetic nervous system [105]. Keratinocytes however have also been shown to secrete catecholamines which are anti-motogenic and anti-mitogenic[106, 107] and thus delay wound re-epithelialisation. βARs are expressed in the majority of skin cells and the receptors that are expressed on keratinocytes[108], fibroblasts[109] and melanocytes[110] are of exclusively of the β2-AR subtype which together form a βARs skin network with both autocrine (epidermis) and paracrine (dermis) systems[111].

Pullar et al (2006) demonstrated that use of a β-AR antagonist (Timolol) blocked β2-AR receptors and enhanced keratinocyte motility and subsequent wound healing[112] and this finding has been echoed by Sivamani et al (2009) in animal burn wound models[113] and beta-blocker use in adult burn patients has been shown to be associated with reduced time to healing[114]. Conversely, the activation of β-AR by β-AR agonists (e.g. Clenbuterol) has been shown to significantly delay skin re-epithelialisation[115]. Further studies by Pullar et al however has shown that β2ARag (e.g. Salbutamol, Formeterol) use reduced fibroblast differentiation, contraction and ability to sense tension (through mature focal adhesions,) as well as reducing inflammation and angiogenesis all of which contributed to reduced scarring[116]. Although β2ARag use on porcine wounds led initially to re-epithelialisation delay at 14 days, there was no difference seen in the wound after 28 days[116]. There is currently a Medical Council Research (MRC) funded study that is investigating the use of topical Salbutamol to prevent skin scarring and hyperpigmentation in humans[117].

1.2.3.2 Decorin

In recent years, there has been much interest and increasing evidence that a naturally occurring proteoglycan in our bodies, decorin, which exhibits potent anti-scarring properties and has been shown to reduce fibrosis in fibrotic conditions that affect different organ systems such as the in the central nervous system[118], liver[119, 120], kidneys[121], lungs[122] and skin[123]. The role of decorin and its potential application in burns is discussed later in this chapter.

1.3. Development of an anti-scarring burn dressing

1.3.1 The molecular pathway of scarring: The roles of decorin and Transforming Growth Factor-β2 in scarring

1.3.1.1 Transforming Growth Factor –β

Both Transforming Growth Factor –β (TGF-β) and decorin play important roles in the formation of scar tissue. TGF- β is a growth factor that has a variety of different essential functions. Three isoforms exist which are β1, β2 and β3. All three forms share 60-80% homology even though they are encoded by different genes and are secreted as inactive pre-cursors which require activation (due to the presence of latency associated peptide [LAP] and latent TGFβ binding protein [LTBP] complexed to the TGFβ molecule,) prior to receptor binding[124]. This is achieved in-vivo through factors such as plasmin[125], thrombin, thrombospondin-1[126] or matrix metalloproteinases (e.g. MMP2 and 9)[127, 128] but in-vitro generally through the use of a mild acid[129] such as citric acid which denatures the LAP.

All three isoforms are present during wound healing but differ in terms of expression and duration in the wound. The different isoforms are also though to play different roles in healing and scarring, with TGF-β1 and 2 being implicated as important factors for hypertrophic scarring whilst TGF-β3 being thought to have anti-scarring actions[130-132].

Damaged platelets in blood clots present in wounds are thought to be one of the main sources of TGF-β1, with two different pools: the first pool (TGF-β1 with LTBP, LAP and a smaller TGF-β1 dimer,) which is released into the serum and tissues and a second pool (with TGF-β1 with LAP only) which is

slowly released as the clot is dissolved by plasmin[133]. Other sources of TGF-β1 include macrophages and fibroblasts.

Signalling by all three isoforms occur through the binding to two TGF-β receptors (TβRI and TβRII; also known as Activin-receptor-like kinase [ALK]), though TGF-β2 has been shown to require TβRIII for high affinity binding[134].

The main pathway for intra-cellular signalling of TGF-β1 is through the phosphorylation of cytoplasmic Smad proteins via the TβRI and TβRII receptors. TGF-β binds to phosphorylated TβRII and subsequently phosphorylates TβRI. This phosphorylated complex then activates the SMAD intracellular pathway through the receptor Smads (Smad-2 and 3) and co-Smad 4. Smad 2,3, and 4 then traverse the nuclear membrane to influence the regulation of genes[135].

During the inflammatory phase, TGF-β encourages the migration of leukocytes[136] and also influences the transformation of monocytes into macrophages[137]. In the proliferative phase of wound healing, TGF-β plays a role in re-epithelialisation by stimulating keratinocyte migration (both TGF-α and TGF-β; TGF-β1 may induce integrin expression in epidermal keratinocytes that facilitate migration[138]) and proliferation and also angiogenesis[139]. Fibroblasts are also stimulated by TGF-β to transform into myofibroblasts which secrete the constituents of ECM such as collagen and form granulation tissue. The myofibroblasts then contract to promote wound closure. Remodelling of the wound then occurs with TGF-β again influencing the process for e.g. by the inhibition of MMPs to allow collagen accumulation.

1.3.1.2 Decorin

Decorin is a proteoglycan (average 90-140 kilodaltons in molecular weight) that is one of the most abundant proteoglycans present in the connective tissue[140], produced predominantly by fibroblasts located in the dermis of adult human skin[140]. It belongs to a family of called the small leucine-rich proteoglycans (SLRPs), characterised by leucine-rich repeats (LRR) within a 40kD core protein[141, 142], and which also consists of biglycan, lumican and fibromodulin. SLRPs have not just structural roles

within the extracellular matrices but instructive roles as well, playing an important part in the regulation of collagen fibril growth, organisation and assembly[143]. SLRPs can be divided into 5 classes (I-V), based on multiple parameters such as the conservation and homology at protein and genomic levels, chromosomal organisation and the presence of N-terminal Cys-rich clusters[144] of which decorin belongs to Class I (along with biglycan, asporin and ECM2).

As with most SLRPs, decorin possesses both a core protein, of approximately 38 kDa with 10 leucine-rich repeat sequences[145], and a single glycosaminoglycan side chain (GAG) linked to its N-terminal 4th amino acid residue of the core protein[140]. The GAGs play an important role in cytokine binding, extracellular matrix assembly and hydration. Li et al showed that although the size of the decorin core protein did not change with age, the size and amount of decorin GAG chains were found to be reduced with age and is thought to contribute to the skin fragility commonly seen in the elderly[140].

Studies have shown that the decorin core protein possesses a curved solenoid fold that is characteristic of LRR proteins[146]. It has an banana-like arched shape with an inner concave surface consisting of curved β-sheets and the outer convex surface being formed by α-helices (Figure 2)[147].

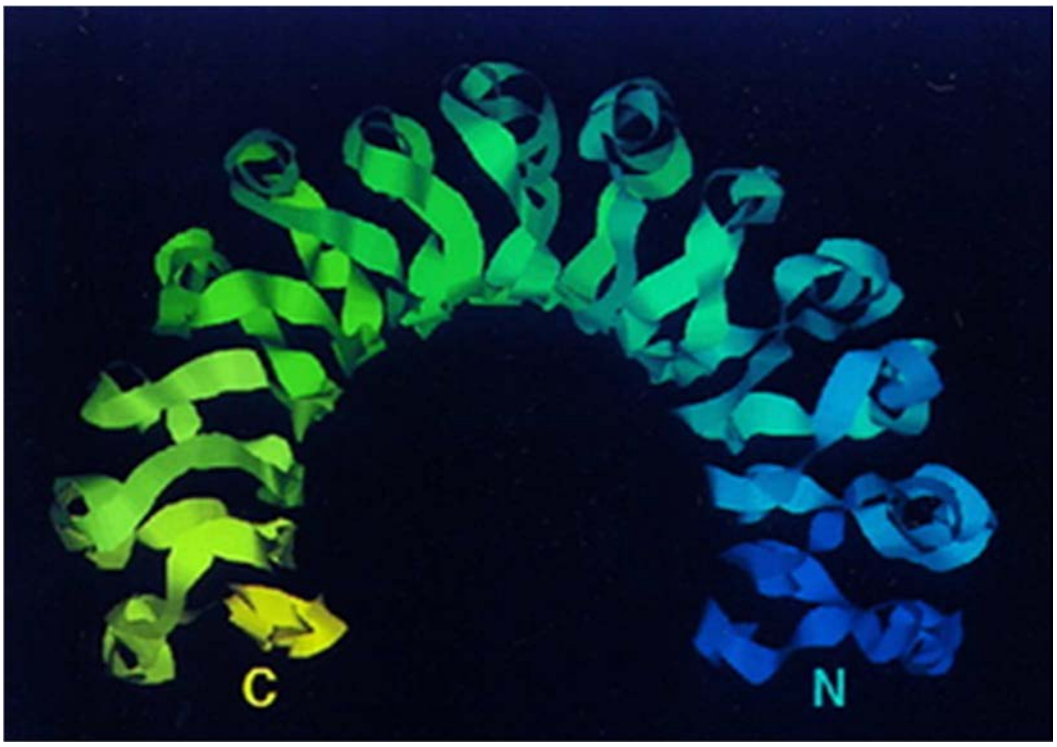

Figure 2: Model structure of decorin, with its Carboxyl (C) and NH_2-terminals (N). Adapted from Weber et al, 1996, Journal of Biological Chemistry, Volume 271, page 31769. Copyright 1996 The American Society for Biochemistry and Molecular Biology. Reprinted with permission.

Decorin is important for the regulation of the fibrillogenesis of type I, II and VI collagen[145], and binds to collagen fibrils at the "d" or "e" bands[148]. The binding of collagen molecules is thought to occur on the inner concave surface of the decorin protein, and is able to accommodate a single collagen triple helix[149]. Further studies by Scott et al (2004) however has shown through decorin crystal analysis that decorin exists in a dimeric form (Figure 3)[146], and that the two monomers interact through their concave surfaces, extending from the N-terminus to more than three-quarters of the concave surface length, resulting in a large area of the concave surface being buried. However other authors have claimed that the crystallographic decorin dimer is an artifact[150]. Studies by Islam et al (2013) have helped to resolve this controversy by showing that the decorin dimer is in equilibrium with its stable monomeric form, and that the decorin dimer must disassociate in order to bind collagen[151]. This has further relevance when the heating of decorin is discussed.

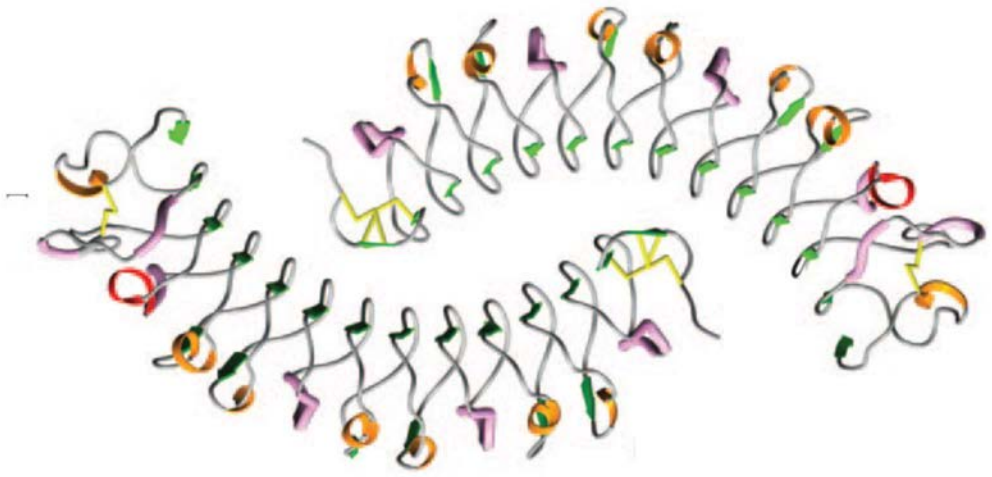

Figure 3: Dimeric structure of decorin. Adapted from Scott et al, 2004, Proceedings of the National Academy of Sciences of the United States of America (PNAS), Volume 101, page 15635. Copyright 2004 National Academy of Sciences. Non-commercial, educational use.

Decorin has been shown to be able to either enhance[152] (in low concentrations,) or inhibit the activity of TGF-β through its binding and sequestration. The decorin core protein contains at least two binding sites for TGF-β1 and 2 of differing affinities[152, 153]. Schonherr et al (1998) showed the high affinity binding site to be in the Leu155-Val260 peptide sequence, with several possible low affinity binding sites (e.g. Asp45-Leu155 and Arg63-Gly190). This high affinity Leu155-Val260 peptide sequence was also found to form complexes with TGF-β, and thus could play a role in modulating TGF-β by storing it in the extracellular matrix[153]. Furthermore, it was shown that collagen-bound decorin maintained the ability to interact with TGF- β, thus suggesting independent binding sites for TGF- β and collagen.

Decorin has been shown in animal models to be linked to both the processes of cutaneous wound healing and scarring. Jarvelainen et al (2006) showed that decorin-deficient mice had statistically significant delay in both excisional and incisional full thickness dermal wound healing compared to wild type controls. Furthermore, greater fibro-vascular invasion was also seen in decorin deficient mice[154].

Contrary to this, an animal study by Beanes et al (2001) has showed that a decrease in decorin expression is associated with scarless healing[155]. Nakamura et al (2000) also demonstrated that suppression of decorin (via decorin antisense gene therapy) improved the functional healing of early rabbit ligament scar by suppressing decorin expression and therefore allowing the formation of larger collagen fibrils in the scar which improved the mechanical properties of the scar[156]. Hosaka et al (2005) further showed that decorin antisense oligodeocynucleotide treatment of tendinocytes not only improved collagen fibril diameter but also suppressed TGF-β1 expression[157]. Al-Tarrah et al (2017) has also demonstrated higher levels of serum decorin in patients with worse long term scar severity although it should be noted that these higher levels may be proportionally related to the increase in injury severity and hence higher rates of scar remodelling and release of decorin into the systemic circulation[158].

These studies show that there is still much that needs to be understood about the role of decorin in the wound healing and scar formation process and that different levels of decorin may be required at different stages of healing and scarring depending on the desired action (e.g. improve mechanical strength of a scar or tendon,) and to optimise long term outcomes.

1.3.1.3 Gellan: a polysaccharide based dressing material

In order for decorin to exert its effects, an effective system that delivers it to the fibroblasts at the site of thermal injury needs to be devised. This is especially so as decorin is expensive to acquire as it is difficult to manufacture. A variety of methods have therefore been devised for decorin delivery and these are discussed below.

1.3.2 Decorin delivery methods in literature

1.3.2.1 Injection

A commonly used method, especially in animal studies, is to inject decorin into the area of its intended action and has been used in multiple anatomical locations. Abdel et al (2014) performed intra-articular decorin injections into knee joints[159] and this was found to be able to increase the mRNA expression of genes though no functional improvement in flexion contracture could be

elicited. Fukushima et al (2001) showed that injection of decorin into sites of muscle laceration was effective in preventing fibrosis as well as enhancing muscle regeneration and strength[160]. Hill et al (2014) found that intra-cameral injection of decorin was effective in lowering intraocular pressure by reversing established trabecular meshwork fibrosis [161]. Botfield et al (2013) showed that an initial bolus decorin injection followed by an infusion could prevent the development of juvenile communicating hydrocephalus post-trauma [162].

1.3.2.2 Intravenous injection

Besides local injection, decorin has also been delivered systemically via intravenous injection[150] and has been shown to still be able to exert its effects at the intended sites. Several research groups have sought to optimise the delivery of decorin to target sites. The native decorin protein has been reported to possess homing properties that target angiogenic vasculature through a core protein dependent interaction by binding to Vascular Endothelial Growth Factor Receptor (VEGFR-2)[163], which may be further enhanced by the its glycosaminoglycan (GAG) chain binding to integrins[164]. Jarvinen et al (2010) further enhanced this homing mechanism by combining an additional wound-homing 9-amino acid peptide (CARSKNKDC, or CAR) with decorin which allows it to more effectively target and home towards regenerating skin, skeletal muscle and tendons by recognising angiogenic blood vessels[165]. Both native decorin and the fusion CAR-decorin also have an advantage in that they do not accumulate in normal tissues[165, 166].

1.3.2.3 Decorin gene transfection

Another approach that has been investigated is the delivery of decorin gene via recombinant virus containing decorin complementary DNA (cDNA) into cells which results in overexpression of the exogenous decorin gene. This has been shown to successfully inhibit TGF-β mediated fibrosis in the lung and cornea[167].

1.3.2.4 Surface coating of implants

The encapsulation of medical devices can occur after implantation by fibrous tissue due to foreign body response, infection or inflammation[168]. This can lead to device reduced function, malfunction,

failure, pain and deformity. Furthermore, bacteria can also become embedded in the fibrous tissue and are hard to treat with antibiotics due to the poor blood supply. This is a common complication of devices such as breast implants[169], hip replacements and artificial heart valves.

Sylvester et al[170] (2012) successfully bound decorin onto poly(2-hydroxyethyl methacrylate) (pHEMA) based implants using a type 1 collagen affinity coating. However this coating with its decorin overexpression failed to reduce fibrous capsule thickness and density. This failure was thought to due to the difference in the wound environment where the presence of a foreign body led to a chronic stimulation of the inflammatory response.

1.3.2.5 Topical application and dressings

Although the previously discussed systems have shown some promise, such systems are invasive and likely to be quite costly or could cause considerable patient discomfort, for example the study by Hill et al (2014) required bi-weekly injections for 1 month[161]. A dressing based delivery system on the other hand could potentially be cheaper, easier to administer and cause less distress to the patient[171, 172]. For example the cost of topical Ibuprofen gel (10%) is approximately £63[173] compared to £12,400 for parenteral ibuprofen (based on a conversion rate of £1 to USD 1.22)[174].

Topical application of decorin can be via direct administration however without a suitable reservoir, the time available for decorin to exert its effects would be limited. Sustained topical decorin delivery can be achieved via the use of naturally decorin rich tissue based dressings i.e. via the application of human amniotic membrane. This has been used successfully to enhance wound healing and reduce fibrosis in the eyes[175], wounds[176] (including burn[177] and surgical wounds[178]) and skin graft donor sites[179].

Amniotic membrane however has several disadvantages. Being derived from human donors, there is a risk of viral and bacterial infection especially with amniotic membranes recovered from vaginal deliveries which have been shown to have a high level of bacterial contamination[180]. As a human derived product, amniotic membrane is also limited in its supply and size which makes its use in

large burn wounds difficult. The cost of amniotic membranes can also be prohibitive to its use especially for cryo-preserved membranes, which also require special storage conditions which further limit its availability. The use of freeze-dried amniotic membrane is cheaper but may not be effective in preventing fibrosis compared to cryo-preserved membranes[181].

In contrast to the large amount of literature on amniotic membrane, there is scant literature on the use of artificial decorin impregnated dressings for topical delivery. A search of the literature only revealed a study by Turkoglu et al (2014) who utilised a decorin solution soaked gelatin sponge to deliver decorin topically to dura mater after laminectomy and showed reduced epidural fibrosis[182].

The ideal topical delivery method for decorin would be via a dressing that is non-toxic, optically clear, easily modifiable and freeze-dryable. The gellan polysaccharide fulfils all these criteria optimally and is further discussed in the next section.

1.3.3 Characteristics of gellan: Suitability as a dressing material

Gellan is one of the many natural gums that have seen an increase in uses in various different fields due to their low cost and low potential for toxicity. Gellan is a bacteria synthesized polysaccharide discovered in 1978 by Kaneko and Kang et al[183] and is currently commercially produced by C.P. Kelco in the USA and a handful of other smaller companies. It is most commonly used by food companies as an FDA approved thickener and stabiliser. Gellan is significantly more expensive (cost approximately £400 per kilogram[184]) compared to other polysaccharide based gelling agents such as xanthan and gelatine (six and ten times the cost respectively)[185].

Derived from a newly discovered species of *Sphingomonas elodea* (formerly *Pseudomonas elodea*), gellan is a water-soluble polysaccharide comprised of approximately 46% D-glucose and 30% rhamnose (a naturally occurring deoxy sugar), 21% glucuronic acid (a sugar acid) and 3% O-acetyl[183] which forms a linear tetrasaccharide repeat unit: 1,3-β-D-glucose, 1,4-β-D-glucuronic acid, 1,4-β-D-glucose, and 1,4-α-L-rhamnose[186, 187] (Figure 4).

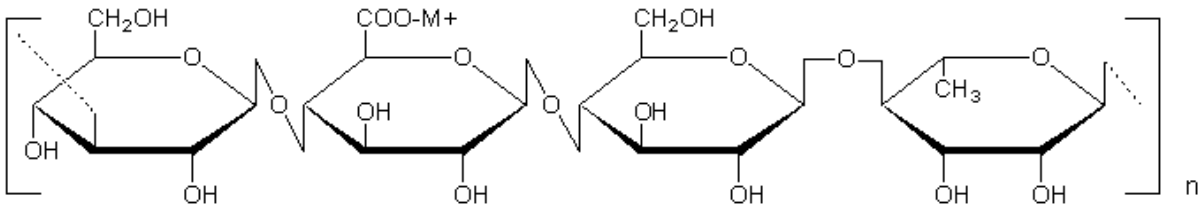

Figure 4: Gellan gum structure. Gellan consists of a linear tetrasaccharide repeat unit: 1,3-β-D-glucose, 1,4-β-D-glucuronic acid, 1,4-β-D-glucose, and 1,4-α-L-rhamnose. Image by Sensonet, distributed under a CC-BY-SA-3.0 license via Wikimedia Commons.

An advantage of gellan is its modifiable texture property. It can be formed as either an elastic soft gel (acetylated or high acyl form, with O-5-acetyl and O-2-glyceryl groups that are present on the 1,3-β-D-glucose) or a firm, non-elastic brittle gel (deacetylated or low-acyl form,) which lacks these additional acetyl and glyceryl groups. These two different forms can be combined in different ratios to produce different texture properties with superior deformability whilst retaining compressive strength similar to low acyl gellan gels[188]. The gelation of gellan is a temperature-dependent process and the polysaccharide transitions between random coiled and double helix conformations. The double helices then assemble into oriented bundles known as junction zones. A three dimensional gel network is formed when the untwined polysaccharide regions at the ends of these helices link the junction zones together as shown in Figure 5[189].

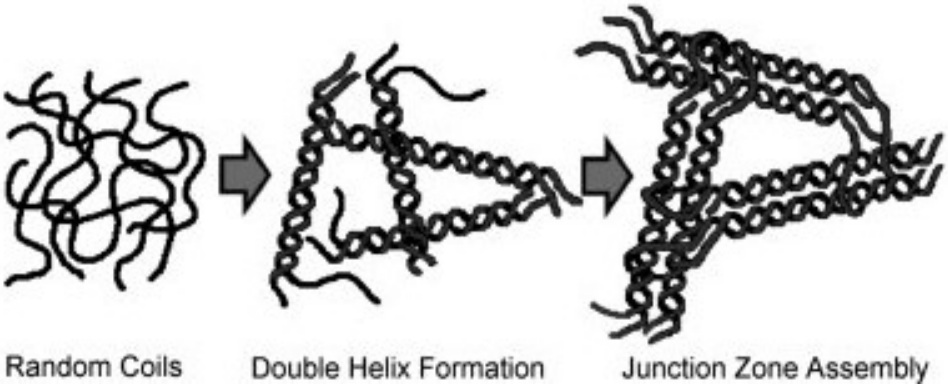

Figure 5: The mechanism of gellation of gellan gum. The gelation of gellan is temperature dependent and transitions between random coiled and double helix formations. These double helices then assemble into oriented bundles (junction zones). Reprinted from Optimizing gelling parameters of gellan gum for fibrocartilage tissue engineering, by Haeyeon Lee et al, 2011, Journal of Biomedical Materials Research Part B: Applied Biomaterials, Volume 98B, page 239. Copyright 2011 Wiley Subscription Services, Inc., A Wiley Company. Reprinted with permission.

The presence of cations is required for the formation of a stable hydrogel and the textural property of gellan is also dependent on the type and concentration of salts added. Unlike other gels such as carrageenan which is limited to potassium, ammonium, caesium and rubidium for gelation, most monovalent, di- or trivalent salts can be used for gellan gelation such as magnesium or calcium. The addition of cations increases the setting temperature by decreasing repulsion by binding to the helices around the carboxylate groups of gellan[190] and crosslinks them and therefore results in a more stabilised gellan structure[191] . Conversely, delay in gelling can be achieved by the addition of sodium citrate to complex free Ca^{2+} ions prior to use[192].

In order for non-modified gellan to be fully dissolved into water, a temperature of at least 70°C is required (though the manufacturer recommends 90°C,) and once cooled it sets almost instantaneously when the setting temperature is reached, which causes some problems which will be discussed later in this chapter. The gelling temperature of gellan can be modified as it is dependent on the concentration of gellan gum as well as the concentration and type of cations present[193]. A study by Lee et al (2011) showed that for low acyl gellan gum, gelling temperatures from around 32°C to around 67°C could be achieved by varying the gellan gum concentration as well

as cation concentration ($CaCl_2$ was utilised in this study)[189] with increasing cation concentration leading to higher gelling temperatures.

Gellan can be manufactured into many different forms such as tablets, sheet dressings, gels and drops. Additionally, multiple properties of gellan (gel strength, texture, clarity etc.) can be adjusted by varying the type and concentration of salts (cations) or sugars used and also the pH[194]. Gellan is also moisture-retentive and thus is able to provide a moist wound environment which is beneficial to the healing process of the wound by promoting keratinocyte migration[195]. Another useful property of gellan based fluid gels is that it can be formulated to have shear thinning characteristics[196]. Shear thinning is the non-Newtonian behaviour of fluids that when under shear strain, its viscosity decreases. This characteristic will enable gellan based fluid gels to be easily applied, but also avoid dripping and running as it will regain its viscosity immediately after application. Other useful properties of the gel include a good thermal stability capable of withstanding multiple autoclaving cycles and resistance to enzymatic degradation[183].

1.3.3.1 Gellan toxicity studies in literature

Gellan is a widely used as a food thickener and also in eye drops (e.g. Timoptic XE®) and no significant toxic effects have been reported in the literature. The Food and Drug Administration (FDA) has also classified gellan as a safe food additive[197]. Toxicity studies for gellan have mostly been ingestion studies due to gellan's predominant use as a food thickener, no studies on topical (skin) gellan application were found. A study by Anderson et al (1988) showed that ingestion of gellan gum at a high level (175-200mg/kg) caused no adverse dietary or physiological effects in human healthy volunteers and acted as a faecal bulking agent[198]. In an animal studies by Cao et al (2007 & 2009), no cilio-toxicity or mucosal irritation was demonstrated after administration of intra-nasal gellan gel[199, 200].

1.3.3.2 Pharmaceutical use of gellan

The most widely used application of gellan is in ophthalmic formulations for the delivery of drugs such as anti-glaucoma agents such as Timolol maleate[201] and antibiotics[202]. Gellan based eyedrops

have an advantage over traditional eyedrops due to its ability to enhance bio-availability through its in-situ adhesion and gelling properties[202].

Gellan can also been developed to aid oral drug delivery as an excipient[203] or disintegrating agent[204]. The gel form of gellan has also been developed to produce nasal gels.

More recently, injectable gellan systems have also been developed for sustained antibiotic delivery in bone infections[205].

1.4 Scar assessment

In order to accurately assess the efficacy of interventions that alter the formation and severity of pathological scars, reliable and objective scar measurement tools are required. Traditionally, subjective scales such as the Vancouver Scar Scale (VSS, also known as the Burn Scar Index,)[206] and the Patient and Observer Scar Assessment Scale (POSAS)[207] have been used for this purpose as they are free and simple to use. Furthermore, scales such as the POSAS also incorporate a patient rated scale that allows the opinion of patients regarding their own scars to be evaluated and recorded. However these scales are limited by their subjective nature and can be poorly reproducible[208].

The burns research community have in recent years recognised the importance of objective scar measurement tools and an increasing number of studies now utilise both subjective and objective tools in the evaluation of scars.

The majority if not all objective scar measurement devices have been adapted from existing devices used in the aesthetic industry. As such, before these devices are re-purposed for the evaluation of pathological scars, their reliability and validity need to be assessed.

Objective scar measurement device parameters mirror those assessed in the subjective scar scales and the most commonly measured ones are briefly described below:

- **Colour**
  The main measured colour parameters are erythema and pigmentation and are chiefly evaluated by instruments which utilise the reflectance principle and are broadly divided into tristimulus colorimeters (e.g. Labscan XE[209]) which describes colour using the CIE L*a*b* system and devices which use the narrow band spectrometry system (e.g. Mexameter[210]).

- **Pliability**
  The most commonly used devices utilise the principles of torque (e.g. Dermal Torque meter[211]), resistance to suction (e.g. Cutometer[212]) or pressure (e.g. Durometer[213]).

- **Thickness**
  This traditionally could only be measured using biopsies, but advances in ultrasound technology have produced high frequency ultrasound systems (e.g. Dermascan C[214]) which provide high resolution images at the expense of depth of penetration.

1.5. Aims of the study and processes involved in development of a new therapeutic dressing membrane and clinical outcomes

The aims of the study are twofold: to develop an anti-scarring burn scarring burn dressing and to develop a reliable and validated panel of objective scar measurement devices which can be used to investigate the efficacy of the anti-scarring burn dressing.

New therapeutic product development (e.g. drug, biologic, wound dressing) is a long and arduous process which can take up to 10 or more years from the initial identification of the target therapy to commercialisation, although in some cases, accelerated pathways are available where speeding up the availability of drugs or devices that are able to treat serious disease are in the public's best interest.

The common pathway that new drugs or devices go through are listed below[215]:

- **Discovery/Concept:** identification of the target therapy (drug/device) for the treatment of a condition

- **Development:** can be divided into preclinical and clinical studies. Pre-clinical studies assess the potential therapeutic effects and safety of the drug/device in non-human subjects (in-vitro or animal studies,) prior to human studies and include pharmacodynamics, pharmacokinetics, toxicity and efficacy studies. Clinical trials then evaluate the safety and efficacy of the drug/device in humans and can be divided into four phases (I-IV). Phase I

studies investigate the safety and tolerability of the product in humans (usually healthy volunteers) whereas Phase II and III studies investigate the therapeutic efficacy of the product in patients. Phase III studies differ from phase II studies in that they compare the investigated product with the best existing treatment/standard of care and are done in larger numbers of patients (and thus requiring multi-centre trials).

- **Regulatory body review:** Submission of product safety, efficacy and quality data for regulatory review

- **Commercialisation and safety monitoring:** Phase IV of the clinical studies, which is the on-going compliance regulation through safety reports

The anti-scarring burn dressing is currently in the pre-clinical development phase with an early clinical (Phase I) study of the gellan dressing carrier (without decorin).

The outline of the development phase and its associated work packages (WP) provided by the study funders and aims are outlined in Figure 6 along with the associated thesis chapters. The relevant work packages are discussed below:

Hypothesis: Hypertrophic scarring as a result of excessive collagen deposition can be reduced by the administration of decorin via a gellan carrier dressing and that this can be measured reliably utilising a panel of objective scar measurement tools.

- **Work package 2:**

  Aim 1 (Chapter 4):
  To characterise decorin (in terms of cell toxicity) and to investigate its effects on fibroblast collagen production. In the designing of a dressing membrane, several factors need to be considered including the cytotoxicity of the agent (decorin) and its effective dose (to prevent excessive collagen formation,) in order to determine the optimal delivery dose.

  Aim 2 (Chapter 5):
  To characterise the thermal stability of decorin. This is important as the both the therapeutic agent and the carrier may be affected during the manufacturing process, storage and clinical use, particularly as burn theatres are typically run at higher temperatures to prevent hypothermia in patients.

- **Work package 3:**

  Aim 3 (Chapter 6):
  To investigate the dermatological safety of gellan based dressings (sheet and fluid gel). Gellan is an FDA approved food additive but has also been promoted for use by the company in skincare products such as lotions, creams and non-dissolving cosmetic films. Despite this, there are no published studies that investigate the use of gellan in intact or injured skin. The

aim of this work package is thus to investigate the epidermal response of healthy volunteers to gellan.

- **Work package 5:**

  Aim 4 (Chapters 2 & 3):
  To create a panel of burn scar measurement devices/tools that have an acceptable level of reliability for use in a clinical trial investigating the effectiveness of a decorin based dressing in preventing or reducing pathological scarring. In order to determine the efficacy of the anti-scarring properties of the dressing, reliable tools are required to assess scarring severity in patients.

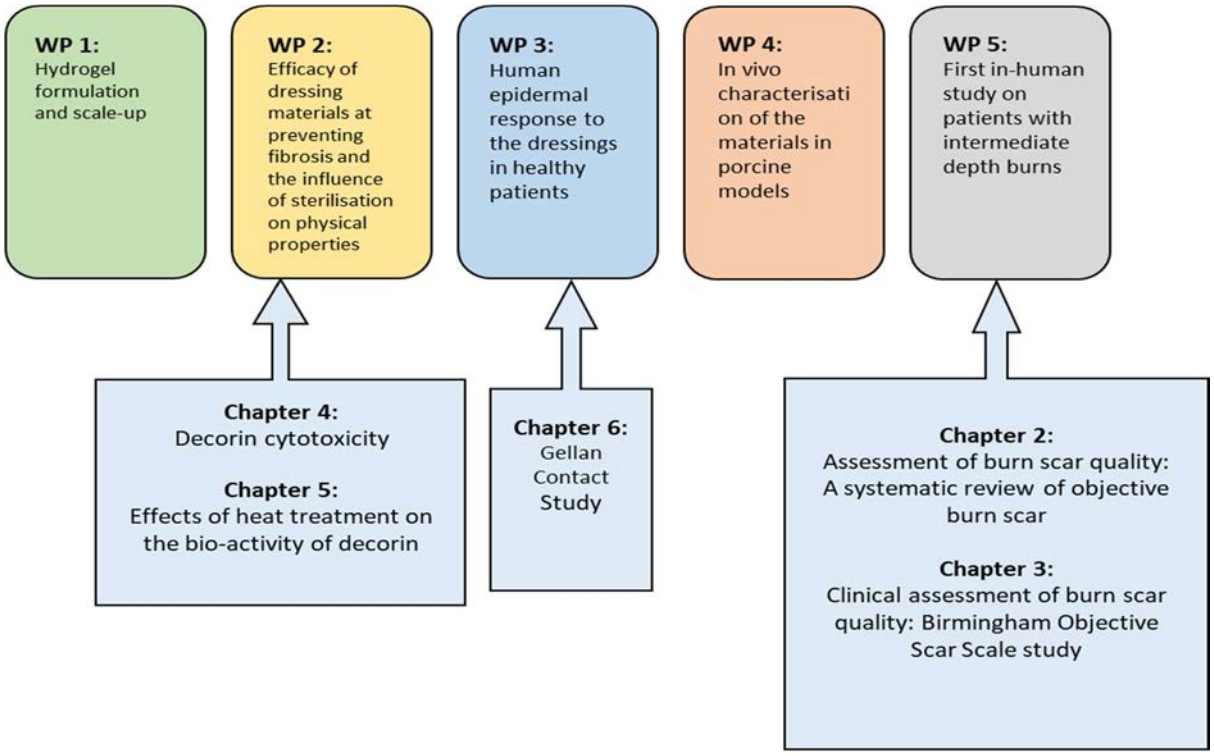

Figure 6: Development phase of the anti-scarring burn dressing, its work packages and the associated thesis chapters.

SECTION 1- SCAR ASSESSMENT

CHAPTER 2

ASSESSMENT OF BURN SCAR QUALITY:

A SYSTEMATIC REVIEW OF OBJECTIVE BURN SCAR

2. Assessment of burn scar quality: A systematic review of objective burn scar measurements

2.1 Background

Burn injury is one of the most common type of traumatic injuries in the world with an estimated incidence of 1.1 per 100,000 population[216] and remains one of the leading causes of deaths, accounting for 5.2 % of 5.1 million deaths due to injuries and violence in 2012[217]. In the last few decades, major advances in burn care have greatly improved survival rates[218] and an increased number of patients are surviving large burns. Non-fatal burns however is a leading cause of morbidity, as many of these patients develop hypertrophic scars that may lead to significant disfigurement and disability (e.g. contractures).In order to assess and track the evolution of scars over time; subjective rating scales have been introduced into clinical practice. These scales in general are free or low cost and require minimal training to utilise. Several such scar scales have been developed and are used widely, including the commonly used Vancouver Scar Scale (VSS) and the Patient and Observer Scar Assessment Scale (POSAS)[207].

However, these scar scales are considered to be subjective and the resulting scores can vary between different assessors (inter-assessor variation)[219], different scar severities[220] and age of the scar[221], and some studies have suggested that more than one rater (sometimes as many as five), and utilising the average, is required in order to produce reliable ratings[221, 222]. The POSAS attempts to improve the method of rating scars by including the patients' perspective; however, patients' perception and subjective evaluation of their scars have been shown to be influenced by depressive symptoms[223]. The physical characteristics of scars further add to the complexity of rating as changes in both the vascularity and pigmentation can occur simultaneously, and scars are also rarely homogenous in both colour and texture, which makes estimation of mean values difficult and inaccurate for a human observer.

Standardised, quantifiable, reliable (reproducible) and valid assessment tools that provide a more objective evaluation of scars are essential for monitoring the changes in scar quality over time and also to determine the effectiveness of scar treatments.

The various objective measures that relate to scar severity can be divided into the following categories:

- **Colour:** erythema and pigmentation contribute significantly to the appearance of a scar.
- **Dimensions:** it includes planimetry (surface area), thickness and volume.
- **Texture:** surface texture or scar roughness has a significant effect on the patient's and observer's opinion of the scar.
- **Biomechanical properties:** it includes pliability and elasticity. Stiffness and hardening of scars are due to increased collagen synthesis and lack of elastin in the dermal layer and can lead to impairment of skin function, especially when the scar is located around joints.
- **Pathophysiological disturbances:** it includes transcutaneous oxygen tension and transepidermal water loss and moisture content.
- **Tissue microstructure:** new non-invasive in vivo imaging techniques analyse the morphological tissue architecture of the scar, providing measurements previously only possible by histopathological analysis of biopsy samples.
- **Pain/sensation:** pain is a commonly measured parameter in many subjective scales however objective methods to measure it are yet to be available. However the measurement of altered sensation may be useful.

2.2 Aims

In this review, we describe and compare the underlying principles and performance of various currently available objective measurement devices in order to inform clinicians and researchers about their clinical utility for scar assessment. In addition, we discuss innovative technologies that may be applicable to burn scar assessment in the near future.

2.3 Methods

2.3.1 Criteria for considering articles for inclusion

Published articles that describe non-invasive burn scar measurements were included in this systematic review. Studies that used scar scales which utilise subjective scoring systems were

excluded, as studies that made histopathological evaluations of scars via biopsies had no potential to be used in vivo (i.e. requiring the use of ex vivo processing and staining). We chose to include studies comparing the outcomes of wound or scar treatments as well as animal studies and in some cases non-burn scars if appropriate, as excluding these studies may prevent us from identifying new or emerging technologies.

2.3.2 Search methods

A computerised literature search (until October 2015) was performed using the web-based Web of Science (http://wok.mimas.ac.uk/; years 1900–2015) and PubMed services (www.ncbi.nlm.nih.gov/pubmed/; years 1950–2015) and utilising the Web of Science Core collection and Medline databases. No language limit was set.

The following search strategies were used:

- (Skin OR derma* OR dermis OR epidermis OR epiderma*) AND (scar OR cicatrix OR fibrosis) AND (objective OR quantitative) AND (burn OR burn$ OR hypertrophic).
- (Skin OR derma* OR dermis OR epidermis OR epiderma*) AND (scar OR cicatrix OR fibrosis) AND (evaluation OR assessment) AND scale
- ((burn$ or burn) and hypertrophy)
- ((burn$ or burn) and (scar or cicatrix))
- ((scar or cicatrix or fibrosis) and hypertrophy)
- ((Objective assess* or objective evaluat* or objective measure* or assess$ instrument or assess$ tool or device or measurement system or objective) adj3 assess$)
- (objective evaluat* or objective measur* or assess$ instrument or assess$ tool or (device or scale or measurement system))
- NOT (uterus or cardio* or neoplasm or cancer or metastas$ or malignancy)

Web of Science core collection results were further refined by the following terms: surgery or dermatology or critical care medicine or emergency medicine or medicine research experimental or computer science interdisciplinary applications or computer science artificial intelligence or imaging science photographic technology or rehabilitation or medical laboratory technology or engineering biomedical or medicine legal or medical informatics or biophysics or anatomy morphology.

This search produced 5062 articles after duplicates (n = 2334) were removed. After filtering by review of titles and abstracts, 140 suitable articles were chosen.

A separate search was also conducted using the PubMed database (www.ncbi.nlm.nih.gov/pubmed) using the following keywords/terms (including MeSH [Medical Subject Headings] terms): skin AND (scar OR cicatrix OR fibrosis) AND (evaluation OR assessment OR assess OR measure OR measurement) AND (objective OR quantitative) AND (burn OR burns OR hypertrophic). A further broader search was conducted using the following keywords and MeSH terms: skin AND (scar OR cicatrix OR fibrosis) AND (evaluation OR assessment) AND scale. No language limit was set. This search retrieved 613 articles, and after filtering by review of titles and abstracts and removal of duplicates, a further 27 articles were included. The reference lists of the selected articles were also searched for suitable studies, and an additional 12 articles were included.

A search of the Cochrane database retrieved no suitable articles.

A grey literature search was performed using the Bielefeld Academic Search Engine (BASE) database with the term “objective measurement of scarring”. This search included books, reports, papers, lectures, theses, reviews, and primary data document types and excluded article, journals, audio, videos, images, maps, software and sheet music document types. This search produced 180 hits (after 50 duplicates removed), and after review, 6 articles were deemed suitable for inclusion into the review.

Full text articles were obtained for the articles where possible, and a further 28 records were removed after evaluating the full text. Articles which were only available in abstract form and had no extractable data were also excluded.

Thus, the total number of articles selected for review was 157. This includes 9 review articles.

The selection process for the eligible articles is outlined in Figure 7 below.

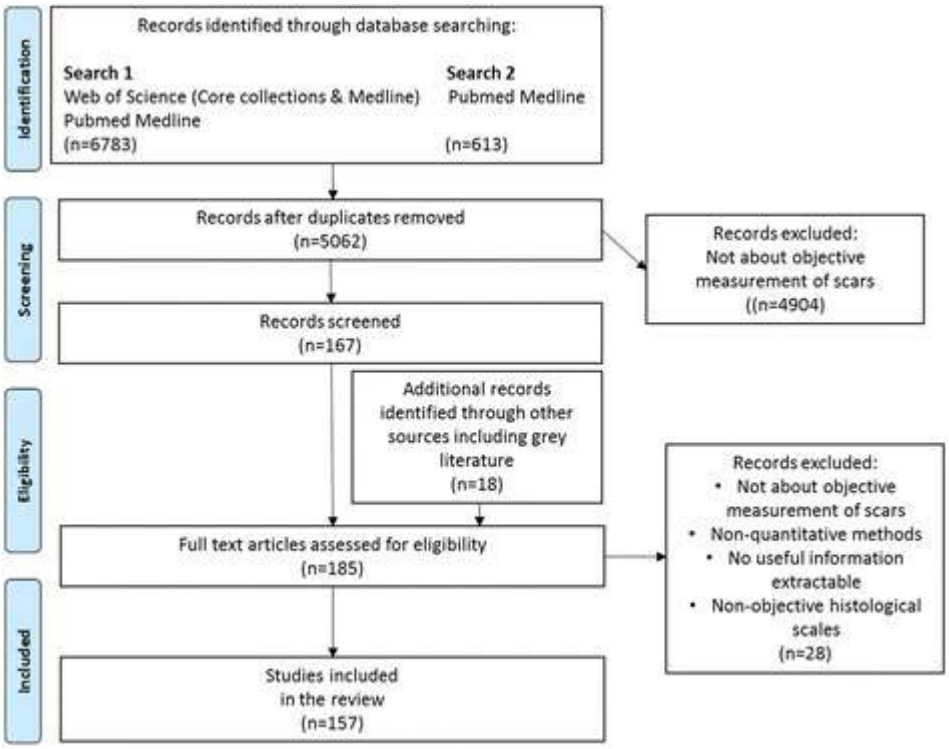

Figure 7: Preferred Reporting Items for Systematic Reviews and Meta-Analyses (PRISMA) flowchart. The search produced 5062 articles and after a process of filtering, a final list of 157 suitable articles was chosen.

2.3.3 Quality assessment

The validity and reproducibility of the devices were evaluated when statistical data were available especially in terms of reproducibility of the assessments. Where available, the additional value of the device compared with subjective scar scales and/or other tools is discussed.

In terms of interpreting the intra-class correlation coefficients (ICC), some guidelines have been provided by Landis and Koch [224] (1977) for Kappa coefficients (which are also reasonable for the ICC) suggesting that:

- Kappa of <0.00 indicates “poor” agreement
- Kappas from 0.00 to 0.20 indicate “slight” agreement
- Kappas from 0.21 to 0.40 indicate “fair” agreement
- Kappas from 0.41 to 0.60 indicate “moderate” agreement
- Kappas from 0.61 to 0.80 indicate “substantial” agreement
- Kappas from 0.81 to 1.00 indicate “almost prefect” agreement

However, it should be noted that these guidelines are subjective.
Feasibility of devices was assessed via the commercial availability, portability and cost of the devices. An economical assessment of the devices based on the literature was not possible due to the lack of such data in the articles; however, several of the companies with commercially available devices were contacted to provide quotes, and although it was not possible to publish the exact prices due to confidentiality issues, the devices are categorised into price ranges (<£5000, £5000–10,000, >£10,000, >£30,000).

2.4 Results

Articles, reviews and editorials that described objective burn scar assessments were retained. These were then classified into six categories based on the assessed variables: (1) colour, (2) scar dimensions (e.g. thickness or height, surface area), (3) texture, (4) biomechanical properties (e.g. elasticity, pliability), (5) physiological disturbances (e.g. hydration) and (6) non-invasive morphological imaging techniques.

2.4.1 Colour

Colour is a major factor that affects the aesthetics of a scar and is mainly composed of two components: melanin (the brown pigment made by activated cutaneous melanocytes) and erythema (the redness that is caused by haemoglobin in the dilated/congested remodelled cutaneous vasculature). Other pigments that localise in scars, such as bile and carotene, may also contribute to the overall appearance of the scar. Colour measurements can be used to gauge the effectiveness of anti-scarring treatments since they reflect abnormal skin architecture/composition[225]. Measurement of the scar colour can be complicated by several factors, such as skin layer thickness, reflection from the skin surface and environmental factors including light and temperature. The measurement of erythema is further influenced by patient-related factors such as activity and positioning of affected areas as such movements may affect the blood circulation and hence the erythema of the skin.

Although visual assessment of colour has been incorporated into various scar scales, it is a subjective evaluation method that provides relative rating systems. Even in normal circumstances, the human

brain cannot accurately quantify colour or its intensity. A famous recent example of this is the "blue and black dress" which shows that human colour discrimination may be affected by the illuminant colours, level of ambient illumination and the background colours of a visual display terminal[226, 227]. Neuropsychiatric conditions have also been shown to affect colour discrimination[228]. In scars, changes in vascularity and pigmentation occur simultaneously and overlap each other which make colour observation and reporting even more difficult for a human observer, e.g. it is difficult to assess the pigmentation of a scar in a highly vascularised scar as the erythema would obscure the increase or lack of pigment. Additionally, as scars often have an uneven colour distribution, human observers cannot easily or accurately provide a mean value for a certain area.

More recently, several objective and reproducible methods of colour evaluation have been developed and they can be broadly classified as follows:

- Reflectance spectroscopy: tristimulus reflectance colorimetry and narrow-band spectrophotometry
- Laser imaging: it measures the microcirculation in the scar which influences the erythema of the scar.
- Computerised analysis of digital photographs: it can include two-dimensional (2D) and three-dimensional (3D) images which are then digitally analysed to quantify colour values.

2.4.1.2 Reflectance spectroscopy

Reflectance spectroscopy is a well-established technique of more than 50 years[221] and currently one of the most commonly used methods for measuring colour. Techniques that utilise reflectance spectroscopy quantitatively measure the colour and intensity of reflected light. For example in Figure 8, when light consisting of red, blue and green is shone upon a surface, if the material absorbs red and green light, then only the blue light is reflected which will make us perceive the material as blue. A biological example is the detection of the oxygenation of haemoglobin. When haemoglobin is illuminated with white light, oxygenated haemoglobin will absorb a higher proportion of blue light

and reflect back red light whereas de-oxygenated haemoglobin absorbs more red light and thus appears bluer. In reality, the process is more complicated as the light that is shone (termed incident light) onto biological tissues can be reflected in many different trajectories, and this scattering also influences our perception of the colour of an object.

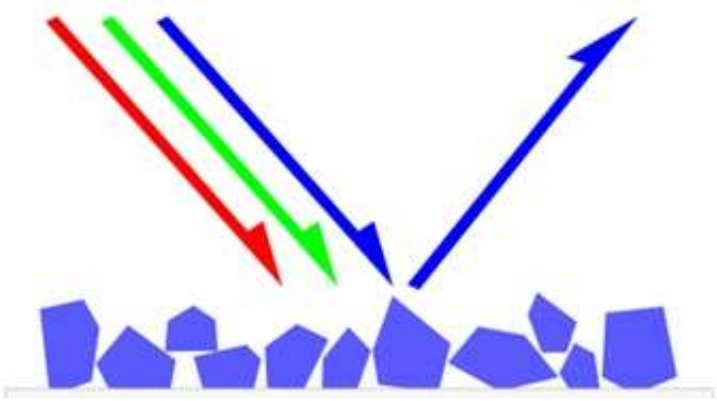

Figure 8: Graphical illustration of the concept of reflectance spectroscopy. If a material absorbs red and green light, then only the blue light is reflected which will make us perceive the material as blue. (Source: http://commons.wikimedia.org/wiki/File:Simple reflectance.svg)

Tristimulus reflectance colorimetry and narrow-band simple reflectance (or spectrophotometry) are both based on the principle of reflectance spectroscopy.

Tristimulus reflectance colorimetry[210] describes colour by three values: L* (clarity, lightness or brightness); a*, the amount of red or green (erythema); and b*, the amount of yellow or blue (pigmentation) (see Figure 9). For example, a white coloured object would have a higher L* value compared to a darker coloured object and a scar that it is redder than normal skin would give a higher a* value than normal skin. Additionally, another approach to quantify colour is by using the saturation or chroma of colour ($C*$) which is a vector magnitude in the chromatic plane calculated from a* and b* values[229, 230].

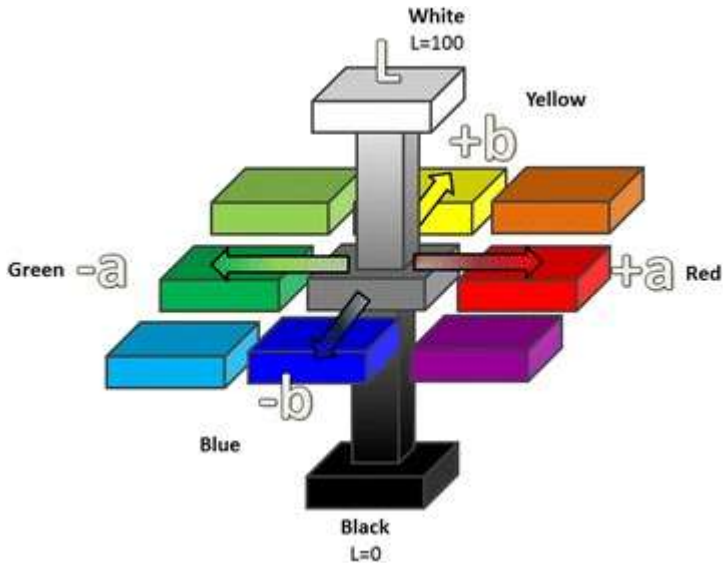

Figure 9**:** Graphical representation of the L*a*b* colour measurement system. Tristimulus reflectance colorimetry181 describes colour by three values: L* (clarity, lightness or brightness); a*, the amount of red or green (erythema); and b*, the amount of yellow or blue (pigmentation) (Source: Kwang Chear Lee).

There are currently several spectrocolorimeter devices that utilise the principle of tristimulus reflectance colorimetry, including the Minolta Chromameter[210, 231, 232] (Minolta Camera Co., Osaka, Japan), the Labscan XE[209] (Hunter Associates Laboratory, Inc., Reston, VA), DSM II Colormeter[233], NF-333[234] (Nippon Denshoku Co. Ltd, Japan), Micro Color (Dr. Bruno Lange GmBH, Dusseldorf, Germany)[235] , X-Rite SP64 Spectrophotometer (X-rite Inc, Michigan, USA)[236] and the Visi-Chroma VC-100 (Biophotonics, Belgium)[235, 237]. Camera systems such as the Eykona 3D camera can also be calibrated to report colour values using the L*a*b* system[238]. However, a drawback of the Eykona 3D camera is that although its cost is low, it currently requires consumables in the form of one-use targets (about £70 for 25 targets) that have to be placed next to the area of interest when taking an image, although there are plans to introduce reusable targets in the coming months according to the company.

A study by Li-Tsang et al[209] (2003) showed that the intra- and inter-rater reliability for the Labscan XE device for hypertrophic scars was satisfactory, with an intra-class correlation coefficient (ICC) ranging from 0.95 to 0.99 for intra-rater reliability, and 0.50 to 0.99 for inter-rater reliability in all the

three colour parameters (L*, a* and b*). A strong positive correlation was also found between VSS scores and the readings obtained from the Labscan XE device. The device that was utilised in the literature was not portable; however, newer portable versions are currently available. A study by Draaijers et al. (2004) showed that the overall evaluations of scar colour with both the Dermaspectrometer and the Minolta Chromameter are more reliable than the visual evaluation and scoring of scar colour carried out by observers using a 10-step score, whereby a score of 1 reflects normal skin and a score of 10 reflects the worst scar imaginable[210]. However, devices that rely solely on tristimulus colorimetery have been shown to have poor correlation scores with patient scar scales when measuring pigmented or hypo-pigmented scars due to the scar scales scoring hyper- and hypo-pigmented scars higher as deviations from normal skin.

Narrow-band spectrophotometry[210] devices on the other hand measures the vascularisation and pigmentation of the scar based on differences in red and green light absorption by haemoglobin and melanin, respectively. The Dermatospectrometer (or the newer version, DSM II Colormeter)[233, 239, 240] (Cortex Technology, Hadsund, Denmark) and Mexameter[233, 241] (Courage + Khazaka, Germany) are examples of a device that uses this principle. In comparison with the Minolta Chromameter and Labscan XE, the Dermaspectrometer is a smaller and hence a more portable device and the use of the erythema and melanin indexes is less complicated to understand and analyse compared to the L*, a* and b* of the Minolta Chromameter. It has also been shown to have a slightly better correlation with clinical scores when compared with the Chromameter[242]. Unfortunately, the Dermatospectrometer has been withdrawn from the market but it has been replaced with a newer model, the DSM II Colormeter. The DSM II Colormeter[233] (Cortex Technology, Denmark) is a small, fully hand-held device that utilises both tristimulus colorimetry and narrow-band spectrophotometry technology and produces reliable readings. It has an improved utility, in terms of cost and assessment time as it utilises one instrument instead of two to obtain both tristimulus colorimetry readings as well as narrow-band spectroscopy readings. The Mexameter also has good intra-observer and inter-observer reliability in scar assessments[233].

Caution however must be used when using erythema to grade the severity of scars. This is because scars can often be very vascular initially but this does not mean that they will become hypertrophic, e.g. in the study by Nedelec et al (2008).[243], the Mexameter was unable to differentiate hypertrophic scars from normal scars as donor sites were very erythematous, but we know that donor sites rarely progress to become hypertrophic scars.

A common disadvantage of all of the aforementioned devices is that they employ a small measuring area, e.g. the measuring area for the Minolta Chromameter is only 3 mm[231] and the other devices range from 5 to 8 mm[221]. Therefore, multiple measurements, especially in larger scars, need to be performed to provide accurate scores, but these increase the risk of observational bias. Additionally, these devices also require contact with the skin which can change the colour if too much pressure is applied. Environmental lighting may also affect the readings obtained, although many of the companies of these devices (e.g. DSM II Colormeter) claim that the flash that is utilised by these devices is strong enough to overcome and compensate for any differences in colour caused by indoor lighting.

2.4.1.3 Large area spectrophotometry

Some investigators have attempted to overcome the problem of small measurement areas by utilising camera systems to allow the imaging of larger areas. Cheon et al (2009 & 2010) utilised digital photographs taken with a digital camera (Nikon D70s, Tokyo, Japan) under the same light source and obtained L*a*b* values for the regions of interest (whole scar lesions when possible) using Adobe Photoshop (Adobe systems Incorporated, San Jose, CA). The test–retest consistency (or intra-rater reliability) of the L*a*b* as determined by the intra-class coefficient ranged from 0.95 to 0.99 and the inter-rater reliability was also good with values ranging from 0.94 to 0.98[244, 245].

Another method of spectral modelling developed by Kaartinen et al (2011) utilised standardised digital imaging (SDI) with computer controlled lighting to quantify colour changes[221, 222]. This system allows a larger area of the skin to be analysed with an only slightly weaker accuracy compared to the

previously mentioned spectroscopy-based systems[246]. This method, however, is yet to become commercially available, but a similar system, Scanoskin (Leniomed Ltd, London, UK), is available. The Scanoskin system utilises polarised light, which has the advantage of blocking the reflectance from the skin which allows better analysis of the epidermal and superficial dermal layers[247]. The system is currently used only to assess burn depth via the imaging of haemoglobin (erythema/vascularisation) and haemosiderin or melanin. Images which are taken (with a modified SLR camera with polarised lenses) are processed by the provided software which splits them into separate erythema and melanin components. Quantification of erythema and pigmentation (melanin) has to be performed on the exported images using software such as ImageJ[248-250].

The evidence for using objective measures in measuring colour is encouraging and is based on a relatively small number of studies, and more research is needed[251].

2.4.1.4 Spectrophotometric intra-cutaneous analysis (SIA)

Analysis of colour information purely in the visible spectrum is insufficient to provide information relating to a lesion's deeper structures, and it was this realisation that prompted research at the University of Birmingham to extend the spectrum of light used into the infrared region (700–1000 nm). Spectrophotometric intra-cutaneous analysis via the clinical device, SIAscope, utilises a probe (12 × 12 mm or 24 × 24 mm) that utilises radiation ranging from 400–1000 nm and produces 8 narrow-band spectrally filtered images of the skin which are then processed by software algorithms and allows the visualisation and quantification of melanin, collagen and blood[252]. Although developed for diagnosing skin cancers, it can and has been used to monitor the changes in scar tissue in response to treatment[253].

2.4.1.5 Computerised analysis of digital photographs

Digital photographs can be taken with any standard digital camera, e.g. the Nikon 8400[232]. Photos are then downloaded for analysis by proprietary software packages such as KS400 (Kontron Electronic GMB, Carl Zeiss Micro-Imaging, Inc., Thornwood, New York, United States of America)[254] or the freely available ImageJ. One study utilised an artificial neural network to perform chromatic

analysis of the digital image of a burn scar[255]. Colour measurements using ImageJ have been shown to be equivalent to those obtained using a colorimeter (Chromameter, Konica-Minolta)[232]. Several studies have attempted to improve the objectivity of photograph analysis of scars by standardising factors such as distance and lighting[232] or using computerised image capturing systems[256-258]. However, even this method fails to allow scars to be compared objectively as humans vary in terms of how we set the measurement criteria for and analyse colour[241, 259] and the photographs have been shown to have limited utility when assessed using computer-based subjective scales[260]. Improved computer programmes may overcome the limitations of the human brain and provide objective analysis of the digital photographs. However, computer programmes cannot properly "see" colour and thus have to convert colour information into digital data, thereby losing valuable information.

Computer programmes utilise two methods to analyse colour. The Hue-Saturation-Value (HSV) method analyses colour by separating it into three main components: hue (dominant wavelength), saturation (amount of white) and value (amount of black). The other method utilises colour models of which there are two main ones: the Red, Green and Blue (RGB) model and the Cyan, Magenta, Yellow and Black (CMYK) model. Measurement techniques using other systems such as the L*a*b* system have also been described[261].

To remove the influence of light and camera settings, generally a card carrying standard colours (e.g. Pantone colour chart [Pantone Inc, USA][229], Macbeth Digital Colorchecker SG colour chart [Munsell Colour services Laboratory, X-Rite Inc, Michigan, USA][238, 257]) is recommended to be placed beside the scar being photographed so that every photo taken would include areas of known colour properties, allowing an objective colour evaluation[229]. Table 1 summarises the colour measurement devices in terms of parameter measured, reliability, correlation with clinical score and cost.

Table 1: Comparison of colour measurement devices in terms of parameter measured, reliability, correlation with clinical score and cost.

Device	Company	Parameter	Intra-rater Reliability	Inter-rater reliability	Correlation with clinical score	Cost	Portability	References
Computerised colour analysis	Sony Hi-8 Handycam CCD-TR 705E video camera recorder and Adobe Photoshop	Hue, saturation, value	No data	No data	VSS Vascularity score significantly correlated with hue (r = 0.311) and saturation (r = 0.35) (p < 0.051), index with hue and saturation combined correlated even better (r = 0.42).	£5000–10,000	Yes	Davey et al. 1999[229]
Computerised colour analysis	Nikon D70 camera and Adobe Photoshop	Tristimulus colorimetry (L*a*b*)	0.95–0.99	0.94–0.95	L* and a* values are more important than b* values in distinguishing colour features between normal skin and scars.	No data	Yes	Cheon et al. 2010[245]
Labscan XE (non-portable version)	Hunterlab	Tristimulus colorimetry (L*a*b*), chroma and hue.	Good (0.95–0.99)	Acceptable to good (0.50–0.99, outlier low value of 0.50 for a* [ranged from 0.01 to 0.77])	L*, a*, b* and hue had moderate to strong correlation with VSS pigmentation and vascularity scores. Chroma had low correlation with pigmentation and vascularity (r = −0.40 and −0.17)	>£10,000	Poor	Li-Tsang et al. 2003[209]
Labscan XE (portable version)	Hunterlab	Tristimulus colorimetry (L*a*b*)	No data	No data	No data	£5000–10,000	Yes	Li-Tsang et al. 2005[262]
Chromameter	Konica-Minolta	Tristimulus colorimetry (L*a*b*)	Acceptable (0.73–0.89)	Good (0.91–0.97)	Unable to differentiate between hypo- and hyper-pigmented scars and normal and 'red' skin (On Seattle, Hamilton and Vancouver scar scales)	£5000–10,000	Yes	Draaijers et al. 2004[210], Oliveira et al. 2005[242]
Eykona 3D camera	Fuel 3D	Tristimulus colorimetry (L*a*b*)	No data	No data	Good correlation (Manchester scar scale)	<£5000	Yes	Hallam et al 2013[238]
Colorimeter	Courage + Khazaka	Tristimulus colorimetry (L*a*b*) and ITA (Individual Typology Angle)	No data	Good (0.91–98)	No data	£5000–10,000 (including cost of hub)	Yes	van der Wal et al[233]

(Table 1 continues on next page)

Mexameter	Courage + Khazaka	Narrow-band spectrophotometry (melanin and erythema)	Good for melanin (0.89–0.97) and acceptable for erythema (0.74–0.90)	Good for melanin (0.95) and erythema (0.82–0.85)	No data	<£5000	Yes	Nedelec et al. 2008 (I)[243], Nedelec et al. 2008 (II)[263], van der Wal et al. 2013[233].
Dermaspectrometer/DSM II Colorimeter	Cortex	Both tristimulus colorimetry and narrow-band spectrophotometry	Erythema: 0.29–0.94 Melanin: 0.72–0.87 L*a*b*: no data.	Erythema: 0.68–0.91 Melanin: 0.91–0.94 L*a*b*: no data.	Erythema: Moderate but significant $r = 0.50$ (<0.001) Melanin: weak but significant $r = 0.32$ (0.02)–0.63 (<0.001)	<£5000	Yes	Gankande et al. 2014[220], Gankande et al 2015[264], van der Wal et al. 2013[233], Oliveira et al. 2005[242].
Standardised digital imaging (SDI) + Spectral modelling (SpM)	Custom made	Estimated concentration change of haemoglobin and melanin	Good for haemoglobin (0.875) and melanin (0.886)	Good for haemoglobin (0.955) and melanin (0.959)	Acceptable correlation with POSAS (0.63 for haemoglobin, 0.60 for melanin) and VSS (0.74 for haemoglobin, 0.53 for melanin)	<£5000	Yes	Kaartinen et al. 2011[221, 222].
Dermoscopy	Hong Kong Productivity Council	RGB values: lightness and redness	Redness: 0.980 Lightness: 0.965	Redness: 0.93 Lightness: 0.871	Strong correlation between the VSS scores of vascularity and the RGB values of redness obtained from the dermoscope ($r = 0.625$, $p < 0.01$). Strong correlation also found between transformed VSS scores of pigmentation and the lightness of the dermoscope pictures when vascularity was blanched out (i.e. when measuring pure pigmentation) ($r = 0.783$, $p < 0.01$).	No data	Yes	Wei et al. 2015[265]

2.4.2 Laser imaging

The amount of haemoglobin or erythema present in a scar can be measured indirectly via laser imaging[266, 267] that measures the blood flow in a scar. Immature scars show a significantly increased blood flow due to their higher vascularity compared to mature scars. Increased microcirculatory blood flow (as measured by Laser Doppler Flowmetry (LDF)) has also been shown to be a potential indicator for the occurrence of hypertrophic scarring[268]. Hypertrophic scars will typically generate readings that are two to three times greater than that made in normal skin[32, 267, 269] and four times greater than that in a non-hypertrophic scar[267]. Laser-based methods have the advantage of being fast, reproducible and having a good correlation with the VSS; however, they are subject to structural changes in the skin and environmental and body temperature fluctuations[270-272].

Laser-based methods can be divided into three techniques: LDF, Laser Doppler Imaging (LDI) and Laser Speckle Imaging (LSI)/Laser Speckle Perfusion Imaging (LSPI). With the older Laser Doppler Flowmeter, the fibre optic probe is in contact with the tissue surface and is a single-point measure[266, 273]. Laser Doppler Flowmeter[32, 242, 274, 275] systems, such as the DRT4[269] (Moor instruments, Devon, UK) or the LaserfloBPM[276] (Vasamedics Corp, St Paul, Minnesota, USA), the fibre optic probe is in contact with the tissue surface and provides a single-point measure of an indirect evaluation of scar colour by measuring the cutaneous bloodflow present in a scar[266, 273]. LDF systems are more limited compared to the other laser-based methods (see below) as they measure flow within a small area and, thus, are unsuitable for use with larger, heterogeneous scars.

In contrast, Laser Doppler Imaging (LDI) devices, such as the Lisca PIM1.0 imager (Lisca Development AB, Linköping, Sweden) and The Moor LDI (Moor Instruments, Devon, UK)[266], utilise a laser beam to scan several points across a tissue surface and generates a 2D colour-coded image that is correlated to the blood flow[266]. They are primarily used for burn depth assessment but have been utilised for scar evaluation[266, 277]. The method is, however, hampered by long measurement times and low resolution[273]. LSI and LSPI are alternative perfusion monitoring techniques that generate rapid, high-resolution images of tissue. As red blood cells move during circulation, dynamic interference

patterns that change with time are created. Blood flow maps can then be created from the coherent light that is reflected from stationary tissue, generating a high contrasted speckle pattern that remains static in time. As indicated previously, high measurements reflect high blood flow and immature/hypertrophic scars. LSI devices compare favourably with the more established LDI instruments, but offer advantages in terms of a faster scan time, higher resolutions and the ability to zoom in with increased resolution of a smaller field of view, a feature that is not possible with LDI[273, 278].

A major disadvantage common to all laser imaging systems are that they are not very portable (with the exception of a new commercially available laser speckle imaging device developed by Moor instruments[279]) due to their size and are often very expensive, with costs of >£30,000.

Table 2 summarises the comparison of laser devices in terms of parameter measured, reliability, correlation with clinical score and cost.

Table 2: Comparison of laser devices in terms of parameter measured, reliability, correlation with clinical score and cost.

Device	Company	Parameter	Intra-rater reliability	Inter-rater reliability	Correlation with clinical score	Cost	Portability	References
Laser Doppler Flowmeter	Moor	Blood flow	No data	No data	LDF showed significant difference in blood flow within hypertrophic and keloid scars and normal skin (2.6–2.8-fold higher).	>£30,000	Poor	Clark et al. 1996[275], Timar-Banu et al. 2001[269].
Laser Doppler Imaging	Lisca, Moor	Blood flow (red and near infrared wavelengths)	No data	No data	Correlations with clinically assessed grades (VSS) of pigment, vascularity, pliability, and height ranged from $r^2 = 0.63$ to 0.95.	>£30,000	Poor	Stewart et al. 2005[278], Bray et al. 2003[266].
Laser Speckle Perfusion Imaging	Moor	Blood flow	No data	No data	Correlations with clinically assessed grades (VSS) of pigment, vascularity, pliability, and height ranged from $r^2 = 0.73$ to 0.94.	>£30,000	Poor	Stewart et al. 2005[278]

2.4.3 Thermographic analysis of burn scars

Thermographic cameras detect radiation in the long-infrared range of the electromagnetic spectrum (9–14 μm) and can be used to produce images or videos of that radiation. Thermography can be divided into passive (where the object can be imaged directly as it has a higher or lower temperature than the background) and active thermography (where an energy source is required to produce a thermal contrast between the imaged object and the background). Several studies have looked at using thermography to assess the depth of burn wounds[250, 280-282].

Our literature search however has only been able to identify one small study done in 1985 (n = 12) which utilised thermographic analysis of the scar temperature in an attempt to differentiate hypertrophic and non-hypertrophic scars[283]. No relationship between scar temperature and hypertrophic scar formation was found.

A more recent case report by Horta et al.[284] (2015) which utilised a thermography camera (FLIR SC7000 thermography camera; FLIR Systems, Wilsonville, OR, USA) showed that factors such as muscle activity or the lack of mucosa, cartilage and bone can influence the thermographic reading of scars rather than the degree of hypertrophy itself. This further complicates the use of thermography to objectively quantify scars.

2.4.4 Scar dimensions

2.4.4.1 Surface area and volume

Planimetry is the measure of the surface area of a scar and, when done over time, can be used to assess the contraction or expansion of a scar.

The most basic method of planimetry, that does not require specialist equipment or trained personnel, is the linear method where the maximum length and width of the wound is measured directly on the patient and the surface area is then calculated by multiplying the maximum length and width. As can be expected, this technique is inaccurate as scars are rarely rectangular or square

in shape and will produce results that are significantly different from those obtained with tracing and photography methods[285].

The second method involves the tracing of scar margins either on sheets of paper, clear plastic film or any transparent non-stretchable material[258, 286]. The surface area traced on these sheets can then be calculated by outlining wound margin with the tip of a planimeter (Koizuni Sokk Manufacturing Ltd., Nagoaka-shi, Japan)[285] or by digitising the tracings on these sheets and using software such as NIS-Elements (Nikon, Amstelveen, The Netherlands)[240] , ImageJ[287] or Digimizer software[288] to calculate the surface area. Dedicated systems have also been developed such as the Visitrak (Smith & Nephew) which have been shown to have high intra- and inter-rater reliability and high validity in the measurement of the surface area of ulcers[289] although the maximum size of the area that can be measured at a time is limited by the disposable tracing grid used (14 cm × 14 cm).

The third method uses digital photography combined with image analysing programmes such as ImageJ, Image Tool (C.D. Wilcox and colleagues, San Antonio, TX, USA)[242] or Adobe Photoshop (Adobe Systems Inc., San Jose, California, USA)[290] to measure the surface area. A significant problem with 2D photography is that it is subject to parallax errors and projecting a three-dimensional object onto a two-dimensional image. Due to this, the 2D surface area (or planimetric area) calculated does not take into account the wound surface topography and will nearly always underestimate the true three-dimensional surface area (see Figure 10).

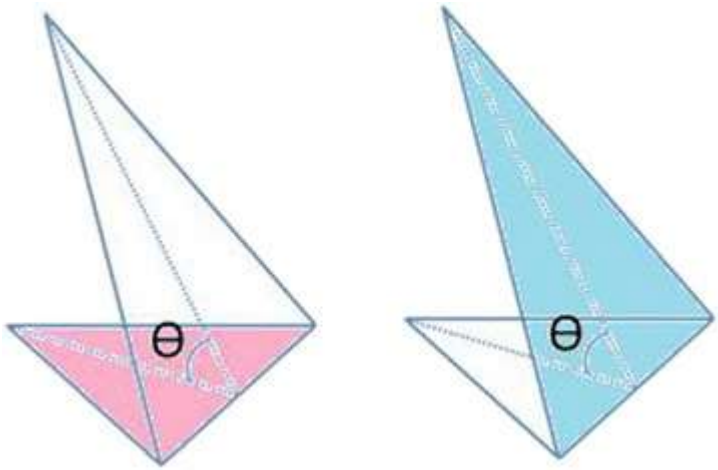

Figure 10: Comparison of 2D and 3D areas. The 2D or planimetric area (in pink) is always smaller than the 3D area (in blue). (Source: Kwang Chear Lee)

With smaller scars, this error would be small but will increase as the size increases. A study by van Zuijlen et al. (2004) compared the direct and indirect (through 2D photography) tracing methods[290]. It found that both techniques were reliable ($r \geq 0.82$, $p < .001$) for surface lesions with a scar surface area of 25 cm^2, but planimetry by photography was superior to planimetry by direct tracing in respect to inter-observer reliability for surface lesions of 50 and 75 cm^2, with increasing scar size resulting in decreasing inter-observer reliability. However, planimetry by direct tracing was more accurate on curved surfaces (e.g. forearm), with a statistically significant reduction of the surface area obtained when compared to results with planimetry after photography. The use of photography[242, 256] to measure surface area, although useful, is subject to variance caused by lighting conditions, distance and camera settings and does not provide any information on volume.

Three-dimensional (3D) measurement systems can overcome the limitation of 2D photograph, and in addition to surface area measurements, the 3D camera systems are also able to measure the volume of scars much more quickly and easily compared to traditional moulage and moulding methods[291].

A 3D image can be achieved via various methods. A method that is commonly used in the medical is stereo-photogrammetry. These systems are non-contact and involve taking two or more pictures using either one or multiple cameras which can be on the same device (e.g. Eykona wound measurement system, Fuel 3D, UK[238]) or separate devices (e.g. 3D MD static systems, 3dMD, USA[292]). Some authors have even developed their own systems with standard cameras (e.g. Stereoimage optical topometer (Korea University, Seoul, South Korea) with PC vision plus (AES, Sydney, Australia))[293]. Other devices utilise mirrors to achieve a similar effect for, e.g. LifeViz I, II, Mini or Micro (Quantificare S.A., Sophia Antipolis, France)[294, 295] and Vectra H1 3D imaging system (Canfield Scientific Inc, Fairfield, NJ, USA)[296-299]. Other systems utilise the projection of a complex speckled pattern in combination with a colour camera to produce the 3D images[300].

These software are able to provide information about the surface area[301] and tissue volume above the skin[302] (including correction for curved surfaces) as well as geometry, texture and, as mentioned above, the colour of scars for which the performance of the Eykona device has been shown to compare favourably with the subjective Manchester Scar Scale (MSS)[238]. These devices share a few common drawbacks. Firstly, none of them have been validated in scar studies, but their ability to measure the area[302-304] and volume of wounds and tissue (e.g. breasts[301]) has been shown in other non-scar related studies. Additionally, the maximum area that can be imaged is limited to the size of about an A4 size sheet of paper which is not ideal for large burns scars. Furthermore, although stitching of images is possible, this really only applies to the face as it is easy to identify anchor points such as the eyes and nose, but to do so for other highly curved surfaces such as the forearm or the whole body would be technically challenging and time consuming and requires high-end hardware and thus a true 360° view would not be easily possible[299]. Hairy areas of the body can also pose a problem[299].

The Lifeviz and Vectra H1 systems have an advantage over the Eykona in that they have adjustable light-beam pointers to aid positioning and do not require one-use disposable targets which the

Eykona system does but they are also significantly more expensive. Furthermore, the Eykona is no longer being developed by the company and has not been updated recently, thus its resolution is significantly lower (250 micron sampling via two 5 MP sensors)[305] compared to the Lifeviz Mini (13.5–24 MP, 0.5–2 mm geometry resolution)[306] or Vectra H1 cameras (18 MP, 0.8 mm geometry resolution)[307].

More recently, light field or plenoptic technology has been introduced. Cameras utilising this technology (Raytrix 3D camera systems, Raytrix, Germany[308]) capture information about the intensity and also direction of the light rays utilising an array of micro-lenses[308]. The images or data are then processed and merged using dedicated image analysis software into a single 3D image. Additionally, other commonly used 3D imaging techniques include structured light scanner systems (or coherence scanning interferometery) such as the Artec[309] (Artec Group, United States of America/Luxemborg/Russia) and ATOS series of scanners[310], and laser scanning devices such as the Minolta Vivid 900 or 910 3D linear laser scanner (Konica-Minolta, Osaka, Japan)[311, 312]. Whole body scanners such as the Cyberware Whole Body Color 3D Scanner (Model WBX, Cyberware Inc, Monterey, California)[313] are also available. These other systems have the ability to scan much larger areas (up to the size of a car with some systems) compared to the Eykona, Lifeviz and Vectra; however, they have not been specifically manufactured or optimised for medical use. For example with the Artec Eva system, the software supplied is able to calculate the surface area and volume of an object on a flat surface but not on curved surfaces. Specialised 3D analysis software such as Rapidform (Inus technology, Seoul, South Korea)[312] is required to measure and quantify surface area and volume information obtained from these scans. The authors are not aware of any published studies that have validated the surface area and volume measurements produced by these devices or software.

A different approach to calculating the surface area of scars is through the use of a combination of 2D photography and 3D models. The Burncase 3D (RISC Software GmbH, Austria) software has been

developed for the estimation of burn surface areas primarily, but it theoretically can be adapted to measure the surface area of scars. With the Burncase 3D programme, 2D photographs of the lesions are superimposed onto a 3D model that can be adjusted according to the height, weight, age and gender of the patient. The outline of the lesion is then traced onto the 3D model from the photographs (which can be multiple and is aided by an automated alignment algorithm that uses corresponding landmarks to allow quick matching[314]) and the software then estimates the surface area. The areas can also be classified into different categories if needed (e.g. normal and hypertrophic scar areas) and thus useful to track the progression of the wounds from time of burn through to scar formation. As it uses standardised 3D models to estimate surface area, much work is still required to validate the accuracy and precision especially in small children (currently in progress[315, 316]) and obese patients[314]. In a study which utilised mannequins, the inter-class correlation between the single raters of the mean percentage of artificially created burn areas was 0.988 with relative underestimations of burn wound areas of 0.4 % in the child mannequin, and overestimations of 2.8 and 1.5 % for the female and male mannequins when compared to areas as measured with 2D planimetry imaging[316].

Table 3 below summarises the comparison of 3D measurement devices in terms of parameter measured, reliability, correlation with clinical score and cost.

Table 3: Comparison of 3D measurement devices in terms of parameter measured, reliability, correlation with clinical score and cost.

Device	Company	Parameter	Intra-rater Reliability	Inter-rater reliability	Correlation with clinical score	Cost	Portability	References
Eykona 3D camera	Fuel 3D	Surface area and volume	Intra-operator variability: area: 0.9 %; volume: 4.0 %	Intra-operator variability: area: 1.7 %; volume: 4.0 %	No data	<£5000 for the camera unit. ~£3 for each disposable target but device can now be configured to use reusable targets.	Yes	Paterson et al. (Eykona Medical Imaging FAQ)[305]
Lifeviz I, II, Micro	Quantificare	Surface area and volume	No data	Surface area: ICC = 0.99 (Coefficient of variation 5.9–6.8 %) Volume: no data	Surface area: Excellent level of agreement with Visitrak (ICC 0.96, 95 % CI 0.93, 0.97); however greater level of variability in larger wounds especially circumferential wounds. Volume: r^2 = 0.9678 when correlated with actual volumes of model scars	£10,000–£15,000	Yes	Lumenta et al. 2011[295], Stekelenburg et al. 2013[294].
Vectra H1	Canfield Imaging Systems Inc.	Surface area and volume	No data	No data	No data	£10,000–£15,000	Yes	Tzou et al. 2014[317], Urbanova et al. 2015[299].
Artec Eva	Artec	Surface area and volume	No data	No data	No data	<£10,000 (depends on package)	Yes	N/A
Minolta Vivid 910 3D linear laser scanner	Konica-Minolta	Surface area and volume	No data	No data	No data	>£15,000	Yes	Taylor et al. 2007[312]
Moulding (positive–negative moulage)	N/a	Volume	ICC = 0.921–0.995	ICC = 0.759–0.977	No data	Dependent on moulding material and measurement techniques used	Yes	Berman et al. 2015[291]

2.4.5 Thickness

The accuracy of subjective estimation of scar thickness has been shown to be quite low, 67 % (when measured against ultrasound measured thickness)[318] and thus unreliable.

Objective thickness or height of a scar can be evaluated by measurement by 3D photography (see above) or the use of negative–positive moulage[319]. A negative–positive moulage is performed by firstly making a negative impression cast (negative moulage) of the scar using materials such as alginate, silicon, siloxane[276, 291], dental impression material[320] or plaster of Paris. A positive impression cast (positive moulage) is then made by pouring a material that will harden (e.g. plaster of Paris, wax) into the negative moulage. Once hardened, this positive moulage can then be measured. These techniques have some limitations and are inaccurate as the portion of the scar below the surface of the skin is not included in the measurement[321].

This limitation can be overcome by using high-frequency (5–20 MHz) ultrasound systems such as the Tissue Ultrasound Palpation System (TUPS; Biomedical Ultrasonic Solutions, Hong Kong)[262, 322-324], the Dermascan C[243, 263, 269, 325] (Cortex, Hadsund, Denmark) devices, Acuson Sequoia 512[326] (Siemens, Germany; highest frequency probe available is 10 MHz), HDI 5000 (Philips, Amsterdam, Netherlands)[327], and the Dermcup 2020 (Atys Medica, Soucieu-en-Jarret, France)[328]. High-frequency ultrasound systems have previously been used in many dermatological applications[329].

Ultrasound skin imaging is performed by firing an acoustic pulse into the skin and measuring the acoustic response from the skin which is picked up by an ultrasound transducer. The signals are then processed, and a cross-sectional image is produced which represents an intensity/amplitude analysis of these returned signals. Areas with small changes in density between structures such as scar tissue and fat will produce a low reflection and be visualised as dark colours, whereas areas with significant changes in density between structures (e.g. healthy dermis) will be visualised as bright areas (Figure 11).

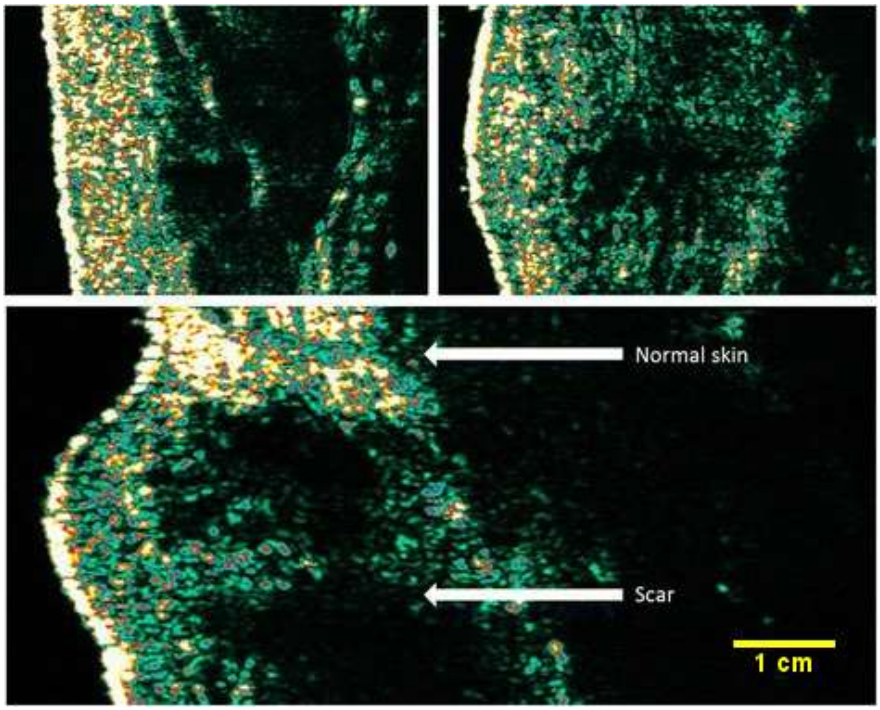

Figure 11: High-frequency ultrasound image of normal and scarred skin. High frequency ultrasound image of Normal skin (top left, site: forearm). High-frequency ultrasound image of hypertrophic scar (top right, site: shoulder). High-frequency ultrasound image of normal skin (top) and adjacent scar tissue (bottom) which shows that normal skin has a higher ultrasound intensity compared to scar tissue. (Source: Kwang Chear Lee)

An advantage of ultrasound systems are that they allow real-time measurement on changes of scar thickness upon pressure loading[330]. Additionally, high-frequency ultrasound systems will also allow the identification of aberrant structures within the scars which may affect treatment[331].

The frequency of the ultrasound determines the resolution and penetrance of the measurement. A low frequency will allow deeper penetration but lower resolution images; whereas a higher frequency will have a shallower penetrance but produce higher resolution images (Figure 12). High-frequency ultrasound systems utilise a frequency above 18 MHz to obtain images of the skin structure with acceptable resolution. In earlier studies, 7.5-MHz probes have been used to measure and track the change in thickness of healing burn scars[321, 332]. These lower frequency systems allow evaluation of deeper tissues (penetration of >15 mm) but have a low resolution of 2–3 mm which may not be sufficient for the evaluation of superficial skin structures[333]. More recently, higher frequency ultrasound probes (20 MHz) have been used to allow more detailed images of the

structures of the skin to be visualised, producing higher resolutions of at least 50 µm[214, 333, 334]. Probes with frequencies below 50 MHz are advised as systems with higher frequencies and will not be able to penetrate to the average depth of hypertrophic scars which is around 4–5 mm.

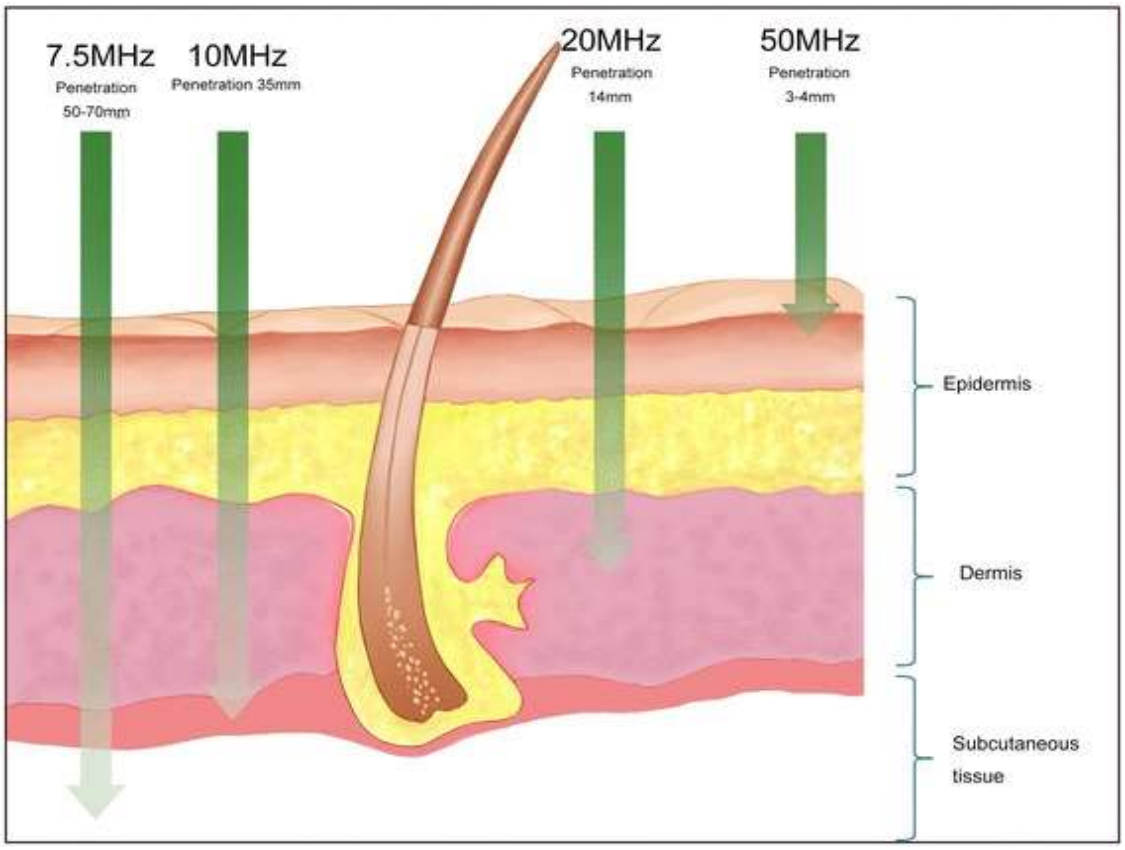

Figure 12: Different frequencies of ultrasounds and their penetrance into the skin. A low frequency will allow deeper penetration but lower resolution images; whereas a higher frequency will have a shallower penetrance but produce higher resolution images.
(Source: Kwang Chear Lee, adapted from image from http://www.eotech.fr/Fiches/produits/107_DUB_Brochure_English_DB10_2012_O.pdf)

It is advisable to always check with the manufacturer the actual penetrance of the systems as cheaper portable ultrasound systems (e.g. Dermalab USB Ultrasound, Cortex, Hadsund, Denmark) only penetrate a maximum of 3.4 mm despite being a 20-MHz system[220].

These high-frequency ultrasound devices both show good inter-observer reliability and moderately correlate with the modified VSS[335] (modified version of the Vancouver Scar Scale by Nedelec et al. [2008]), with the Dermascan C system having the better correlation of the two (0.41–0.50 versus

0.34). It has to be noted that the VSS measures clinical scar thickness (i.e. the thickness of the scar that is above the surface of the skin), whereas the two ultrasound systems measure histological thickness (i.e. the whole thickness of the scar above and below the surface of the skin). The Dermascan system would thus be preferred, although it is more expensive than the TUPS (however at the time of writing, there was no method to purchase the TUPS from their website). Other ultrasound systems that are commercially available include the Acuson Sequoia 512 (Siemens, Germany)[326], Episcan (Longport, USA)[336, 337] and the DUB®SkinScanner (EOTech, France)[338], although at present there are no published studies that have utilised these for scar measurement.

Ultrasound systems that can capture a 3D image of a scar have now become commercially available, albeit only from one company (Cortex, Hadsund, Denmark). However, this system has not been trialled on scars, is limited to a small measurement area (22 × 22 mm) and costs significantly more compared to the 2D system (Table 4).

A summary of the different ultrasound systems is given in Table 4.

Table 4: Comparison of ultrasound devices in terms of parameter measured, reliability, correlation with clinical score and cost.

Device	Company	Parameter	Intra-rater reliability	Inter-rater reliability	Correlation with clinical score	Cost	Portability	References
Dermascan C (2D)	Cortex	Thickness (2D)	ICC = 0.91–0.93	ICC = 0.90–0.91	Modified VSS and ultrasound thickness: Spearman's r = 0.41–0.50	£15,000–20,000	Yes	Nedelec et al. 2008[243, 263]
Dermalab USB (2D)	Cortex	Thickness (2D)	ICC = 0.92–0.97	ICC = 0.86–0.98	No data	<£10,000	Yes	Gankande et al. 2014[220]
Dermascan C (3D)	Cortex	Thickness (3D)	No data	No data	No data	£30,000–40,000	Yes	N/a
Tissue ultrasound palpation system	Biomedical Ultrasonic Solutions	Thickness (2D)	ICC = 0.98	ICC = 0.84	Spearman Correlation of 0.42 between VSS thickness score and TUPS measurement ($p < 0.01$), and r = 0.34 ($p < 0.01$) between VSS total score and TUPS.	Not currently commercially available.	Yes	Lau et al. 2005[339]

2.4.6 Texture

2.4.6.1 Skin topography

Scar roughness has a significant effect on the patient's and observer's opinion of the scar[207]. Indirect methods of measuring skin topography that involve creating a negative replica of the skin using materials such as polymers (e.g. Silflo silicon polymer; Flexico Developments Ltd., Hertfordshire, UK[340]) and then further analysing this with devices (e.g. mechanical, optical, laser or interference fringe projection profilometry[340-342]), although accurate can be very time consuming and not appropriate for clinical use[343]. Transparency profilometry (using the Visiometer; Courage + Khazaka, Germany) uses the Silflo silicon polymer but analysis is much easier and quicker[344, 345]. However, these indirect measurement techniques have been clinimetrically evaluated[340].

The Phaseshift Rapid In Vivo Measurement Of the Skin[346] (PRIMOS; Omniscan, GFMesstechnik GmbH; Germany) and the Visioscan VC 98 (Courage + Khazaka, Germany) are the only devices currently on the market that can be used to measure skin topography directly, but only the PRIMOS system has published studies in scars.

Three parameters were used for the evaluation of the PRIMOS system by Bloemen et al[346] (2011). These were the peak count (PC, number of peaks per unit length), arithmetic mean of surface area roughness (Sa, in micrometres) and the mean of five highest peaks and five deepest valleys form entire measurement (Sz, in millimetres).

The PRIMOS has been shown to have excellent intra-observer and inter-observer reliability on both normal skin and scars and a high correlation with the relief score of the Patient and Observer Scar Assessment Scale (POSAS) on scar (The relief score in the POSAS questionnaire is the rating given by patients and clinicians on the surface irregularity of their scar compared to normal skin).

An added advantage of the PRIMOS system is that it can also be used to measure scar height[347].

The Visioscan VC 98 is a UVA-light video camera with high resolution that utilises the Surface Evaluation for Living Skin (SELS) method to evaluate the roughness of skin[348]. This method analyses

the grey level distribution of the image captures and allows the calculation of four clinical parameters to quantitatively and qualitatively describe the skin surface as an index: skin smoothness (Sesm), skin roughness (Ser), scaliness (Sesc), wrinkles (Sew). As mentioned previously, this system has not been used to evaluate scars but has shown a high reliability for the measure of in vivo skin roughness in normal skin[348]. However, the Visioscan only measures an area of 6 × 8 mm at a time which is probably too small for the analysis of the irregularity of a burn scar.

The aforementioned 3D camera systems can potentially also be used for skin topography analysis. However, these systems are already becoming the preferred devices in the clinic for scar surface area measurement as they are significantly more portable than the PRIMOS system although portable versions of the PRIMOS system are now commercially available (PRIMOS lite, GFMesstechnik GmbH; Germany). Lumenta et al. (2011) showed that the Lifeviz Micro 3D camera system (Quantificare S.A., Sophia Antipolis, France) was able to detect surface irregularities (SI) much better than subjective visual assessment which failed to detect at least half of the broader changes in SI of ≥34 %[295]. Moon et al. (2002) utilised a self-developed 3D camera system (Stereoimage Optical Topometer, Korea University, Seoul, Korea) to calculate the mean surface area roughness (Sa) and root mean square roughness (Sq) for acne scars which were found to have a positive correlation with visual gradings (Spearman correlation coefficient $\rho = 0.463$ and 0.438 respectively, $p < 0.001$)[349]. Table 5 below summarises the surface topography devices.

Table 5: Comparison of surface topography measuring devices in terms of parameter measured, reliability, correlation with clinical score and cost.

Device	Company	Parameter	Intra-rater reliability	Inter-rater reliability	Correlation with clinical score	Cost	Portability	References
PRIMOS	GFMesstechnik	Surface roughness (PC, Sa, Sz)	ICC of PC = 0.97, Sa = 0.99, Sz = 0.98	ICC of PC = 0.9, Sa = 0.96, Sz = 0.94	Correlation with POSAS: $r = 0.617$ ($p < 0.001$)	£17,000–£14,000	Yes	Bloemen et al. 2011[346]
Visioscan VC 98	Courage + Khazaka	Skin parameters (Sesm, Ser, Sesc, Sew)	Not been used in scars	Not been used in scars	Not been used in scars	£5000–£10,000	Yes	N/a
Eykona 3D camera	Fuel 3D	Not been used in scars	Not been used in scars	Not been used in scars	Not been used in scars	<£5000	Yes	N/a
Lifeviz Micro	Quantificare	Surface Irregularity	No data	No data	Performed better than subjective visual assessment	£10,000–£15,000	Yes	Lumenta et al. 2011 [295]

PRIMOS = Phaseshift Rapid In Vivo Measurement Of the Skin; ICC = intra-class correlation coefficient; PC = peak count; Sa = mean surface area roughness; Sz = mean of five highest peaks and five deepest valleys; POSAS = Patient and Observer Scar Assessment Scale.

2.4.7 Biomechanical properties

2.4.7.1 Pliability, elasticity or stiffness

The biomechanical properties of skin can be measured with a variety of methods including suction, tonometry, torsion, adherence and reviscometry. Other methods include elastometry, ballistometry, quantitative electrical methods (dielectric measurements and bio-impedance)[350] as well as ultrasound and Magnetic Resonance Imaging (MRI) techniques[351].

2.4.7.2 Non-suction extension methods

Older methods of measuring skin elasticity relied on extension methods (i.e. physical stretching) to measure the viscoelastic properties of skin tissue using ex vivo[352] or in vivo extensometers[353-358] or elastometers[276], which utilises a constant-tension spring and a strain gauge to distract two points on the skin[276, 359]. The majority of these devices suffer from an unwanted peripheral force contribution due to the deformation of surrounding tissues during measurement which can lead to reduced accuracy and reproducibility of results, although newer designs have sought to improve their accuracy[355].

2.4.7.3 Suction extension methods

Extension of the skin by suction is the method used by devices such as the Cutometer[212, 231, 241, 263, 360-370] (Courage + Khazaka, Germany) and the DermaLab elasticity probe[362, 371] (Cortex Technology, Hadsund, Denmark). With the Cutometer, negative pressure is created in the device by vacuum and the skin is drawn into the aperture of the probe and after a defined time is released again. Inside the probe, height of skin that is drawn up is determined by a non-contact optical measuring system which consists of a light source and a light receptor, as well as two prisms facing each other, which project the light from transmitter to receptor (Figure 13). The resistance of the skin to the negative pressure (firmness) and its ability to return into its original position (elasticity) are displayed as curves (penetration depth in mm/time) in real time during the measurement (Figure 14). This measurement principle allows getting information about the elastic and mechanical properties of the skin surface.

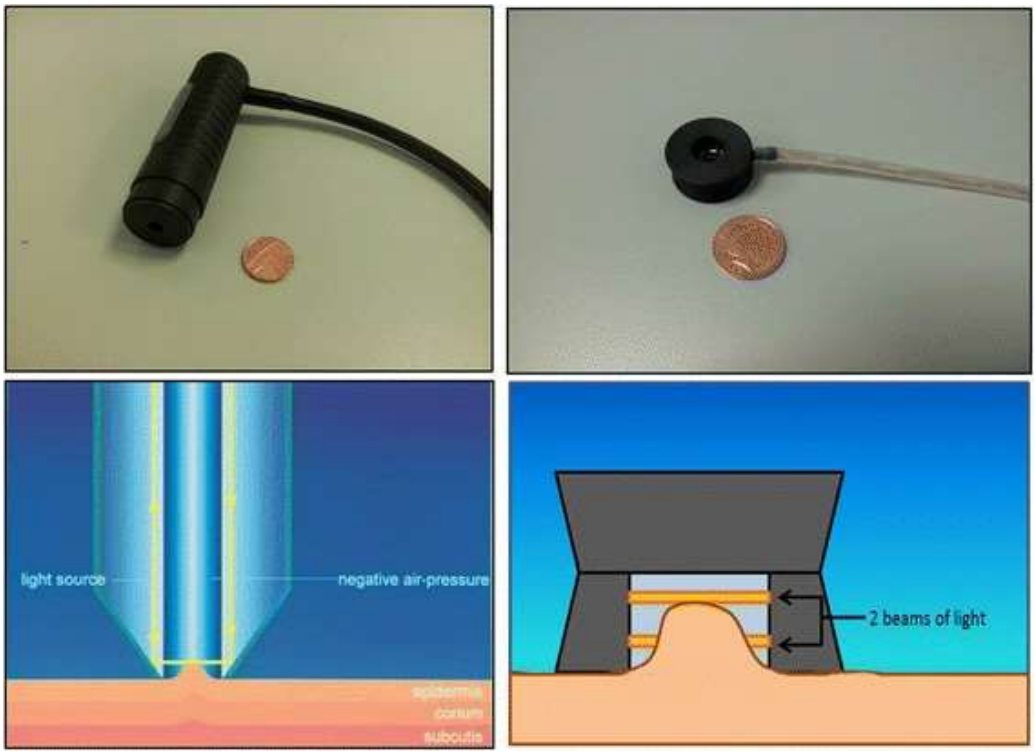

Figure 13: Cutometer and Dermalab probes. The Cutometer (top left) and Dermalab elasticity probe (top right) are shown with a one penny coin Is placed next to probes to provide an idea of the size of the probes. Illustration of the mechanism of the Cutometer and Dermalab elasticity probe (bottom left and right, respectively). (Source: photographs and diagram of elasticity probe by Kwang Chear Lee; Cutometer image source: Courage + Khazaka Electronic GmbH, http://www.courage-khazaka.de/index.php/en/products/scientific/140-cutometer, reprinted with permission).

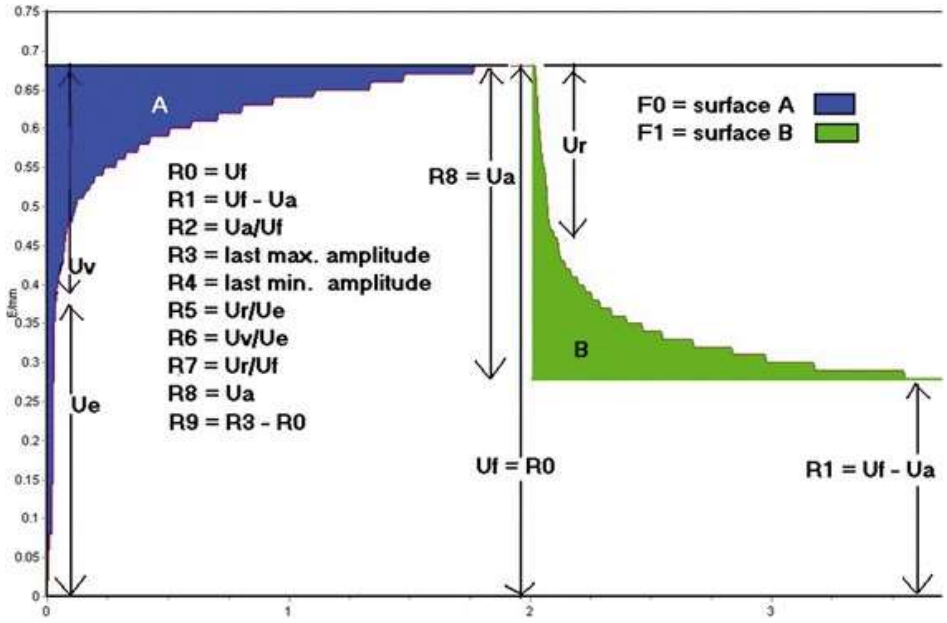

Figure 14: Example of skin deformation curve obtained with the Cutometer. (Source: Courage + Khazaka Electronic GmbH, reprinted with permission).

The Cutometer is reliable for measurement of the elastic and mechanical properties in scars and normal skin; however, its measurements only have a weak to moderate correlation with the pliability score of the POSAS and the subjective pliability assessment of the VSS[360]. Rennekampff et al. (2002) also suggested that the Cutometer may not be sensitive enough to pick up small changes in pliability as he found no correlation was found between subscale VSS pliability rating and Cutometer readings[372].

It was also found to be unreliable for severe scars due to a ceiling effect when rigid tissue is encountered[263]. However, the low ICC values have more to do with difficulty in relocating device to same measurement spot and the high sensitivity of the device[243, 263].

The mechanical parameters of the skin can be divided into absolute and relative parameters:

- **Absolute (in milimetres):** Ue (immediate deformation), Uv (delayed deformation), Uf (maximal deformation), Ur (immediate retraction), Ua (final detraction), R (residual deformation), R8 (visco part).
- **Relative (in percentage):** Ua/Uf (gross elasticity), Ur/Uf (biological elasticity), Ur/Ue (net elasticity), Uv/Ue (viscoelastic to elastic ratio), H (hysteresis).

Absolute parameters are likely to be influenced by skin thickness which in turn is dependent on various factors such as age, gender, anatomical region thus to compare values you will need to standardise them for skin thickness using an ultrasound and this is not always possible thus the relative parameters are more useful as it can be assumed to be independent of skin thickness which allows the values in different subjects, anatomical regions and times to be compared.

Various different opinions regarding the value that should be used (Table 6); however, Draaijers et al. (2004) concluded that either Ue or Uf is sufficient for the evaluation of scar as they found a high correlation between the parameters Ua, Ue, Uf, Ur and Uv, and that Ue and Uf were found to have the highest reliability[364]. Nedelec et al. (2008) agreed with this and also found Uf to have a higher reliability (but not for severe scars) but concluded that as Uf is more convenient to record (automatically calculated by computer software, whereas Ue requires manual calculations), it should be used instead[243, 263].

Table 6: Comparison of used and recommended parameters for the Cutometer in the literature.The most commonly recommended parameters are Ue and Uf (R0).

Authors and papers	Parameter used/recommended
Fong et al. 1997[212].	Uf, Ur/Uf, Ur/Ue, R8
Draaijers et al. 2004[364]	Recommends Ue or Uf
Dobrev et al. 2005[373]	Recommends Ue and Uf (distensibility), Ua/Uf and Ur/Uf (elasticity) and Uv and Uv/Ue (viscoelasticity)
Nedelec et al. 2008[243, 263]	Recommends using only Uf
Rennekampff et al. 2002[372] and 2006[360]	Uf, Ua, Ur, Ue, Ur/Ue and Ur/Uf

Other studies have also utilised the R (dimensionless parameters derived from the U values) and Q (maximum recovery, elastic recovery and viscous recovery areas) values[361].

The Dermalab elasticity probe[220, 374] consists of a light plastic probe that is much smaller than that of the Cutometer (Figure 12). This probe is attached to the skin using double-sided adhesive rings to

form a closed chamber. Within this chamber, two narrow beams of light run at different heights parallel to the skin surface and serve as elevation detectors[371] . A computer controlled vacuum pump connected to the probe is then used to increase the suction within this closed chamber over 30–60 seconds. In contrast to the Cutometer where a set pressure is applied and the skin deformation is measured, the Dermalab elasticity probe measures the amount of suction (in kilopascals, kPa) that is required to lift the skin to pass the height of the two light beams. This may cause problems when the measured skin is too stiff to be stretched enough to reach the level of the detectors[371]. The stiffness of the skin (or Young's modulus, E) is then calculated and expressed in millimetre per kilopascal. Skin that is firm, e.g. scar tissue will have a higher stiffness index compared to normal skin.

A study by Gankande et al. (2014) with the Dermalab elasticity probe showed that the test–retest reliability for pliability was "excellent" (ICC 0.76–0.91) in scar areas but only "good" (ICC 0.45, 95 % CI 0.30–0.76) in contralateral normal skin areas[220]. It should be noted that significant difficulties were encountered by the researchers in the study in obtaining elasticity measurements and they failed to obtain matched measurements for test–retest analysis in 31–52 % of the subjects[220].

Both devices have the advantage of being a "hub" to which other measuring devices can be attached. For example, the Dermalab combo device provides additional probes that can be fitted to provide spectrophotometry data (melanin and erythema) and ultrasound measurement of dermal thickness[220].

2.4.7.4 Tonometry

Tonometry measures the firmness and flexibility of skin and scars by exerting pressure either via an airflow system that is blocked at a certain pressure (e.g. Pneumatometer[375] (Medtronic Solan Model 30 Classic, Jacksonville, Florida, USA), Cicatrometer[332], Tissue Tonometer[376] (Flinders Medical Centre Biomedical Engineering, Australia) or an indentional load in a vertical direction, e.g. durometer[332 213, 376, 377] (Rex model H 1000, Rex Gauge company, Illinois, USA), Schiotz tonometer[378], and Tissue Compliance Meter[379] (Model and company not stated by author). In the study by Lye et al. (2006),

the Tissue Tonometer showed good intra-observer reliability and a moderate correlation with the pliability score of the VSS scale, but the measure is a relative one as it requires a contralateral reference point[376]. A study by Corica et al.[380] (2006), utilising a modified Tissue Tonometer, showed that the intra-class correlation coefficient for averaged measures between measurers (inter-rater reliability) was 0.957, and the standard error of measurement was 0.025 mm. A significant difference ($p = .0000$) between scar (2.64 ± 0.5 mm) and normal tissue (3.23 ± 0.46 mm) measurements was also demonstrated in the study. Tonometry devices are, however, less suitable for skin locations with hard bony structures underneath—as the hard underlying structures limit the degree in which the skin can be compressed. At the time of writing, the mechanical tonometer is no longer commercially available, but a digital version is in the experimental phase. Other shortcomings with the mechanical design include the need to place the device accurately (must be within 5° of upright to measure correctly).

The durometer also showed good reliability and validity in one study but this was performed on sclerodermal skin[377] which demonstrates symmetrical skin thickening compared to scars where thickening can vary from area to area depending on the initial injury.

2.4.7.5 Torsional force and adherence measurement methods

Torsional force can be used to measure the elasticity of skin (Dermal Torque Meter; Dia-Stron, UK) [211] and the device is able to differentiate between native skin, autographs and cultured skin substitutes; however, rigorous clinical appraisals of the device have not yet been performed.

2.4.7.6 Acoustic methods

The Shear Velocity Device (SVD) is a portable tool that can be used to analyse soft biologic tissue by measuring the propagation of an auditory shear wave through the skin surface[381, 382] . The device works on the principal that an acoustic shear wave will have a higher velocity in a hard material (e.g. scar tissue) compared to softer material (e.g. normal skin). Experimental validation of the SVD by McHugh et al. (1997) claims that it provides similar results to the Shore Type A durometer; however, this data has yet to be published[381]. The coefficient of variation (CV) for the device in measurements

of 254 hypertrophic scar locations was ±4.8 % whilst on 210 normal skin sites this was ±4.4 %. Unfortunately, the authors have not been able to locate any subsequent publications on this device and it is not currently commercially available.

Reviscometry[383] (Reviscometer; Dermaviduals and Courage + Khazaka, Germany) is another portable tool that measures the elastic and viscoelastic features of skin and scars by utilising an acoustic shock wave and reports this as resonance running time (RRT). Scars have a significantly lower mean RRT compared with normal skin (52.3 versus 91.6). It has been shown to be reliable with inter-rater observer reliability of more than 0.86 on scars but more studies are required to establish its validity and comparative performance.

2.4.7.7 Electrical of bio-impedance methods

Utilising an impedance device, the capacitance of scar tissue has been shown to be stronger than that of normal skin and the resistance of scar tissue is lower than that of normal skin. The impedance of scar tissue however varies according to the depth and density of scar tissue[350] . This electrical property of scar tissue could be utilised to quantify scars; however, no method has been developed as of yet.

2.4.7.8 Modelling and other techniques

All of the methods that have been discussed thus far rely on measurements in a small area of the scar which may not be representative of the scar as a whole.

The Adheremeter[384] (Fondazione Salvatore Maugeri, Italy) uses an entirely different approach and measures the restriction of scar mobility with respect to the underlying tissue at the worst adherent point when stretched in 4 orthogonal directions using a transparent film print-out of 9 concentric rings with varying radii. It is a relatively new device and has only been tested in one study[384] but it showed an adequate level of reliability and validity when compared to the VSS. However, it has a degree of subjectivity in operation as the measurement is based on the rater's evaluation of the

force required to stretch the skin and on the patient's judgement of comfort. It is also not suitable for use on highly concave surfaces.

A different approach to measuring the elasticity of skin is to use computerised models of skin motion analysis[385, 386]. These experimental methods are able to detect and measure the differences in elasticity between normal and scar tissue by comparing images taken at two time instances before and after deformation. Regular 2D images, combined with 3D data, can offer a method of estimating scar pliability in a more global manner[313]. In simple terms, these methods utilise a grid painted onto the skin which will then deform according to the elasticity of the skin. Grid portions that are less pliable (scar tissue) will deform less than areas which are more pliable (normal skin). A technique called Finite element modelling (FEM) can then be used to analyse this information[385-388]. This technique is still experimental and yet to be commercially available. Some devices that may be commercially available soon that utilise this technique include CutiScan CS 100 (Courage + Khazaka, Germany) which is still under development. Other methods include the measurement of ranges of movement to determine the severity of burn contractures and thus indirectly the viscoelasticity of the scars. The current standard involves the measurement of the passive and active range of motion of an extremity in a single plane or functional movements (which are better related to activities of daily living)[389] using conventional measurements[390] (e.g. goniometry, tape measures, inclinometer) or 3D motion analysis[389, 391, 392] . The Faciometer (University of Vienna) measures the ranges of mimic movements, e.g. the distance between the tragus and the mouth using calipers and an electronic display[393]. A survey by Parry et al. (2010) however showed that there is a lack of consensus in the methods and tools used clinically for the measurement of burn contracture and these methods are also rarely checked for reliability or performance competency[390]. Table 7 gives a summary of the comparison of viscoelasticity devices in terms of parameter measured, reliability, correlation with clinical score and cost. Comparing the devices that measure biomechanical properties of scars, the Cutometer seems to be the best choice at present as it is reliable (in normal, non-hypertrophic scars), shows a reasonable validity and can be used over bony areas. Additionally, the Cutometer is

the most often used device for skin viscoelasticity measurements with more publications than most of the other devices reviewed in this paper.

Table 7: Comparison of viscoelasticity devices in terms of parameter measured, reliability, correlation with clinical score and cost.

Device	Company	Parameter	Intra-rater Reliability	Inter-rater reliability	Correlation with clinical score	Cost	Portability	References
Cutometer	Courage + Khazaka	Viscoelastic parameters	Ranges from unacceptable to good (0.12–0.76)*; poor in severe firm scars	Ranges from unacceptable to good (0.11–0.93)*, poor in severe firm scars	Low to moderate, but significant (Spearman's *r* = −0.29 to −0.53). Rennekampf et al. could not find any significant correlation between objective viscoelastic measurements and the subjective pliability assessment of the VSS.	£5000–£10,000 (with hub)	Yes	Nedelec et al. 2008[243, 263], Draaijers et al. 2004[394], Rennekampf et al. 2006[360].
Dermalab Elasticity probe	Cortex	Viscoelastic parameters	ICC = 0.90–0.93; limited ability to measure rigid scars	ICC = 0.86–0.93; limited ability to measure rigid scars	No data	£5000–£10,000 (with hub)	Yes	Gankande et al. 2014[220]
Tonometer	Flinders Medical Centre Biomedical Engineering	Viscoelastic parameters	ICC = 0.90–0.94	ICC = 0.948	Negative correlation between VSS pliability scores and tonometer readings: −0.457 and −0.442 respectively for 3 and 6 second readings.	No longer commercially available	Yes	Corica et al. 2006[380], Lye et al. 2006[376].
Durometer	Rex Gauge company	Viscoelastic parameters	No data	No data for scars but ICC = 0.82–0.92 for sclerodermal skin	Good correlation with modified Rodnan skin score (0.70) for sclerodermal skin	<£1000	Yes	Merkel et al. 2008[377].
Dermal Torque meter	Dias-tron	Viscoelastic parameters	No data	No data	No data	N/a	Yes	Boyce et al. 2000[211].
Adheremeter	Fondazione Salvatore Maugeri	Viscoelastic parameters	Good (0.96)	Good (0.87–0.99)	Moderate correlation with VSS and Pliability subscale of VSS (rs = −0.58 to −0.66)	Free	Yes	Ferriero et al. 2010[384].
Reviscometer	Courage + Khazaka	Resonance running time	Good (>0.86)	No data	No data	£10,000–15,000 (with hub)	Yes	Verhaegen et al. 2010[383].
Vesmeter	Wave Cyber Co. Ltd.	No data	No data	No data	No data	N/a	Yes	Niyaz et al. 2012[395].
Shear Velocity Device	N/a	Shear wave propagation velocity	No data for ICC. (CV for scars is ±4.8 %)	No data	No data	Not commercially available	Yes	McHugh et al. 1997[381].

2.4.8 Pathophysiological disturbances

Pathophysiological disturbances are defined as functional changes in the skin associated with, or resulting from, disease or injury, with measurable parameters including gas perfusion and moisture content.

2.4.9 Transcutaneous oxygen tension

Transcutaneous oxygen tension ($tcpO_2$) is perturbed in injured tissues and can be used as an index of maturity in hypertrophic scars. The $tcpO_2$ in scar tissue is lower compared to healthy skin, and an increase in $tcpO_2$ is correlated with a reduction in scar thickness assessed both clinically and by ultrasound[396]. This is thought to be due to low oxygen diffusibility through scar tissue. A study by Ichioka et al.[397] (2008) has also shown in animal and human tissues that immature repairing tissues consumed more oxygen than mature tissues and that the oxygen consumption rate in keloid and hypertrophic scars were significantly higher when compared to mature scars which may also explain the lower tcpO2 in scar tissues. The method for measuring transcutaneous oxygen tension exploits the redox reactions that occur in a modified Clark electrode that measures the oxygen ($tcpO_2$) and carbon dioxide ($tcpCO_2$) tension on the surface of the skin. The $tcpCO_2$ is considered non-specific and highly dependent of external factors, whilst the tcpO2 is a much more precise indicator of local perfusion[398]. This technique seems to have been recently abandoned from clinical practice.

2.4.10 Transepidermal water loss and moisture content

The water content of the skin is an important factor that influences the softness and smoothness of the skin, and transepidermal water loss and skin hydration are key indicators of skin function. Transepidermal water loss (TEWL) and moisture content can be measured by open and closed chamber systems. Open systems such as the Dermalab TEWL module[399] and Tewameter[400] (Courage + Khazaka, Germany) are the most frequently used (Figure 15). Closed systems such as the Vapometer (Delphin Technologies, Finland) are also available, but one study has shown that the Tewameter is able to detect significantly smaller differences in TEWL when compared to the Vapometer[401]. Anthonissen et al. (2013) showed a significant difference in mean TEWL values between normal skin and spontaneously healed scars ($p = 0.036$) and a significant negative relation

between mean TEWL values and time after burn (p = 0.008); however, high SEM values were reported[374].

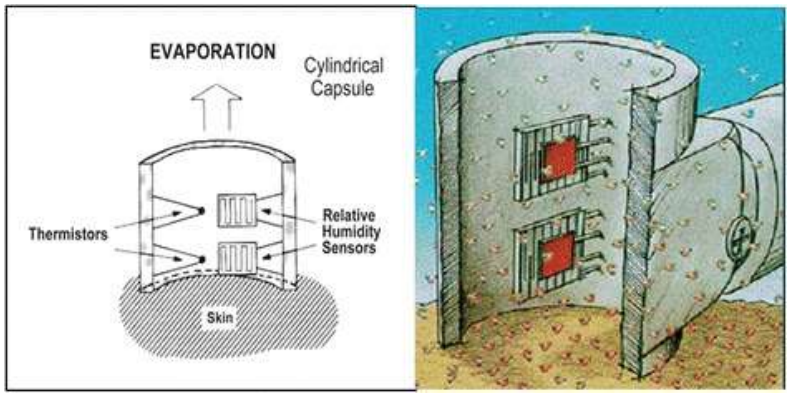

Figure 15: Open chamber transepidermal water loss system. The sensors in the probe (temperature and relative humidity) indirectly measure the density gradient of the water evaporation from the skin indirectly inside the hollow cylinder. (Source: Courage + Khazaka Electronic GmbH and Cortex Technology, reprinted with permission)**.**

The hydration of the skin layers, specifically the stratum corneum, can also be measured using electrical methods, such as the conductance method (for example, the Skicon-200 conductance meter[402, 403], IBS Co, Hamamatsu, Japan, Location, and the NOVA Dermal phase Meter[404], Nova, Technology Corp., Gloucester, Mass.) and impedance method (for example, the Corneometer[402], Courage + Khazaka, Germany). One study has shown that the Corneometer is suitable for use in clinical trials, with useful intra-class correlation coefficient (ICC) values (ICC_{intra} = 0.985; ICC_{inter} = 0.984), but only under very strict conditions with a standardised test protocol[405]. Another method for measuring hydration (and protein content) is to measure the dielectric properties of the skin. This is based on the interaction of high-frequency electromagnetic (EM) waves and biological material[406, 407]. The EM waves are generated using a network analyser (HP8753B, Agilent, USA).

A study by Suetake et al. (1996) found that TEWL was a better parameter for the functional evaluation of scars than was the hydration state of the skin surface measured by high-frequency conductometry[408].

2.4.8 Multispectral imaging systems

A novel polarised multispectral imaging system that combines out-of-plane Stokes polarimetry and Spatial Frequency Domain Imaging has been developed by Ghassemi et al. (2014) and allows the colour (haemoglobin, melanin), pathophysiology (blood oxygenation, hydration) as well as structural features (cellularity and roughness) of hypertrophic scars to be analysed in vivo[409, 410]. The results obtained with this multi-modal system showed a good agreement with the VSS and with histological examinations[409]. Although still in experimental stages, it could potentially simplify the scar measuring process due to its multi-modal measurements.

2.4.9 Non-invasive morphological imaging techniques

Previously, histopathological analysis of biopsy samples was the only method of morphological investigation of damaged biological tissues. Now, recent advances in imaging techniques have made non-invasive in vivo morphological investigation of tissue microstructure possible.

2.4.9.1 Optical coherence tomography

With the advances in fibre optics and other technologies such as ultra-broadband light sources and frequency domain techniques, optical coherence tomography (OCT) imaging that is capable of generating 3D images of tissue microstructure is now possible. OCT is most frequently used in ophthalmology[411] but can be adapted to be used to analyse the skin[412-419]. OCT can be utilised in various different modes for the assessment of scars[418, 419]. The layered arrangement of normal skin is perturbed in scarred skin so that OCT can be used to provide information about microstructure as well as depth and volume[412]. Scar tissue imaged by OCT appears dense and bright due to the increased collagen content, and this parameter can be used to measure the collagen status of scars[420]. Scar microvasculature density has been quantified using an automated OCT system and found to be increased in hypertrophic scar tissues (38 %) when compared against normal, unscarred skin (22 %)[417]. Vessels in scars have also been shown to be much larger compared to normal skin on OCT[421]. However, due to the strong scattering and absorption of light by skin, current OCT methods are only capable of imaging to a depth of 1 to 2 mm, whereas scar thickness is usually greater than 2 mm (as determined by ultrasound)[220, 322, 422]. Nevertheless, in areas where scar tissue is thinner (e.g.

in fingers), OCT (utilising the 1300-nm wavelength region) may still be useful[412]. Another way of differentiating scar tissue from normal tissue using OCT is the use of the attenuation rate, which is defined as the rate at which the OCT signal decreases with depth in the tissue[419]. Lower attenuation coefficients are seen in scarred tissue compared with normal skin tissue[419]. This method bypasses the problem of penetration depth but yields less detailed morphological data when compared to standard OCT methods. A form of OCT (termed "Polarization-sensitive Optical Frequency Domain Imaging") can also be used to image collagen remodelling[423].

OCT imaging has been demonstrated to be feasible for use in the clinical monitoring of scar progression automated quantification of vascularity in cutaneous burn scars[411]. OCT imaging for scarring and fibrosis is currently still in its infancy and further development in the technology is required. In a study by Eraud et al.[424] (2014), although OCT was able to detect dermal nodules (which are present in hypertrophic but not keloid scars[425]) in 100 % of the specimens, it was not helpful in identifying hyalinised collagen (which is present in keloids) and cells. The technology however has the potential for tremendous growth[420].

2.4.9.2 Other in vivo tomography/microscopy techniques

Imaging techniques utilising specialised optical microscopes have been used to image scar tissue. Nonlinear spectral imaging, such as multi-photon tomography based on both two-photon excited fluorescence (TPEF) and second harmonic generation (SHG), can be utilised to demonstrate the morphological structure and spectral characteristics of collagen (with SHG) and elastin fibres (with TPEF) and thus can be used to potentially distinguish hypertrophic scar tissues from normal skin and to evaluate the effects of treatments[426-432]. Information on the orientation of collagen fibres can also be investigated and analysed from these images using fast Fourier transform methods[433, 434]. Advantages these techniques have are that several extracellular matrix components and endogenous biomolecules such as collagen, keratin, melanin and elastin can be visualised in living tissue without the need for specialised processing or staining[435, 436] and high-resolution, high-contrast three-dimensional images can be obtained[436, 437].

These techniques however have similar drawbacks to OCT. The maximum depth of two-photon imaging has been reported to reach up to 1 mm in living brains[438] and thus is comparable to OCT imaging but clinical use in the skin is typically only up to 200 µm, thereby limiting its potential utility for deep scar assessment. In addition, advances in the miniaturisation of spectral imaging apparatus need to be made before it can become of practical use in a clinical setting. The multi-photon technique also has high overall system costs, a long measurement times and the inability to quantify skin redness[439]. Other non-invasive in vivo imaging techniques which currently being developed, such as confocal laser microscopy (CLM)[440, 441], also have a limited imaging depth (~300 µm) due to tissue-related aberrations and light scattering[442].

Other similar microscopy techniques include phase-contrast microtomography with synchrotron radiation technology to detect the 3D structure of dermal tissues[437].

2.4.9.3 Spectroscopy techniques

Another imaging method that holds future promise is the use of optical spectroscopy methods in the UV-visible-near-infrared wavelength range, including diffuse reflectance (DR) and auto-fluorescence (AF) spectroscopies. DR spectroscopy is based on the scattering of photons (350–800 nm) inside biological tissues due to the differences in the refractive indices and morphology of the constituents of skin such as collagen fibres. AF spectroscopy, on the other hand, is based on the fluorescence emissions from endogenous fluorophores such as collagen and elastin when excited by light in the 350–459 nm wavelength range. A combination of both spectroscopy methods increases its accuracy[443] and has been used successfully in a rabbit hypertrophic scar model with high sensitivity and specificity[444, 445]. DR spectroscopy on its own has also been shown to be able to differentiate keloids from normal skin in terms of collagen concentration, haemoglobin oxygen saturation and scattering coefficient in an in vivo human study[433] and can potentially be used to evaluate keloid scar severity[446].

2.4.9.4 High-frequency ultrasound systems

High-frequency ultrasound systems (such as the Dermascan and Dermalab systems[220], Cortex, Denmark) are able to provide a much greater depth of imaging (~8 mm at 20 MHz) but the resolution is inferior to OCT, CLM and multi-photon technology (MPT)[412]. Pathological scars appear as easily identified echo-poor areas that are clearly distinguishable from normal skin and with densitometry analysis with dedicated software, scars are also shown to have significantly reduced densitometric values compared with normal skin (7.6 ± 4.7 versus 31.79 ± 10.8)[447]. More detailed architectural information such as collagen arrangement and cell structure cannot currently be visualised with 2D nor 3D ultrasound techniques.

2.4.9.5 Intravital video-capillaroscopy

Intravital video-capillaroscopy[448] is a technique that utilises an optic contact probe microscope that is attached to a computerised video microscope (e.g. Microwatcher Model VS-901, Mitsubishi Kasei Corporation, Tokyo, Japan[448]) which allows photographic images of skin capillaries to be taken. Scarred skin has a deranged capillary organisation. The pictures are then scored either subjectively and/or objectively. Subjective methods score images according to angiogenic markers[448, 449] such as enlarged or tortuous loops, architectural derangement, neoangiogenesis and quantitative changes of capillary lesions. These scoring systems can be modified to allow objective quantification[450, 451]; for example, the methods used in a study by Hern et al. (2007) allowed for both non-stereological measurements (microvessel density and vessel image width) and stereological measurements (image area fraction and microvessel length density)[451]. Intravital capillaroscopic measurement of capillary density (CD) has been shown to be reliable and reproducible with a mean coefficient of intra-observer variation of CD estimate of 5.6 % and the inter-observer correlation coefficient of 0.94[452].

A similar technique, dermoscopy, and its use in the examination of vascular structures can be a clinically useful diagnostic tool for differentiating between keloids and hypertrophic scars[453].

The dermoscopy can be used to visualise capillaries and pigmentation in the epidermal and dermal layers of the skin. An added advantage is that since dermascopes have their own light source, it is not likely to be affected by differences in environmental lighting which has been shown by Wei et al[265] (2015).

Wei et al.[265] (2015) showed that the L* (or lightness reading) from the Dermoscope (Hong Kong Productivity Council, Hong Kong) had a significant correlation (0.448–0.536, $p < 0.01$) with the readings from the MiniScan XE Plus spectrocolorimeter (HunterLab, Reston, Virginia, USA) and VSS scores of pigmentation (when the skin was blanched with pressure; $r = 0.783$, $p < 0.01$). The RGB values of redness also showed a strong correlation with the VSS scores of vascularity ($r = 0.625$, $p < 0.01$). Both the intra-rater and inter-rater reliability of the dermoscope were found to be excellent (0.965–0.98 and 0.871 to 0.930, respectively).

2.4.10 Measurement of sensory change

A majority of patients with burn scars experience a change in sensation of the scarred skin such as pruritus, pain and hyper- or hypo-sensitivity is common in scars and this can often last for years after the initial injury[454]. However, the objective measurement of such sensory deficits is challenging task and the only gold standard for pain assessment available currently is self-report.

Functional MRI (fMRI) scans have shown promise in assessing pain in the absence of self-report however it is far from ready for regular clinical use[455]. However, skin sensitivity/touch and (indirectly) pain can be examined in an objective manner with the touch pressure threshold method (TPT) using for example Semmes Weinstein monofilaments, which have been shown to have good intra- and inter-rater reliability (ICC = 0.822 and 0.908, respectively) in patients with scars[456].

More recently, an electronic version of the von Frey filaments is also available and showed better reproducibility compared to the traditional von Frey with good to almost perfect intra-observer reliability (ICC ranges from 0.61 to >0.8) (study done on normal skin, not scars)[457, 458].

2.5 Discussion

There have been significant advances in many aspects of burn treatment, but hypertrophic scarring remains as one of the major chronic problems after severe burns with few therapeutic options currently available. The accurate assessment of scarring is an important aspect of research into better treatments for this condition. Despite this, scar assessment is still mostly subjective and there is still little consensus regarding the ideal scar measurement tool[459].

Most if not all currently used subjective scales used in evaluating skin scars assume that scar dimensions conform to linear models and thus employ equal appearing interval (EAI) scales. However, a study by Brandt et al. (2009) showed that whilst pliability, thickness and surface area were defined well using linear models, the dimensions of vascularity and pigmentation were more accurately described using curvilinear functions[460].

Tools for scar measurement are often modified from tools developed for other industries, e.g. dermatological use in the cosmetic industry, such as the Cutometer; colour probes for measuring the colours of materials in the food and building industries and durometers such as the Vesmeter for testing the hardness of materials in the manufacturing industry[395]. As such, their utility for burns patients is mostly unproven. Accordingly, trials on these tools to evaluate their accuracy and reliability are scarce and few trials have compared the different devices.

The ideal assessment of scars should include the objective and subjective aspects of scars as well as an assessment of the functional limitations that are caused by the scar tissues[313]. The different physical aspects of scars can all change independently of each other during the course of scar evolution and as such a hybrid method of scar assessment which incorporates the most reliable and feasible methods should be used[461]. Combination systems such as the Dermalab combo which incorporate multiple scar measurement tools (e.g. colour, thickness and pliability[220, 264]) are now available[264] to facilitate this although improvement in the clinical interpretation of the measurements is required[461].

A problem with validating objective scar measurement tools is the lack of an ideal gold standard.

Biopsies and standard histological analysis whilst proven to be accurate mostly rely on subjective scoring systems[462] unless quantitative measurement techniques are used[463]. Furthermore, Singer et al. (2000) showed that histomorphologic scales have been shown to only correlate fairly with gross macroscopic scores[462]. Beausang et al. (1998) also found that the clinical scar appearance correlated better with the upper portion of the skin (epidermis and papillary dermis) compared to the deeper parts of the scar[256]. Therefore, the lack of correlation of objective measurement techniques with clinical subjective scores should be considered carefully and not used to dismiss the objective methods.

Future validation studies of pigmentation and vascularity may be possible with standard colour reference cards developed for the cosmetic industry[464].

Objective scar measurement tools are important, especially for interventional clinical studies, as scars and the effect of therapies can be described, analysed and compared more accurately than is possible with subjective scar scales. Subjective scar scales however should still be incorporated into studies as they can provide a more global assessment of the scar and allow the measurement of variables that are currently not possible with objective measurement devices, such as pain and itch. Indeed, several published studies have incorporated both subjective and objective scar measuring tools[465, 466].

The implementation of objective measurement devices into standard clinical practice still faces many obstacles and there are multiple reasons why potentially great technologies are struggling to get incorporated into the health care system.

As mentioned previously, many new technologies (including all if not most of the devices mentioned in this review) have been developed for non-medical uses and very little if any input has been sought from clinicians or patients during the design process, and thus these devices may have limited

practical clinical use. The lack of data security features is also a factor although this issue probably applies more to mobile apps rather than physical devices.

Some clinicians also view the use of new technologies in clinical practice as a crutch to the development of clinical acumen even though many studies have shown that clinical judgement to perform poorer, e.g. in determining surface area[467] or burn depth[468].

Another main issue is the high cost of these devices. Even the simplest of devices, e.g. colour probe, costs at least >£3000 not including annual servicing costs. Without solid research evidence of clinical and patient benefit, it is difficult to justify the costs and use of these devices outside of research.

Despite many of these devices being fairly simple to use, a certain level of technical expertise and additional clinical time to collect and analyse the data generated is still required. To take an example, electronic health records have been used more frequently in hospitals nowadays but it takes longer for an average clinician to input data into the electronic system than onto a paper record for months, even years, after they have started using them[469]. This has been anecdotally quoted as one of the main reasons why some burn clinicians have been slow to adopt new technologies such as LDI in determining burn depth even though there is strong evidence for its accuracy compared to clinical judgement. Staff specially trained in the use of these devices and who are responsible for training of other staff and championing their use in regular clinical practice may be the way forward[469].

Lastly, the scope of this review largely did not include journals or articles in physical sciences or engineering which may have unearthed more potentially useful objective scar measurement devices.

2.6 Conclusions

In this review, we aimed to recommend a panel of objective scar measurement tools for burn scars to be used in conjunction with subjective scar scales, that were reliable, patient friendly, and easy to use (feasibility in terms of cost and portability have now been commented on in the tables in the

various sections); generated simple data; and were appropriate for use in a clinical (bedside) environment (i.e. portable). We included in the panel the least number of devices that could measure surface area, colour, thickness, pliability, texture or topography and pathophysiological skin disturbances in order to reduce measurement time and cost. All of the devices considered for inclusion have to be commercially available. As such, the recommended device panel for burn scar assessment is as follows:

- **3D wound measurement camera systems** (Eykona/Lifeviz/Vectra H1): for surface area, texture, volume (including clinical thickness) and colour.
- **Dermascan**: for histological thickness measurements (the TUPS is an alternative but not commercially available).
- **DSM II Colormeter:** for colour measurements (both Tristimulus reflectance colorimetry and narrow-band simple spectrophotometry).
- **Cutometer system:** for viscoelastic measurements of the skin.
- **Tewameter** (optional probe for the Cutometer system): for the measurement of transepidermal water loss.

Further studies are needed to validate the performance and utility of this scar panel and to compare them with the commonly used subjective scar scales, such as the POSAS.

It is recommended that new technologies to be utilised in objective measurement should ideally be evaluated in terms of intra- and inter-rater reliability (with at least two observers) before being used in trials; however, this could be time and resource consuming. Collaborations should be established between the industry, clinical research, and patient groups to streamline and refine this process and encourage the testing and introduction of improved devices.

Although there is a greater emphasis now compared to previous decades on developing and evaluating devices that measure physical scar parameters, scarce attention has been given to measure the physiological characteristics of scars. It is essential to develop tools that can be used to measure and quantify metabolic and cellular activity in scars so that treatments can be tailored to the individual.

CHAPTER 3

CLINICAL ASSESSMENT OF BURN SCAR QUALITY:
BIRMINGHAM OBJECTIVE SCAR SCALE STUDY

3. Clinical assessment of burn scar quality: Birmingham Objective Scar Scale study

3.1 Background

Hypertrophic scarring is not merely an aesthetic problem but can result in physical and psychological problems in burn patients. Traditionally, scars have been assessed only visually and tactilely with subjective methods such as scales. Such assessments, although done routinely in some centres, rarely contribute to the patients' care unless treatment is actively being administered and monitored for effectiveness. The most commonly used scales include the Vancouver Scar Scale (VSS) and Patient and Observer Scar Assessment Scale (POSAS). These methods are widely used in clinical practice due to their ease of use and speed[470]. However they are subjective and may have low reproducibility among different assessors (or low inter-rater reliability) and are best used to monitor change within the same individual rather than between different individuals[471]. Subjective scar scales are subject to the experience of the assessor e.g. An assessor who has seen highly severe scars would tend to rate normal severity scars lower compared to a more inexperienced assessor who has only seen minor scars.

At present, there are few available treatments that target scars and none that can prevent or improve the scarring process however new pharmacological anti-scarring treatments are currently in development, and the comparative efficacy of these treatments has to be evaluated in a systematic and objective manner to ensure that the adoption of potential promising treatments is evidence-based. The clinical measurement of scars is an important obstacle to the development of scar treatments as most assessments are not performed systematically and are based on subjective measurements of scars either by the patient or clinician. Due to the large variability in scars and their parameters, research into the efficacy of treatments on scars can only be valid if no substantial variability is introduced by the measurement tool used. Objective measurements are parameters

that can be quantified and are not observer dependent i.e. influenced by the clinician's or patient's personal opinions or feelings.

Scars are difficult to measure due to a variety of reasons including:

1) **Anatomical region**: the normal parameters of skin vary from region to region. For example, skin on the back and on our palms and soles is thicker compared to other areas. Additionally, scars that occur in areas which are curved are inherently more difficult to measure accurately.

2) **Size:** Most devices only have a small measuring area and thus it is difficult to get an accurate overall measurement of scars especially large scars.

3) **Irregularity:** The irregular nature of burn scars which can be due to pathological developments (e.g. infection) or surgery (e.g. meshed grafts), compounded by the small area of measurements of most devices makes accurate measurement difficult as even a small change in the area measured may produce highly different readings.

4) **Lack of instruments specific to scars:** Most scar measurement tools have been adopted from other fields such as cosmetics and even the manufacturing industry (e.g. colour probes) but not been validated in burn scars.

There is currently a lack of sensitive and specific tools that can aid clinicians in making an objective evaluation of a scar.

Histological methods of evaluating scars via punch biopsies have been touted as the gold standard however it has limitations:

- Invasive, painful, and impractical
- Trained pathologist required to interpret the results
- Unable to monitor the same site over a period of time

Scar assessment consists of the measurement of multiple components including colour (erythema and pigmentation), pliability, thickness, and irregularity. Pain and itch are also important aspects of burn scars that can have significant implications on the quality of life of patients[472, 473] and are included in many subjective scar assessments that are completed by patients such as the POSAS

patient scale[207] however there are currently no commercially available objective pain and itch measurement tools[219, 474].

A small number of devices have been adapted from the cosmetics industry for burn scar measurements as there is an increasing awareness of the importance of reproducible and objective scar measurements for both clinical practice and research. However, these tools are often still in the experimental stage and few have been validated in the study of scars. Thus, there is currently no consensus on the most suitable tools for measurement of the different aspects of scars due to the scarcity of scientific studies in these instruments. One of the aims of our study is to provide this consensus and create a panel of objective scar scale tools that can be used to create a global objective scar scale i.e. the Birmingham Objective Scar Scale.

After performing a review of the current literature on methods of objective scar measurements (Chapter 2), we have identified three parameters of scar assessment that are the most commonly measured as well as the tools required to measure them:

1) Pliability: Cutometer[212]
2) Colour: DSM II Colormeter[233], Scanoskin[475]
3) Thickness: Dermascan C high frequency ultrasound (20MHz)[243, 263]

These tools have been chosen on the basis of their reliability and feasibility (in terms of cost and portability). They have the advantage of being non-invasive and have no or very low risks to the patients. Additionally, histological measurement of skin thickness via skin biopsy will be included as the gold standard as comparison.

3.2 Aims and Objectives

This study aimed to measure the reliability of both subjective measurement tools, a panel of objective measurement devices and histological measurements.

3.2.1 Primary Objectives

To measure the intra and inter-rater reliability of the objective scar measurement tool panel: The objective of this study is to measure the intra and inter-rater reliability of a panel of selected objective scar measurement tools in burn scars in terms of reproducibility (single and multiple assessors).

3.2.2 Secondary Objectives

- Comparison of objective to subjective scores: To compare the scores of the devices to subjective and validated scar measurement scales i.e. Patient and Observer Scar Assessment Scale (POSAS) and modified Vancouver Scar Scale (mVSS).
- Patient Satisfaction: To determine patient satisfaction with the various devices.
- Creation of a global objective scar scale.
- Testing for associations that have not been pre-specified. Major scientific discoveries have been made by “trawling/ sifting”. If any specific association is observed at the data analysis stage of this study, this could be the basis of further research to replicate or refute these findings.

3.3 Methods

3.3.1 Location

The study was conducted in the Wellcome Trust Clinical Research Facility at the Queen Elizabeth Hospital (QEHB), Birmingham, United Kingdom. This study was approved by the South Birmingham National Research Ethics Service (NRES) Committee West Midlands (REC reference 15/WM/0378) as well as the Research and Development Governance of the University Hospitals of Birmingham.

3.3.2 Subjects

Fifty-five adult patients who have been treated at QEHB were invited to participate in this study, and participation was voluntary. Subjects were included in the study if they met the following inclusion criteria: age >16 years, hypertrophic but non-keloid burn scar, scar aged more than 3 months (calculated from time of 95% healing,) or have had a skin-grafted area, or a burn that has had delayed healing (>2 weeks), scar size of at least 10cm^2. We excluded patients if they had other pathological skin conditions, chronic steroid use as we required normal skin to compare the results of the scar areas for further analysis. Scar areas on the genitalia or face were also excluded. Scars on the genitalia areas were excluded as we wanted to protect patients' dignity and avoid unnecessary exposure. Scars on the face were excluded as scars on the face are known to be more challenging to measure due to technical reasons such as increased surface curvatures which increases measurement angle variability[476] as well as greater variability in subjective measurements due to the greater psychological impact of facial scars[223].

Hypertrophic scars were differentiated from keloid scars by the raters involved in this study based on clinical features and history including whether the scar exceeds the boundaries of the initial injury and regression of the scar over time[477]. Hypertrophic and keloid scars can sometimes be difficult to differentiate clinically[18] however in our study, the reason for exclusion of keloid scars was purely for practical reasons due to the depth measurement limitation of the high frequency ultrasound.

Potential subjects were identified from outpatient scar management therapy lists by clinicians and therapists or from multi-disciplinary team meetings and ward rounds. They were then contacted by a member of the research team; either by telephone or during routine clinical appointments and a brief explanation of the trial was given. If they agreed to participate in the study, a Patient Information Leaflet (PIL) was then sent to the participant.

3.3.3 Study design

The study was a prospective, non-blinded single-arm observational study using three independent assessors. A graphical overview of the study design and pathway for the scar assessment study day is shown in Figure 16.

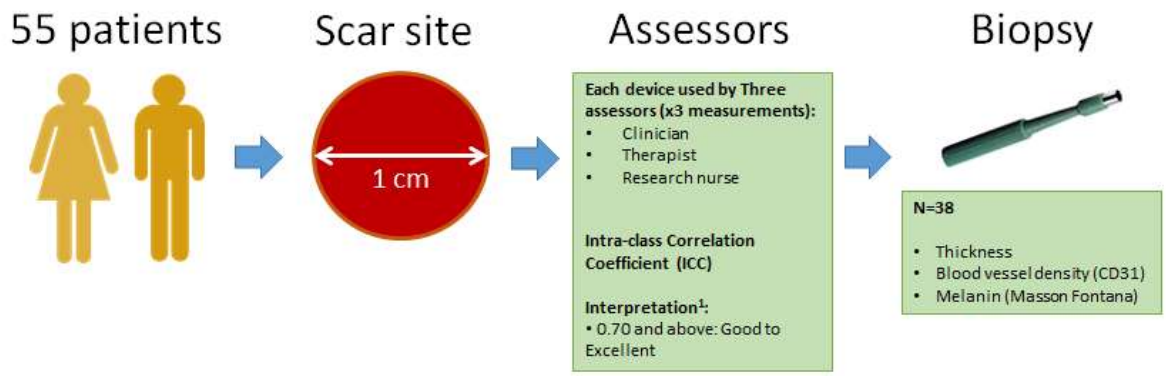

Figure 16: Diagrammatic overview of study design and patient pathway for the scar assessment day. 55 patients had 1 selected scar site (and corresponding normal skin site) evaluated by three assessors with each different device after which a biopsy of the evaluated scar site is taken.

3.3.4 Scar assessment

3.3.4.1 Scar Selection and Measurement procedures

All study participants had a single scar site which was deemed the worse by both patient and clinician chosen. Within this scar site, a 3 x 3 cm area is then selected and marked. One 1cm circle site is then selected and marked (with a stencil and marker pen) for evaluation within this area on each participant. One site of Normal skin (1cm circle area) that is corresponding to the same anatomical site (contralateral site, or adjacent anatomic site) is also chosen for measurements. Similarly, the site is selected and marked for evaluation within this area on each subject.

This scar site (as well as a normal skin site which was contralateral or adjacent to the measured scar site) was measured by 3 different assessors 3 times over a period of one day with the panel of objective scar measurement tools. As the scars were measured in the same day, subjective scar scales (mVSS and POSAS) were only completed once by each of the three assessors and patient. For the objective measurement devices, the normal skin sites (contralateral or adjacent) of the patients

served as the control groups. No control groups were used for the biopsy samples i.e. no biopsies of normal skin sites were taken from the subjects.

If the patients were wearing pressure garments or gels/moisturisers, they were asked to remove them at least 20 min before their appointment- this was confirmed with patients before the start of each session and any residual pressure marks from the pressure garments were noted, the areas were either avoided or were only measured when the skin had recovered. Measurements were conducted in the same temperature-controlled room (22+/-1°C) with the patient lying in the same position for each consecutive measurement. The temperature and humidity of the room was measured and monitored. Figure 16 gives a diagrammatic overview of study design.

3.3.4.2 Raters

All three raters had comprehensive training in the use of the objective scar measurement devices under the supervision of the company representative of the respective devices. Prior to the study commencing, training sessions which involved the raters using the devices on actual patients with burn scars were run to allow the raters to familiarise themselves further with the devices and also the running of the study.

3.3.5 Measurement tools

3.3.5.1 Subjective measurement tools

3.3.4.1.1 Modified Vancouver Scar Scale (mVSS)

A modified version of the VSS that was adapted from the modified version used by Nedelec et al[243, 263] (2008) is used in this study (Table 7). This scale uses a numerical assessment of four skin characteristics including: Height (range, 0-4), Pliability (range, 0-4), Vascularity (range, 0-3), and Pigmentation (range, 0-3). The assessors choose a numerical value for each of these characteristics based on a comparison with normal skin.

Table 7: Modified Vancouver Scar Subscales and parameters. Skin characteristics are divided into pliability, height, vascularity (erythema) and pigmentation subscales.

Skin characteristics	Parameters
Pliability	
0	Normal
1	Supple
2	Yielding
3	Firm
4	Ropes
5	Contracture
Height	
0	Flat
1	<2mm
2	2-5mm
3	>5mm
Vascularity/Erythema	
0	Normal
1	Pink
2	Red
3	Purple
Pigmentation	
0	Normal
1	Hypo-pigmented
2	Mixed
3	Hyper-pigmented

3.3.4.1.2 Patient and Observer Scar Assessment Scale (POSAS)

The Patient and Observer Scar Assessment Scale (POSAS, version 2.0) is a subjective scar scale that consists of two parts: a Patient Scale and an Observer Scale[478] (Figure 17). Both scales contain six items that are scored numerically on a ten-step scale and together they make up the 'Total Score' of the Patient and Observer Scale. Furthermore, category boxes are available to score nominal parameters (e.g. type of colour).

The POSAS Patient scale assesses the scar in terms of pain, itching, scar colour, stiffness, thickness and irregularity, and overall opinion.

The POSAS Observer scale assesses the scar in terms of vascularity, pigmentation, thickness, relief, pliability, surface area and overall opinion.

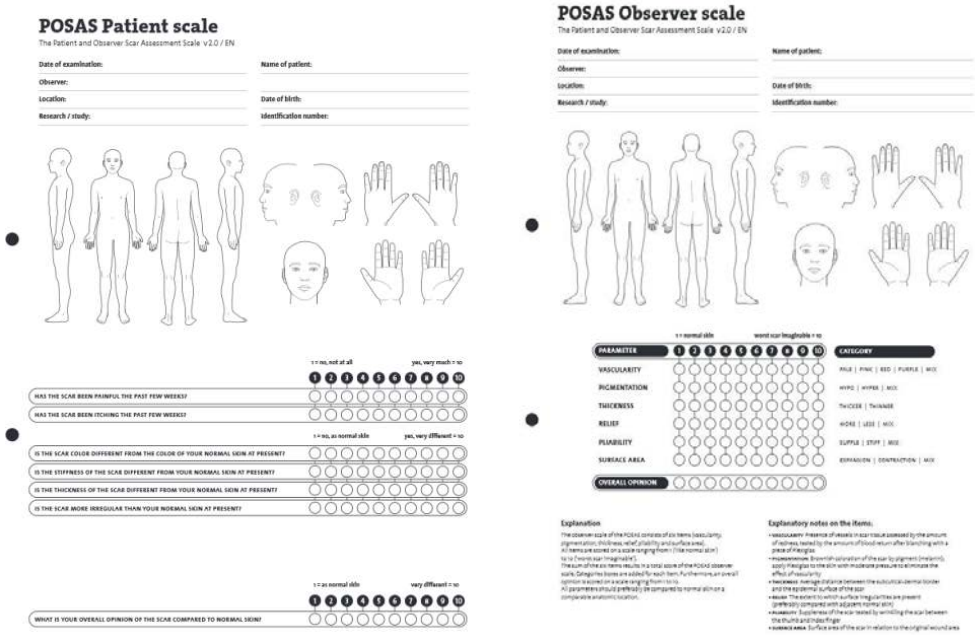

Figure 17: Patient and Observer Scar Assessment Scale. Anatomical figures are included to indicate the site(s) being evaluated. The POSAS Patient scale assesses the scar in terms of pain, itching, scar colour, stiffness, thickness and irregularity, and overall opinion whereas the POSAS Observer scale assesses the scar in terms of vascularity, pigmentation, thickness, relief, pliability, surface area and overall opinion.

3.3.4.1.3 Fitzpatrick skin type

The Fitzpatrick scale is a recognised numerical classification schema for human skin colour developed as a way to classify the typical response of different skin types to ultraviolet light[479]. Participants answer a series of questions pertaining to the colour of their eyes, hair, and skin and also the reaction of their skin when exposed to the sun.

3.3.4.2 Objective measurement tools

3.3.4.2.1 DSM II Colormeter

The DSM II Colormeter (Cortex Technology ApS, Denmark) is a small handheld device which combines two methods of quantifying colour: narrow-band spectrophotometry (melanin, erythema) and tristimulus reflectance colorimetry in a single measurement. These 2 colour systems were

previously explained in Chapter 2. The Colormeter consists of a probe which is made of a transparent dome which houses 2 white LED lights and a colour sensor has a skin measuring area of 4mm in diameter. Measurements were done by placing the probe over the selected areas on the scar. The probe is to be held perpendicular to the scar using minimal pressure to avoid blanching of the scar.

3.3.4.2.2 Scanoskin camera

The Scanoskin camera system (Leniomed Ltd, United Kingdom) is a new device which is a type of spectrophotometer which is a device that can measure a light beam's intensity as a function of its colour (wavelength).

The system consists of a standard DSLR camera, a polarising light filter, ring flash and Scanoskin software. The polarising light filter and ring flash produces a standard controlled lighting which illuminates the skin. Some of this light is reflected and scattered from the surface of the skin. This reflected light is captured with the Digital Single-Lens Reflex (DSLR) camera and the raw image is then processed by the Scanoskin software which then splits it into 2 images, one for melanin (pigment found in skin) and the other for haemoglobin (pigment found in red blood cells).

The following settings were used:

- Distance: 50cm
- Focus: Manual mode
- Aperture size: f/5.6 to f/6.0
- ISO= 100

The images were then analysed with the ImageJ software to quantify the amount of melanin and haemoglobin in the image.

The original image (Figure 18a) is first processed with the Scanoskin software which processes the image into a “Perfusion” (Figure 18b) and a “Pigment” (Figure 18c) image. The “Perfusion” image is used to quantify the erythema of the scar whereas the “Pigment” image is used to quantify the melanin in the scar.

The image is first inverted (thus darker pixel intensity will have higher values,). The Region Of Interest (ROI) is then traced using the Image-J software and then the Histogram function is used to give the mean pixel intensity. The ROI used for the Scanoskin is the larger 3cm square instead of the 1cm circle.

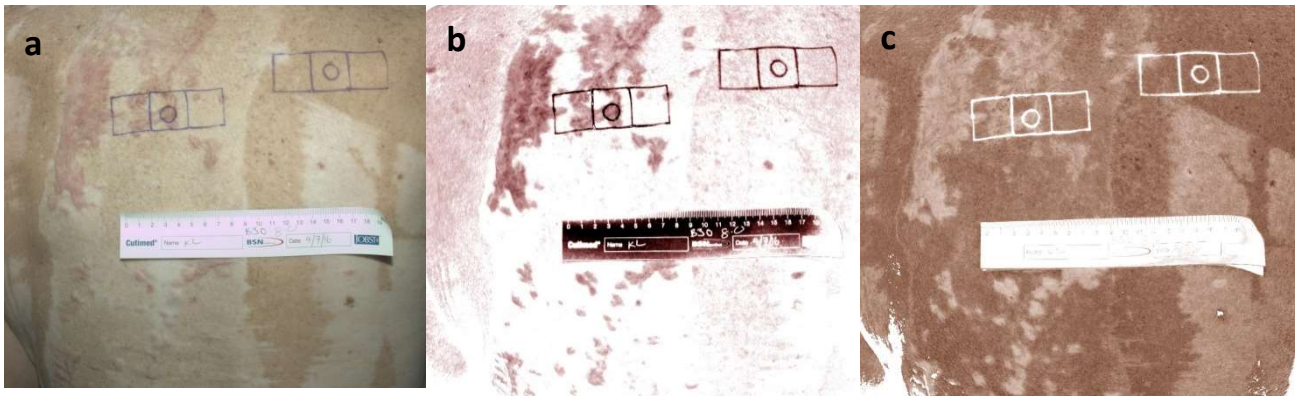

Figure 18: Scanoskin image processing**:** (a) Original photograph, (b) Perfusion image, (c) Pigment image.

3.3.4.2.3 Dermascan 20MHz high frequency ultrasound

The Dermascan C USB (Cortex Technology ApS, Denmark) is a high-frequency (20MHz) ultrasound scanner that enables the imaging of soft tissue at high resolution with a computer and comes with software that allows automated skin thickness measurement.

In the study, a medium focus transducer was used with a 12mm wide viewing field and penetration depth of 15mm. Before measurement, a thin layer of conducting ultrasound gel is applied to the transducer and the transducer is to be held perpendicular to the scar sites to record a single echographic image for each site. Mode 4 and a gain profile of 13 were set for all scans.

All measurements were performed with an ultrasound frequency set at 1580m/s. Thickness measurements are then generated by a single researcher with the provided dedicated software (Advance Control 6 Analysis SW package, Cortex). The B-mode is utilised to analyse the images[327]. This mode provides a two-dimensional ultrasound image display consisting of pixels with varying intensities to represent the amplitude of the returned echo signal. The thickness measured is

defined as the distance between the echogenic stratum corneum and the inner surface of the dermis (in millimetres). Normal dermis is highly echogenic due to the high amount of connective tissue and collagen[447]. Scar tissue appears hypoechoic compared to normal skin (Figure 19), and this may be due to the increased water content of scar tissue due to aberrant proteoglycan metabolism[447].

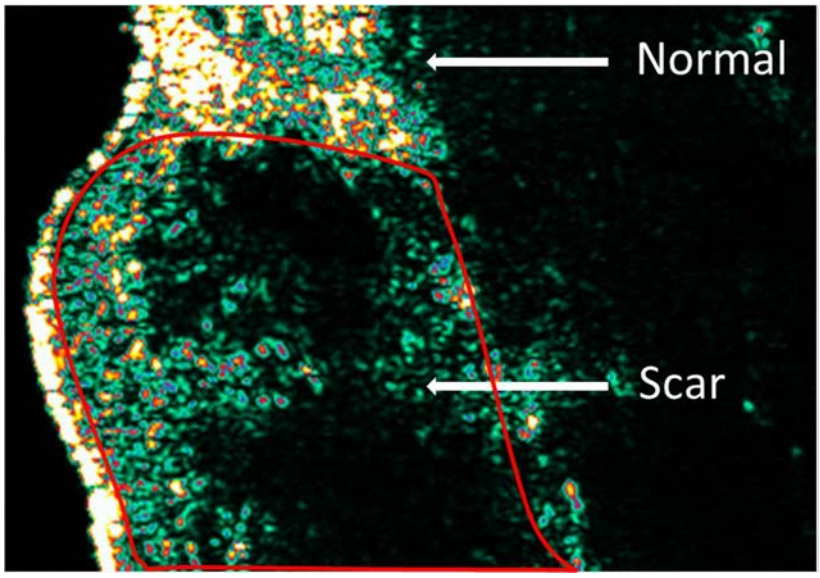

Figure 19: Dermascan ultrasound image of scar and normal skin. Normal skin has a higher ultrasound intensity compared to scar tissue (outlined in red).

3.3.4.2.4 Cutometer Elasticity probe

The Cutometer (MPA 580, Courage and Khazaka GmbH, Germany) is an electronic instrument that assesses skin elasticity. The probe of the device is placed over the area of measurement, which then generates a negative pressure that draws the skin into a hollow aperture in the centre of the probe and then uses a laser to estimate the amount of skin displacement.

The probe with a 6-mm diameter hollow aperture was chosen for this study as previous studies have determined it to be the most efficient size to measure the visco-elasticity properties of the dermis[243, 480, 481]. For this study, mode 1 was chosen. This delivers three cycles of negative air pressure (500 mbar) for 2 seconds, followed by 2 seconds of no pressure. Results are expressed as the means of the three measurement cycles.

The most commonly reported R-parameters, R0 and R2 were used in this study. R0 describes the maximum deformation (extension) of the skin. R2 is the ratio of the final retraction and the maximum deformation.

3.3.4.3 Histology

At the end of the three assessment cycles, a 3mm full thickness punch biopsy is obtained from the site of the assessed scar. The biopsy was optional for the patients thus not all patients had biopsy samples done after measurements. Skin biopsy samples were preserved in 10% formalin saline and paraffin embedded. The sections were prepared and stained by the technical staff at the Human Biomaterials Resource Centre (HBRC, University of Birmingham, UK). Assessment of the following parameters was performed:

1) Dermal thickness: Assessment of the dermal thickness was performed using biopsy sections stained with the Orcein stain. This allowed the differentiation between new scar dermis from the old uninjured dermis[482]. The 9 measurements per slide throughout the breadth of the biopsy sample were performed to enable the calculation of the average dermal thickness.

2) Vascularisation: Immunohistochemistry analysis to determine vascularisation was performed using antibodies to the vascular endothelial cell marker CD31. Images of the stained slides were analysed using the Definiens Tissue Studio version 2.0 (Munchen, Germany). The regions of interest (dermis only) were selected manually after segmentation of the image (up to 12 subsets). The following settings were then used: IHC threshold 0.35, gap to close set to 5µm to close small holes in the vessel wall. The vessel density is reported per mm^2. Only vessels with lumens were quantified.

3) Pigmentation: Assessment of melanin pigmentation was performed using Fontana-Masson staining. The technique described by Billings et al[483] (2015) was used to analyse melanin pigmentation. Images of the stained slides were taken at x20 magnification and three sections of the epidermis where imaged per biopsy sample (total length analysed ~2500µm per sample). The GIMP (GNU Image Manipulation Program, GIMP Development team) open source graphics editor was used

to specifically extract the pixels associated with pigment staining from the photomicrographs (Figure 20). The Image J image processing program, version 50 (National Institutes of Health, Maryland, USA) was then used to quantify the pixels.

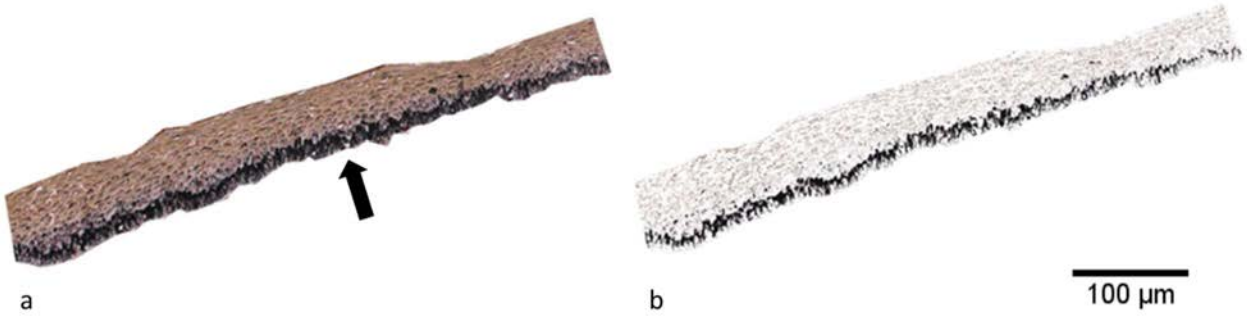

Figure 20: Fontana-Masson staining for melanin pigmentation**.** (a) Melanin pigmentation rich keratinocytes can be seen at the basal layer of the epidermis (arrow). (b) Melanin pixel extraction using the GIMP graphics editor for further analysis with the ImageJ program. (Note that the stratum corneum and dermis have been removed during image extraction process to ease analysis.)

3.3.4.4 Patient satisfaction with devices questionnaire

At the end of the session, patients were asked to score each of the devices that have been used in the trial in terms of overall satisfaction, comfort, and time taken to measure scar; using a 5 point scale, rating levels from very poor to very good is given (Table 8).

Table 8: Patient satisfaction with devices questionnaire.

	Very poor	Poor	OK	Good	Very Good
Overall satisfaction	□	□	□	□	□
Comfort	□	□	□	□	□
Time taken to measure scar	□	□	□	□	□
Would you be happy for your clinician to use this device on you in the future?					(Yes / No)
Additional comments					

Additionally, patients were also be asked to rank the different scar parameters (Surface area, thickness, colour (erythema and pigmentation), pliability, and pain/itch in terms of importance to them, with 1 being the most important, to 6 being the least important to them.

3.4 Statistical analysis

All statistical analyses of the data were performed using IBM SPSS Statistics, version 23 (IBM Corporation, New York, USA). P values of <0.05 are considered to signify statistical significance.

3.4.1 Sample size

The primary outcome is the intra and inter-reliability of a panel of objective scar measurement devices. After a search of the available literature, the lowest ICC value among our panel of devices (that was published,) was for the Cutometer. The results from a trial by Draaijers et al[394] (2004) showed that the single ICC for the Extension parameter (R0) was 0.74 (95% CI 0.63-0.87). To estimate 95% CI for the ICC with an interval no greater than 0.2, according to the methods in Shoukri et al[484] (2004), the required sample size is a minimum of 54 subjects.

3.4.2 Reliability

Reliability of a measurement refers to the consistency of the data when the same trait is measured by the same assessor (intra-rater reliability) or by different assessors (inter-rater reliability) with the same measurement device.

The intra- and inter-rater reliability of the objective (DSM II Colormeter, Cutometer, Dermascan, Scanoskin) and subjective measurement tools (total mVSS and POSAS Scores; sum of pliability, height, and vascularity subscales) were examined via the Intraclass Correlation Coefficient (ICC) with its 95% Confidence Interval (CI). P-values are not typically reported for the ICC. The ICC (2,3) was computed as per Shrout and Fleiss[485] based on the two-way random effect analysis of variance model and the absolute agreement type were selected for ICC calculations. The two-way random effect method was selected as the raters in this study are consistent (i.e. the same three raters throughout the study) and are a sample of raters (rather than a fixed population).

The ICC can be reported as a "single measure ICC" or an "average measure ICC". The single measure ICC is based on a randomly taken single measurement and is equivalent to the reliability of a measurement carried out by a single observer. The average measure ICC is based on the average measurements of three observers and thus is equivalent to the reliability of a measurement carried out by three observers. An ICC value of 0.70 was selected as the minimal threshold requirement for measurements to be deemed reliable (based on previous similar studies[394]).

In addition to the ICC, the Standard Error of Mean (SEM) and the Coefficient of variation ([CV=Standard error/mean] x 100) are also reported. The CV is used to allow comparison of the standard error of measurements between the different devices.

As the POSAS subscales are rated from 1 to 10 (and ordered,), they can be treated as a continuous variable and hence the ICC is used to calculate the reliability. For the mVSS subscales, as the scoring is categorical, the Fleiss kappa[486] was used (instead of the Cohen's kappa which is only suitable for 2 raters). The reliability of the total score of the mVSS however was calculated using the ICC as it is the sum of the scores and can be viewed as a continuous variable.

3.4.3 Concurrent validity

Concurrent validity is a term that describes the extent to which the results of a particular measurement corresponds (or correlates) to an accepted and established measure that is measuring the same trait[487].

The Spearman's ρ correlation coefficient was used to calculate the concurrent validity between the subjective assessments of erythema, pigmentation, pliability and thickness with the relevant objective assessments. Average values of the measurements of the three assessors were used for the correlation calculations of the DSM II Colormeter, Dermascan, Cutometer and Scanoskin camera. The two-tailed significance criterion for the correlation measurements was set at 0.05.

The range of the spearman rho ranges from -1 to +1, a positive correlation indicates a positive relationship between two variables while a negative one expresses a negative relationship. The closer the rho value to -1/+1, the stronger the relationship, and we have defined the ranges as follows: 0.00-0.19 denotes a “very weak” relationship, 0.20-0.39 “weak”, 0.40-0.59 “moderate”, 0.60-0.79 “strong”, and 0.80-1.0 “very strong”. Receiving Operating Characteristic Area Under the Curve (ROC AUC) curves were generated using the mVSS individual subscales as a “gold standard” comparator to determine the sensitivity and specificity of the corresponding objective parameters. The Youdens index was then utilised to ascertain the cut-off values for each objective parameter to distinguish between hypertrophic scars from normal skin and non-hypertrophic scars. These cut-off values were then used to dichotomise the objective parameters and the Chi-square (X^2) test was performed for the dichotomised parameters against the total mVSS score to select the best performing objective parameters to form a combination objective score. The discriminatory power of these various combinations to differentiate between hypertrophic scars (with a total mVSS score of 6 or more) and normal skin and non-hypertrophic scars were then assessed using the ROC AUC.

3.5 Results

3.5.1 Demographics

In total, 55 participants were successfully recruited for this study. There were 37 males and 18 females, with an average age of 46 years (range: 17-77 years). The majority of participants were Caucasian (82%). The demographics of the participants and the clinical characteristics of the scar sites chosen for evaluation are reported in Table 9.

Most of the participants were male (67.2%) with a mean age of 46 years and a mean total body surface area (TBSA) burned of 16.5%. The scars were measured an average of 14.6 months after time of 95% healing (which was calculated as 7 days after the last grafting procedure unless there is evidence in the patient records of delayed healing,). The most commonly measured scar area was on

the upper limb (41.8%) and the most common cause of scars in our cohort were flame burns (58.2%).

Table 9: Demographics of participants and clinical characteristics of the scar sites chosen for evaluation.

Clinical characteristics		n=55
Gender	**Female**	18
	Male	37
	Age (Mean ±SD)	46 ±17.8 years
	Range	17-77
TBSA of burn injury		
	Mean ±SD	16.5 ±18.2%
	Range	0.50-60.0%
Age of Scar (Months after burn)		
	Mean ±SD	14.6 ±10.9
	Range	2-43
Aetiology		
	Flame	32
	Scald	16
	Contact	5
	Electrical	2
Location		
	Upper limb	23
	Lower limb	12
	Chest	2
	Abdomen	13
	Back	5
Fitzpatrick skin type		
	I	1
	II	11
	III	14
	IV	18
	V	11
	VI	0

3.5.2 Subjective Scar Scales

The ICC and kappa values for the mVSS and POSAS scores are presented in Tables 10 and 11. The total score of the mVSS (Pliability + Height + Vascularity + Pigmentation) and the POSAS (Vascularity + Pigmentation + Thickness + Relief + Pliability + Surface area) are the sums of the individual subscales. As both the mVSS and POSAS requires the comparison of the evaluated site (scar site)

with the normal skin, the ICC of these two scores for normal skin cannot be evaluated as there should be total agreement. Additionally, the intra-rater kappa and ICC values also could not be performed as each assessor only completed the subjective scores once. This was because all assessments for the patients had to be completed in the same day and the subjective scores would be heavily influenced by recall bias. Analyses of both the total scores as well as the individual subscales were performed.

For the mVSS, the kappa values for all the subscales of pliability, height, vascularity and pigmentation all fell well below the study set threshold of 0.70, with the lowest being for pigmentation (-0.02) (Table 11). A low or negative kappa score (0—0.10) indicates "no agreement"[488]. Further analyses were performed to investigate the source of the disagreement by calculating the kappa values between assessor pairs. The single and average ICC scores for the mVSS Total score performed better than the subscales, with a value of 0.415 and 0.68 but still remained below the acceptable threshold (Table 10). There was a general disagreement between the assessors with all paired kappa values remaining below the threshold, however the highest disagreement occurred between Assessor 3 with Assessors 1 and 2 (Table 12). For the POSAS score, the ICC (Single) values for the Total score and the individual subscales all fall below the 0.70 threshold with the lowest score being for Surface area (0.003). The POSAS however performs better with higher reliability scores compared with the mVSS in the corresponding subscales: mVSS Pliability versus POSAS Pliability (0.149; 0.384), mVSS Height versus POSAS Thickness (0.031; 0.492); mVSS Vascularity versus POSAS Vascularity (0.241; 0.646) and mVSS Pigmentation versus POSAS Pigmentation (-0.02; 0.304). The ICC scores of the Total scores for both mVSS and POSAS were similar (0.415 versus 0.438). The removal of the subscale with the lowest reliability (Surface area) improved the ICC (Single) value of the POSAS Total score but not enough to reach the acceptable threshold (ICC Single=0.528). The ICC (Average, three assessors) for the POSAS individual subscales and Total score showed improved reliability compared to the ICC (Single) with the Vascularity, Thickness subscales and Total scores showing ICC values above the set threshold for acceptability or

close to the threshold (Relief, Pliability, Overall subscales). However, other subscales (Pigmentation and Surface area) were still below the acceptable limit. Further analyses were then performed to investigate if the ICC (Average) of two assessors were equivalent or similar to three assessors, however as Table 13 shows, the ICC (Average) of three assessors for the subscales and Total score were better compared to two assessors.

Table 10: Inter-rater reliability values for the mVSS individual subscales.

	Subscale	ICC(Single)	(95% CI)	ICC(Average)	(95% CI)	CV%
mVSS	Total	0.415	(0.249-0.578)	0.680	(0.499-0.804)	47.3 (0.82)
POSAS	Vascularity	0.646	(0.511-0.761)	0.846	(0.758-0.905)	41.0 (0.60)
	Pigmentation	0.304	(0.139-0.478)	0.568	(0.327-0.733)	45.2 (0.78)
	Thickness	0.492	(0.298-0.656)	0.744	(0.561-0.851)	44.1 (0.84)
	Relief	0.359	(0.144-0.553)	0.627	(0.335-0.788)	45.2 (0.89)
	Pliability	0.384	(0.207-0.556)	0.652	(0.439-0.790)	44.1 (0.86)
	Surface area	0.003	(-0.033-0.059)	0.008	(-0.106-0.158)	47.3 (1.04)
	Overall	0.394	(0.148-0.600)	0.661	(0.342-0.818)	46.2 (0.69)
	Total	0.438	(0.174-0.642)	0.700	(0.387-0.843)	46.2 (2.92)

Table 11: Inter-rater reliability values for the mVSS total score, POSAS subscale and total scores.

	Subscale	Kappa	(95% CI)	CV%
mVSS	Pliability	0.149	(0.063-0.234)	49.4 (0.41)
	Height	0.031	(-0.74-0.135)	42.1 (0.36)
	Vascularity	0.241	(0.135-0.347)	31.5 (0.25)
	Pigmentation	-0.02	(-0.119-0.079)	46.2 (0.47)

Table 12: Comparison of paired Fleiss kappa values with multiple combinations of assessors**.** A1=Assessor 1, A2=Assessor 2, A3=Assessor 3.

	Fleiss kappa values		
mVSS subscale	**A1 and A2**	**A1 and A3**	**A2 and A3**
Pliability	0.132	0.155	0.128
Height	0.286	-0.091	-0.128
Vascularity	0.190	0.291	0.210
Pigmentation	0.093	-0.003	-0.254
Average kappa	0.175	0.088	-0.011

The single measure inter-rater reliability scores for both the mVSS and POSAS total and subscale scores all fell below the 0.70 threshold which means that they are poorly reproducible if done by only 1 assessor. However with three assessors (average measure), an improvement in the reproducibility of most of the scores is seen although some scores remain below the accepted threshold. This finding agrees with previous studies which also showed poor reliability for the subjective scores[208, 263]. Nedelec et al (2008) noted that the low reliability for the mVSS could be due to the small scale range where a small amount of disagreement could have a substantial impact[263]. The finding of increased reliability scores for the POSAS (which has a rating scale of 1 to 10) compared to the mVSS supports this hypothesis.

Table 13: The ICC (Average) of two assessors versus three assessors. The ICC (Average) of three assessors for the subscales and Total score were better compared to two assessors.

	ICC (Average)	
POSAS subscales	Two assessors	Three assessors
Vascularity	0.78	0.85
Pigmentation	0.41	0.57
Thickness	0.65	0.74
Relief	0.54	0.63
Pliability	0.55	0.65
Surface area	-0.03	0.01
Overall	0.57	0.66
Total	0.61	0.70

3.5.3 DSM II Colormeter: Erythema and Pigmentation

3.5.3.1 Erythema measurements

Erythema can be measured with the DSM II a* and the narrow band Erythema parameters. The inter- and intra-rater ICC values for the a* and narrow band Erythema parameters can be seen in Tables 14-16.

The a* value was found to have acceptable and good inter- (ICC [Single, Average] =0.718, 0.884) and intra-rater (Average ICC [Single, Average] =0.73, 0.87) ICC values for scar tissue. The ICC single value for the a* measurement of normal skin however was considerably lower compared to scar tissue (ICC=0.595 versus 0.718) although the average ICC values were comparable (ICC=0.815 versus 0.884). When this is analysed in more detail by looking at the intra-rater ICC values for the individual assessors, it can be seen that this reduction in ICC is likely to be due to the reduced reliability of the measurements by Assessor 2 (a* ICC value [Single]=0.398 versus 0.875 for Assessor 1 and 0.920 for Assessor 3). When the ICC measurements were analysed in pairs rather than all three assessors, the lowest ICC values were found with the pairings involving Assessor 2 (A1 and A2 ICC [Single]=0.570; A2 and A3 ICC [Single]= 0.676) versus the A1 and A3 pair (ICC [Single]=0.901).

The narrow band Erythema value was also found to have acceptable and good inter- (ICC [Single, Average] =0.777, 0.912) and intra-rater ICC values (Average ICC [Single, Average] =0.73, 0.87) for scar tissue. Similar to the a* value for normal skin, the ICC of the Erythema measurement for normal skin (ICC [Single] =0.647) was lower than that of scar tissue (ICC [Single] =0.777). As with the a* value, when analysed in pairs, the lowest ICC value was found between with the pairings involving Assessor 2 (ICC [Single] =0.673-0.733). Of the two erythema measures, both the a* and narrow band Erythema measure have similar inter- and intra-rater reliability values as well as %CV, thus both are recommended. However, for erythema measurements on normal skin, more than 1 measurement should be taken to improve reliability.

Table 14: Inter-rater reliability values for the erythema measures of the DSM II Colormeter for scar tissue and normal skin.

	Scar tissue		**Normal skin**	
Measure	a*	Erythema	a*	Erythema
Single ICC (95% CI)	0.718 (0.601-0.813)	0.777 (0.678-0.854)	0.595 (0.424-0.732)	0.647 (0.488-0.769)
Average ICC (95% CI)	0.884 (0.819-0.929)	0.912 (0.863-0.946)	0.815 (0.689-0.891)	0.846 (0.741-0.909)
%CV (SEM)	9.65 (0.83)	9.45 (0.73)	13.77 (1.09)	14.5 (0.90)

Table 15: Intra-rater reliability values for the DSM II Colormeter a* and Erythema parameters for scar tissue. A1=Assessor 1, A2=Assessor 2, A3=Assessor 3.

Single measure-Scar tissue							
Parameter	A1	95% CI	A2	95% CI	A3	95% CI	Average
a*	0.875	(0.813-0.920)	0.398	(0.233-0.561)	0.920	(0.878-0.949)	0.73
Erythema	0.888	(0.832-0.929)	0.423	(0.260-0.582)	0.902	(0.852-0.938)	0.74
Average Measure- Scar tissue							
Parameter	A1	95% CI	A2	95% CI	A3	95% CI	Average
a*	0.954	(0.929-0.972)	0.670	(0.477-0.793)	0.972	(0.956-0.983)	0.87
%CV (SEM)	8.36	(0.72)	15.42	(1.39)	5.71	(0.51)	9.83
Erythema	0.960	(0.937-0.975)	0.688	(0.513-0.807)	0.965	(0.945-0.978)	0.87
%CV (SEM)	8.39	(0.67)	14.82	(1.27)	6.89	(0.57)	10.03

Table 16: Intra-rater reliability values for the DSM II Colormeter a* and Erythema parameters for normal skin. A1=Assessor 1, A2=Assessor 2, A3=Assessor 3.

Single measure-Normal Skin							
Parameter	A1	95% CI	A2	95% CI	A3	95% CI	Average
a*	0.915	(0.871-0.946)	0.508	(0.352-0.653)	0.952	(0.926-0.970)	0.79
Erythema	0.956	(0.933-0.973)	0.444	(0.283-0.600)	0.977	(0.964-0.985)	0.79
Average measure- Normal Skin							
Parameter	A1	95% CI	A2	95% CI	A3	95% CI	Average
a*	0.970	(0.953-0.981)	0.756	(0.620-0.849)	0.983	(0.974-0.990)	0.90
%CV (SEM)	8.22	(0.61)	14.53	(1.31)	5.53	(0.36)	9.43
Erythema	0.985	(0.976-0.991)	0.706	(0.542-0.818)	0.992	(0.988-0.995)	0.89
%CV (SEM)	7.86	(0.42)	13.76	(1.06)	5.16	(0.26)	8.93

3.5.3.2 Pigmentation measurements

Pigmentation can be measured with the DSM II L*, b* and the narrow band Melanin parameters.

The inter- and intra-rater ICC values for the L*, b* and narrow band Melanin parameters can be seen in Tables 17-19.

Table 17: Inter-rater reliability ICC values of the pigmentation measures for the DSM II Colormeter for scar tissue and normal skin.

	Scar tissue			**Normal skin**		
Measure	L*	b*	Melanin	L*	b*	Melanin
Single ICC (95% CI)	0.942 (0.908-0.964)	0.525 (0.370-0.666)	0.930 (0.893-0.956)	0.806 (0.576-0.903)	0.351 (0.178-0.523)	0.836 (0.677-0.909)
Average ICC (95% CI)	0.980 (0.967-0.988)	0.768 (0.638-0.857)	0.975 (0.962-0.985)	0.926 (0.803-0.965)	0.618 (0.393-0.767)	0.939 (0.873-0.968)
%CV (SEM)	6.14(0.88)	32.58 (1.09)	4.06 (1.13)	8.10 (1.63)	32.19(1.60)	6.69 (1.43)

The L* value was found to have very good inter- (ICC [Single, Average] =0.942, 0.980) and intra-rater (Average ICC [Single, Average] =0.90, 0.97) ICC values for scar tissue. The inter-and intra-rater for the L* value for normal skin, although lower, were also all above the set threshold of 0.70 (ICC [Single, Average] =0.806, 0.926). The narrow band Melanin value for scars was also found to have good inter- (ICC [Single, Average] =0.930, 0.975) and intra-rater (Average ICC [Single, Average] =0.93, 0.97) ICC values for scar tissue. The inter-and intra-rater for the Melanin value for normal skin were also similarly high with inter-rater values of 0.836 (ICC Single) and 0.939 (ICC Average); and intra-rater values of 0.90 (ICC Single) and 0.96 (ICC Average). The b* value however performed the worst out of the three objective pigmentation measures. The b* value for scar tissue had a moderate but below threshold inter-rater ICC (Single) value of 0.525, but acceptable ICC (Average) value of 0.768 for scar tissue, although this is with a high %CV of 32.58%. The b* parameter was also found to be prone to significantly aberrant readings as can be seen from the %CV of Assessor 1 in Table 19. The b* intra-rater ICC (Single) value for scar tissue was just below the threshold (ICC Single=0.64) but the ICC (Average) was considered very good (ICC Average=0.82). Both the inter- and intra-rater values of the b* measure were all below the acceptable threshold for normal skin except for the average ICC

which was very good (0.80). Therefore, the L* and narrow band Melanin are both recommended but not the b* measure.

Table 18: Intra-rater reliability values for the DSM II Colormeter pigmentation measures for scar tissue. A1=Assessor 1, A2=Assessor 2, A3=Assessor 3.

Single measure-Scar							
Parameter	A1	95% CI	A2	95% CI	A3	95% CI	Average
L*	0.924	(0.884-0.952)	0.847	(0.774-0.902)	0.941	(0.910-0.963)	0.90
b*	0.729	(0.615-0.820)	0.368	(0.202-0.536)	0.814	(0.728-0.879)	0.64
Melanin	0.902	(0.851-0.938)	0.914	(0.869-0.946)	0.962	(0.98--0.992)	0.93
Average measure- Scar							
Parameter	A1	95% CI	A2	95% CI	A3	95% CI	Average
L*	0.973	(0.958-0.984)	0.943	(0.911-0.965)	0.98	(0.968-0.987)	0.97
%CV (SEM)	6.76	(1.00)	8.62	(1.23)	5.22	(0.80)	6.87
b*	0.890	(0.827-0.932)	0.636	(0.431-0.776)	0.929	(0.889-0.956)	0.82
%CV (SEM)	115.43	(0.92)	44.06	(1.57)	20.47	(0.66)	59.84
Melanin	0.965	(0.945-0.979)	0.970	(0.952-0.981)	0.987	(0.980-0.992)	0.97
%CV (SEM)	4.98	(1.35)	4.81	(1.30)	3.47	(0.91)	4.42

Table 19: Intra-rater reliability values for the DSM II Colormeter pigmentation measures for normal skin. A1=Assessor 1, A2=Assessor 2, A3=Assessor 3.

Single measure-Normal Skin							
Parameter	A1	95% CI	A2	95% CI	A3	95% CI	Average
L*	0.914	(0.871-0.946)	0.815	(0.729-0.880)	0.976	(0.963-0.985)	0.90
b*	0.656	(0.524-0.767)	0.319	(0.152-0.491)	0.890	(0.835-0.930)	0.62
Melanin	0.888	(0.831-0.930)	0.845	(0.771-0.900)	0.975	(0.961-0.984)	0.90
Average measure- Normal Skin							
Parameter	A1	95% CI	A2	95% CI	A3	95% CI	Average
L*	0.970	(0.953-0.981)	0.930	(0.890-0.957)	0.992	(0.987-0.995)	0.96
%CV (SEM)	5.17	(1.05)	7.96	(1.52)	2.46	(0.53)	5.20
b*	0.851	(0.767-0.908)	0.584	(0.350-0.743)	0.960	(0.938-0.976)	0.80
%CV (SEM)	-234.10	(1.24)	34.21	(1.82)	8.24	(0.47)	-63.88
Melanin	0.960	(0.937-0.975)	0.942	(0.910-0.964)	0.992	(0.987-0.995)	0.96
%CV (SEM)	5.11	(1.07)	7.34	(1.54)	2.56	(0.51)	5.00

3.5.4 Scanoskin camera: Erythema and Pigmentation

Due to technical difficulties and errors in the flash power (resulting in photo underexposure), only 31 of the patients had Scanoskin camera photos which were analysable (B25 to B55). The inter- and intra-rater ICC values for the Scanoskin erythema and melanin parameters can be seen in Tables 20-22. The Scanoskin erythema measure had very good reliability values for both inter- (ICC [Single, Average] =0.969, 0.972) and intra-rater (ICC [Single, Average] =0.995, 0.998) ICC values for scar tissue. The Scanoskin erythema measure for normal skin also had slightly lower but similarly very good inter- (ICC [Single, Average] =0.926, 0.974) and intra-rater (ICC [Single, Average] =0.985, 0.995) ICC values. The same trend was seen with the Scanoskin pigmentation measure, with analyses showing very good inter- (ICC [Single, Average] =0.972, 0.991) and intra-rater (ICC [Single, Average] =0.989, 0.996) ICC values for scar tissue as well as normal skin, inter-rater (ICC [Single, Average] =0.957, 0.985); intra-rater (ICC [Single, Average] =0.994, 0.997). Both Scanoskin measures are thus recommended.

Table 20: Inter-rater reliability values of the erythema and pigmentation measures for the Scanoskin system for scar tissue and normal skin.

	Scar tissue		**Normal skin**	
Measure	Erythema	Pigmentation	Erythema	Pigmentation
Single ICC (95% CI)	0.969 (0.944-0.984)	0.972 (0.951-0.986)	0.926 (0.871-0.961)	0.957 (0.925-0.978)
Average ICC (95% CI)	0.989 (0.981-0.994)	0.991 (0.983-0.995)	0.974 (0.953-0.987)	0.985 (0.974-0.992)
%CV (SEM)	8.55 (3.32)	6.34 (2.59)	18.05 (2.78)	4.42 (2.43)

Table 21: Intra-rater reliability values for the Scanoskin camera for scar tissue. A1=Assessor 1, A2=Assessor 2, A3=Assessor 3.

Single measure-Scar							
Parameter	A1	95% CI	A2	95% CI	A3	95% CI	Average
Erythema	0.994	(0.986-0.998)	0.995	(0.987-0.998)	0.996	(0.985-0.998)	0.995
Pigmentation	0.979	(0.955-0.990)	0.994	(0.963-0.998)	0.994	(0.974-0.998)	0.989
Average measure-Scar							
Parameter	A1	95% CI	A2	95% CI	A3	95% CI	Average
Erythema	0.998	(0.995-0.999)	0.998	(0.996-0.999)	0.999	(0.995-0.999)	0.998
%CV (SEM)	2.87	(1.03)	3.84	(1.26)	3.60	(1.17)	3.44
Pigmentation	0.993	(0.955-0.990)	0.998	(0.987-0.999)	0.998	(0.991-0.999)	0.996
%CV (SEM)	3.15	1.23	3.75	1.45	2.86	(1.17)	3.25

Table 22: Intra-rater reliability values for the Scanoskin camera for normal skin. A1=Assessor 1, A2=Assessor 2, A3=Assessor 3.

Single measure-Normal skin							
Parameter	A1	95% CI	A2	95% CI	A3	95% CI	Average
Erythema	0.982	(0.962-0.991)	0.987	(0.971-0.994)	0.985	(0.966-0.993)	0.985
Pigmentation	0.981	(0.940-0.992)	0.992	(0.962-0.997)	0.988	(0.945-0.996)	0.994
Average measure-Normal skin							
Parameter	A1	95% CI	A2	95% CI	A3	95% CI	Average
Erythema	0.994	(0.987-0.997)	0.996	(0.990-0.998)	0.995	(0.988-0.998)	0.995
%CV (SEM)	11.46	(1.25)	9.72	(1.08)	9.94	(1.19)	10.37
Pigmentation	0.994	(0.979-0.997)	0.997	(0.987-0.999)	0.996	(0.981-0.999)	0.997
%CV (SEM)	2.64	(1.41)	2.08	(1.11)	2.29	(1.23)	2.34

3.5.5 Dermascan ultrasound: Dermal thickness and intensity

The inter- and intra-rater ICC values for the Dermascan ultrasound dermal thickness and intensity measures are shown in Tables 23-25. Dermascan measured dermal thickness had very good inter- (ICC [Single, Average] =0.957, 0.985) and intra-rater (ICC [Single, Average]=0.951, 0.983) for scar tissue. The dermal thickness measure for normal skin also had similarly very good inter- (ICC [Single, Average] =0.967, 0.989) and intra-rater (ICC [Single, Average] =0.948, 0.982).The Dermascan measured dermal intensity likewise had very good inter- (ICC [Single, Average] =0.918, 0.971) and intra-rater (ICC [Single, Average]=0.928, 0.937) for scar tissue. The dermal intensity measure for normal skin also had similarly very high inter- (ICC [Single, Average] =0.863, 0.950) and intra-rater (ICC [Single, Average] =0.931, 0.976). Although both Dermascan measured dermal thickness and intensity had similarly high ICC values and are thus both recommended, the %CV values for Dermal intensity are higher compared to that for Dermal thickness for both scar (16.4% versus 6.79%) and normal skin (15.9% versus 5.13%).

Table 23: Inter-rater reliability values for the Dermascan ultrasound Thickness and Intensity measurements for scar tissue and normal skin.

	Scar tissue		**Normal skin**	
Measure	Dermal thickness	Dermal Intensity	Dermal thickness	Dermal Intensity
Single ICC (95% CI)	0.957 (0.934-0.973)	0.918 (0.874-0.948)	0.967 (0.949-0.980)	0.863 (0.796-0.912)
Average ICC (95% CI)	0.985 (0.977-0.991)	0.971 (0.954-0.982)	0.989 (0.982-0.993)	0.950 (0.921-0.969)
%CV (SEM)	6.79 (0.10)	16.4 (0.90)	5.13 (0.04)	15.9 (2.42)

Table 24: Intra-rater reliability values for the Dermascan for scar tissue. A1=Assessor 1, A2=Assessor 2, A3=Assessor 3.

Single measure-Scar							
Parameter	A1	95% CI	A2	95% CI	A3	95% CI	Average
Dermal thickness	0.959	(0.937-0.975)	0.915	(0.871-0.946)	0.979	(0.968-0.987)	0.951
Dermal intensity	0.922	(0.881-0.951)	0.904	(0.947-0.979)	0.959	(0.937-0.974)	0.928
Average measure-Scar							
Parameter	A1	95% CI	A2	95% CI	A3	95% CI	Average
Dermal thickness	0.986	(0.978-0.991)	0.970	(0.953-0.981)	0.993	(0.989-0.996)	0.983
%CV (SEM)	6.90	(0.10)	10.04	(0.15)	5.07	(0.07)	7.34
Dermal intensity	0.972	(0.957-0.983)	0.966	(0.947-0.979)	0.986	(0.978-0.991)	0.937
%CV (SEM)	14.90	(0.82)	15.95	(1.00)	10.20	(0.61)	13.68

Table 25: Intra-rater reliability values for the Dermascan for normal skin. A1=Assessor 1, A2=Assessor 2, A3=Assessor 3.

Single measure-Normal skin							
Parameter	A1	95% CI	A2	95% CI	A3	95% CI	Average
Dermal thickness	0.962	(0.941-0.976)	0.916	(0.873-0.947)	0.966	(0.948-0.979)	0.948
Dermal intensity	0.943	(0.913-0.964)	0.904	(0.855-0.939)	0.946	(0.918-0.966)	0.931
Average measure- Normal skin							
Parameter	A1	95% CI	A2	95% CI	A3	95% CI	Average
Dermal thickness	0.987	(0.980-0.992)	0.97	(0.954-0.982)	0.989	(0.982-0.993)	0.982
%CV (SEM)	5.21	(0.04)	5.95	(0.05)	4.88	(0.04)	5.35
Dermal intensity	0.98	(0.969-0.988)	0.966	(0.947-0.979)	0.981	(0.971-0.989)	0.976
%CV (SEM)	12.31	(1.71)	15.03	(2.00)	10.53	(1.59)	12.62

3.5.6 Cutometer: R0 and R2 measurements

Cutometer measurements were only available for 54 patients as 1 patient did not have enough time during the session for the Cutometer measurement. The inter- and intra-rater ICC values for the Cutometer R0 and R2 measures are shown in Tables 26-28. The R0 measure had good and acceptable inter- (ICC [Single, Average] =0.715, 0.883) and intra-rater ICC values (ICC [Single, Average] =0.80, 0.92) for scar tissue. The R0 intra-rater ICC values for normal skin was also acceptable (ICC [Single, Average] =0.85, 0.94) but only the ICC (Average) of the R0 inter-rater ICC was above the set threshold (ICC Average =0.827) but not the ICC Single (ICC Single =0.615). In contrast to the R0 value, the R2 measure for scar tissue only had acceptable Average Inter-rater ICC (ICC Average=0.780) and intra-rater (ICC Average =0.79) values but its Single Inter-rater ICC (ICC Single

=0.542) and Intra-rater (ICC Single =0.58) values were all below the acceptable threshold. Both the single inter- (ICC Single =0.510) and intra-rater (ICC Single =0.52) ICC values for the R0 measure for normal skin were below the threshold but the average inter- (ICC Average =0.758) and intra-rater (ICC Average =0.76) ICC values reached acceptable levels. The R0 measure is thus recommended over the R2 measure.

Table 26: Inter-rater reliability values for the Cutometer R0 and R2 measures for scar tissue and normal skin.

	Scar tissue		**Normal skin**	
Measure	R0	R2	R0	R2
Single ICC (95% CI)	0.715 (0.522-0.834)	0.542 (0.385-0.683)	0.615 (0.373-0.772)	0.510 (0.348-0.660)
Average ICC (95% CI)	0.883 (0.766-0.938)	0.780 (0.653-0.866)	0.827 (0.641-0.910)	0.758 (0.616-0.853)
%CV (SEM)	17.15 (0.06)	7.84 (0.03)	14.74 (0.09)	5.90 (0.03)

Table 27: Intra-rater reliability values for the Cutometer for scar tissue. A1=Assessor 1, A2=Assessor 2, A3=Assessor 3.

Single measure-Scar							
Parameter	A1	95% CI	A2	95% CI	A3	95% CI	Average
R0	0.661	(0.529-0.772)	0.854	(0.782-0.907)	0.888	(0.829-0.930)	0.80
R2	0.392	(0.225-0.557)	0.648	(0.509-0.764)	0.708	(0.586-0.807)	0.58
Average measure-Scar							
Parameter	A1	95% CI	A2	95% CI	A3	95% CI	Average
R0	0.854	(0.771-0.910)	0.946	(0.915-0.967)	0.960	(0.936-0.976)	0.92
%CV (SEM)	15.90	(0.06)	11.98	(0.04)	11.98	(0.03)	13.29
R2	0.659	(0.465-0.791)	0.846	(0.757-0.907)	0.879	(0.809-0.926)	0.79
%CV (SEM)	10.11	(0.04)	7.62	(0.03)	5.95	(0.03)	7.89

Table 28: Intra-rater reliability values for the Cutometer for normal skin. A1=Assessor 1, A2=Assessor 2, A3=Assessor 3.

Single measure-Normal skin							
Parameter	A1	95% CI	A2	95% CI	A3	95% CI	Average
R0	0.886	(0.828-0.928)	0.785	(0.687-0.862)	0.881	(0.820-0.925)	0.85
R2	0.524	(0.368-0.667)	0.378	(0.206-0.551)	0.672	(0.534-0.783)	0.52
Average measure- Normal skin							
Parameter	A1	95% CI	A2	95% CI	A3	95% CI	Average
R0	0.959	(0.935-0.975)	0.916	(0.868-0.949)	0.957	(0.932-0.974)	0.94
%CV (SEM)	7.44	(0.05)	9.28	(0.06)	7.20	(0.04)	7.97
R2	0.768	(0.636-0.857)	0.646	(0.438-0.786)	0.860	(0.775-0.916)	0.76
%CV (SEM)	7.16	(0.03)	9.77	(0.04)	5.12	(0.02)	7.35

Previous studies have shown both low[243, 263] and high reliability[212] values for the Cutometer. In studies that have shown low inter-rater reliability values, this was thought to be due to scars with high rigidity[263] however in the study by Nedelec et al (2008) this was found to be only true for the R0 value where the normal skin R0 ICC value was higher than the scar tissue R0 ICC value. The R2 value for normal skin (ICC=0.55) was however lower than the R2 value for severe scar tissue (ICC=0.71) in that study.

We further analysed our data by dividing the group into scars with mVSS Pliability scores of $\leq$2 and above 2 (Table 29). The inter-rater R0 ICC values for normal scars (ICC [Single, Average] =0.718, 0.884) were better compared to the firmer hypertrophic scars (ICC [Single, Average] =0.568, 0.798). A similar trend was seen for the R2 parameter, with lower inter-rater R2 ICC values for hypertrophic scars compared to non-hypertrophic scars (Single [0.294 versus 0.567]; Average [0.555 versus 0.797). Thus, in firmer hypertrophic scars, more than one measurement is recommended to improve the reliability.

Table 29: Differences in R0 and R2 inter-rater ICC values between non-hypertrophic scars (mVSS Pliability scores of 2 or less) and hypertrophic scars (mVSS Pliability values of >2). Hypertrophic scars were found to have lower reliability values for the R0 and R2 compared to non-hypertrophic scars.

	Non-hypertrophic scars (mVSS Pliability score$\leq$2)		**Hypertrophic scars (mVSS Pliability>2)**	
Measure	R0 (n=21)	R2 (n=21)	R0 (n=33)	R2 (n=33)
Single	0.718	0.294	0.568	0.567
ICC (95% CI)	(0.431-0.876)	(0.024-0.582)	(0.341-0.747)	(0.370-0.737)
Average	0.884	0.555	0.798	0.797
ICC (95% CI)	(0.695-0.955)	(0.070-0.807)	(0.608-0.899)	(0.638-0.894)
%CV (SEM)	14.47 (0.06)	6.52 (0.03)	18.87 (0.05)	8.68 (0.04)

3.5.7 Concurrent validity

Concurrent validity was calculated between the mVSS and POSAS subscales with the relevant objective measures (average of readings from the three assessors,) (Table 30): mVSS and POSAS Pliability (Observer rated pliability and patient rated thickness) with the Cutometer R0 and R2 measures, mVSS Height and POSAS Thickness (Observer and patient rated Thickness) with the Dermascan measured dermal thickness, mVSS and POSAS Vascularity (Observer rated vascularity

and patient rated difference in colour,) with the DSM II Colormeter erythema parameters (a*, Narrow band Erythema) and Scanoskin camera measured erythema, mVSS and POSAS pigmentation (Observer rated pigmentation and patient rated difference in colour) with the DSM II Colormeter pigmentation parameters (L*, b*, Narrow band Melanin). The POSAS patient rated difference in colour does not differentiate between erythema and pigmentation.

Adjustments had to be performed for some of the mVSS and POSAS categories to allow accurate comparisons. To allow for comparisons of the POSAS Pliability subscale, scars which were categorised as “Supple” had 10 points deducted from the scar pliability rating; no adjustments were done to the scars in the “Mixed” and “Stiff” categories. To allow for comparisons of the pigmentation subscale, several adjustments to the parameters had to be made. To allow for comparisons of the pigmentation subscale, adjustments to the mVSS had to be made as the pigmentation subscale was not linear; the original mVSS, hypo-pigmented scars were given a score of 1 which was higher than normal skin. This would cause an error when comparing with the objective scar measurements as hypo-pigmented scars will have measured pigmentation values below that of normally pigmented skin. To prevent this discrepancy, the pigmentation subscale score was adjusted by converting hypopigmentation into a negative value, -1, normal skin was kept at score 0 (and adjusting down the other scores: Mixed from score 2 to score 1; Hyper-pigmented from score 3 to score 2,). For the objective measures, the ratio of the pigmentation parameters at the scar site over the pigmentation at the normal skin site was calculated. These adjustments were only done in calculations to correlate the mVSS and POSAS subscales with the corresponding objective measures and not to calculate the total score of the mVSS or POSAS.

For pliability, the Cutometer R0 (and its scar to normal skin ratio) had significant correlations with both the mVSS and POSAS-Observer Pliability subscales (R0 Spearman’s rho=-0.632, $p<0.01$; -0.585, $p<0.01$; Scar to normal skin ratio Spearman’s rho=-0.556, $p<0.01$; -0.472, $p<0.01$) but not the POSAS-Patient Stiffness subscale (Spearman’s rho=-0.113, $p=0.419$; -0.19, $p=0.173$). The Cutometer R2

subscale (nor its scar to normal skin ratio) however had no significant correlations with all three subjective pliability scores. Interestingly, although the Dermascan dermal thickness and intensity scores are not direct measurements of pliability, analyses show that both correlate significantly with the mVSS, POSAS-Observer and POSAS-Patient pliability/stiffness subscales (Spearman's rho =0.316 to 0.591 and -0.290 to -0.652 respectively, $p<0.05$ to <0.01). This may mean that the Dermascan ultrasound measured thickness and intensities can be used to indirectly assess the pliability of scar tissue. Further analyses were also performed to investigate if the scar/normal skin ratios of the Dermascan dermal thickness and intensity parameters would correlate better than the non-ratio parameters as this would hypothetically adjust for differences in the skin at different anatomical sites. The results however show that the ratios, although still significantly correlating with the mVSS and POSAS-Observer, have lower Spearman's rho values compared to the direct measures of dermal thickness and intensity.

For vascularity/erythema, the most valid measures was the Scanoskin Erythema measure (though not its scar to normal skin ratio,) which correlated significantly and moderate to strongly with the mVSS (Spearman's rho=0.718, $p<0.01$), POSAS-Observer (Spearman's rho=0.675, $p<0.01$) and POSAS-Patient erythema scores (Spearman's rho=0.462, p=0.01). The DSM II narrow-band Erythema measure also performed well and was found to correlate significantly with the mVSS (Spearman rho=0.387, p=0.004), POSAS-Observer (Spearman rho=0.273, p=0.044) and POSAS-Patient Colour (Spearman's rho=0.516, $p<0.01$) scores. The DSM II a* value however correlated significantly but weakly with the mVSS subscale (Spearman's rho =00.278, p=0.04) and did not have any significant correlations with the POSAS-Observer nor POSAS-patient.

For pigmentation, the DSM II L* parameter had significant correlations with the mVSS (Spearman's rho=-0.321, p=0.017), POSAS-Observer (Spearman's rho=-0.583, $p<0.01$) and POSAS-Patient (Spearman's rho=-0.649, <0.01). The correlations are negative as for the L* parameter, 0 is for total blackness and 100 for total whiteness.

Table 30: Concurrent validity of subjective to objective scores: Spearman's rho estimates and their p-values for the comparisons between the mVSS and POSAS subscales and the corresponding objective measurement for the scar sites. Parameters with statistically significant correlations are shaded in grey.

	Spearman estimates					
Parameters compared	**mVSS**	**p-value**	**POSAS-Observer**	**p-value**	**POSAS-Patient**	**p-value**
Pliability subscale versus (modified for POSAS-Observer):						
Cutometer R0 (n=54)	-0.632	<0.01	-0.585	<0.01	-0.113	0.419
Cutometer R2 (n=54)	0.141	0.310	-0.062	0.655	-0.12	0.391
Cutometer R0 Scar/Normal ratio (n=54)	-0.556	<0.01	-0.472	<0.01	-0.19	0.173
Cutometer R2 Scar/Normal ratio (n=54)	-0.134	0.334	-0.062	0.656	-0.199	0.154
Dermascan Dermal Thickness	0.546	<0.01	0.591	<0.01	0.316	0.020
Dermascan Dermal Intensity	-0.624	<0.01	-0.652	<0.01	-0.290	0.033
Dermascan Dermal thickness Scar/Normal ratio	0.410	0.002	0.444	<0.01	0.238	0.083
Dermascan Dermal intensity Scar/Normal ratio	-0.377	0.005	-0.534	<0.01	-0.170	0.219
Vascularity subscale versus:						
DSM II a*	0.278	0.04	0.235	0.084	0.007	0.962
DSM II Erythema	0.387	0.004	0.273	0.044	0.516	<0.01
DSM II a* Scar/Norm ratio	0.346	0.01	0.163	0.234	-0.058	0.677
DSM II Erythema Scar/Norm ratio	0.469	<0.01	0.317	0.018	0.125	0.369
Scanoskin Erythema (n=31)	0.718	<0.01	0.675	<0.01	0.462	0.01
Scanoskin Erythema Scar/Normal ratio (n=31)	0.284	0.121	0.352	0.052	-0.052	0.787
Pigmentation subscale versus (modified for mVSS):						
DSM II L*	-0.321	0.017	-0.583	<0.01	-0.649	<0.01
DSM II b*	0.069	0.617	-0.216	0.114	-0.13	0.350
DSM II Melanin	0.320	0.017	0.586	<0.01	0.604	<0.01
DSM II L* Scar/Norm ratio	-0.334	0.013	-0.495	<0.01	-0.501	<0.01
DSM II b* Scar/Norm ratio	0.014	0.921	-0.201	0.141	-0.276	0.043
DSM II Melanin Scar/Norm ratio	0.336	0.012	0.505	<0.01	0.445	0.001
Scanoskin Pigmentation Scar (n=31)	0.069	0.711	0.184	0.321	0.237	0.207
Scanoskin Pigmentation Scar/Normal ratio (n=31)	0.086	0.646	-0.061	0.744	0.218	0.246
Height/Thickness subscale versus:						
Dermascan Dermal thickness	0.509	<0.01	0.628	<0.01	0.271	0.047
Dermascan Dermal thickness Scar/Normal ratio	0.313	0.02	0.486	<0.01	0.288	0.035

The DSM II narrow band Melanin parameter similarly had significant correlations with all three subjective scores. The DSM II b* and Scanoskin scar Pigmentation parameter (nor their scar to normal skin ratios) however both had no significant correlations with any of the subjective scores. It was however noted that the DSM II b* parameter correlated strongly and significantly with the Scanoskin Pigmentation parameter (Spearman rho=0.782, p<0.01), thus we investigated whether the DSM II b* and Scanoskin Pigmentation parameters were actually correlating with scar vascularity instead of pigmentation (Table 31). Analyses show that this was true as both the DSM II b* (Spearman's rho correlation with mVSS, POSAS-Observer and POSAS-Patient=-0.528, p<0.01; -0.586, p<0.01) and Scanoskin pigment (Spearman's rho correlation with mVSS and POSAS=-0.379, p=0.035; -0.391, p=0.030) parameters correlated significantly with the mVSS and POSAS Erythema subscales. The Scanoskin system is currently being marketed for use in to detect perfusion and pigmentation (haemosiderin or melanin) in acute burns, and thus the software may not be able to accurately detect melanin in mature scar tissue.

Table 31: Concurrent validity of objective vascularity parameters: Spearman's rho estimates and their p-values for the comparisons between the mVSS, POSAS Vascularity and Patient POSAS Colour subscales and the DSM II b* and Scanoskin Pigmentation parameters. Parameters with statistically significant correlations are shaded in grey.

	Spearman estimates					
Parameters compared	**mVSS**	**p-value**	**POSAS-Observer**	**p-value**	**POSAS-Patient**	**p-value**
Vascularity subscale versus:						
DSM II b*	-0.528	<0.01	-0.586	<0.01	-1.30	0.350
Scanoskin Pigmentation Scar (n=31)	-0.379	0.035	-0.391	0.03	0.237	0.207
Scanoskin Pigmentation Scar/Normal ratio (n=31)	-0.408	0.023	-0.426	0.017	0.218	0.246

For Height/Thickness, the Dermascan measured dermal thickness correlated significantly with the mVSS Height (Spearman's rho=0.509, p<0.01), POSAS-Observer thickness (Spearman's rho=0.628, <0.01) and POSAS-Patient Thickness (Spearman's rho=0.271, p=0.047) subscales. The Dermascan

scar to normal skin thickness ratio also had significant correlations with all three subjective subscales but with lower correlation values.

3.5.8 Histological measurements

Biopsies were done in 38 patients and dermal thickness; blood vessel density and melanin concentration were measured as described above and the results are shown in Table 32.

Both subjective and objective measures of scar thickness (other than the POSAS patient rated thickness parameter) were found to have significant correlations with histologically measured dermal thickness with the Dermascan ultrasound dermal thickness having the strongest correlation (Spearman's rho=0.732, $p<0.01$). For blood vessel density as measured by CD31 staining (Figure 21), both the mVSS (Spearman's rho=0.354, p=0.029) and POSAS observer rated vascularity (Spearman's rho=0.486, p=0.002) had significant correlations but the POSAS patient rated colour parameter did not (Spearman's rho=0.008, p=0.962). For the DSM II Colormeter parameters, the a* parameter correlated significantly with blood vessel density (Spearman's rho=0.339, p=0.037) but not the narrow band erythema measure (Spearman rho=0.114, p=0.495). Interestingly, the b* parameter, even though it is a parameter meant for pigmentation, also had a significant negative correlation with blood vessel density (Spearman's rho=-0.487, p=0.002). The negative correlation indicates that the higher the blood vessel density the "bluer" the scar tissue, and thus the b* parameter may possibly be measuring the venous circulation in the scar tissue.

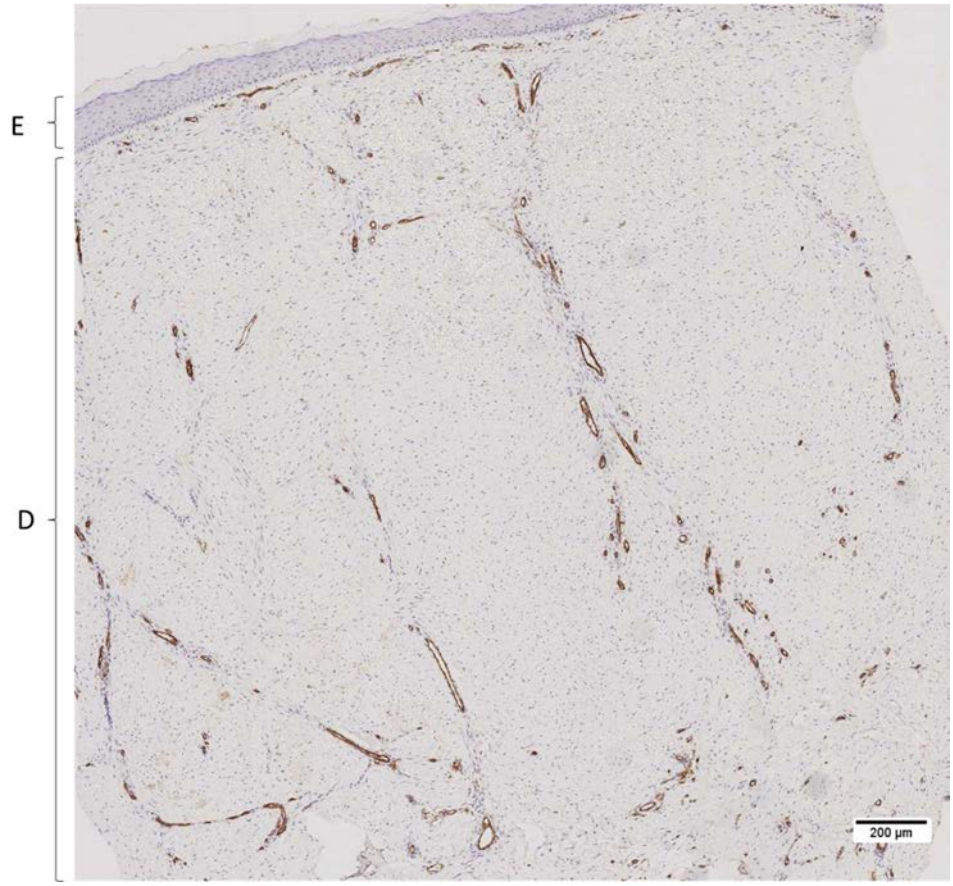

Figure 21: CD31 staining of the blood vessel endothelial cells. E=Epidermis, D=Dermis (Source: Kwang Chear Lee).

For the Scanoskin camera system, the Scanoskin erythema measure did not correlate significantly however, like the DSM II b* parameter, the pigmentation parameter had a significant negative correlation with histologically measured blood vessel density (Spearman's rho=-0.726, $p<0.01$). For Melanin density as measured by the Fontana-Masson stain, none of the subjective parameters had significant correlations. This is in contrast with the objective parameters, all of which had significant moderate to strong correlations with the histologically measured melanin density including the L* parameter (Spearman's rho=-0.491, p=0.002), narrow band melanin (Spearman's rho=0.492, p=0.02).

Table 32: Spearman's rho correlations of histological thickness, blood vessel density (CD31 staining), and melanin (Fontana-Masson staining) with the corresponding subjective and objective parameters. Parameters with statistically significant correlations are shaded in grey.

Parameters	Spearman estimates	p-value
Histological thickness versus:		
mVSS Height	0.436	0.006
POSAS Observer Thickness	0.604	<0.01
POSAS Patient Thickness	0.053	0.752
Dermascan dermal thickness	0.732	<0.01
Blood vessel density (CD31) versus:		
mVSS Vascularity	0.354	0.029
POSAS Observer Vascularity	0.486	0.002
POSAS Patient Colour	0.008	0.962
DSM a*	0.339	0.037
DSM b*	-0.487	0.002
DSM Erythema	0.114	0.495
Scanoskin Erythema (n=19)	0.13	0.596
Scanoskin pigmentation (n=19)	-0.726	<0.01
Melanin (Fontana-Masson) versus:		
mVSS Pigmentation	0.241	0.145
POSAS Observer Pigmentation	0.150	0.368
POSAS Patient Colour	0.288	0.079
DSM L*	-0.491	0.002
DSM b*	0.555	<0.01
DSM Melanin	0.490	0.02
Scanoskin pigmentation (n=19)	0.774	<0.01

The b* and Scanoskin pigmentation parameters also had significant correlations with the melanin density despite previously shown to also correlate significantly with the blood vessel density. This may indicate that these 2 parameters are measuring both blood vessel density (erythema) as well as melanin (pigmentation). For the b* parameter, as the colour spectrum it measures is between blue and yellow, the blue spectrum is hypothesised to be a measure of blood vessel density (specifically venous density, and hence the negative correlation) while the yellow spectrum is most likely a measure of the melanin density (as melanin is a brown pigment and close to the colour yellow, thus the positive correlation). This may explain the poor reliability values for the b* value as it is influenced by 2 different "colours" on opposite sides of its measured spectrum. However, this does

not appear to influence the Scanoksin pigmentation parameter which has been shown to have high reliability values.

3.5.9 Patient Reported Outcome Measures

3.5.9.1 Patient Satisfaction with devices questionnaire

Table 33 shows the patient satisfaction ratings for the objective measurement tools used in the study as well as for the skin biopsy procedure. All of the objective measurement devices had over 90% of "Very good" and "Good" ratings in all three of the patient satisfaction parameters of overall satisfaction, comfort and time to measure.

Table 33: Ratings for the objective measurement tools used in the study and skin biopsy. All of the objective measurement devices had over 90% of "Very good" and "Good" ratings.

	Number of responses (n=)	Rating	Overall Satisfaction	Comfort	Time to measure
Scanoskin	51	Very Good	68.6%	68.6%	66.7%
		Good	25.5%	27.5%	27.5%
		OK	5.9%	3.9%	5.9%
		Poor	0.0%	0.0%	0.0%
		Very Poor	0.0%	0.0%	0.0%
DSM II	52	Very Good	67.3%	67.3%	63.5%
		Good	32.7%	32.7%	34.6%
		OK	0.0%	0.0%	1.9%
		Poor	0.0%	0.0%	0.0%
		Very Poor	0.0%	0.0%	0.0%
Dermascan	51	Very Good	66.7%	70.6%	62.7%
		Good	27.5%	23.5%	29.4%
		OK	3.9%	5.9%	5.9%
		Poor	2.0%	0.0%	2.0%
		Very Poor	0.0%	0.0%	0.0%
Cutometer	49-50	Very Good	65.3%	62.0%	56.0%
		Good	30.6%	30.0%	40.0%
		OK	2.0%	4.0%	4.0%
		Poor	2.0%	4.0%	0.0%
		Very Poor	0.0%	0.0%	0.0%
Skin biopsy	32-33	Very Good	63.6%	54.5%	68.8%
		Good	24.2%	24.2%	21.9%
		OK	12.1%	21.2%	9.4%
		Poor	0.0%	0.0%	0.0%
		Very Poor	0.0%	0.0%	0.0%

Interestingly, high patient satisfaction was also found for the more invasive skin biopsy procedure though slightly lower compared to the non-invasive tools (average %) in terms of overall satisfaction (87.9% versus 96%), comfort (78.8% versus 95.5%), and time to measure (90.6% versus 95.1%).

3.5.9.2 Patient rated scar parameter importance

Responses were available from 54 of the 55 patients for patient rated scar parameter importance. Table 34 shows the rank of the different parameters arranged according to their mean rank. Due to the method of ranking (1 being the most important, to 6 being the least important to them), lower mean rank denotes higher patient perceived importance. There was a statistically significant difference in patient perceived scar parameter importance, $x^2(5) = 11.26$, $p=0.046$).

Table 34: Mean rank of parameters arranged according to rank. Pain and itch were shown to be the most important scar parameter to patients (mean rank=3.01) compared to pigmentation (mean rank=4.03).

	Mean Rank
Pain/Itch	3.01
Thickness	3.17
Pliability	3.41
Surface area	3.68
Redness	3.71
Pigmentation	4.03

Pain and itch were shown to be the most important scar parameter to patients and pigmentation the least. The Wilcoxon signed-rank test was performed to examine where the differences in ranking actually occur with different combinations of the parameters (Table 35). The test showed that patients perceived scar thickness to be significantly more important than pigmentation (0.018) and surface area (0.049), whereas pain and itch was perceived to be more important than pigmentation (p=0.033).

Table 35: Wilcoxon signed-rank test comparison of the scar parameters. Parameters with statistically significant correlations are shaded in grey.

Parameters (p-values)	Redness	Pigmentation	Surface area	Thickness	Pliability	Pain/Itch
Redness	n/a	-	-	-	-	-
Pigmentation	0.16	n/a	-	-	-	-
Surface area	0.956	0.217	n/a	-	-	-
Thickness	0.195	0.018	0.049	n/a	-	-
Pliability	0.574	0.218	0.429	0.258	n/a	
Pain/Itch	0.115	0.033	0.134	0.55	0.28	n/a

Due to the multiple comparisons done, a Bonferroni adjustment was performed, with the adjusted significant p-value calculated to be 0.003 (i.e. 0.05/15 comparisons). After adjustment, there were no statistically significant differences between the parameters in terms of perceived importance. The results may imply that physical comfort (absence of pain and itch) and functionality were more important factors to patients compared to appearance (surface area and colour). However, this may be due to the majority of the scar being assessed being >12 months old which means that the scars are more likely to be mature scars with reduced erythema.

3.5.10 Sensitivity and Specificity

To establish the most accurate cut off point for the objective measurement tools to distinguish between a hypertrophic scar and normal scar, Receiving Operating Characteristic (ROC) curves were generated using the mVSS as a "gold standard" comparator. In order to produce the ROC analysis, two sites from each patient were utilised: the scar site and the matching normal skin site (adjacent or contralateral). Positive cases were scars that received an average score (average of the three assessors) of 2 or more on the mVSS subscale that corresponds to the objective measurement tool: Height for the Dermascan ultrasound measured scar thickness and scar thickness ratio (scar to normal skin), and Pliability for the Cutometer R0 and R2 parameters and their respective ratios (scar to normal skin).

For the mVSS Vascularity subscale for the DSM II a* and narrow band Erythema parameters and their respective ratios (scar to normal skin), the score of 1 or more was used as there were too few cases with scores of 2 or more (n=9). Similarly, for mVSS Pigmentation subscale for the DSM II L* and Melanin parameters, the adjusted mVSS subscale was used and a score of 1 and above was used as there were too few cases with scores of 2 or more for the scars (n=1). Additionally, hypo-pigmented scars were also removed (mVSS score of <0).

The negative cases were the scars that received an average score below 2 on the mVSS subscale (or below 1 for the vascularity and pigmentation subscales as previously explained,) as well as the normal skin cases (regarded as having an mVSS score of 0 for all subscales). For ratios, normal skin was considered as having a ratio of 1 for all cases.

The optimal cut-off point on the ROC curve was determined as the point having the highest Youden's index, defined as (Sensitivity + Specificity)-1. The Area under the curve (AUC) for all the parameters is shown in Table 36 and the ROC curves in Figure 22.

The ROC for the Dermascan scar thickness and thickness ratio both had very strong AUC values of 0.897 (95% CI: 0.818-0.975, p<0.01) and 0.870 (95% CI: 0.795-0.944, p<0.01) which indicates that the Dermascan scar thickness is able to differentiate between hypertrophic scars and non-hypertrophic scars or normal skin. The cut-off point with the highest Youden's index (optimal sensitivity and specificity) for scar thickness is 2.64mm, and for the scar to normal skin ratio, it is the ratio of 1.38. Thus, dermis that is thicker or has a higher ratio can be classified as hypertrophic dermis.

The ROC for the Cutometer R0 (AUC: 0.942, 95% CI: 0.900-0.983, p<0.01) and R0 ratio (AUC 0.944, 95% CI: 0.905-0.983, p<0.01) values perform better than the R2 (AUC: 0.625, 95% CI 0.509-0.741) and R2 ratio (AUC: 0.627, 95% CI: 0.481-0.774) though all were statistically significant. As previously mentioned, the Dermascan measured dermal intensity was found to have significant correlations with the pliability scores and further analysis has also shown that the Dermascan dermal intensity

(AUC: 0.914, 95% CI: 0.861-0.967, p<0.01) and dermal intensity ratio (scar to normal skin) (AUC: 0.919, 95% CI: 0.856-0.983, p<0.01) both have very strong ROC AUC values for pliability though slightly lower than that for the Cutometer R0 value.

For colour measurements, ratios of scar to normal skin were found to perform better than the single measures for both erythema and pigmentation measurements. For the erythema subscale, all parameters had strong to very strong and statistically significant ROC AUC values but the highest values were for the DSM II narrow band Erythema ratio (scar to normal skin) parameter (AUC: 0.885, 95% CI: 0.794-0.975, p<0.01) and the DSM II a* ratio (scar to normal skin) (AUC: 0.848, 95% CI: 0.740-0.956, p<0.01). For the pigmentation subscale, the Melanin (AUC 0.761, 95% CI: 0.626-0.897, p=0.03) and DSM II L* (AUC 0.767, 95% CI: 0.628-0.905, p=0.002) ratios (scar to normal skin) had strong and statistically significant ROC AUC values. The non-ratio DSM II L* (AUC 0.767, 95% CI: 0.628-0.905, p=0.002) and narrow band Melanin (AUC 0.761, 95% CI: 0.626-0.897, p=0.003) parameters had strong and statistically significant ROC AUC values.

3.11 Global Scar Scale

In order to develop a global scar scale, the cut-off points for each of the parameters from the ROC AUC analyses (as shown in Table 36) were used to dichotomise the parameters. A univariate exploratory analysis was then performed on the data set. The X^2 test was performed for the dichotomised parameters against the total mVSS score (with a score of 6 or more being deemed as a positive outcome) (Table 37). Candidate parameters with p<0.10 were tried in different combinations and the ROC AUC for the prediction of a mVSS score of 6 (to indicate hypertrophic scarring: 2 (Pliability) + 2 (Height) + 1 (Erythema) +1 (Pigmentation) and above was calculated (Table 38). The Cutometer R0, Dermascan scar thickness, intensity and their respective scar to normal skin ratios were the only parameters that had p-values of less than 0.10. None of the colour related parameters nor the Cutometer R2 parameters had significant p-values.

As can be seen in Table 38, the highest AUC was for the combination of the all six parameters (AUC: 0.786, p=0.003). A total score of 5 and above (out of the maximum 6) had the highest combined sensitivity and specificity (sensitivity of 69.0% and a specificity of 83.3%) (Table 39).

Table 36: Receiver Operating Characteristic values for the Dermascan, Cutometer and DSM II parameters.

Parameter	mVSS subscale	ROC AUC	p-value	95% CI	Direction	Cut-off value	Sensitivity (%)	Specificity (%)	Youden's index
Dermascan scar thickness	Height	0.897	<0.01	0.818-0.975	Higher than	2.64mm	85.0	86.0	0.700
Dermascan scar Thickness ratio	Height	0.870	<0.01	0.795-0.944	Higher than	1.38	100.00	71.10	0.710
Cutometer R0 ratio	Pliability	0.944	<0.01	0.905-0.983	Lower than	0.88	80.60	100.00	0.806
Cutometer R0	Pliability	0.942	<0.01	0.900-0.983	Lower than	0.67mm	88.90	91.70	0.806
Dermascan dermal intensity ratio	Pliability	0.919	<0.01	0.856-0.983	Lower than	0.70	81.94	97.22	0.792
Dermascan dermal intensity	Pliability	0.914	<0.01	0.861-0.967	Lower than	11.88	83.33	86.11	0.694
Cutometer R2 ratio	Pliability	0.627	0.012	0.481-0.774	Lower than	0.985	81.94	66.67	0.486
Cutometer R2	Pliability	0.625	0.023	0.509-0.741	Lower than	0.765	70.83	50.00	0.208
DSM Erythema ratio	Erythema	0.885	<0.01	0.794-0.975	Higher than	1.17	93.10	81.50	0.746
DSM a* ratio	Erythema	0.848	<0.01	0.740-0.956	Higher than	1.10	86.20	85.20	0.714
DSM Erythema	Erythema	0.818	<0.01	0.730-0.906	Higher than	13.58	82.80	69.10	0.519
DSM a*	Erythema	0.741	<0.01	0.643-0.860	Higher than	16.81	58.60	85.20	0.438
DSM L* ratio	Pigmentation	0.862	<0.01	0.779-0.945	Lower than	0.70	86.40	69.20	0.556
DSM Melanin ratio	Pigmentation	0.854	<0.01	0.778-0.931	Higher than	1.08	68.20	100.00	0.682
DSM L*	Pigmentation	0.767	0.002	0.628-0.905	Lower than	30.67	67.00	84.60	0.517
DSM Melanin	Pigmentation	0.761	0.003	0.626-0.897	Higher than	40.1	64.80	84.60	0.494

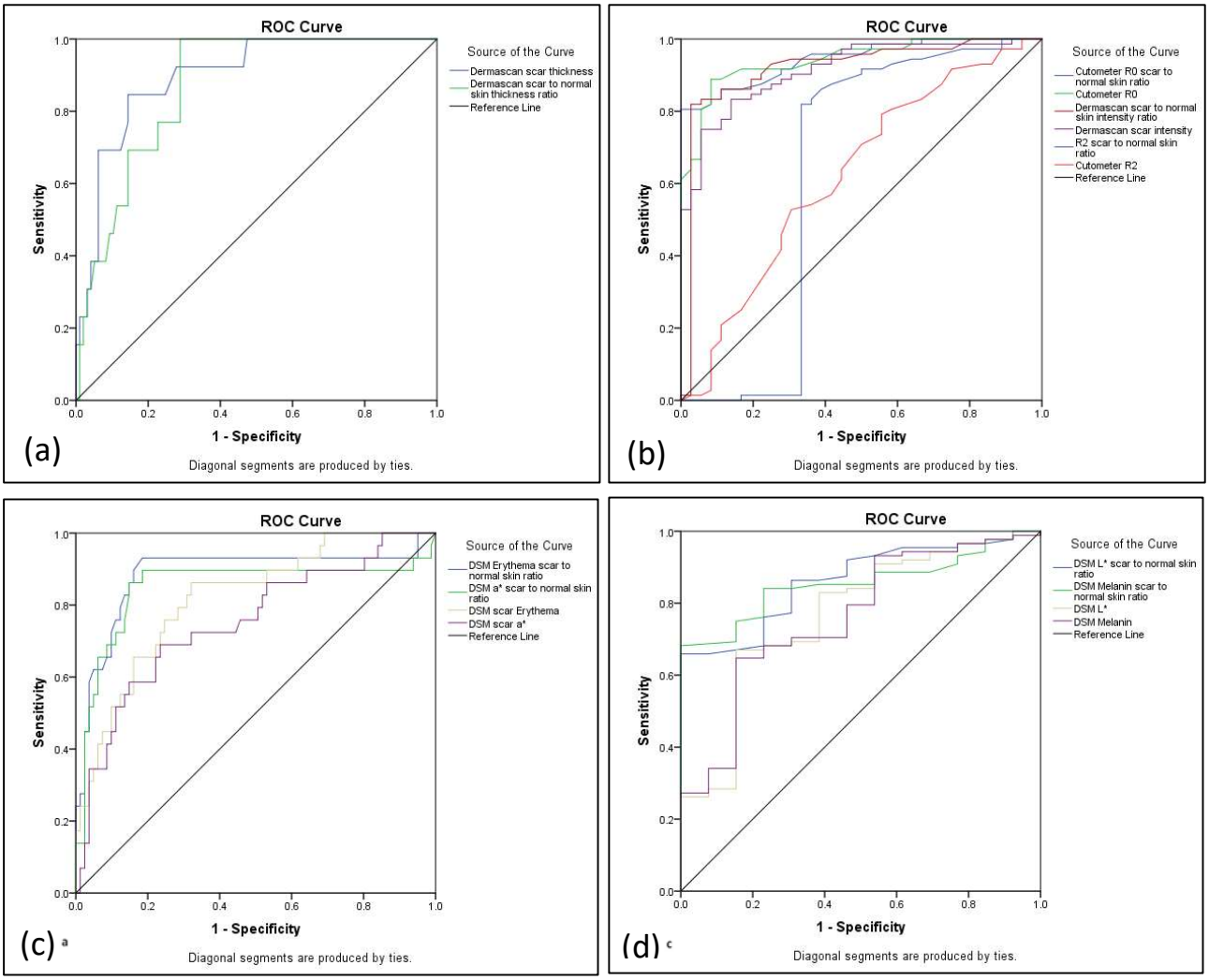

Figure 22: Receiver Operating Characteristic curves for the panel of scar measurement tools. Receiver Operating Characteristic curves for the (a) Dermascan scar thickness and scar thickness ratio to mVSS thickness subscale; (b) Cutometer R0, R2, R0 ratio (scar to normal skin), R2 ratio (scar to normal skin), Dermascan dermal intensity and intensity ratio (scar to normal skin)to mVSS pliability subscale; (c) DSM II a*, narrow band Erythema, a* ratio (scar to normal skin), narrow band Erythema ratio (scar to normal skin) to mVSS erythema subscale; (e) DSM II L*, DSM L* ratio (scar to normal skin), DSM II Melanin and DSM Melanin ratio (scar to normal skin) to mVSS pigmentation subscale.

Table 37: Chi-square test (X^2) values for the objective parameters. The Cutometer R0, Dermascan scar thickness, intensity and their respective scar to normal skin ratios were the only parameters that had p-values of less than 0.10. Parameters with statistically significant X^2 values are shaded in grey.

Parameters	X^2, P-value
Cutometer R0 Ratio	0.008
Dermascan scar intensity	0.012
Cutometer R0	0.014
Dermascan scar thickness ratio	0.027
Dermascan scar thickness	0.046
Dermascan scar intensity ratio	0.077
DSM Melanin ratio	0.490
Cutometer R2	0.513
DSM a* ratio	0.519
DSM a*	0.696
DSM Erythema	0.714
DSM Melanin	0.714
Cutometer R2 Ratio	0.876
DSM L ratio	0.876
DSM Erythema ratio	0.900
DSM L*	0.960

Table 38: Parameter combinations and the ROC Area under the curve values for predicting mVSS scores of 6 or more.

Parameter combinations	AUC	p-value	95% CI
All 6 parameters: R0 Ratio+ Scar intensity+ R0+ Scar thickness ratio+ Scar thickness +Scar intensity ratio	0.786	0.003	0.641-0.931
5 parameters: R0 Ratio+ Scar intensity+ R0+ Scar thickness ratio+ Scar thickness	0.776	0.004	0.626-0.925
4 parameters: R0 Ratio+ Scar intensity+ R0+ Scar thickness ratio	0.748	0.009	0.578-0.918
3 parameters: R0 Ratio+ Scar intensity+ R0	0.758	0.007	0.589-0.927
2 parameters: R0 Ratio+ Scar intensity	0.736	0.013	0.562-0.910
1 parameter: R0 Ratio/ Scar intensity/ R0/ Scar thickness ratio/ Scar thickness/ Scar intensity ratio	0.589-0.685	0.053-0.349	0.415-0.866

Table 39: Objective Scar Scale total scores and their corresponding sensitivities and specificities in predicting an mVSS score of 6 and above. A total score of 5 (highlighted in grey) and above (out of the maximum 6) had the highest combined sensitivity and specificity**.**

Objective Scar Scale Total score	Sensitivity (%)	Specificity (%)	Youden's index
1	100.0	8.3	0.08
2	97.6	16.7	0.14
3	90.5	41.7	0.32
4	76.2	58.3	0.35
5	69.0	83.3	0.52
6	42.9	91.7	0.35

3.6 Discussion

Accurate and reliable measurements of hypertrophic scarring in burns are increasingly being recognised as important in both clinical practice and research. This is especially true in the field of wound healing where long term scarring is an important outcome measure to determine the effectiveness of a surgical procedure or treatment[489, 490].

In this study, both the intra- and inter-rater reliability of the objective tools, i.e. the Cutometer, the Dermascan ultrasound, the DSM II Colormeter, the Scanoskin system were tested on both scar tissue as well as the matching normal skin sites. Additionally, the inter-rater reliability of commonly used subjective scales, the modified VSS and POSAS were also tested. Comparisons of the objective scar measurement tools with the mVSS, POSAS and also histological parameters were made to test for concurrent validity of these tools.

This study differs from previous similar studies in a number of different ways. Firstly, a power calculation was performed to calculate the minimum number of participants required, and as a result of this, a much larger number of patients have been recruited (n=55). Additionally, other reliability studies have performed their measurements over an average 2-week period and not in a single session as in this study. This predisposes these studies to errors due to relocating the exact site of measurement despite rigorous protocols being utilised and this is a common source of error that is acknowledged by several studies[233, 263]. Thus, the ICC values of the tools in these studies are influenced substantially by the reliability of their relocation protocol. Furthermore, although

biopsies were not obtained for all patients, concurrent validity with a superior "gold standard" i.e. histological parameters was performed in this study compared to other studies that relied on subjective scores which have been shown to be poorly reproducible.

3.6.1 Subjective scores

Our study has shown that the traditionally and widely used subjective scar scales, the modified VSS and POSAS have poor reliability when performed by less than three assessors for the majority of the subscales with the exception of the POSAS vascularity subscale which has an acceptable inter-rater average ICC of 0.78 when performed by 2 assessors. Even with three assessors, the mVSS total score as well as the POSAS pigmentation, relief, pliability, change in surface area and overall score still have lower than acceptable ICC values. The reliability of the POSAS subscales is likely to be even lower as these ICC values were calculated without taking into account the additional categorical classifications each subscale possesses, for example the pigmentation subscale can be rated into the categories of "Hypo", "Hyper" and "Mix" in addition to the 1-10 scale. The requirement of having three assessors for acceptable reliability makes these subjective scores impractical for most clinical and research settings. One explanation for the poor reliability of these subjective scores is the lack of a standardised reference on which to score against. The assessors are thus affected by both recall bias and are also biased by their own personal experience of previously seen scars when judging the assessed scar. The POSAS-Patient rated subscales are important to inform clinicians of the patients' perception of their own scars, but as our analyses have shown, the patient rated subscales do not have any significant correlations with the matching histologically measured parameters. In general, the objective direct measures of the scar appear to perform slightly better than the scar/normal skin ratios with correlated with the subjective scar parameters. This may indicate that although the scar tissue is meant to be compared to normal skin when providing subjective scores, the assessors' ratings do not reflect the ability to do this.

3.6.2 Colour

Anecdotally, scar colour, especially the redness of the scar, has been thought to be a highly important to patients and can be a useful feature to gauge the maturity of the scar[491, 492]. Additionally there is also a large academic interest in restoring normal pigmentation in burn scars[493].

The DSM II a* and narrow band Erythema had acceptable inter- and intra-rater ICC values of above 0.7 for both single and average measures for scar tissue. The single assessor ICC values for the a* and Erythema parameters for normal skin however were lower and below the acceptable threshold with larger % CV (14.0% and 15.3%), but the average ICC values were good (ICC average: 0.813 and 0.841). As the intra-rater ICC values for these parameters are higher and above the acceptable threshold (ICC [Single, Average]: 0.79 and 0.90; 0.80 and 0.90), this points towards a difference in the readings between raters, most likely due to different pressures being applied to the measured site resulting in varying levels of blanching, though a greater difference would be expected to be seen in scars compared to normal skin. Another explanation could be that the measured normal skin site had been irritated by multiple measurements (and thus appearing more erythematous,) by the other tools and insufficient time was allowed for the skin to recover fully despite time being allocated in the protocol for this. Our results are in contrast with other studies which show that the erythema ICC values for normal skin are usually similar or higher than that for scar sites[233, 263].

In terms of pigmentation measurement, the DSM II L*, and narrow band Melanin parameters both show high inter- and intra-rater ICC values of above 0.90 for both single and average measures although the b* measure had poor reliability values which is in contrast with the reliability of the b* value of similar colour measurement systems such as the Labscan XE[209]. Our analyses have shown that this is likely to be due to the fact that the b* parameter is affected by both pigmentation (“yellowness”) as well as skin circulation (likely venous circulation, “blueness”) as evidenced by the significant correlations to both histologically measured melanin concentrations and CD31 measured vessel concentration thus leading to greater variability.

Compared to the pigmentation measures (other than the b* measure), the objective measurements for erythema of the DSM II Colormeter have lower ICC values. This again is likely due to the erythema parameters being susceptible to the varying amounts of pressure applied onto the area of measurement which may cause different degrees of blanching in contrast to pigmentation parameters which are not influenced by pressure.

The Scanoskin camera system parameters for both erythema and pigmentation have been shown to have greater reliability compared to the DSM II parameters, although more observations are required to confirm this. An additional advantage of the Scanoskin system is that it allows the measurement of the parameters over a much greater area (up to approximately 3500cm^2, although light exposure at peripheries will be lower than centre,) will be compared to the DSM II which only has a measurement area of 4mm. Similar to the DSM II b* parameter, the pigmentation parameter of the Scanoskin system may also be influenced by the erythema of the measured area as evidenced by the significant correlations with the erythema subscales of both the mVSS and POSAS (p=0.023, 0.017).

Although our study showed that there were statistically significant correlations between the subjective perceptions of skin colour and the objective measurements, only weak correlations were found. This is not surprising as several factors influence the both the redness and pigmentation of skin such as skin thickness, blood vessel density and blood flow. A study by Jaspers et al (2017) showed a similarly moderate but significant correlation between colorimetry measured erythema values and subjective redness assessment (r=0.401, p=0.03)[491]. Additionally, in the same study, no correlation was found between laser Doppler measured blood flow, immunochemistry measured microvasculature and objective colorimetry measurements. Interestingly, in the ROC AUC analyses, we found that the DSM II erythema and pigmentation ratios (scar to normal skin) performed better than the single measures. This shows that the subjective scores are highly likely to be influenced by

the colour of the surrounding normal skin as greater differences between the scar colour and normal skin (and hence higher ratios,) led to higher scar scores.

3.6.3 Thickness

The Dermascan ultrasound system has been shown to have high (ICC>0.90) inter- and intra-rater ICC (Single an Average) values for both dermal thickness and intensity in scar tissue and normal skin. This agrees with the findings of previous similar studies[243, 263, 322].

In addition to this, the dermal thickness parameter also had significant correlations with the subjective height subscale of both the mVSS and POSAS-Observer as well as histologically measure dermal thickness ($p<0.01$). This is in agreement with most studies on the Dermascan system[214, 243, 263]. A study by Agabalyan et al[494] (2017) however reported a weak correlation between the Dermascan measured ultrasound and histological measured dermal thickness (Spearman rank correlation of −0.6242). There are some important methodological differences between this study and ours. This includes the small number of samples (n=10) compared to our study (n=38), and the use of the H&E stain which will not allow the authors to differentiate between scar tissue and uninjured dermis.

As skin thickness is known to vary relative to anatomical site[495], the thickness ratio was initially predicted to perform better compared to direct measurement of the scar thickness, however our analyses have shown that the direct scar measurement has a slightly stronger correlation. This may be due to the fact that when part of the dermis is lost in the case of deep dermal and full thickness burns, the thickness of the scar tissue that replaces it does not necessarily match nor exceed the original dermis in thickness (and hence not dependent on anatomical site,) as is the case in atrophic scars.

A flaw of the Dermascan system however is the inability to adjust the image enhancement (mode) after the image is taken compared to newer systems such as the DUB Skinscanner system (Taberna

Pro Medicum, Germany)[496], which makes the detection of the lower dermal border difficult particularly in thicker scars when using the same enhancement mode as the thinner scars.

3.6.4 Pliability

For pliability measures, the Cutometer R0 parameter had acceptable inter and intra-rater ICC values for scar tissue but the R2 parameter did not reach the required threshold. Previous studies have attributed these errors to the sensitivity of the Cutometer to slight differences in location[263] and also lower reliability in firmer hypertrophic scars. This difference in reliability between softer and firmer scars had been shown to be true for the R0 parameter but not the R2 parameter (Table 29). The R0 parameter also correlated significantly with the subjective pliability measures (mVSS pliability, $p<0.01$; POSAS-Observer pliability, $p<0.01$) but the R2 did not. This could be due to the fact that in the subjective scar assessments, observers typically pinch the scar to test its pliability but do not take into account the time it takes for the scar to return to its baseline after pinching it. Interestingly, the Dermascan ultrasound measured dermal thickness and intensity both also correlated significantly with the subjective scar pliability measures, which could indicate that these ultrasound parameters can be used to indirectly predict the pliability of the scar with the advantage of higher reliability compared to the Cutometer.

3.6.5 Global Scar Scale

One of the secondary objectives of this study was to create a preliminary global objective scar scale that would allow the combination of several different objective scar parameters into a single score. This has an advantage of providing a more accurate picture of the scar compared to just a single parameter, and mirrors what the total scores of the mVSS and POSAS, which are combinations of different parameters, provide.

The use of ROC curves and their associated AUC values allow for the generation of cut-off point values for the various objective tools that can aid in differentiating hypertrophic scars from normal scars and skin. Utilising these cut-off values described earlier as well as ROC AUC analyses, it was found that the combination of six parameters (R0 Ratio+ Scar intensity+ R0+ Scar thickness ratio+

Scar thickness +Scar intensity ratio) gave the highest AUC value (0.786). Interestingly, none of the colour parameters (erythema and pigmentation) were found to be significant enough to be included in the global score.

There has been a previous attempt of creating an objective tool based scar assessment system by Oliveira et al[242] (2014). Similar to this study, scars were evaluated using the same subjective scar scale (modified Vancouver Scar Scale), however there was no mention of how many observers performed the measurements and whether the same observer(s) was used for all the enrolled participants. Part of the study involved subjective scar measurements by three observers, however photos of the scars and photographic scar assessment scales (Seattle and Hamilton Scar Scales) were used compared to the real-time clinical measurements performed in this study. The objective measurement devices used in the Oliveira study were also different to the panel selected in our study: for pliability measurements, they utilised the durometer and pneumatonometer; for colour measurements, they utilised a dermaspectrometer and a chromameter. Additionally, a laser Doppler ultrasound flowmeter was utilised to measure the blood flow in the scar. No objective scar thickness measurement device (such as the high frequency ultrasound system used in this study) was included in the study but rather skin biopsies were utilised to provide objective scar thickness measurements. Despite the detailed findings of the Oliveira et al study, objective measurement tools have still not been widely taken up. Many factors contribute to this, chiefly the cost required to purchase these objective measurement devices, the time required to utilise them and the lack of expertise in interpreting the findings.

A weakness of utilising the mVSS as the gold standard is that the mVSS scores have been shown to have poor reliability, although other studies have also utilised the mVSS for this purpose[243]. Other "gold standards" have been considered apart from the mVSS but these alternatives have their own issues. The POSAS score is unsuitable as there are no studies which have defined the cut-off score for the various subscales which indicate a hypertrophic scar. This applies to the histological

parameters as well in which there is no consensus of the value of dermal thickness or vessel and melanin concentration that define a hypertrophic scar.

Previous studies have shown time to healing as a strong predictor of hypertrophic scarring[10]. However in our study, the only parameters found to have significant correlations with a time of healing of more than 3 weeks were the Dermascan thickness (AUC 0.708, p=0.034), thickness ratio (AUC 0.725, p=0.022) and Cutometer R0 (AUC 0.282, p=0.027). The time to healing was unsuitable for several reasons. Wound healing times were retrospectively corrected and were for the whole burn wound and not specific to the sites measured in the study. Additionally, the ages of the scars measured in this study were different (and thus were in different stages of remodelling) which has a significant impact on many of the measured parameters such as colour and scar thickness but the time to healing does not account for this.

The use of the ROC to dichotomise values and using the Youden's index to create a strict cut-off point can cause problems with diagnosis. Whilst it is useful for research analysis to having definitive values, clinically scars vary tremendously in characteristic. Additionally, a cut-off value that provides a dichotomous result i.e. normal scar vs hypertrophic scar does not provide an indication of the severity of the measured characteristic of the hypertrophic scar itself. We have tried to create differing scores to correspond to the increasing severity of scars but this was not possible due to the sample size as the study was not designed to recruit adequate number of patients with different scar severities.

3.7 Conclusion

In summary, we found that the reliability of the subjective scores mVSS and POSAS both fell below the acceptable threshold. For the objective tools, the following had good to excellent intra and inter-rater reliability scores: (1)The DSM II L* and narrow band Melanin measures for pigmentation and the a* and narrow band Erythema values for erythema, (2) The Dermascan thickness and intensity

measurements and the (3) Cutometer R0. Therefore, these devices are suitable to be used in both clinical practice and research. The findings of this study provide a basis for the creation of an objective scar assessment panel however a further multi-centre validation of this global scar score is required in a separate cohort of patients.

SECTION 2- DRESSING FORMULATION

CHAPTER 4

DECORIN FORMULATION

4. Decorin Cytotoxicity

4.1 Cytotoxicity of decorin

4.1.1 Background

Previous studies have shown that decorin has anti-proliferative effects against tumour cells[497] and is able to reduce fibroblast cell proliferation[498]. Furthermore, at high enough doses, decorin has also been shown to increase apoptosis via the activation of caspase-1, 3 and 8 in various cells including dermal fibroblasts and tumour cells[499-502]. The therapeutic dose of decorin to prevent hypertrophic scarring has yet to be determined, however a study by Zhang et al (2007) showed that normal and hypertrophic scar fibroblast proliferation could be inhibited with decorin concentrations of 100 and 200nm (i.e. 3.8 and 7.2μg/mL; the decorin used in the study had a predicted molecular mass of 38 kDa) and TGF-β1 concentration per cell was found to be significantly lower in hypertrophic scar fibroblasts treated with 10nM of decorin (i.e. 0.38μg/mL, $p<0.05$) compared with fibroblasts without decorin addition[498]. Deep dermal fibroblasts however may be resistant to the anti-proliferative and anti-apoptotic effects of decorin and may thus contribute more significantly, compared to normal fibroblasts, to hypertrophic scarring[500].

In order to safely utilise decorin in human studies, we require information about its toxicity. This is especially so in patients with severe burns as potentially a large surface area of de-epithelialized skin will be exposed to the decorin-loaded dressing leading to increased absorption and raised serum levels. Toxic levels of decorin on wound surfaces could also be detrimental to the wound healing process if it reduces keratinocyte and normal fibroblast proliferation or induces apoptosis in these cells.

4.1.2 Hypotheses

As a naturally occurring proteoglycan, we hypothesised that decorin has no or minimal toxicity.

4.1.3 Aims

The aim of this study was to investigate the concentration of decorin that is cytotoxic to dermal fibroblasts in in-vitro cell cultures.

4.2 Materials and Methods

4.2.1 Materials

Material	Supplier (including address)	Cat/Lot/Batch number
Dulbecco-modified Eagle medium	Sigma-Aldrich	RNBD4073 (exp 08/2015)
Phosphate buffered saline (Dulbecco A, Mg2+ and Ca2+ free)	Oxoid	1293357
Foetal Bovine Serum (FBS, heat inactivated)	Sigma-Aldrich	034M3398 (expiry 03/2019)
Penicillin and Streptomycin	Sigma-Aldrich	SLBB9308
Decorin (Galacorin)	Catalent	200LBRX09018
Human Dermatofibroblasts	European Collection of Cell Cultures	Human dermal fibroblasts (106-05a) cell line Cat no: 06090715
Millex GP filter unit (0.2µm), Milipore Express PES membrane	Sigma-Aldrich	Z359904
MTT (3-4,5-Dimethythiazol-2-yl)-2,5-diphenyltetrazolium bromide) assay	Life technologies	M-6494
Hydrochloride-Isopropranolol	Lab supply	n/a
5-fluoro-2-deoxyuridine	Sigma-Aldrich	F0503
12-well plates (Biolite)	Thermo scientific	130185
24-well plates (Biolite)	Thermo scientific	930186

4.2.2 Cell culture

Human dermal fibroblasts were sourced from an established cell line and cultured in Dulbecco-modified Eagle medium (DMEM) with 1% penicillin and streptomycin. The specimens were maintained in a humidified incubator at 37 C° with a 5% carbon dioxide atmosphere. Medium was changed every second to third day. Cells at the same early passages (10 to 15) were used for all the experiments which examined the effect of decorin on proliferation and cyto-toxicity.

4.2.3 Cell proliferation and cytotoxicity assays

Yellow MTT (3-4,5-Dimethythiazol-2-yl)-2,5-diphenyltetrazolium bromide, a tetrazole) is reduced to purple formazan by metabolically active cells, in the mitochondria of living cells, in part by the action of dehydrogenase enzymes, to generate reducing equivalents such as NADH and NADPH. Mitochondrial dehydrogenases of viable cells cleave the tetrazolium ring, yielding purple MTT formazan crystals which are insoluble in aqueous solutions. The resulting purple formazan can be

solubilised in acidified isopropanolol (HCl-isopropanolol), and the absorbance of this coloured solution can be quantified by measuring with a spectrometer at 620nm.

This reduction only takes place when mitochondrial reductase enzymes are active, and thus the readings can be directly related to the number of viable (living) cells, i.e. an increase in cell numbers results in an increase in the amount of MTT formazan formed and subsequently an increase in absorbance. Thus when the amount of purple formazan treated with an agent (e.g. decorin,) is compared with the amount of formazan produced by untreated control cells, the effectiveness of the agent in causing cell death can be deduced through the production of a dose response curve. This method however cannot distinguish between reduced proliferation and cell death as the cause of reduced cell numbers. Thus, an additional agent that halts cell growth (but does not result in cell death) is needed. This can be achieved by adding 5-Fluoro-2-deoxyuridine (FDU-to limit fibroblast proliferation) (Merck Biosciences, Feltham, UK) at a final concentration of 30 μM[503] to the Dulbecco-modified Eagle medium (DMEM) (Invitrogen) that is used to suspend the cells.

4.2.4 Haemocytometer calibration, and determining optimal cell counts and Calibration of the MTT with haemocytometer readings

The MTT assay provides optical density readings which gives an indication of cell numbers but not actual cell counts. The assay can however be calibrated with haemocytometer readings to give an estimate of cell numbers.

A 175ml flask of fibroblasts was trypsinised using 4mls of TrypLE (Life Technologies) to detach the cells. After 5 minutes, 16 mls of DMEM was added to neutralise the trypsin and to make up the cell solution to 20 mls. 1ml of this cell solution was taken and put into a bijoux bottle from which a small sample (approximately 10 μL,) was loaded onto each of the counting chambers of an Improved Neubauer haemocytometer.

4.2.5 Haemocytometer calibration

A calibration was firstly done with the haemocytometer to determine the minimum number of grids that needed to be counted to give an accurate estimate of cell numbers. 1 reading is the count obtained from one grid on the haemocytometer (Figure 21).

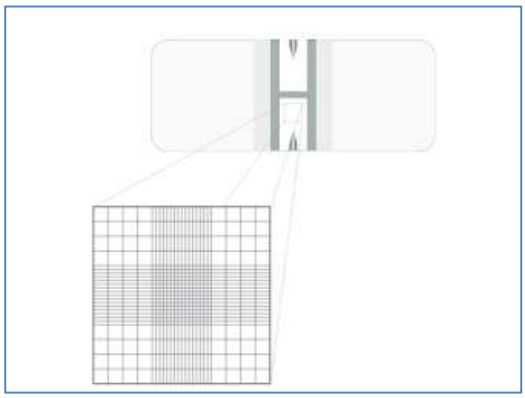

Figure 23: Haemocytometer grid used in the experiment. One reading is the count obtained from one grid on the haemocytometer.

A series of one to five readings with the haemocytometer (each performed in triplicate) was then done. The standard deviation of the readings was then plotted against the number of readings. Where the graph plateaus is the minimum number of grids that was needed to be counted for an accurate estimate of cell numbers.

4.2.6 MTT assay calibration

The rest of the solution was then centrifuged at 1000 rpm for 3 minutes to obtain a cell pellet and the excess DMEM was then aspirated. 19mls of DMEM was added to obtain a $1x10^5$ cells/ml solution (calculated from the previous reading from the haemocytometer using the $C_1V_1=C_2V_2$ formula). Serial dilutions of cells in culture medium of $1x10^5$ to $1x10^3$ cells were then prepared from this solution in a 96-well plate. A control row of DMEM without cells was also included. The cells were then left to attach overnight in a humidified incubator at 37 °C with a 5% carbon dioxide atmosphere.

The next day, 10µL of MTT reagent (i.e. 10%) was added to all wells including controls and the plate was returned to incubator for another 4 hours. Once the purple precipitates (Formazan crystals) had

formed, 100µL of isopropanol acidified with 0.1N hydrochloric acid was added to each well. The wells were left for another hour and checked under a microscope to ensure all crystals have dissolved before the absorbance in each well was read at 620nm in a microtiter plate reader (Glomax Multi Detection system, Promega, Wisconsin, United States of America).

The average values were calculated, and the absorbance reading was plotted against the number of cells/mL. The number of cells to use in the assay should lie within the linear portion of the plot and yield an absorbance of 0.75 - 1.25.

4.2.7 Cell proliferation and cytotoxicity assay

5 x 10^3 fibroblasts were seeded into each well in two sets of 96 well plates and left to attached overnight. The next day, the spent media was aspirated and replaced with 100 µL of normal DMEM that was supplemented with concentrations of decorin of 0, 5, 10, 15, 25, 50, 100 µg/mL per well in one plate. The decorin that was used was sterilised by filtering it with a 0.22 µm filter unit (Millex GP filter unit, Milipore Express PES membrane). This was repeated with the second plate except that the decorin-containing DMEM was additionally supplemented with 30 µM 5-FDU. MTT assays were then performed at 12, 24, 48 and 72 hours as described above. Eight replicate wells were used to obtain all data points. This experiment was then repeated with higher doses of decorin of 100, 200, 300, 400 and 500µg/mL, but the 5-FDU was increased to 50 µM as results from the earlier experiment showed that the fibroblast still showed some growth in the early phases.

4.3 Results

4.3.1 Haemocytometer calibration

When the standard deviation of the triplicate readings obtained from the haemocytometer was plotted against the number of readings, the graph obtained plateaued at 5 readings (Figure 24). It can be concluded that a minimum of 5 grids will need to be counted to give a reliable average of the number of cells.

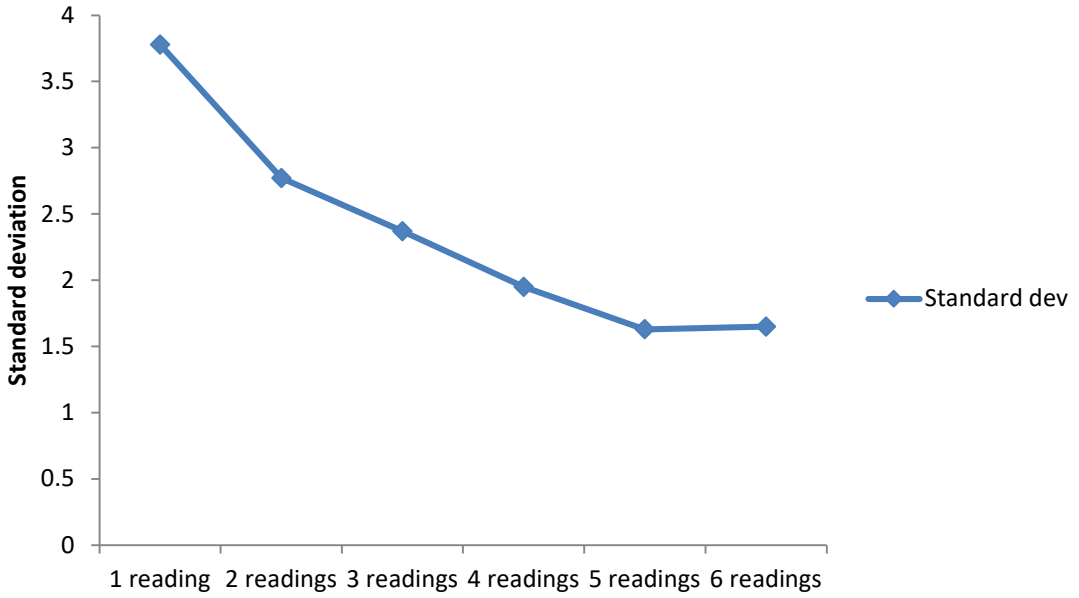

Figure 24: The standard deviation of readings 1-6 plotted against the number of readings. The lowest standard deviations were found with 5 and above readings.

4.3.2 MTT assay calibration results

As can be seen from Figure 25a, the graph of the optical density readings plotted against cell number seeded per well shows a good linearity (R^2=0.876) up to 10,000 cells. However, when the graph is limited to 5,000 cells, the linearity is further improved (R^2=0.917) (Figure 25b). The best linearity was actually obtained when the graph was limited up to 2500 cells (R2=0.984), but it was felt that this was too low a density and may affect the results of later experiments thus 5,000 cells per well was chosen as the preferred seeding density.

The manufacturers of the assay recommend that the linear portion of the graph should yield absorbance units between 0.75 to 1.25; however, our results are significantly less than this.

Fibroblasts are much larger and elongated compared to other cells, and thus they reach confluency at 5000-10,000 cells when viewed under light microscopy and it would be ideal not too have them growing in multiple layers. Thus, from the graph, 5000 cells per well appeared to be the optimal seeding density.

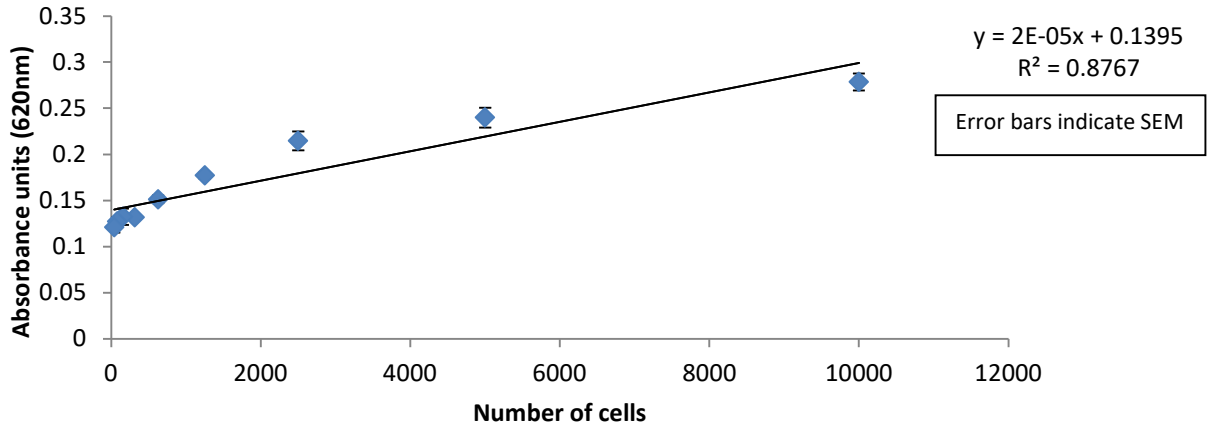

Fig. 23(a)

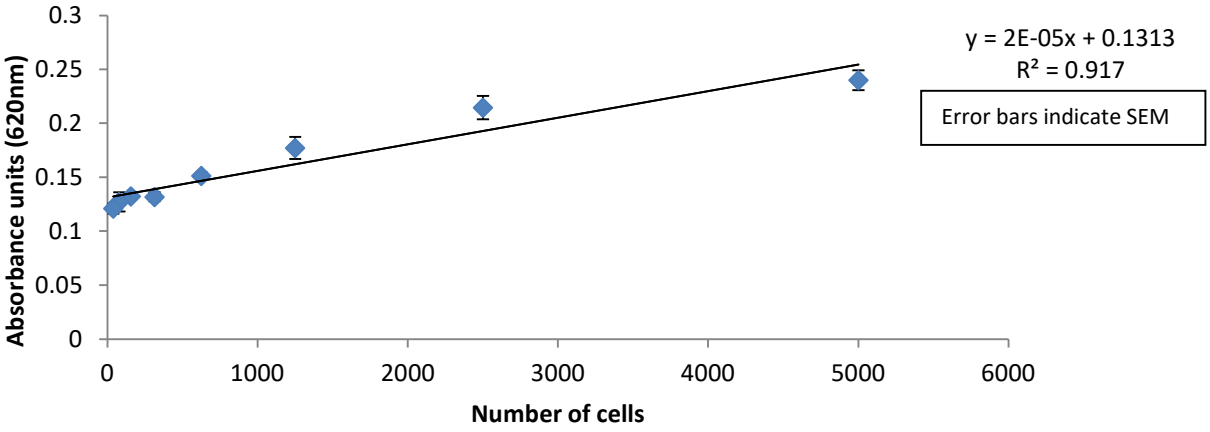

Fig. 23(b)

Figure 25 (a & b): MTT assay spectrometer optical density readings (Absorbance units, 620nm) plotted against the number of cells seeded per well in a 96 well plate. 23(a) MTT assay spectrometer optical density readings for 10,000 cells. 23(b): MTT assay spectrometer optical density readings for 5000 cells. Data were represented mean +/- standard deviation of mean (SEM; n=8). From these two graphs, it can be inferred that 5000 cells per well appeared to be the optimal seeding density.

4.3.3 Cell proliferation and cytotoxicity assay

Fibroblasts were cultured in the absence (0µg/mL) of decorin or presence of various concentrations of decorin (0, 5, 10, 15, 25, 50, 100, 200, 300, 400, and 500 µg/mL) for 12, 24, 48 and 72 hours in

normal DMEM (Figures 26a and 26b) and DMEM supplemented with 30µM of 5-FDU (Figure 26c) or 50µM of 5-FDU (Figure 26d).

Cell numbers at 0 hours appeared to be below the 5000 cells seeded but rose rapidly to 5000 cells and above at 12 hours for all groups. This is likely due a combination of an increase in fibroblast cell numbers (human dermal fibroblast doubling time is 18-24 hours) and also the restoration of cell metabolism after the cells have had time to recover after the initial seeding process.

No significant difference in the absorbance units could be seen in the decorin only plate amongst the various concentrations ($p=0.275$). In the 5-FDU supplemented plates, a difference can be seen between the wells with no decorin (0µg/mL) and decorin containing wells at 48 and 72 hours ($p<0.05$) although there was no significant differences between the different concentrations (100 to 5 to 500µg/mL).

Interestingly, the significant difference in fibroblast cell numbers between untreated (decorin 0µg/mL) and decorin treated groups at 72 hours is only seen in cells which were cultured with 5-FDU.

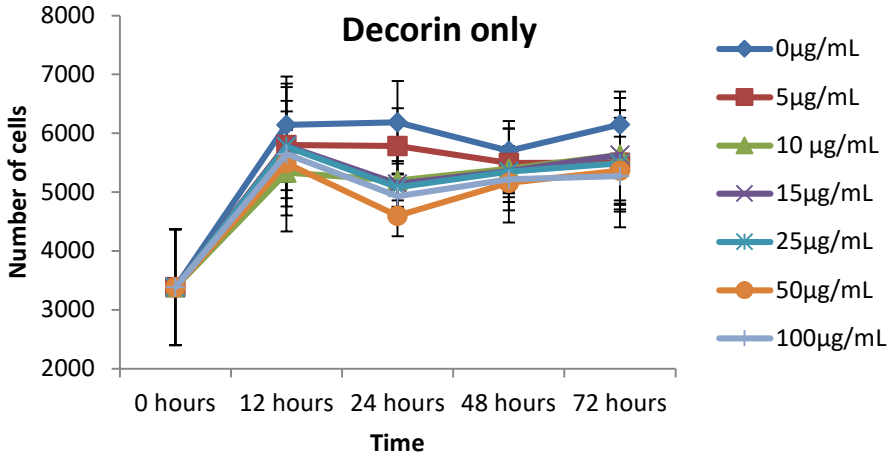

Fig. 24(a)

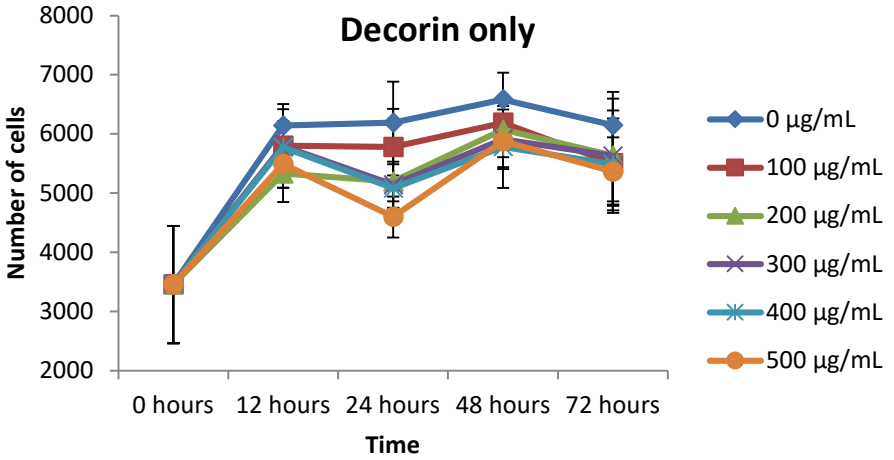

Fig. 24(b)

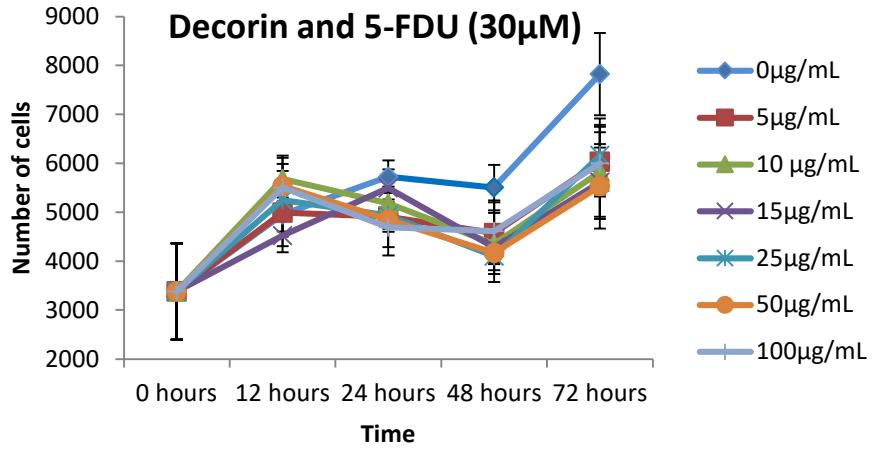

Fig. 24(c)

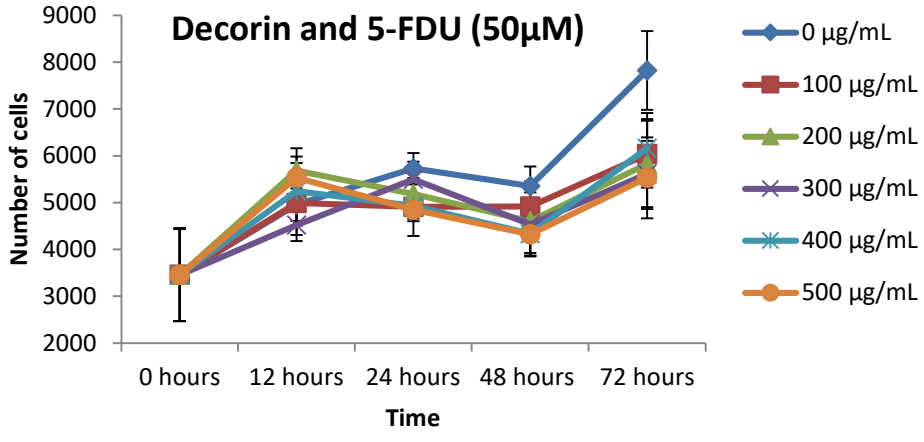

Fig. 24(d)

Figure 26 (a-d): MTT assay of human dermatofibroblasts cultured with different concentrations of decorin. Dermatofibroblasts cultured in the absence (0µg/mL) of decorin or presence of various concentrations of decorin (0, 5, 10, 15, 25, 50, 100, 200, 300, 400, and 500 µg/mL) for 12, 24, 48 and 72 hours in normal DMEM (4(a) and 4(c)) and DMEM supplemented with 30µM of 5-FDU (4(b)) & and 50 µM of 5-FDU (4(d)). Data were represented as their mean +/- standard deviation (n=8). No significant difference in the absorbance units could be seen among the different decorin concentrations in the 5-FDU supplemented and non-supplemented fibroblasts.

4.4 Discussion

Our present study confirms the results of previous work by Zhang et al[498] (2007) that decorin does not appear to have any significant cytotoxic effects on fibroblasts. Furthermore, we have shown that this non-toxicity extends up to 500µg/mL, whereas Zhang's study only tested decorin concentrations up to 100nM which is equivalent to about 3.8µg/mL. This is important as although fibroblasts through their excess secretion of collagen can cause problematic scars, they are still a vital component of the wound healing process and any toxicity to these cells may prolong the wound healing process and conversely results in poorer scars.

4.5 Conclusions

Our experiments have shown that decorin has a low potential for toxicity. This is important in the treatment of burns as patients with a high surface area of burns could potentially receive large doses of decorin through topical absorption of decorin. However, studies that investigate the systemic toxicity of decorin are required.

CHAPTER 5

EFFECTS OF HEAT TREATMENT ON THE BIO-ACTIVITY OF DECORIN

5. Effects of heat treatment on the bio-activity of decorin

5.1 Background

Information on the thermal stability of decorin is important when manufacturing the carrier dressing as it may need to be added in to the dressing at higher than room or body temperatures, e.g. gellan is required to be heated to 90°C to allow it to dissolve in water. Additionally, patients with large area burns often need to be kept warm in rooms with temperatures up to 40°C, and they can also spike fevers of 40°C or higher. Thus, it is essential to know that the integrity of decorin is maintained in these conditions. Although many studies have looked into its effects on cells, to date, few studies have looked at the thermal stability of the decorin proteoglycan.

There is currently no available commercial kit that will determine the bioactivity of decorin. Although enzyme-linked immunosorbent assay (ELISA) kits and various spectrophotometry techniques can allow us to measure the quantity of decorin, these techniques do not provide any information on the biological activity of decorin that is present.

Decorin however has known effects on different cell types such as proliferation[498, 504] , differentiation[505] , production of extracellular matrix components such as collagen[506] and expression of cell markers such as smooth muscle actin[507]. Thus, we can utilise these effects of decorin on cells as a marker of bio-activity and we thus designed experiments to test the bio-activity of decorin based its different effects on cells.

Additionally, decorin is known to affect collagen deposition in the extra-cellular matrix. It is thought to exert its effects by binding and neutralizing the effects of transforming growth factor β[508-511] and interacting with the various components of the extracellular matrix including collagen[512], fibronectin[513] and thrombospondin[514]. Decorin is known to play a crucial role in the production[498, 506], fibrillogenesis [515] and phagocytosis[516] of collagen. Experiments were thus designed to demonstrate the effects of decorin on collagen production by skin fibroblasts (Human dermatofibroblasts). Collagen in these experiments was quantified using the Pico-sirius red method[517, 518]. This method

uses the Sirius red dye which binds to the [Gly-x-y] triple-helix structure that is found in collagen fibres. The advantage of this method is that the stain can be dissolved (with an alkaline solution such as sodium hydroxide) and the optical density of the resulting solution determined spectrophotometrically using a microtiter plate assay system[519]. This binding of Sirius red dye has been shown to be proportional to the amount of collagen present and sensitive down to 0.5µg of collagen[520].

5.2 Hypothesis

As decorin is a protein, it is expected to be sensitive to changes in temperature.

5.3 Aims

To investigate the effects of heat treatment on the structural stability and bio-activity of decorin.

5.4 Materials and Methods

5.4.1 Materials

5.4.1.1 Thermal stability studies

Material	Supplier (including address)	Cat/Lot/Batch number
Phosphate buffered saline (Dulbecco A, Mg2+ and Ca2+ free)	Oxoid	1293357
Decorin (Galacorin)	Catalent	200LBRX09018
Glass cuvette (0.5mm, 1cm)	Lab supply	N/A
Circular Dichroism Spectrometer	Jasco UK	J-800
Decorin ELISA kit	R&D systems	Catalogue: DY143 Lot number: P152005
Wash buffer (0.05% Tween 20 in PBS)	Lab supply	N/A
Eppendorf Block heater (Techne Dri-Block)	Techne	DB-3
Glomax multi-detection system (spectrophotometer)	Promega	N/A

5.4.1.2 Cell proliferation bio-activity studies

Material	Supplier (including address)	Cat/Lot/Batch number
Dulbecco-modified Eagle medium	Sigma-Aldrich	RNBD4073 (exp 08/2015)
Phosphate buffered saline (Dulbecco A, Mg2+ and Ca2+ free)	Oxoid	1293357
Foetal Bovine Serum	Sigma-Aldrich	034M3398

(FBS, heat inactivated)		(expiry 03/2019)
Penicillin and Streptomycin	Sigma-Aldrich	SLBB9308
Human TGF-β2 (Cat. #100-35B)	Peprotech Inc	#08055345
Decorin (Galacorin)	Catalent	200LBRX09018
Human Dermatofibroblasts	European Collection of Cell Cultures	Human dermal fibroblasts (106-05a) cell line Catalogue no: 06090715
Alamar blue assay (Resazurin)	Sigma-Aldrich	R7017
12-well plates (Biolite)	Thermo scientific	130185
24-well plates (Biolite)	Thermo scientific	930186

5.4.1.3 Immunohistochemistry bio-activity studies

Material	Supplier (including address)	Lot/Batch number
Dulbecco-modified Eagle medium	Sigma-Aldrich	RNBD4073 (exp 08/2015)
Phosphate buffered saline (Dulbecco A, Mg2+ and Ca2+ free)	Oxoid	1293357
Foetal Bovine Serum (FBS, heat inactivated)	Sigma-Aldrich	034M3398 (expiry 03/2019)
Penicillin and Streptomycin	Sigma-Aldrich	SLBB9308
Human TGF-β2 (Cat. #100-35B)	Peprotech Inc	#08055345
Decorin (Galacorin)	Catalent	200LBRX09018
Human Dermatofibroblasts	European Collection of Cell Cultures	Human dermal fibroblasts (106-05a) cell line Catalogue no: 06090715
8 Chamber Chamber Polystyrene vessel tissue culture treated glass slides	BD Falcon	1001138000
Formaldehyde 36% w/v solution	TAAB	Lot: 90900
Normal Goat Serum (NGS)	Vector Laboratories	Lot: Z0325; Cat S-1000
Triton-X100 solution	Sigma-Aldrich	Lot: 121K0090
Bovine Serum Albumin (BSA)	Sigma-Aldrich	Lot: SLBH9984V; Cat A3294
Vectashield with DAPI (4',6-diamidino-2-phenylindole)	Vector Laboratories	ZA0210
Fibronectin (produced in Rabbit)	Sigma-Aldrich	F3648 Batch: 032M4752V Concentration: 0.5mg/mL
Goat & Rabbit secondary antibody, Alexa Fluor 594	Sigma-Aldrich	SAB4600 Lot: 1420978 Concentration: 2 mg/mL
Axioplan2 Imaging Microscope	Carl Zeiss MicroImaging GmbH	N/A
Imaging software: Axiovision	Carl Zeiss MicroImaging GmbH	Version 4.8.2.0

5.4.1.4 Collagen assay studies

Material	Supplier (including address)	Lot/Batch number
Dulbecco-modified Eagle medium	Sigma-Aldrich	RNBD4073 (exp 08/2015)
Phosphate buffered saline (Dulbecco A, Mg2+ and Ca2+ free)	Oxoid	1293357
Foetal Bovine Serum (FBS, heat inactivated)	Sigma-Aldrich	034M3398 (expiry 03/2019)
Penicillin and Streptomycin	Sigma-Aldrich	SLBB9308
Human TGF-β2 (Cat. #100-35B)	Peprotech Inc	#08055345
L-Ascorbic acid 2-phosphate sesquimagnesium salt hydrate	Sigma-Aldrich	A8960
L-Glutamine (200mM)	Sigma-Aldrich	G7513
Decorin (Galacorin)	Catalent	200LBRX09018
Human Dermatofibroblasts	European Collection of Cell Cultures	Human dermal fibroblasts (106-05a) cell line Cat no: 06090715
Trypan blue solution (0.4%)	Sigma-Aldrich	RNBC5948
24-well tissue culture plates (flat bottom with low evaporation lid)	Falcon	3319737 (Ref 353047)
Sirius Red (Direct Red 80)	Sigma-Aldrich	Cat: 365548
Bouin's solution	Sigma-Aldrich	HT10132
Picric Acid solution	Sigma-Aldrich	P6744
Hydrochloric acid solution	Lab supply	n/a
Sodium Hydroxide solution	Lab supply	n/a
Glomax multi-detection system (spectrophotometer)	Promega	n/a

5.4.2 Methods

5.4.2.1 Decorin heating protocol

A 0.05mg/mL solution of decorin was firstly prepared by adding 1mL of the 5mg/mL decorin stock solution to 99mls of Phosphate buffered saline (PBS). 1ml of this solution was then transferred to an eppendorf and placed in an eppendorf block heater at the 40 °C, 50 °C, 60 °C, and 90 °C for 30 minutes, 1 hour, 2 hours, 6 hours and 12 hours (Samples at 90°C were heated for 30 and 60 minutes only). The samples were then stored in a fridge at 8 °C until all samples had been prepared and ready for testing.

5.4.2.2 ELISA analysis of decorin post-heat treatment

Samples were further diluted from the heated stock samples to a working concentration of 500 pg/mL and decorin concentrations were determined using a human decorin ELISA kit ((Enzyme-Linked Immunosorbent Assay, R&D systems). All samples were performed in triplicate. The general ELISA protocol is described below.

5.4.2.2.1 Plate preparation

The capture antibody was diluted to working concentration without carrier protein (2.0ug/mL in PBS). A 96-well plate was then coated with 100µL of the capture antibody, sealed with paraffin film and incubated overnight at room temperature. The following day, each well was aspirated and washed with wash buffer (0.05% Tween 20 in PBS) three times. Plates were then blocked by adding 300µL of reagent diluent to each well and incubated at room temperature for 1 hour. After this, each well was again aspirated and washed with wash buffer (0.05% Tween 20 in PBS) three times.

5.4.2.2.1 Assay procedure

All reagents and samples were brought to room temperatures before use.

100µL of each standard (Standards used were 2000pg, 1000pg, 500pg, 250pg, 125pg 62.5pg, 31.2pg and 0pg of decorin) and samples were added into the appropriate wells. Wells were then covered and incubated for 2 hours at room temperature. After this, each well was again aspirated and washed with wash buffer (0.05% Tween 20 in PBS) three times.

100 µL of the Detection Antibody, diluted in reagent diluent (250 ng/mL), was then added to each well. The wells were then covered with a new adhesive strip and incubated for 2 hours at room temperature. After this, each well was again aspirated and washed with wash buffer (0.05% Tween 20 in PBS) three times.

100µL of working dilution of Streptavidin-HRP (Undiluted concentration ranges between 3-5µg/mL; diluted to 1:200) was then added to each well. The plate is then covered and incubated for 20 minutes at room temperature. After this, each well was again aspirated and washed with wash buffer (0.05% Tween 20 in PBS) three times.

100µL of substrate solution was then added to each well, followed by 20 minutes of incubation at room temperature. 50 µL of stop solution was then added to each well and gently tapped to ensure thorough mixing. Plates were then read with a spectrophotometer (Glomax multi-detection system).

5.4.2.3 Circular dichroism analysis of heat treatment of Decorin

We have shown through ELISA studies that decorin is rapidly denatured in temperatures above 40°C. In the in-vitro arm of our studies, we thus sought to look at the effects of heat more closely by investigating the effects of heat on the secondary and tertiary structure of decorin via circular dichroism. We also sought to develop a bio-activity assay to determine the efficacy of decorin in order to evaluate the effect of different conditions such as change in temperature on the biological activity of the proteoglycan.

5.4.2.3.1 Non-continuous heat treatment

Decorin was prepared in a concentration of 0.6mg/mL in PBS and 500uL of the decorin solution was placed in each eppendorf. The eppendorfs were then subject to heat treatment in an eppendorf block heater at temperatures of 40°C, 60°C, 70°C and 90°C for the time periods of 30 minutes, 1 hour, 2 hours, and 3 hours. The samples, including a PBS baseline sample, were then loaded into a 0.5mm glass cuvette and analysed with a circular dichroism spectropolar-meter (J-810, Jasco) with the following parameters:

- Wavelengths analysed: 190nm to 300nm
- Data pitch: 0.2nm
- Scanning mode: Continuous
- Scanning speed: 200nm/minute
- Accumulations: 10

5.4.2.3.2 Continuous heating and cooling treatment

Decorin was prepared in a concentration of 0.6mg/mL in PBS and 1mL of the decorin solution was placed in a 1cm glass cuvette which had a seal to minimise evaporation. The cuvette was then placed in the circular dichroism spectropolarmeter (J-810, Jasco) with a Peltier controller (Jasco PTC-4235/15) which is capable of heating and cooling the sample. The following parameters were used:

- Wavelength monitored: 217nm
- Temperature rate: 0.7°C/minute
- Temperature ranges: 20°C to 30°C, 20°C to 45°C, 20°C to 90°C

5.4.4.4 Effects of heat treated decorin on ECM production

5.4.4.4.1 Cell proliferation bioactivity assays

Rat C6 glioma cells were sourced from an established cell line and cultured in Dulbecco-modified Eagle medium (DMEM) with 1% penicillin and streptomycin. The specimens were maintained in a humidified incubator at 37 C° with a 5% carbon dioxide atmosphere.

2 x10^5 cells were seeded per well in a 24 well plate, with each well topped up with media to a total of 2mls. The cells are then left to attach overnight. The next day, the media was removed and replaced with 2mls of media supplemented with decorin in concentrations of 0 µg/mL (control), 5µg/mL, 20 µg/mL and 100 µg/mL. The media was exchanged with fresh treatment media every 24 hours for 5 days. Every 3 wells per treatment group was trypsinised and the cells counted.

5.4.4.4.2 Immunohistochemistry bioactivity assays

2.0 x 10^4 human dermal fibroblasts were seeded per well in 8-chamber wells, with x3 wells for each treatment group. The wells were then topped up to 100µL per well. 400µL of prepared treatment solutions were then added to make a total of 500µL of solution per well with the below treatment groups:

1. Control (No TGF-β2 & no decorin)
2. Decorin 100ng/mL
3. Decorin 500ng/mL
4. Decorin 1000
5. TGF-β2 50ng/mL
6. TGF-β2 50ng/mL + decorin 100ng/mL
7. TGF-β2 50ng/mL + decorin 500ng/mL
8. TGF-β2 50ng/mL + decorin 1000ng/mL

The cells were then left to attach and grow for 3 days before being prepared for immuno-histochemical staining.

On day 3, the media was removed, and the cells washed with PBS (without calcium and magnesium and using plastic Pasteur pipettes). The cells were then fixed with a solution of 4% Formaldehyde for 10 minutes. After which they were again washed with wash buffer three times (10 minutes each time). 150µL of blocking solution was then added and left for 30 minutes at room temperature. The cells were then washed again three times in wash buffer (5 minutes each time). The primary antibody for fibronectin was then added (rabbit fibronectin, 1:200 dilution i.e. 2.5µg/mL) to each well and left to incubate at 4°C overnight or 1 hour at room temperature. After incubation, the antibody solution was removed, and the cells were again washed with wash buffer three times (5 minutes each time). After this, secondary antibodies (Goat and rabbit Alexa Fluor 594, 1:400 dilution i.e. 5.0 µg/mL) were then added and incubated at room temperature for 1 hour. The cells were again washed with wash buffer three (5 minutes each time) before the chamber plastic was removed from the slides before a drop of DAPI Vectashield was applied to each well and a coverslip attached on the surface. The slides were then imaged with an Axioplan2 Imaging Microscope (Carl Zeiss) at 180ms exposure.

The images obtained were then analysed with an image analysis software (ImageJ). Quantification of the area staining positively for fibronectin was performed after processing of the images was done using thresholding techniques to remove background staining.

5.4.4.4.3 Collagen assays

The fibroblasts were sourced from an established cell line and cultured in Dulbecco-modified Eagle medium (DMEM) with 1% penicillin and streptomycin. The specimens were maintained in a humidified incubator at 37 C° with a 5% carbon dioxide atmosphere. Cells at the same early passages (10 to 15) were used for all the experiments.

1.0×10^5 of HDF cells were seeded per well in a 24-well plate, with x3 wells seeded for each treatment group. The wells were then topped up with DMEM supplemented with FBS and Pen/Strep and the cells were allowed attach overnight. The cells were left to grow for 3 days to ensure that they were confluent before the treatments were started.

On day 3, the spent media was aspirated and 500µL of the following treatment solutions were added to each well:

First set of experiments:

1. DMEM without ascorbic acid supplementation
2. DMEM supplemented with ascorbic acid (50µg/mL)
3. DMEM supplemented with ascorbic acid (50µg/mL) + TGF-β2 (50µg/mL)
4. DMEM supplemented with ascorbic acid (50µg/mL) + TGF- β2 (50µg/mL) + decorin 0.1µg/mL
5. DMEM supplemented with ascorbic acid (50µg/mL) + TGF- β2 (50µg/mL) + decorin 0.5µg/mL
6. DMEM supplemented with ascorbic acid (50µg/mL) + TGF- β2 (50µg/mL) + decorin 1.0µg/mL
7. DMEM supplemented with ascorbic acid (50µg/mL) + TGF- β2 (50µg/mL) + decorin 10µg/mL
8. DMEM supplemented with ascorbic acid (50µg/mL) + TGF- β2 (50µg/mL) + 40°C heated decorin 10µg/mL*

*For the 40°C heated decorin, decorin was prepared at 10µg/mL in DMEM sup, and 2mLs were placed in an Eppendorf. This Eppendorf was then heated in an Eppendorf block heater to 40°C for 30 minutes and then removed and cooled in iced water. This solution was then used to make up the treatment solution number 8.

All treatment solutions were prepared fresh on the day of media change except for treatment solution number 8. Media was changed on days 3, 7, 10, and 14. The Sirius red assay for collagen was done on days 4, 7, 10, and 14.

Second set of experiments:

1. Control: No TGF-β2 and no decorin.
2. TGF- β2 only: TGF-β2 (50ng/mL) only given on days 3, 7 and 10.

3. TGF- β2 + DCN 40°C: TGF- β2 (50ng/mL) + decorin (10ug/mL, heated to 40°C, stored together from day 3 onwards)
4. TGF-β2 + DCN 90°C: TGF- β2 (50ng/mL) + decorin (10ug/mL, heated to 90°C, stored together from day 3 onwards)
5. TGF-β2 + DCN 40°C (fresh): TGF-β2 (50ng/mL) + decorin (10ug/mL, heated to 40°C, made fresh on day 3, 7, and 10)
6. TGF-β2 + DCN 90°C (fresh): TGF-β2 (50ng/mL) + decorin (10ug/mL, heated to 90°C, made fresh on day 3, 7, and 10)
7. TGF-β2 till day 7 only then DCN 40°C: TGF-B2 (50ng/mL) on days 3, then stopped and then decorin (10ug/mL, heated to 40°C) added fresh with each media change on days 7 and 10
8. TGF-β2 till day 7 only then DCN unheated: TGF-β2 (50ng/mL) on days 3, then stopped and then decorin (10ug/mL, unheated) added fresh with each media change on days 7 and 10

Media was changed on days 3, 7, 10, and 14. The Sirius red assay for collagen was done on days 4, 7, 10, and 14.

Sirius red assay protocol

Sirius Red (Direct 80) – dissolved in saturated aqueous picric acid at a concentration of 100mg/100ml.

Staining of cell layers and quantification of the dye reaction (cultured in 24 well plates):

- DMEM discarded and cells washed with PBS
- 1ml of Bouin's fixation fluid added and left for 1 hour (Fume Cupboard used)
- Fixation fluid aspirated.
- Cells immersed in distilled water for 15min
- Cultures air dried and Sirius red solution added to cover the well (250µL)
- Plate shook for 1 hour on a plate shaker, and excess dye aspirated and washed with 1mL of 0.01N hydrochloric acid to remove all the non-bound dye (repeat x3 times).
- 500µL of 0.1N sodium hydroxide was then added into each well and placed on a microplate shaker for 30 minutes at room temperature.
- The dye solution was then transferred to a 96-well plate (100µL per well) and measured at an optical density (OD) of 550nm against a 0.1N sodium hydroxide blank.

5.5 Results

5.5.1 ELISA analysis of decorin post-heat treatment

Concentrations of decorin free in solution were determined using an ELISA kit on samples treated at 40, 50, 60, 70 and 90°C for 30 minutes, 1, 2, 6 and 12 hours. Figure 27 shows that decorin remains stable at 40°C even up to 12 hours and that it was even possible to detect a rise in decorin concentration when samples were held at this temperature. At temperatures above 50°C, decorin started to degrade and no decorin survives at 90 °C even at 30 minutes. Decorin levels in samples heated to 50 °C or higher for more than 30 minutes were all significantly lower than decorin kept at 40 °C ($p<0.05$). Interestingly, the decorin samples heated at 40°C showed a higher decorin concentration compared to the decorin sample kept at room temperature. This may possibly be because the heat treatment caused a change in the configuration of the proteoglycan and exposed more functional groups which were detected by the antibodies in the ELISA kit. Decorin exists in dimeric form at room temperature. It is possible that the elevation of temperature caused dissociation of the monomers, allowing for the measurement of a higher concentration of the molecule. This data indicated that the decorin has to be added to the gellan mixture only after it has cooled to 40°C. We followed this experiment with a circular dichroism study to determine the exact temperature decorin unfolds at and whether this process is reversible.

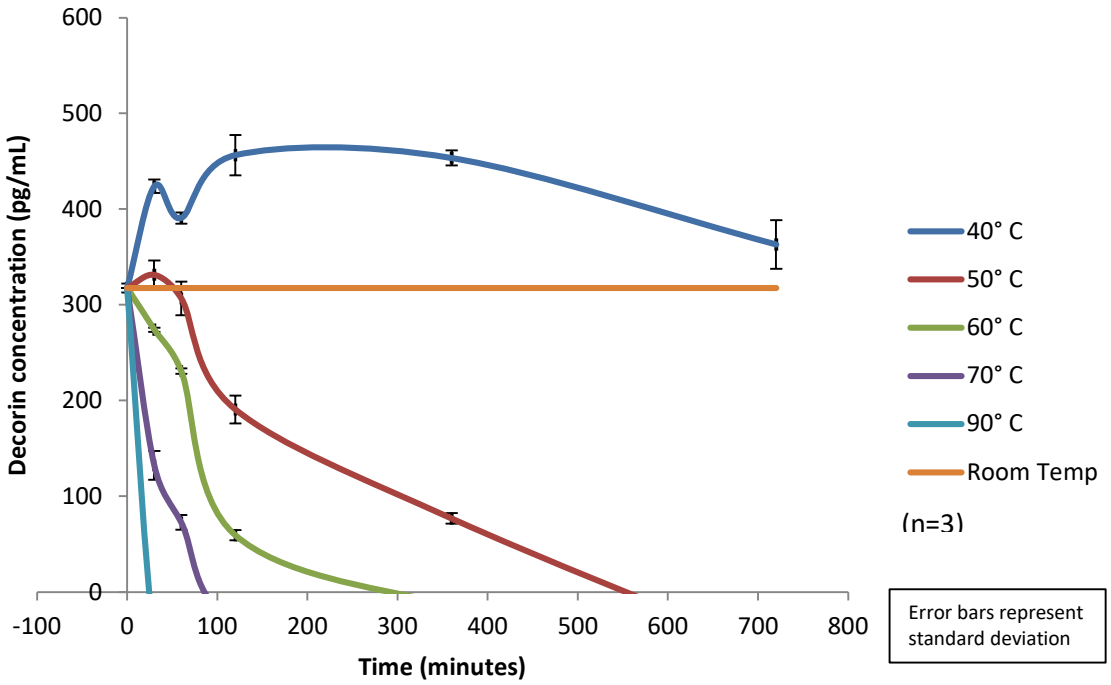

Figure 27: Decorin concentration as measured using an ELISA assay during heat treatment. Decorin was treated at 40 °C, 50 °C, 60 °C, and 90 °C for 30 minutes, 1 hour, 2 hours, 6 hours and 12 hours and compared with decorin that was left at room temperature. Compared to decorin heated at temperatures at higher temperatures and even room temperature, decorin heated at 40°C showed higher concentrations. All samples were performed in triplicate (n=3).

5.5.2 Circular dichroism analysis of heat treatment of decorin

Thermal stability tests with the circular dichroism method have confirmed that decorin starts to lose its tertiary structure at temperatures above 40 °C. This change in the structure of decorin after heat treatment was also found to be non-reversible. Decorin heated at 40°C shows 2 nadirs, one at approximately 210nm and the other at approximately 217nm (Figure 28a). The nadir at approx. 217nm is lost in decorin heated at 60°C at 1 hour, though it is present but reduced at 0.5 hours (Figure 28b). At 70°C (Figure 28c) and 90°C (Figure 28d), the nadir at 215nm is lost even at 0.5 hours.

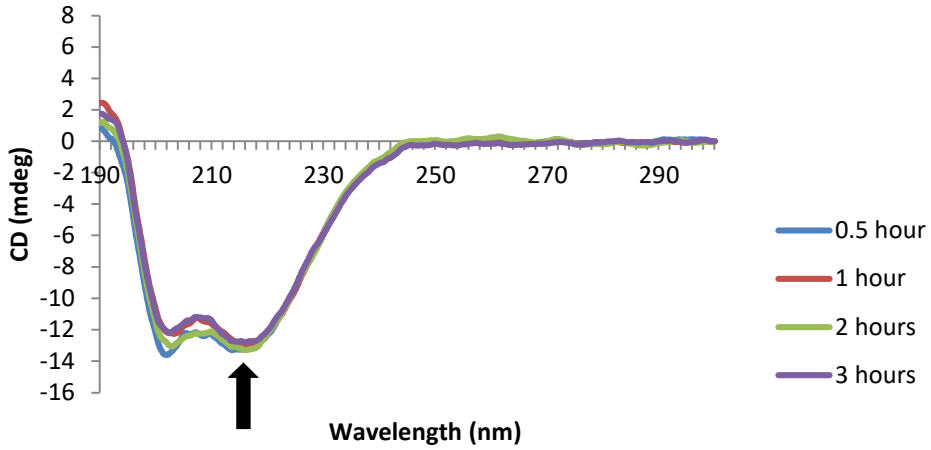

Fig. 26(a)

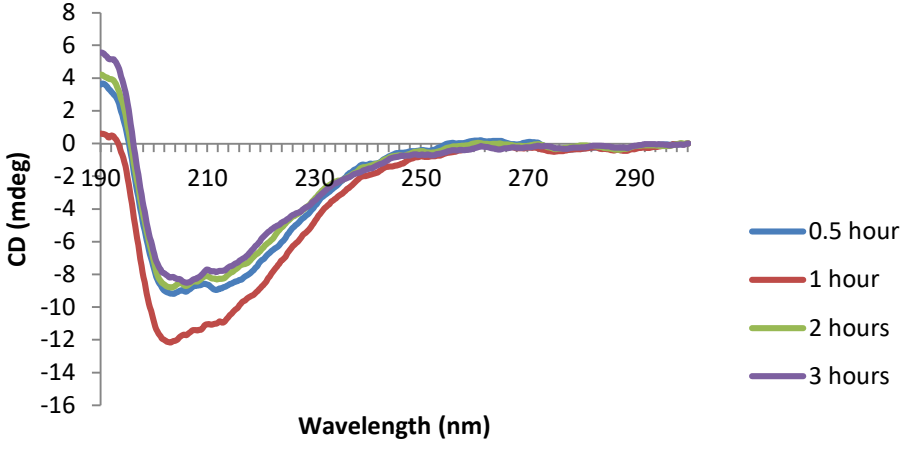

Fig. 26(b)

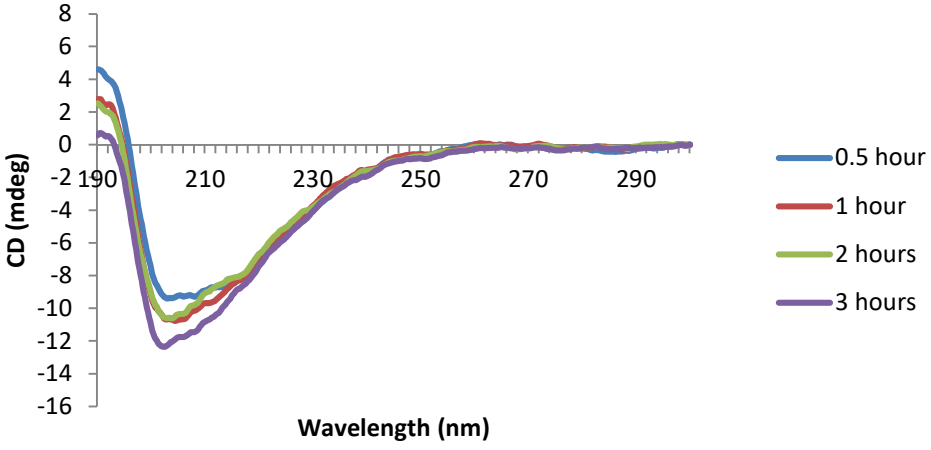

Fig. 26(c)

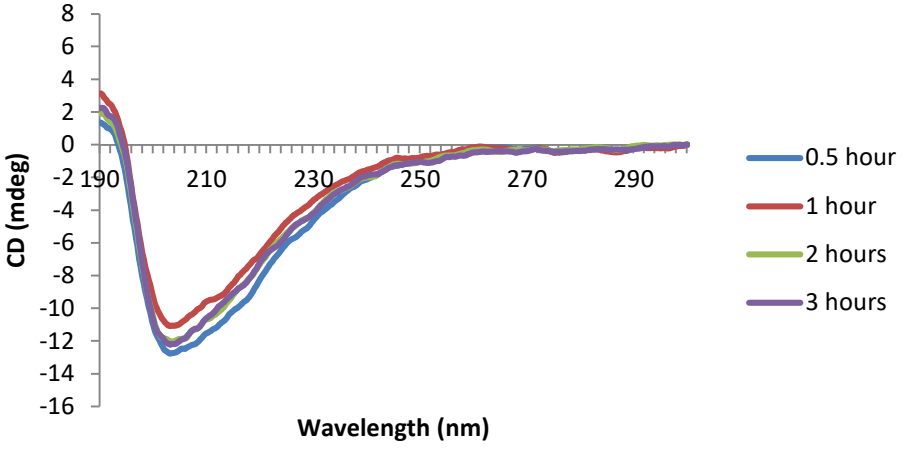

Fig. 26(d)

Figure 28 (a-d): Circular dichroism analysis of decorin heated at 40°C (a), 50°C (b), 70°C (c) and 90°C (d)over 0.5, 1, 2 and 3 hours. The nadir at 217nm in (figure a, black arrow) is present in decorin heated at 40°C but is absent at higher temperatures.

The results of the continuous heating and cooling treatment of decorin are shown in Figures 29(a) to 29(d). The decorin sample that is heated to 45°C shows CD spectra and absorbance readings that return to the same value after cooling indicating that no structural change in the decorin has occurred (Figures 29(a) and (b)). For decorin heated to 70°C and 90°C, a significant increase in the CD spectra is seen at about 42°C, and the absorbance graphs (29(c) & 29(d)) show that the absorbance values of decorin after cooling is significantly different to the original values indicating that the structural changes to the protein are not reversible even after cooling occurs.

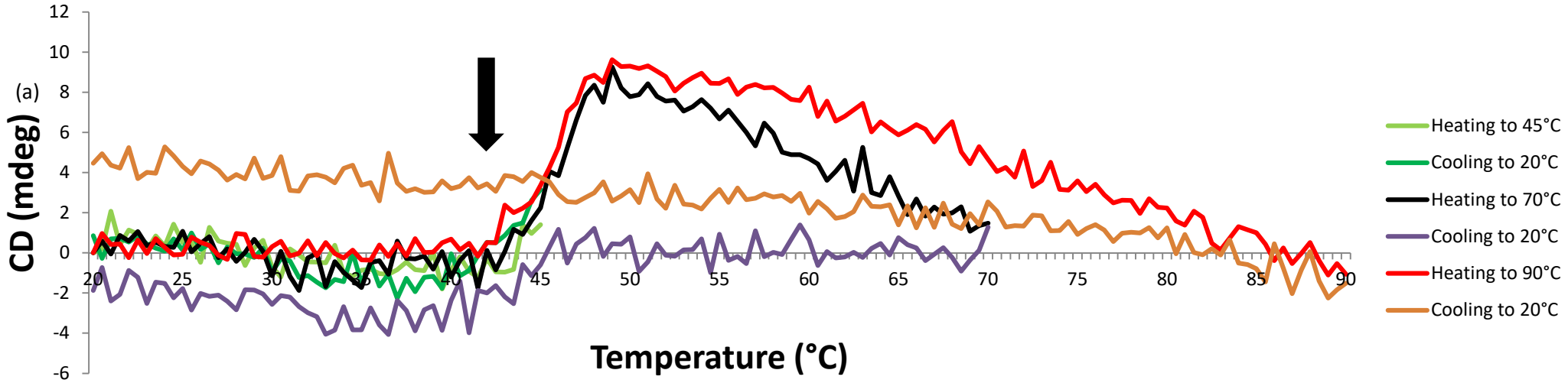

Fig 27(a)

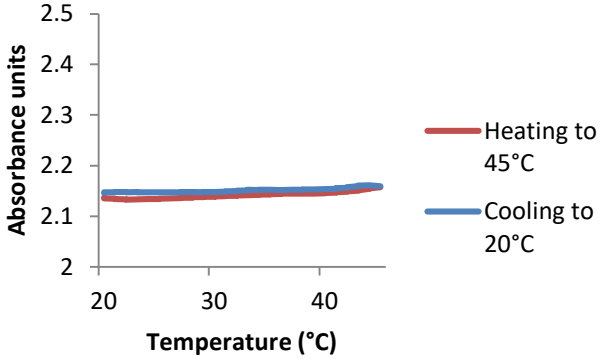

Fig. 27(b)

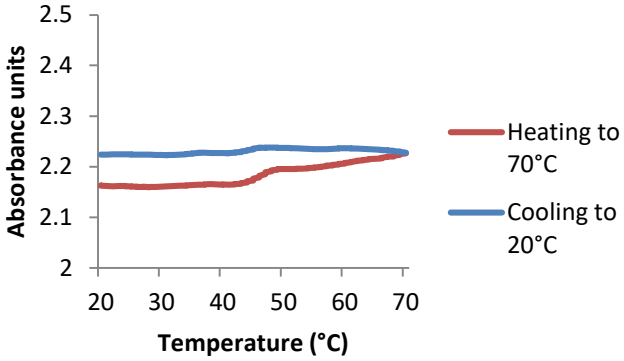

Fig 27(c)

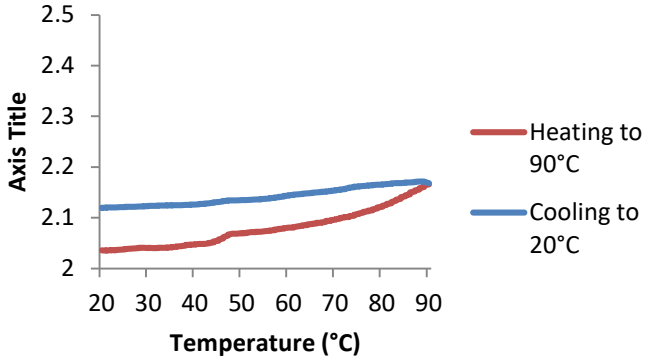

Fig 27(d)

Figure 29 (a-d): Circular dichroism of decorin: (a) Circular dichroism of decorin with continuous monitoring of the 217nm wavelength as it is heated from 20 to 45°C, 70°C and 90°C and then cooled back down to 20°C. A significant increase in the CD spectra is seen at about 42°C (black arrow). Figures (b) to (d) show the corresponding absorbance of decorin throughout the heating (to 45°C, 70°C and 90°C) and cooling cycles (back to 20°C). The original and final absorbance values of decorin heated to 45°C remain the same whereas those of decorin heated to 70°C and 90°C differ.

5.5.3 Proliferation based Bioactivity studies

As previous experiments showed that decorin did not significantly affect the proliferation of HDF cells, we tested decorin on a different cell line, i.e. rat glioma C6 cells, as previous experiments done by other colleagues had shown an effect. However, in our experiments, at concentrations of decorin from 0 to 200µg/mL, no significant differences in the cell count can be seen even at day 4 and 5 (Figures 30(a) and 30(b)).

In terms of bio-activity, proliferation of cells (both HDFs and C6 glioma) cells were found to be an unreliable indicator of the bio-activity of decorin i.e. we could not demonstrate any differences in the cell counts after decorin treatment.

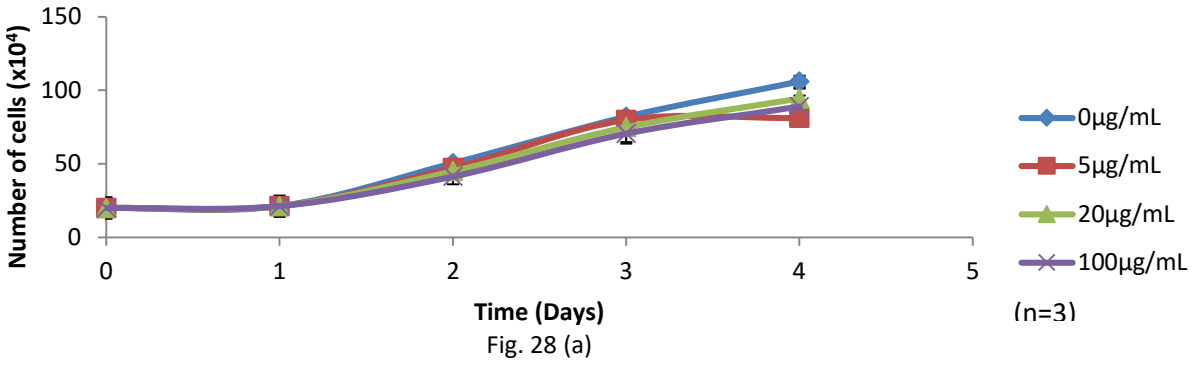

Fig. 28 (a)

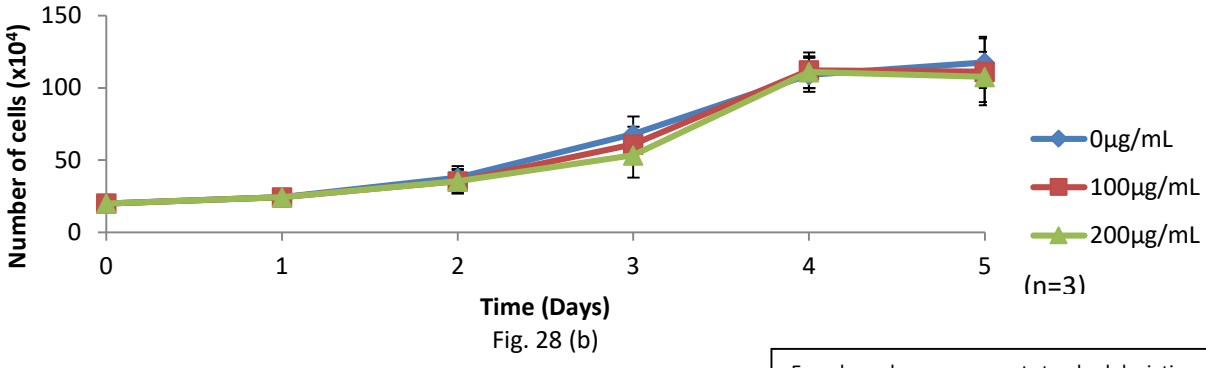

Fig. 28 (b)

Error bars shown represent standard deviation

Figure 30 (a & b): Rat glioma C6 cell proliferation in the presence of decorin at concentrations of 0µg/mL, 5µg/mL, 20µg/mL, 100µg/mL and 200µg/mL. Figure 8(a) Rat glioma C6 cell counts with decorin treatment groups of 0, 5, 20 and 100µg/mL. Fig 8 (b) Rat glioma C6 cell counts with decorin treatment groups of 0, 100, 200µg/mL. Error bars shown represent standard deviation. No significant differences in the cell count can be seen even at day 4 and 5 at all concentrations of decorin. All samples were performed in triplicate (n=3).

5.5.4 Immunohistochemistry based bio-activity studies

Fibronectin in fibroblasts was investigated as a possible marker of decorin bio- activity. Immuno-histochemical staining for fibronectin was performed in human dermatofibroblasts after 3 days of treatment with a fixed dose of TGF-β2 (50ng/mL) and various concentrations of decorin (1 to 1000ng/mL). Visual examples of fibronectin staining can be seen in Figure 31.

Figure 32 shows the quantification of the surface area staining positively for fibronectin after immuno-histochemical staining. As can be seen from the graph, there is a significant decrease seen in fibronectin staining in HDFs treated with 100 and 1000ng/mL of decorin ($p<0.05$) . HDFs treated with 1000ng/mL of decorin show levels of fibronectin similar to control. The experiment was then repeated with both heated and non-heated decorin. As can be seen from Figure 33, only HDF's that were treated with decorin (1000ng/mL) at 40°C showed a significant decrease in area of fibronectin staining to the control group ($p=0.02$). When compared to the TGF-β2 (50ng/mL, with no decorin), the following groups showed a significant decrease in area staining for fibronectin: HDF's and DCN (500ng/mL) only, TGF-β2 + DCN (1000ng/mL) treated at 40°C, TGF-β2 + DCN (1000ng/mL) treated at 50°C and TGF-β2 + DCN (1000ng/mL) treated at 90°C. Although not significant, there is a trend of increasing area staining for fibronectin when decorin is treated at increasing temperatures (except for decorin treated at 90°C) which infers that heat treatment with increasingly higher temperatures reduces the anti-fibronectin effects of decorin.

The results of this experiment (Figure 33) are significantly different from the previous experiment (Figure 32), and this may be due to a difference in protocol: in the previous experiment (Figure 32), the slides were incubated with the secondary antibody overnight which resulted in stronger staining as evidence by the level of thresholding used to analyse the images (Thresholding value of 140 versus 75). Immunohistochemistry experiments which stained for fibronectin showed that it could possibly be used as a bio-activity assay as decorin at 1000µg/mL reduced the area staining positively

for fibronectin significantly. Further standardisation of the experiment procedure is required to increase its reproducibility. However, the current results do support the hypothesis that decorin that is treated at 40°C appears to have good bioactivity that is even greater than non-heat treated decorin.

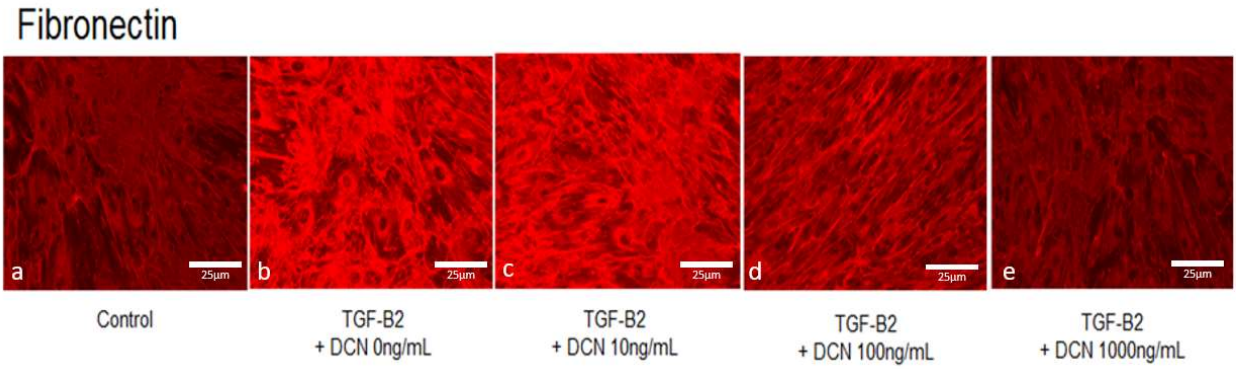

Figure 31: Immuno-histochemical staining for fibronectin (red) in human dermatofibroblasts after 3 days of treatment with TGF-β2 (50ng/mL) and various concentrations of decorin: (a) Control, (b) 0ng/mL, (c) 10ng/mL, (d) 100ng/mL, and (e) 1000ng/mL. HDFs treated with TGF-β2 and 0 or 10ng/mL of decorin show much brighter and greater surface area of staining for fibronectin whereas there is a decrease in staining intensity in the HDFs treated with 100 and 1000ng/mL of decorin. The intensity of fibronectin staining appears to return to the levels of the control group in HDFs treated with 1000ng/mL of decorin. All samples were performed in triplicate (n=3).

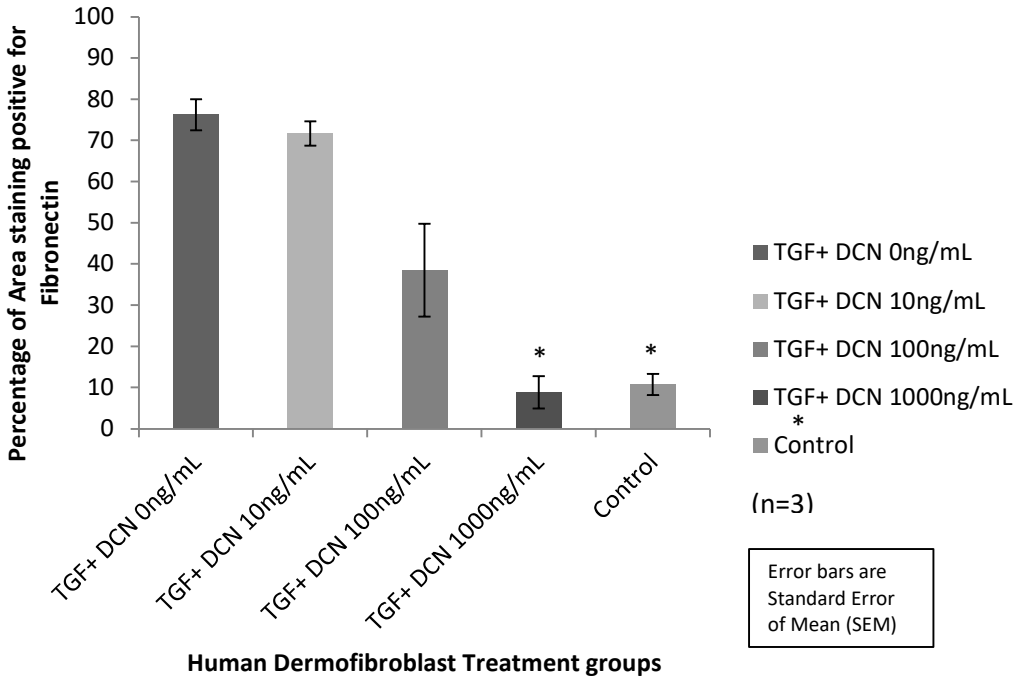

Figure 32: Quantification of surface area staining positively for fibronectin after immuno-histochemical staining. Both of the groups treated with TGF and 1000ng/mL of Decorin and control (asterixed) had fibronectin positive surface areas (%) lower than the group treated with TGF but no decorin. All samples were performed in triplicate (n=3).

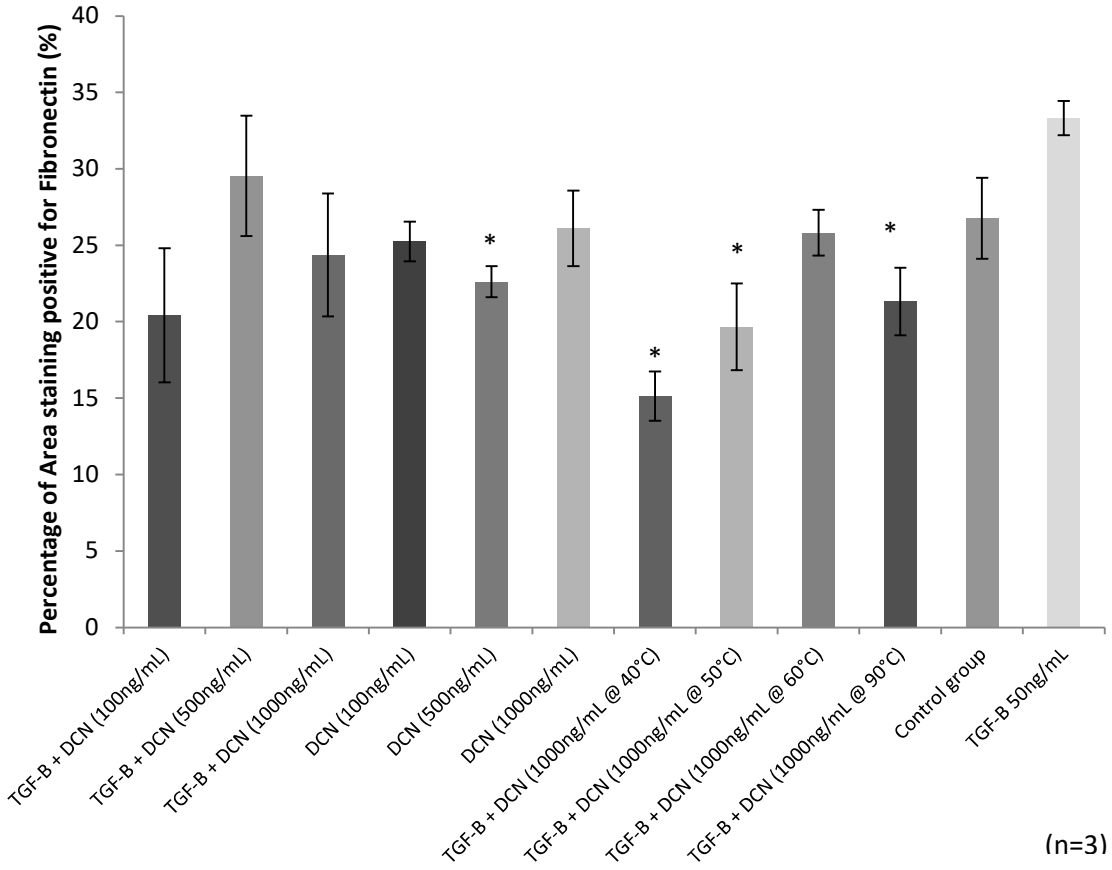

Figure 33: Quantification of immune-histochemical staining of fibronectin in human dermato-fibroblasts after treatment with TGF- β2, unheated decorin and heated decorin: the graph shows the percentage of area of fibroblasts staining positively for fibronectin after 3 days of treatment with TGF-β2 (50ng/mL) and various concentrations of decorin (100, 500 and 1000ng/mL) and decorin (at a concentration of 1000ng/mL) and treated at temperatures of 40, 50, 60 and 90°C for 30 minutes. The treatment groups that showed a statistically significant difference to the TGF only treatment group are denoted with an asterisk. All samples were performed in triplicate (n=3).

5.5.5 Collagen based bio-activity studies

Figures 34 and 35 show the quantification of collagen via the Sirius red assay in HDF's treated with TGF-β2 and various concentrations of decorin (0.1, 0.5, 1, and 10ug/mL and also 10ug/mL heat treated decorin [40°C]) over 14 days. This experiment showed that ascorbic acid supplementation is important in increasing the amount to collagen formed by HDF's as it significantly increases the amount of collagen produced by HDF cells ($p<0.05$).

TGF-β2 (50ng/mL) also significantly increases collagen production when compared to non-TGF-β2 treated control groups (both ascorbic and non-ascorbic acid supplemented). Only decorin at 10ug/mL reduced collagen levels to a significant level compared to the TGF-β2 only treated group. Decorin at 10ug/mL (non-heat treated) significantly reduces the amount of collagen deposited at day 14(p=0.00) by 12%. Decorin at 10ug/mL which had been heated to 40°C (and co-incubated with TGF-β2 up to 14 days) appears to significantly reduce the amount of collagen deposited at day 14 (p=0.00) by 44%. This may be due to decorin binding all the TGF in the treatment solution, and the excess decorin seems to then (from day 7) have a fibrinolytic effect on the collagen as the amount of collagen reduces from day 7 onwards and becomes significantly less than the control group on day 14 (p=0.02).

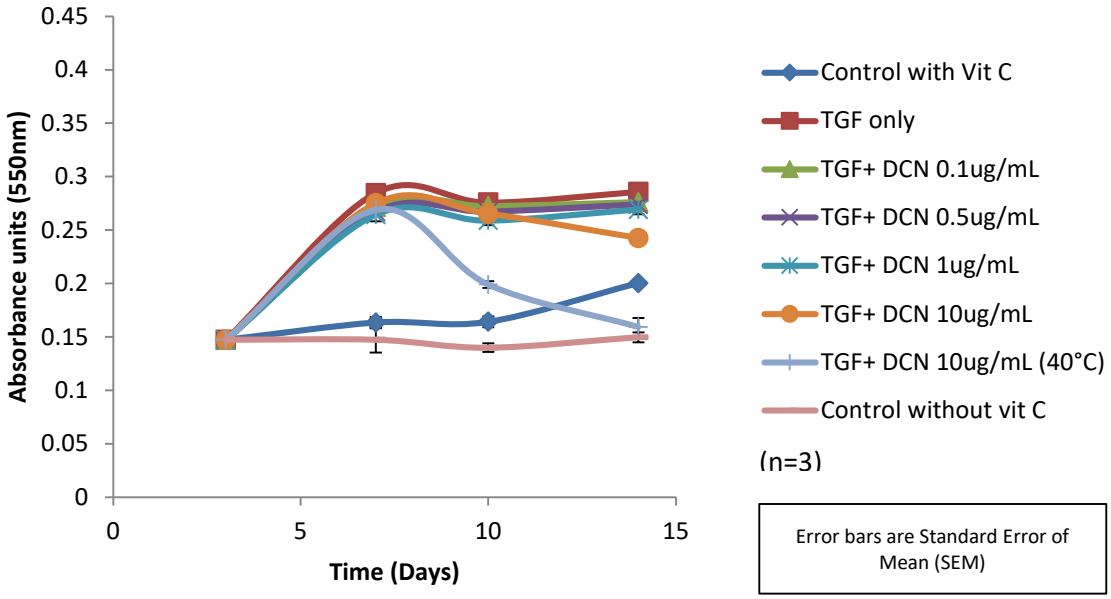

Figure 34: Quantification of collagen via the Sirius red assay in HDF's treated with TGF-β2 and various concentrations of decorin (0.1, 0.5, 1, and 10ug/mL and also 10ug/mL heat treated decorin [40°C]) over 14 days. The biggest difference in final collagen deposition is seen with the decorin at 10ug/mL which had been heated to 40°C (and co-incubated with TGF-β2 up to 14 days). Ascorbic acid supplementation significantly increases the amount of collagen deposited compared to the controls without supplementation. All samples were performed in triplicate (n=3).

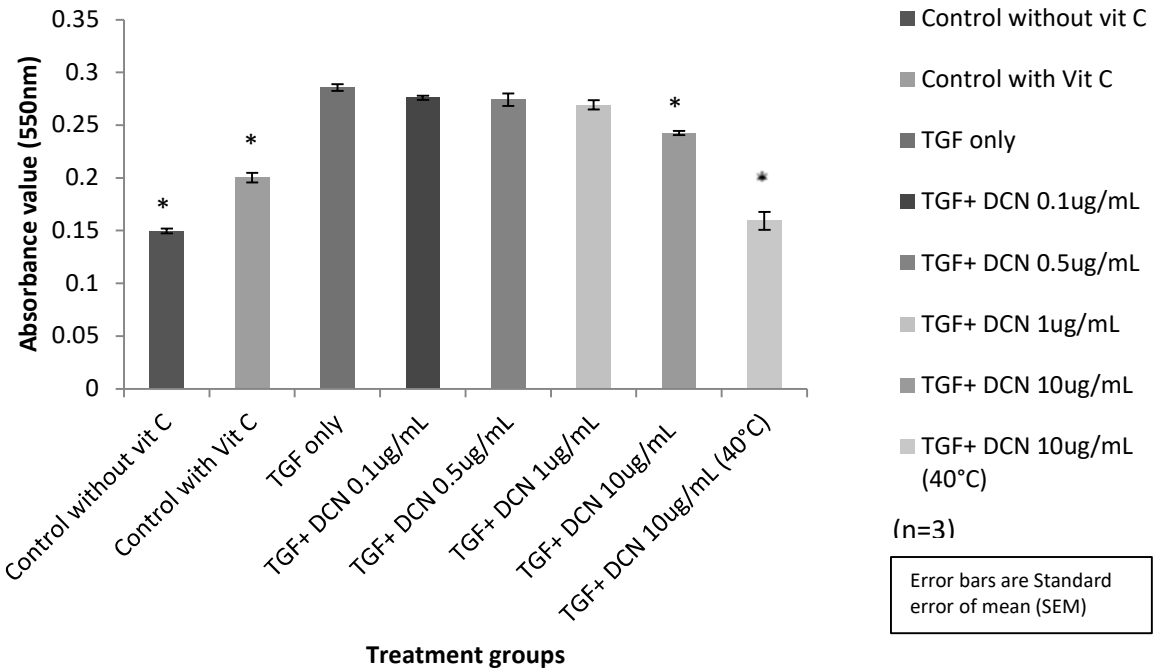

Figure 35: Bar chart showing the levels of collagen as ascertained by the Sirius red assay on day 14 of HDF's treated with TGF-β2 and various concentrations of decorin (0.1, 0.5, 1, and 10ug/mL and also 10ug/mL heat treated decorin [40°C]). The treatment groups that showed a statistically significant difference to the TGF only treatment group are denoted with an asterisk. Error bars are Standard error of mean (SEM). All samples were performed in triplicate (n=3).

The objective of the next experiment (Figures 36 and 37) was to determine firstly if increased temperature would affect the effect of decorin on collagen deposition and secondly if the dissolution of deposited collagen seen in the previous experiment was due to the sequestration of TGF-β2 by decorin (thus in two of the groups, TGF-β supplementation was stopped after day 7).

According to the results of the previous ELISA and CD experiments on the heat stability of decorin, an increase of temperature from 40 to 90°C should destroy the tertiary structure of decorin and cause it to denature. Thus, decorin heated at 90°C treated should have theoretically shown less or no bio-activity. However contrary to the hypothesis, decorin heated at 90°C not only retained but actually showed a small but statistically significant increased activity in both the groups that decorin was stored with TGF-β2 ($p<0.001$) and the freshly prepared groups ($p<0.001$).

In the treatment groups where TGF-β2 treatment was stopped after day 7 and then only treated the cells with decorin, no significant differences in both the 40°C and non-heat treated decorin groups were found when compared to the TGF-β2 only control.

In the collagen experiments, ascorbic acid was found to be important in the deposition of collagen as it increased the amount of collagen detected with the Sirius red assay significantly ($p<0.05$). Decorin at the concentration of 10µg/mL was found to be effective in decreasing the amount of collagen deposited ($p<0.05$). Decorin heated at 40°C and 90°C unexpectedly showed increased bio-activity compared to non-heated decorin. Prolonged storage of decorin together with TGF-β markedly increased the effect of decorin on the dissolution of deposited collagen.

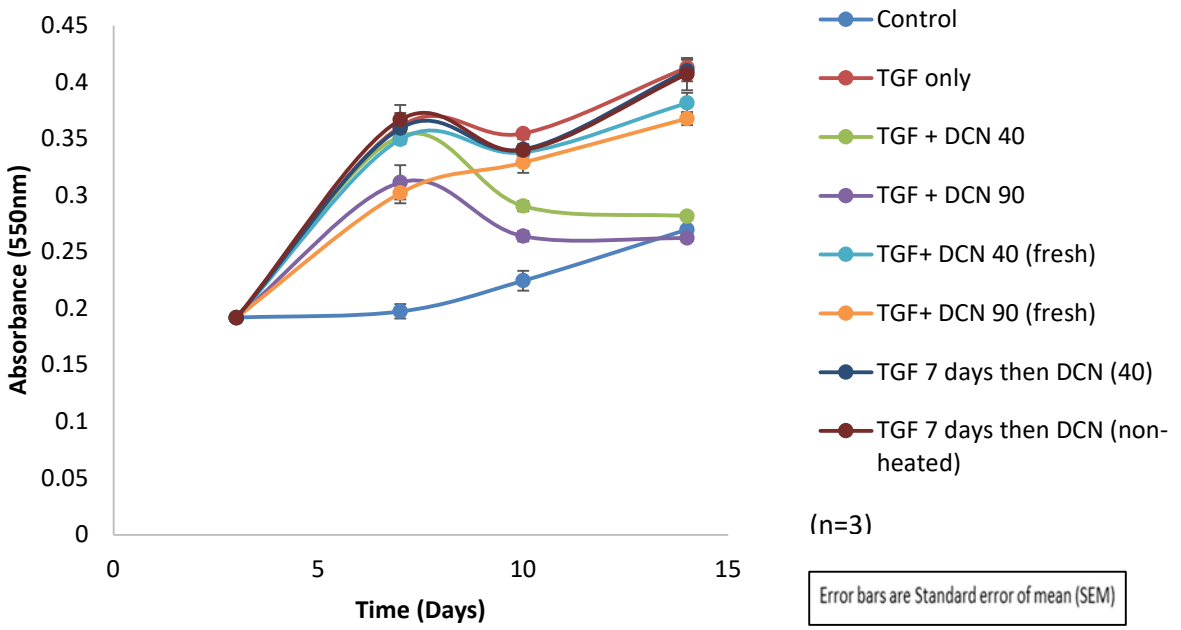

Figure 36: Quantification of collagen via the Sirius red assay in HDF's treated with TGF-β2 and various preparations of decorin (Heat treated decorin [40°C & 90°C, prolonged storage with TGF-β and fresh]) over 14 days. Fibroblasts treated with decorin heated at 40°C and 90°C showed significantly less deposited collagen compared to non-heated decorin. Prolonged storage of decorin together with TGF-β further enhanced the effect of the heat treated decorin on the dissolution of deposited collagen. All samples were performed in triplicate (n=3).

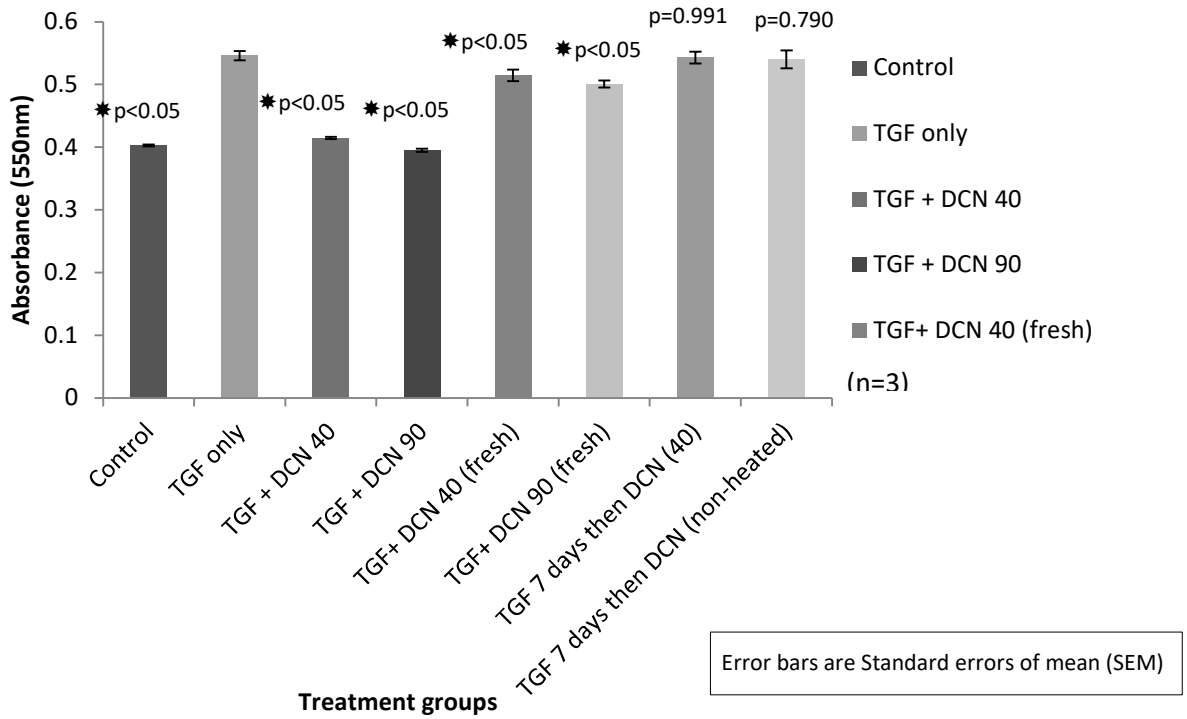

Figure 37: Bar chart showing the levels of collagen as ascertained by the Sirius red assay on day 14 of HDF's treated with TGF-β2 and various preparations of decorin. The treatment groups that showed a statistically significant difference to the TGF only treatment group are denoted with an asterisk. The p-values of each treatment group (compared to TGF only) is shown above each bar. All treatment groups except for the groups treated with TGF for 7 days and then decorin (heated at 40°C) and non-heated decorin showed significantly lower absorbance compared to the TGF only group. All samples were performed in triplicate (n=3).

5.6 Discussion

We have shown through circular dichroism testing that decorin will start to unfold and degrade over temperatures of approximately 42 °C and that this process is irreversible. This agrees with previous studies that show that decorin undergoes a structural transition at a temperature of 45-46°C[521].

Regarding the reversibility of the heat induced unfolding of decorin, our data agrees with the study by Krishnan et al[522] (1999) which showed that the process is irreversible. However a study by Scott et al[521] (2006) showed that the unfolding of decorin by heating (up to 60°C) was reversible after cooling the decorin to 25°C in contrast to our data. They theorized that the lack of one or more disulfides in the decorin used in the study by Krishnan was responsible for the difference in the ability to refold

as they also showed that disulfide bonding was important for the refolding process. Additionally this study by Scott et al (2006) also showed that the concentration of protein affects the refolding process with refolding occurring at slower rates in lower concentrations[521]. Our study differs in several aspects, including the source of decorin, the length of time decorin (>30 mins in our study versus <10 minutes in the study by Scott et al) was exposed to the elevated temperatures as well as the concentrations of decorin (0.6mg/mL in our study versus 1mg/mL in the study by Scott et al). Additionally the experiments in which the structure of decorin was analysed with CD (Figures 28(a) to 28(d)), the heated decorin was prepared at least 1 day in advance of the CD experiments which would have provided more than enough time for the refolding process to occur but yet we did not detect the reappearance of the peak at 217nm which shows that refolding did not occur.

The low temperature stability of decorin means a low temperature method of introducing decorin to the gellan dressing will need to be developed. This will need to be considered when developing the upscaling and production of the gellan dressing as gellan needs to be dissolved in water at 90°C. However, in our latter bio-activity experiments, we have shown that actually rather than decreased activity, the heat treated decorin showed increased bio-activity. We theorized that this effect may be due to the heat treatment of decorin causing either the conversion of decorin from its dimer state to a monomer state or that the denaturation by heat causes exposure of additional biologically active sites in the protein.

Decorin has been shown to be a “banana” shaped protein with a curved solenoid form with a β-sheet forming the inner concave face[146]. It is this inner β-sheet surface that has been suggested by Weber et al[147] (1996) to bind to a single collagen triple helix. Decorin has be shown to be a stable dimer in solution in light and x-ray scattering experiments (at concentrations of 1 to 5mg/mL)[523] most likely from interactions between the inner β-sheet surfaces[523]. Thus dimerization of decorin buries a significant portion of the inner surface[146], and may render this binding site mostly unavailable for binding to collagen but this is debatable[146]. Goldoni et al [150] (2004) demonstrated,

through collagen fibrillogenesis assays and quantification by scanning densitometry of the degree of tyrosyl phosphorylation of the Epidermal Growth Factor Receptor (EGFR) in serum-starved A431 cells (model human cell line (epidermoid carcinoma)), that the dimeric form of decorin showed reduced biological activity compared to the monomeric form. However it should be noted that Goldoni also claimed that decorin exists as a monomer in solution and that dimerization is an artefact of the removal of water or salts, a fact that is contested by Scott et al[146] (1996). The reported molecular weight of the decorin core protein in Goldoni's study was 55 kDa whereas we have been informed by our supplier that our decorin has a molecular weight of about 70kDa which may mean that our form of decorin may indeed exist as a dimer. Thus we hypothesize that as the denaturation of decorin via heat treatment disrupts the β-sheet inner surface of decorin, it causes it to exist in a monomeric form which avails a larger area of the active site to interact with collagen and TGF-β.

Alternatively, heat treatment may also sufficiently denature decorin as to break it into several separate chains of amino acids of which several would be able to bind to TGF-β. Scott et al (1986) showed that the isolated decorin protein core was as effective as the intact proteoglycan in retarding the precipitation of fibrils from soluble collagen despite heat treatment which led to an almost complete loss of the secondary structure of decorin[524]. Only reduction of the disulphide bridges in the core protein reduced the bio-activity of the core protein. Schonherr et al (1998) demonstrated that different sectional fragments of the decorin core protein were able to bind to TGF-β albeit with different affinities[153]. This study also hypothesized and presented evidence that independent binding sites of decorin for TGF-β and collagen existed. This is supported by findings by Hausser et al (1994) which showed that collagen-bound decorin could still interact with TGF-β[525].

We experimented with both freshly prepared solutions of decorin and TGF-β (mixed together on the day of media change) and also with solutions of decorin that was stored together with TGF-β for a prolonged period (prepared on day 3 of experiment and same stock used for subsequent media

change days of experiment). Unexpectedly, the decorin that was stored with TGF-β showed a far greater bio-activity and was able to reduce deposited collagen levels to levels similar to that of non-TGF-β treated controls. To our knowledge, there is no existing literature that has showed this phenomenon. It is hypothesized that this could be due to the increased time for decorin to bind the TGF-β in the treatment solution. To test this theory, two groups in the subsequent experiment were included in which TGF-β treatment was stopped after day 7, and the cells were thereon only treated with decorin to simulate the effect of TGF-β being completely bound and neutralized by decorin. However, these two groups showed no decrease in the amount of collagen deposited. Thus, this suggests that a decorin & TGF-β complex may be responsible for the collagen dissolution seen in the experiment.

5.7 Conclusions

In conclusion, further experiments will be needed to refine the bio-activity assays for decorin, and it has been shown that proliferation bio-activity assays are unlikely to be suitable. However, the immunohistochemistry staining for fibronectin and the Sirius red assay for collagen have been shown to be promising techniques. Additionally, studies to understand the effect of heat treatment on the structure and binding sites of decorin and the interaction between decorin and TGF-β are also required e.g. small angle x-ray scattering are required.

CHAPTER 6

GELLAN CONTACT STUDY (GCS)

6. Gellan Contact Study (GCS)

6.1. Background

Although both animal and human safety data for oral ingestion of gellan is available, to date there is no published safety evidence for the topical application of gellan to the skin. Before we are able to proceed with clinical testing of a gellan based dressing, we need to show that the gellan sheet and fluid gel dressings can be applied to skin with no adverse dermatological reaction. This can be achieved through a contact study where the dressing is applied onto the skin of healthy volunteers and any reaction to the dressing will be recorded.

6.2. Aims

The primary objective of our study is therefore to establish the safety of the two different gellan formulations (sheet and fluid gel) following its application to the epidermis of healthy volunteers compared to a control dressing; Mepitel One (Polyurethane net with soft Silicone). We also aim to evaluate the performance of the dressings in terms of user feedback in the areas of comfort, itch, pain and ease of removal.

6.3. Materials and Methods

6.3.1 Materials

The two formulations tested in this study are 2.0% gellan sheet (2% gellan and water and 2.0% gellan fluid gel (2% gellan, 0.58% sodium chloride and water).The gellan sheet was rehydrated either with Hartmann's solution (Macoflex N, Macopharma, UK) or 0.9% Sodium chloride (Versol, United Kingdom) for at least 1 minute prior to application. Mepitel One (Mölnlycke Health Care, Gothenburg, Sweden) was used as the control dressing. It consists of polyurethane net with soft silicone on one side only.

The gellan sheets and gellan fluid gel were manufactured by Ms. Maryam Esmaeili (PhD student) and sterilised with UV light.

6.3.2 Location

This prospective, assessor blinded, randomised control study was performed in a clinical room within the Wellcome Trust/NIHR Clinical Research Facility of the Queen Elizabeth Hospital Birmingham, UK. Approval was granted by the Black Country National Research and Ethics Committee (West Midlands, UK; Project ID: 189413) prior to the running of the study.

The study was performed in room with standard temperature and humidity regulation. Average temperature of 24.6 Celsius (range: 20.8 to 26.2 °C) and average humidity of 32.3% (range: 24 to 45%).

6.3.2 Subjects

We aimed to recruit 30 healthy participants of both genders (15 subjects per different formulation) and aged > 18 years for this study. The inclusion and exclusion criteria are listed in Table 40.

Table 40: Study inclusion and exclusion criteria.

Inclusion Criteria
• Male or female subjects aged ≥ 18 years old • Subjects who can provide informed consent
Exclusion Criteria
• Subject with existing skin conditions/diseases which may interfere with the aim(s) of the study. Examples include pathological fibrosis e.g. scleroderma; pathological thinning e.g. epidermolysis bullosa and collagen disorders e.g. Marfan's syndrome • Chronic steroid use, history of skin malignancy or chronic papulo-squamous disease (e.g. eczema, pemphigus) and history of Steven Johnson or TENS disease • Blemishes, marks (e.g. tattoos, scars or burns,) on the test site(s) which may interfere with assessment on the test site • Use of medication which may affect skin response • Known allergy to the materials used in the study • Known allergy to adhesive plasters or tapes • Fitzpatrick skin type VI (due to the difficulty of identifying erythema) • Irritated skin on the test site • Known pregnancy (confirmed by urine pregnancy test) or lactating • Inability to commit to attending all sessions. • Participation in another study which may affect the results of this contact study. • Any other reason that clinician considers will interfere with the objectives of the study

6.3.3 Study design

These participants had to complete 2 phases of the study: an open epicutaneous phase (Phase 1) where the test and control dressings were applied to a 10 x 10 cm area (marked with a surgical marker pen) on contralateral upper arm sites for 1 hour (+15 minutes). If the participants did not develop a reaction (erythema/dryness/oedema) above a set precaution threshold, they then continued to the second closed epicutaneous phase (Phase 2) where the test and control dressings were again applied to a 10 x10cm area on contralateral inner forearm sites and covered with a waterproof transparent film dressing (Tegaderm film, 3M Wound Care, USA) and left for 72 hours (+/- 3hours). The study design conforms to the standards set out by the International Organization for Standardization (ISO) for biological evaluation of medical devices[526].

6.3.3.1 Measured outcomes

The primary outcome measured is the reaction (presence/absence of Erythema, Dryness or Oedema) of the skin after application of gellan (sheet/fluid gel) after a minimum of 1 hour (+15 mins) and 72 hours (+/- 3 hours) compared to the baseline. The presence of erythema, dryness and oedema suggest an inflammatory response to the dressing material.

The scoring scale that was used to quantify the skin reaction to the dressing is shown in Table 41. This scale is supplemented with a photographic guide that has examples of the different grades of erythema, dryness and oedema (Appendix B).

Table 41: Scoring scale used to quantify erythema, dryness and oedema of the subject's skin.

Erythema	Dryness (scaling)	Oedema
0 = No evidence of erythema	0 = No evidence of scaling	0 = Absence of oedema
0.5 = Minimal or doubtful erythema	0.5 = Dry without scaling, appears smooth and taut	0.5 = Presence of mild/patchy oedema
1 = Slight redness, spotty and diffuse	1 = Fine or mild scaling	1 = Presence of moderate or severe oedema
2 = Moderate uniform redness	2 = Moderate scaling	
3 = Strong uniform redness	3 = Severe scaling with large flakes	
4 = Fiery redness		

The assessments were performed by 2 clinical assessors who were blinded to the allocation of treatment and control sites. Assessors performed both a baseline score before the dressing is applied and rescore the site after the dressing is applied for the specified time period. The assessor performing both the baseline and post-dressing score is always the same. The final score is then calculated by averaging the score of the 2 assessors.

The precautionary threshold that would disqualify the participant in phase 1 to proceed to phase 2 was set at >0.5 for redness, dryness and oedema. This was implemented to improve the safety of the study and minimise the risk to participants. The set threshold of failure for the dressings was set at as score of >1.0 for redness and dryness and a score of 1 for oedema.

Secondary outcomes measured include usability, comfort and feel (itch and pain) which were collected via a clinician evaluation questionnaire and participant evaluation questionnaire.

6.3.3.2 Randomisation

For this study, participants were randomised to 4 different treatment groups (See Table 42). Randomisation was performed straight after participant enrolment. An online block randomisation tool was used to generate the randomisation list (Sealed Envelope Ltd. 2016. Simple randomisation service. [Online] Available from: https://www.sealedenvelope.com/simple-randomiser/v1/ [Accessed 5 May 2016]). Before recruitment commenced, a randomisation list was created by a member of the team not involved in the recruitment or treatment of participants. The independent member then placed the results into chronologically labelled sealed envelopes. The research team then opened the envelope in chronological order to determine the group the participant is randomised to.

Table 42: Treatment groups of the first (open cutaneous test) and second (closed cutaneous test) phases of the study.

Treatment group	Open cutaneous test		Closed cutaneous test	
	Left upper arm	Right upper arm	Left upper forearm	Right upper forearm
A	Gellan sheet	Mepitel One	Gellan sheet	Mepitel One
B	Mepitel One	Gellan sheet	Mepitel One	Gellan sheet
C	Gellan fluid gel	Mepitel One	Gellan fluid gel	Mepitel One
D	Mepitel One	Gellan fluid gel	Mepitel One	Gellan fluid gel

6.3.3.3 Statistical analysis

Data was analysed on an intention to treat basis. Statistical tests were performed using Graphpad statistical software (GraphPad Software, San Diego, United States of America). Differences in groups were calculated using Fisher's exact test. The significance level was predetermined to be less than 0.05.

6.4 Results

6.4.1 Demographics

33 participants were recruited (gellan sheet: 18; gellan fluid gel: 15) however 3 participants who received the gellan sheet did not proceed to the 2nd phase due to scoring skin erythema above the specified precaution threshold. The average age of participants was 28.7 years (Range: 19 to 57). The gender distribution for the participants was 16 females and 17 males.

The average Fitzpatrick score of the participants was 3 (range 1 to 5) (Figure 38).

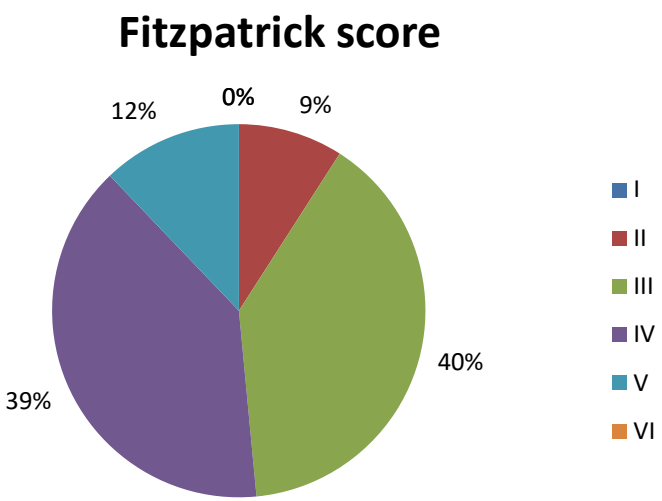

Figure 38: Distribution of participants according to Fitzpatrick score classification.

6.4.2 Erythema

None of the participants in any of the test (gellan fluid or sheet) or control groups developed an erythema grade above the milestone threshold, i.e. a grade of >1.0, after Phase 1 (1 hour) and Phase 2 (3 days).

For the gellan fluid formulation, there was no significant difference between the Mepitel One control group for any erythema more than doubtful erythema (grades >0.5) during phase 1 (0% vs 3.03%, p=1.00) (Table 43). However for phase 2, there was a significant difference in the number of participants developing mild erythema (Grades 0.51 to 1.0) to the gellan fluid gel compared to the Mepitel One control group (53.3 vs 6.7%, p= 0.0009) (Table 44). This difference may be due to the dry residue left by gellan fluid after it dries causing a mild irritative effect to the skin.

Conversely for the gellan sheet formulation, there was a significant difference between the number of participants who developed a mild erythematic reaction (grades >0 to 1.0) to the gellan sheet compared to the Mepitel One control group (83.33% vs 33.33%, p=0.001). However, after 3 days participants who received the gellan sheet had less mild erythemic reactions compared to participants in the Mepitel One (46.67% vs 53.33%, p=0.7575), and a higher proportion of

participants in the gellan group had no reactions (i.e. Grade 0; 53.33% vs 46.67, p=0.7575), however both differences did not reach statistical significance.

We observed that participants who received the gellan sheet rehydrated in Hartmanns solution developed a stronger erythema reaction compared to when rehydrated with normal saline. Some participants in the Mepitel One control group also developed a mild erythema after 1 hour as the sites were cleaned with normal saline before the dressings were applied, but the reaction was milder compared to the gellan sheet sites. This may be due to the gellan sheet releasing the absorbed rehydration fluid during the 1-hour time period. This is not seen at 3 days as the dressings possibly because the gellan sheets become drier after 72 hours.

Table 43: Distribution of erythema grades of participants after 1 hour of dressing application.

Phase 1 (1 hour)				
Grades (%)				
	0	0.25-0.5	0.51-1.0	>1.0
Gellan fluid gel	53.33%	46.67%	0.00%	0.00%
Gellan Sheet	16.67%	50.00%	33.33%	0.00%
Mepitel One	66.67%	30.30%	3.03%	0.00%

Table 44: Distribution of erythema grades of participants after 3 days of dressing application.

Phase 2 (3 days)				
Grades (%)				
	0	0.25-0.5	0.51-1.0	>1.0
Gellan fluid gel	20.00%	26.67%	53.33%	0.00%
Gellan Sheet	53.33%	40.00%	6.67%	0.00%
Mepitel One	46.67%	46.67%	6.67%	0.00%

6.4.3 Dryness

None of the participants in any of the test (gellan fluid or sheet) or control groups developed a dryness grade above the milestone threshold, i.e. a grade of >1.0, after Phase 1 (1 hour) and Phase 2 (3 days).

For the gellan fluid gel formulation, there was no significant difference in skin dryness compared to the control group after 1 hour (Grades >0: 0% vs 3.03%, p=1.00) (Table 45). However there was a

significant difference in the number of participants who developed mild dryness of the skin after receiving the fluid gel formulation and (Grades 0.25-1.00) after 3 days (Phase 2) compared to the control group (66.67% vs 6.67%, p= 0.0001) (Table 46). On further investigation, we found that this was due to the assessors being unable to differentiate between the white flaky residues left by the fluid gel after it dries at 3 days from the appearance of dry skin scales.

For the gellan sheet formulation, we found that no differences in skin dryness between the gellan sheet group and the Mepitel One control group at 1 hour (Grades >0: 0% vs 3.03%, p=1.00) and 3 days (Grades >0: 6.7% vs 6.7%, p=1.00). The difference between the results of the Gellan sheet and fluid gel again can be explained by the presence of white flaky residues present after the Gellan fluid dries which does not occur with the gellan sheet.

Table 45: Distribution of dryness grades of participants after 1 hour of dressing application.

Phase 1 (1 hour)				
Grades (%)				
	0	0.25-0.5	0.51-1.0	≥1.0
Gellan fluid gel	100.00%	0.00%	0.00%	0.00%
Gellan Sheet	100.00%	0.00%	0.00%	0.00%
Mepitel One	96.97%	3.03%	0.00%	0.00%

Table 46: Distribution of dryness grades of participants after 3 days of dressing application.

Phase 2 (3 days)				
Grades (%)				
	0	0.25-0.5	0.51-1.0	≥1.0
Gellan fluid gel	33.33%	60.00%	6.67%	0.00%
Gellan Sheet	93.33%	6.67%	0.00%	0.00%
Mepitel One	93.33%	6.67%	0.00%	0.00%

6.4.4 Oedema

None of the participants in any of the test (gellan fluid or sheet) or control groups developed an oedema grade above the milestone threshold, i.e. a grade of 1.0, after Phase 1 (1 hour) and Phase 2 (3 days).

For the gellan fluid formulation, no participants developed any degree of oedema in phase 1 (1 hour) (Table 47). However, some participants who received the fluid gel formulation (n=5) developed mild skin puffiness (Oedema grade0.25-0.50) compared to the control group (33.3% vs 0%, p= 0.0025) (Table 48) after 72 hours. This was expected as the fluid gel will rehydrate the skin over the 3 days and give rise to a fuller appearance compared to the Mepitel One dressing. Of these 5 participants, none of these participants had any signs of an urticarial reaction.

For the gellan sheet formulation, there was no significant difference between the numbers of participants developing a mild degree of oedema (grades 0.25 to 0.5) compared to the control group. None of the participants in the gellan sheet group developed oedema in the 1st phase. In the 2nd phase, there was no significant difference in the participants who developed mild oedema (Grades 0.25-0.50) between the gellan sheet and Mepitel One groups (6.67% vs 0.00%, p=0.3333).

Table 47: Distribution of oedema grades of participants after 1 hour of dressing application.

Phase 1 (1 hour)				
Grades (%)				
	0	0.25-0.5	0.51-1.0	1
Gellan fluid gel	100.00%	0.00%	0.00%	0.00%
Gellan Sheet	100.00%	0.00%	0.00%	0.00%
Mepitel One	100.00%	0.00%	0.00%	0.00%

Table 48: Distribution of oedema grades of participants after 3 days of dressing application.

Phase 2 (3 days)				
Grades (%)				
	0	0.25-0.5	0.51-1.0	1
Gellan fluid gel	66.67%	33.33%	0.00%	0.00%
Gellan Sheet	93.33%	6.67%	0.00%	0.00%
Mepitel One	100.00%	0.00%	0.00%	0.00%

6.4.5. Participant feedback

In terms of comfort, the majority of participants found the gellan fluid (86.7% versus 86.7%, p=1.00) and sheet formulations to be as comfortable as the Mepitel One dressing (100% versus 100%, p=1.00).

Some participants who received both the test and control dressings developed a mild itch after 3 days but there was no significant difference between the groups. 33.3% of participants receiving the Fluid gel formulation developed a mild itch after 3 days comparted to 20% of the participants in the control group (p=0.6817). For the Sheet formulation, 53% developed mild itching compared to 40% in the control group (p=0.7152). There was no significant difference in the number of participants developing itch between the Fluid gel and Sheet formulations (p=0.4621). None of the participants experienced any pain at the skin site as a result of the test or control dressings after 3 days. Participants felt that dressing removal was as equally comfortable compared to the control dressing for both the Fluid gel (Fluid vs Mepitel One; comfortable removal in 93.3% vs 93.3%, p=1.00) and Sheet formulations (Sheet vs Mepitel One; comfortable removal in 93.3% vs 86.7%, p=1.00).

In terms of clinician feedback, both the gellan fluid and sheet formulations had the same levels of ease of application, removal and handling durability compared to the Mepitel One control dressing. The gellan sheet dressing however was vulnerable to tears and fragmentation in 53.3% and 25.7% of cases respectively at 3 days. This is due to the dressing drying out and becoming more brittle at 3 days. This would unlikely be a problem in actual burns patients as burn wounds then to produce significant amounts of exudate especially in the first 48-72 hours.

6.5 Skin patch test

Two participants (GCS03 and GCS08) who developed erythema reactions over the phase 1 threshold that prevented them from proceeding to phase 2 of the study were referred to a consultant dermatologist (Dr. Tang Shim Ngee, University Hospital Coventry) for skin patch tests. The two participants were patch tested to British standard and acrylate series and also to the following:

- 2.0% gellan fluid sheet, rehydrated in Hartmann solution
- 2.0% gellan fluid sheet, rehydrated in normal saline (0.9%)
- 2.0% gellan fluid sheet, rehydrated in sterile water
- 2.0% gellan fluid gel
- Mepitel One dressing, rehydrated in Hartmann solution
- Mepitel One dressing, rehydrated in normal saline (0.9%)
- Mepitel One dressing, rehydrated in sterile water
- Tegaderm film dressing

Participants were reviewed after 2 and 4 days after the patches were applied. Additionally, a quick contact test was also done on day 2 for 15 and 30 minutes with only the dressing materials.

For participant GCS03, no contact allergen was identified on day 2 and 4. On day 2 of the investigation, the dressing sheets and fluid gel were repeated and observed at 15 and 30 minutes. No type 1 hypersensitivity reaction was seen.

For participant GCS08, no contact allergen was identified except for an irritant reaction to potassium dichromate and cobalt on day 2 and 4. On day 2 of the investigation of the investigation, the dressing sheets and fluid gel was repeated and observed at 15 and 30 minutes. No type 1 hypersensitivity reaction was seen. However, an irritant reaction was seen in 2% gellan dressing rehydrated with water, Mepitel dressing rehydrated in Hartmann's solution and Mepitel dressing rehydrated with sterile water.

The results show that the participants had irritation reactions that were not specific to gellan, rather than true allergic contact reactions.

6.6 Discussion

The objective of this study was to address the safety and comfort of two novel gellan dressings, namely a gellan fluid gel and a gellan sheet formulation and is the first clinical trial to evaluate the suitability of gellan dressings for the treatment of cutaneous injuries such as burn wounds.

Topical dressings are widely used and although largely deemed safe, their allergic potential should not be underestimated. Some dressing constituents have been known to cause allergic contact dermatitis such as regenerated oxidized cellulose[527], colophonium resins such as Vistanex or Pentalyn (which are commonly used tackifying agents [adhesives] for hydrocolloid dressings)[528-531], and other constituents of hydrogel or hydrocolloid based dressings[532-534]. Patients with chronic wounds[534] or auto-immune conditions such scleroderma appear to be particularly at risk of developing dressing related allergic contact dermatitis[533, 534].

Skin irritation due to dressings may also be due to mechanical irritation of the skin upon dressing removal[535-537] or low conformability of the dressing to skin[538].

Gellan is an extensively studied bacterial polysaccharide[194] that is currently widely used in the food industries since its approval in Japan in 1988[539] as a stabilizer, thickening and gelling agent[540]. Gellan has also more recently seen an increasing trend in its use in pharmaceutical products as disintegrating or binding agent, excipient and thickening and gelling agent[194, 540]. Additionally, it has also been investigated for the topical delivery of drugs on both skin[541] and mucosa[542]. Gellan has been shown to be non-toxic through the oral administration route[197], but there have been few studies that have investigated its toxicity when applied topically. A study by Lee et al (2010) applied gellan gum based films (GG40, a film made with gellan cross linked with 1-ethyl-3-(3-dimethylaminopropyl) carbodiimide (EDC) on the wounds of rats. The GG40 film was shown to cause minor inflammation in the early post-operative period but no fibrosis or stromal reaction in both long and short-term implantations[543]. Additionally the film was found to be compatible to L929 fibroblast cells and platelets, had beneficial effects on wound healing and wound size reduction, and

also showed low adhesion to the wound surface compared to the control hydrocolloid dressing (Duoderm, Convatec, Deeside, United Kingdom) thus preventing further trauma to the wound on dressing removal[543]. In a separate study by the same author, a photo-crosslinked gellan gum-cinnnamate film was applied to denuded peritoneal walls in rats[544]. This study showed that the film showed promising anti-adhesion potential and anti-inflammatory effects with reduced neutrophils in the peritoneal fluid. This difference in inflammation seen could be due to the wound location (skin versus peritoneum) or the cross-linking agents used (EDC versus cinnamate). Other bacterial polysaccharides (e.g. from Bacteroides fragilis) have been shown to have both pro-inflammatory and anti-inflammatory effects [545].

In our study, some participants developed a mild erythema skin reaction, which although was seen in a higher percentage of the gellan treated group, was also seen in the participants who had the control Mepitel dressings. This is most likely an irritative rather than allergic contact dermatitis reaction as three of the participants who underwent further skin patch testing showed no hypersensitivity to any of the agents used in the study. The Hartmanns solution was initially thought to be more irritative compared to the normal saline solution used in this study although a quantitative analysis was not performed between Hartmann and saline treated participants. A search in the literature did not show any reports or studies regarding skin reactions to Hartmanns as it is commonly used intravenously and not topically. Furthermore, the second participant in the formal skin patch test developed irritant reactions to the control dressing rehydrated with both Hartmanns and sterile water which points to the reaction being due to increased moisture rather than specific to the rehydrating agent.

The assessment technique used to evaluate erythema, dryness and oedema in this study was subjective in nature, but is in line with the scoring of skin patch tests according to International Contact Dermatitis Research Group recommendations which also utilises clinical subjective grading

of erythema (with scores of "?+", "+", "++" or "+++") and the presence of skin infiltration and vesicles to determine the aetiologic agent(s) of allergic contact dermatitis[546].

Objective assessment tools were not used in the skin contact study as there are no current guidelines on the interpretation of the results e.g. cut-off values for determining the positivity of a test. Several studies have attempted to introduce objective methods of skin patch interpretation but with mixed results. A study by Held et al (1998) investigated the use of the erythema index as measured with the Dermaspectrometer (Cortex Technology, Hadsund, Denmark) to interpret allergic patch test reactions but concluded that readings from a Dermaspectrometer did not provide better information than visual readings[547]. In the study, erythema indices were significantly higher for visually rated positive patch tests than for negative tests ($p<0.05$) however the Dermaspectrometer could not differentiate between the grades of positive reactions i.e. between the categories of "?+", "+", "++" or "+++".

Another study by Gawkrodger et al (1991) investigated the use of laser-Doppler flowmetry to quantify allergic and irritant patch test reactions[548]. Although both irritant and allergic responses produced statistically significant increases in laser-Doppler flow index, there was a low correlation between the laser-Doppler flow index and conventional clinical subjective scoring and the index could not differentiate between allergic and irritant patch test reactions.

Several modifications however have been used in this study to reduce the variability in assessments including the use of two assessors, and a photographic guide. Objective quantitative methods may be considered in future studies such as the use of colorimeters (such as the DSM II Colormeter) or camera systems (Scanoskin) previously described in Chapter 2 and 3 however the accuracy of these systems and cut-off values to guide interpretation of results will have to be further investigated before use.

6.7 Conclusion

Both the gellan fluid and sheet formulations were found to be safe for use on intact skin as none of the participants developed any severe dermatological reactions in terms of erythema, dryness of oedema. This was confirmed with further testing via skin patch tests performed by a consultant dermatologist which showed either no reaction or non-dressing specific skin irritation.

The rehydrated gellan sheet however may cause a mild irritative effect (most likely attributable to the rehydration fluid used) in some participants acutely (1 hour) but this effect is not seen after 3 days. Similarly, the gellan fluid gel may also cause a mild erythematous reaction after it dries after 3 days.

CHAPTER 7

OVERALL DISCUSSION AND CONCLUSIONS

7. Overall Discussion and Conclusions

7.1 Main findings and future work

This thesis has described selected several investigations which help inform different stages of the anti-scarring dressing development process. In addition to this, suitable and reliable scar measurement tools are identified and validated to be used in the assessment of the anti-scarring effects of the dressing when used in clinical trials.

In order to show that the anti-scarring dressing is effective in preventing or reducing pathological scar formation, objective and reliable scar measurement tools are required. In Chapter 2, a systematic review was performed and allowed the identification of a panel of suitable objective scar that allow the measurement of the colour, pliability and thickness of a burn scar. As these tools were originally developed for the cosmetic industry, they required testing in pathological burn scars as well as validation with the traditionally used subjective scar scales as well as histology. Chapter 3 thus addresses this and it was found that the high frequency ultrasound system, DSM II Colormeter and Cutometer pliability probe all had acceptable reliability and good correlations with both subjective and histological parameters of burn scars. Further analysis allowed the creation of a "Global objective scar score" that incorporated the ultrasound measured dermal thickness and intensity measures as well as the Cutometer maximum extension measurements (direct and ratio with normal skin). Further work is required to validate this global scar score in a larger cohort of patients. A significant factor of reduced reliability in scar measurements is the relocation of the site of measurement, and future work needs to be done in this area with temporary tattoos being a promising solution.

Chapter 4 investigated the cytotoxicity of decorin in in-vitro fibroblast cell cultures using cell proliferation based cytotoxicity assays. As decorin is a ubiquitous vertebrate extra-cellular matrix

protein[549], it was hypothesised to have no or very low cytotoxicity. The experiments confirmed the hypothesis with no cytotoxicity seen even at high concentrations of decorin. Further experiments on keratinocytes, especially non-immortalised cells from patients need to be carried out in order to ensure that the topically applied decorin will not impede the wound healing process as well as tests on systemic toxicity in animal models.

Chapter 5 investigated the effects of heat treatment on the bio-activity of decorin. The process of manufacturing the gellan based dressing requires a heating process which exposes the decorin to high temperatures. Additionally, burn patients are routinely nursed at higher room temperatures as they are prone and intolerant to hypothermia. Both of these factors may potentially change denature and alter the bio-activity of decorin. Circular dichroism studies show that decorin undergoes a non-reversible change in protein configuration at 42°C and exposure to temperatures above 50°C will start reducing the concentration of bio-active decorin after 30 minutes. This will have implications on the sterilisation methods that can be used for the dressing as techniques which utilise or cause high temperatures (e.g. autoclaving, irradiation) will not be suitable. Heating decorin to 40°C however appears to increase the availability of the binding sites on decorin as evidenced by the increased concentration of decorin seen on ELISA, most likely by decoupling of decorin dimers. Future work should also include the designing of decorin proteins that naturally exist in monomer form without the need for heat treatment to enhance its bio-activity.

Successful pre-clinical safety testing of the decorin gellan dressing has been conducted in guinea pig animal models by our group and large animal burn models (pig model) are currently being run in the University of Manchester to provide data on the effects of the dressing on wound healing and subsequent scarring.

Chapter 6 describes the first clinical study on humans of the gellan only dressing. Clinical trials can be divided into four different phases and the first phase investigates the safety of the dressing. The gellan contact study aimed to investigate the epidermal response of intact skin on gellan in healthy volunteers. It showed that the dressing did not cause any significant skin reaction in terms of erythema, dryness or oedema although in some individuals, mild skin irritation can be expected though this is not specific to gellan itself. The next phase would be the testing of the decorin gellan dressing in actual burn patient wounds with the initial primary endpoint being safety tests and eventually wound healing and scarring.

If the clinical trials in burn patients are successful, the dressing could then be modified for application in other surgical fields such as intraabdominal, gynaecological and neurological surgery where an anti-fibrosis layer could be instrumental in preventing adhesions and reduce complications.

8. References

1. Stokes MAR, Johnson WD. Burns in the Third World: an unmet need. Annals of burns and fire disasters. 2017;30(4):243-6.
2. Brusselaers N, Monstrey S, Vogelaers D, Hoste E, Blot S. Severe burn injury in europe: a systematic review of the incidence, etiology, morbidity, and mortality. Critical Care. 2010;14(5):R188.
3. Smolle C, Cambiaso-Daniel J, Forbes AA, Wurzer P, Hundeshagen G, Branski LK, et al. Recent trends in burn epidemiology worldwide: A systematic review. Burns : journal of the International Society for Burn Injuries. 2017;43(2):249-57.
4. Klein MB, Goverman J, Hayden DL, Fagan SP, McDonald-Smith GP, Alexander AK, et al. Benchmarking Outcomes in the Critically Injured Burn Patient. Annals of surgery. 2014;259(5):833-41.
5. Kawasumi A, Sagawa N, Hayashi S, Yokoyama H, Tamura K. Wound Healing in Mammals and Amphibians: Toward Limb Regeneration in Mammals. Current topics in microbiology and immunology. 2012;367.
6. Stephens P, Thomas DW. The cellular proliferative phase of the wound repair process. Journal of wound care. 2002;11(7):253-61.
7. Slemp AE, Kirschner RE. Keloids and scars: a review of keloids and scars, their pathogenesis, risk factors, and management. Current opinion in pediatrics. 2006;18(4):396-402.
8. Kirsner RS, Eaglstein WH. The wound healing process. Dermatologic clinics. 1993;11(4):629-40.
9. Guo S, DiPietro LA. Factors Affecting Wound Healing. Journal of Dental Research. 2010;89(3):219-29.
10. Chipp E, Charles L, Thomas C, Whiting K, Moiemen N, Wilson Y. A prospective study of time to healing and hypertrophic scarring in paediatric burns: every day counts. Burns Trauma. 2017;5.
11. Rowlatt U. Intrauterine wound healing in a 20 week human fetus. Virchows Archiv A, Pathological anatomy and histology. 1979;381(3):353-61.
12. Ferguson MW, Whitby DJ, Shah M, Armstrong J, Siebert JW, Longaker MT. Scar formation: the spectral nature of fetal and adult wound repair. Plastic and reconstructive surgery. 1996;97(4):854-60.
13. Bayat A, McGrouther DA, Ferguson MW. Skin scarring. BMJ (Clinical research ed). 2003;326(7380):88-92.
14. McDougall S, Dallon J, Sherratt J, Maini P. Fibroblast migration and collagen deposition during dermal wound healing: mathematical modelling and clinical implications. Philosophical transactions Series A, Mathematical, physical, and engineering sciences. 2006;364(1843):1385-405.
15. Linares HA, Kischer CW, Dobrkovsky M, Larson DL. The histiotypic organization of the hypertrophic scar in humans. J Invest Dermatol. 1972;59(4):323-31.
16. Dunkin CS, Pleat JM, Gillespie PH, Tyler MP, Roberts AH, McGrouther DA. Scarring occurs at a critical depth of skin injury: precise measurement in a graduated dermal scratch in human volunteers. Plastic and reconstructive surgery. 2007;119(6):1722-32; discussion 33-4.
17. Wallace HJ, Fear MW, Crowe MM, Martin LJ, Wood FM. Identification of factors predicting scar outcome after burn injury in children: a prospective case-control study. Burns & Trauma. 2017;5(1):19.
18. Atiyeh BS, Costagliola M, Hayek SN. Keloid or hypertrophic scar: the controversy: review of the literature. Ann Plast Surg. 2005;54(6):676-80.
19. Glass DA, 2nd. Current Understanding of the Genetic Causes of Keloid Formation. The journal of investigative dermatology Symposium proceedings. 2017;18(2):S50-s3.
20. Gauglitz GG, Korting HC, Pavicic T, Ruzicka T, Jeschke MG. Hypertrophic scarring and keloids: pathomechanisms and current and emerging treatment strategies. Mol Med. 2011;17.
21. Jumper N, Paus R, Bayat A. Functional histopathology of keloid disease. Histology and histopathology. 2015;30(9):1033-57.

22. Lee JY, Yang CC, Chao SC, Wong TW. Histopathological differential diagnosis of keloid and hypertrophic scar. The American Journal of dermatopathology. 2004;26(5):379-84.
23. Goverman J, He W, Martello G, Whalen A, Bittner E, Schulz J, et al. The Presence of Scarring and Associated Morbidity in the Burn Model System National Database. Annals of Plastic Surgery. 2019;82(3S):S162-S8.
24. Bock O, Schmid-Ott G, Malewski P, Mrowietz U. Quality of life of patients with keloid and hypertrophic scarring. Archives of Dermatological Research. 2006;297(10):433-8.
25. Wiechman SA, McMullen K, Carrougher GJ, Fauerbach JA, Ryan CM, Herndon DN, et al. Reasons for Distress Among Burn Survivors at 6, 12, and 24 Months Postdischarge: A Burn Injury Model System Investigation. Archives of physical medicine and rehabilitation. 2018;99(7):1311-7.
26. Carrougher GJ, Martinez EM, McMullen KS, Fauerbach JA, Holavanahalli RK, Herndon DN, et al. Pruritus in adult burn survivors: postburn prevalence and risk factors associated with increased intensity. Journal of burn care & research : official publication of the American Burn Association. 2013;34(1):94-101.
27. Cubison TC, Pape SA, Parkhouse N. Evidence for the link between healing time and the development of hypertrophic scars (HTS) in paediatric burns due to scald injury. Burns. 2006;32.
28. Janzekovic Z. A new concept in the early excision and immediate grafting of burns. The Journal of trauma. 1970;10(12):1103-8.
29. Westra I, Pham H, Niessen FB. Topical Silicone Sheet Application in the Treatment of Hypertrophic Scars and Keloids. The Journal of Clinical and Aesthetic Dermatology. 2016;9(10):28-35.
30. Puri N, Talwar A. The Efficacy of Silicone Gel for the Treatment of Hypertrophic Scars and Keloids. Journal of Cutaneous and Aesthetic Surgery. 2009;2(2):104-6.
31. Suetak T, Sasai S, Zhen YX, Tagami H. Effects of silicone gel sheet on the stratum corneum hydration. British journal of plastic surgery. 2000;53(6):503-7.
32. Musgrave MA, Umraw N, Fish JS, Gomez M, Cartotto RC. The effect of silicone gel sheets on perfusion of hypertrophic burn scars. The Journal of burn care & rehabilitation. 2002;23(3):208-14.
33. Ahn ST, Monafo WW, Mustoe TA. Topical silicone gel: a new treatment for hypertrophic scars. Surgery. 1989;106(4):781-6; discussion 6-7.
34. Quinn KJ, Evans JH, Courtney JM, Gaylor JDS, Reid WH. Non-pressure treatment of hypertrophic scars. Burns. 1985;12(2):102-8.
35. O'Brien L, Jones DJ. Silicone gel sheeting for preventing and treating hypertrophic and keloid scars. The Cochrane database of systematic reviews. 2013(9):Cd003826.
36. Reno F, Grazianetti P, Cannas M. Effects of mechanical compression on hypertrophic scars: prostaglandin E2 release. Burns. 2001;27(3):215-8.
37. Candy LH, Cecilia LT, Ping ZY. Effect of different pressure magnitudes on hypertrophic scar in a Chinese population. Burns. 2010;36(8):1234-41.
38. Kim JY, Willard JJ, Supp DM, Roy S, Gordillo GM, Sen CK, et al. Burn Scar Biomechanics after Pressure Garment Therapy. Plastic and reconstructive surgery. 2015;136(3):572-81.
39. Anzarut A, Olson J, Singh P, Rowe BH, Tredget EE. The effectiveness of pressure garment therapy for the prevention of abnormal scarring after burn injury: a meta-analysis. Journal of plastic, reconstructive & aesthetic surgery : JPRAS. 2009;62(1):77-84.
40. Chi CF, Lin CH, Yang HS. The causal analysis of requested alterations for pressure garments. Journal of burn care & research : official publication of the American Burn Association. 2008;29(6):965-74.
41. Ripper S, Renneberg B, Landmann C, Weigel G, Germann G. Adherence to pressure garment therapy in adult burn patients. Burns. 2009;35(5):657-64.
42. Brown CA. A comparison of the outcomes of two clinical audits of burn pressure garment satisfaction and compliance in Saudi Arabia. Burns. 2001;27(4):342-8.
43. Li-Tsang CW, Zheng YP, Lau JC. A randomized clinical trial to study the effect of silicone gel dressing and pressure therapy on posttraumatic hypertrophic scars. Journal of burn care & research : official publication of the American Burn Association. 2010;31(3):448-57.

44. Khan KM, Scott A. Mechanotherapy: how physical therapists' prescription of exercise promotes tissue repair. British Journal of Sports Medicine. 2009;43(4):247-52.
45. Ogawa R. Mechanobiology of scarring. Wound Repair and Regeneration. 2011;19:s2-s9.
46. Yusko EC, Asbury CL. Force is a signal that cells cannot ignore. Molecular Biology of the Cell. 2014;25(23):3717-25.
47. Yagmur C, Guneren E, Kefeli M, Ogawa R. The effect of surgical denervation on prevention of excessive dermal scarring: a study on rabbit ear hypertrophic scar model. Journal of plastic, reconstructive & aesthetic surgery : JPRAS. 2011;64(10):1359-65.
48. Brown NJ, Kimble RM, Rodger S, Ware RS, Cuttle L. Play and heal: randomized controlled trial of Ditto intervention efficacy on improving re-epithelialization in pediatric burns. Burns. 2014;40(2):204-13.
49. Meirte J, Moortgat P, Anthonissen M, Maertens K, Lafaire C, De Cuyper L, et al. Short-term effects of vacuum massage on epidermal and dermal thickness and density in burn scars: an experimental study. Burns & Trauma. 2016;4:27.
50. Moortgat P, Anthonissen M, Meirte J, Van Daele U, Maertens K. The physical and physiological effects of vacuum massage on the different skin layers: a current status of the literature. Burns Trauma. 2016;4:34.
51. Fodor PB. Endermologie (LPG): does it work? Aesthetic Plast Surg. 1997;21(2):68.
52. Marques MA, Combes M, Roussel B, Vidal-Dupont L, Thalamas C, Lafontan M, et al. Impact of a mechanical massage on gene expression profile and lipid mobilization in female gluteofemoral adipose tissue. Obesity facts. 2011;4(2):121-9.
53. Majani Ugo, Aldo M. Tissue mechanostimulation in the treatment of scars. . Acta Medica Mediterranea. 2013;29:133–4.
54. Taheri A, Mansoori P, Al-Dabagh A, Feldman SR. Are corticosteroids effective for prevention of scar formation after second-degree skin burn? J Dermatolog Treat. 2014;25(4):360-2.
55. Wagner W, Alfrink M, Micke O, Schafer U, Schuller P, Willich N. Results of prophylactic irradiation in patients with resected keloids--a retrospective analysis. Acta oncologica (Stockholm, Sweden). 2000;39(2):217-20.
56. Manuskiatti W, Fitzpatrick RE. Treatment response of keloidal and hypertrophic sternotomy scars: comparison among intralesional corticosteroid, 5-fluorouracil, and 585-nm flashlamp-pumped pulsed-dye laser treatments. Arch Dermatol. 2002;138.
57. Shah VV, Aldahan AS, Mlacker S, Alsaidan M, Samarkandy S, Nouri K. 5-Fluorouracil in the Treatment of Keloids and Hypertrophic Scars: A Comprehensive Review of the Literature. Dermatology and Therapy. 2016;6(2):169-83.
58. Zhang ZY. Therapy function of 5-Fu associate with steroid to keloid (In Chinese). J Tongji University. 2007(28:79–82.).
59. Bodokh I, Brun P. [Treatment of keloid with intralesional bleomycin]. Annales de dermatologie et de venereologie. 1996;123(12):791-4.
60. Espana A, Solano T, Quintanilla E. Bleomycin in the treatment of keloids and hypertrophic scars by multiple needle punctures. Dermatologic Surgery. 2001;27(1):23-7.
61. Lee SY, Park J. Postoperative Electron Beam Radiotherapy for Keloids: Treatment Outcome and Factors Associated with Occurrence and Recurrence. Annals of Dermatology. 2015;27(1):53-8.
62. Sclafani AP, Gordon L, Chadha M, Romo T, 3rd. Prevention of earlobe keloid recurrence with postoperative corticosteroid injections versus radiation therapy: a randomized, prospective study and review of the literature. Dermatologic surgery : official publication for American Society for Dermatologic Surgery [et al]. 1996;22(6):569-74.
63. Flickinger JC. A radiobiological analysis of multicenter data for postoperative keloid radiotherapy. International journal of radiation oncology, biology, physics. 2011;79(4):1164-70.
64. Carvajal CC, Ibarra CM, Arbulo DL, Russo MN, Solé CP. Postoperative radiotherapy in the management of keloids. ecancermedicalscience. 2016;10:690.

65. Song C, Wu H-G, Chang H, Kim IH, Ha SW. Adjuvant single-fraction radiotherapy is safe and effective for intractable keloids. Journal of Radiation Research. 2014;55(5):912-6.
66. Ogawa R, Yoshitatsu S, Yoshida K, Miyashita T. Is radiation therapy for keloids acceptable? The risk of radiation-induced carcinogenesis. Plastic and reconstructive surgery. 2009;124(4):1196-201.
67. Hultman CS, Friedstat JS, Edkins RE, Cairns BA, Meyer AA. Laser resurfacing and remodeling of hypertrophic burn scars: the results of a large, prospective, before-after cohort study, with long-term follow-up. Ann Surg. 2014;260(3):519-29; discussion 29-32.
68. Levi B, Ibrahim A, Mathews K, Wojcik B, Gomez J, Fagan S, et al. The Use of CO2 Fractional Photothermolysis for the Treatment of Burn Scars. Journal of burn care & research : official publication of the American Burn Association. 2016;37(2):106-14.
69. Alster TS, Tanzi EL, Lazarus M. The use of fractional laser photothermolysis for the treatment of atrophic scars. Dermatologic surgery : official publication for American Society for Dermatologic Surgery [et al]. 2007;33(3):295-9.
70. Naouri M, Atlan M, Perrodeau E, Georgesco G, Khallouf R, Martin L, et al. High-resolution ultrasound imaging to demonstrate and predict efficacy of carbon dioxide fractional resurfacing laser treatment. Dermatologic surgery : official publication for American Society for Dermatologic Surgery [et al]. 2011;37(5):596-603.
71. Lee S-J, Suh D-H, Lee JM, Song K-Y, Ryu HJ. Dermal Remodeling of Burn Scar by Fractional CO2 Laser. Aesthetic Plastic Surgery. 2016;40(5):761-8.
72. El-Zawahry BM, Sobhi RM, Bassiouny DA, Tabak SA. Ablative CO2 fractional resurfacing in treatment of thermal burn scars: an open-label controlled clinical and histopathological study. Journal of cosmetic dermatology. 2015;14(4):324-31.
73. Kumar N, Kumar P, Nayak Badagabettu S, Prasad K, Kudva R, Raghuveer CV. Quantitative fraction evaluation of dermal collagen and elastic fibres in the skin samples obtained in two orientations from the trunk region. Dermatol Res Pract. 2014;2014:251254.
74. Borges AF. Relaxed Skin Tension Lines (RSTL) versus Other Skin Lines. Plastic and reconstructive surgery. 1984;73(1):144-50.
75. Connolly KL, Chaffins M, Ozog D. Vascular patterns in mature hypertrophic burn scars treated with fractional CO2 laser. Lasers in surgery and medicine. 2014;46(8):597-600.
76. Giordano CN, Ozog D. Microstructural and molecular considerations in the treatment of scars with ablative fractional lasers. Seminars in cutaneous medicine and surgery. 2015;34(1):7-12.
77. Alves ACA, Vieira RdP, Leal-Junior ECP, dos Santos SA, Ligeiro AP, Albertini R, et al. Effect of low-level laser therapy on the expression of inflammatory mediators and on neutrophils and macrophages in acute joint inflammation. Arthritis Research & Therapy. 2013;15(5):R116-R.
78. Kuo YR, Jeng SF, Wang FS, Chen TH, Huang HC, Chang PR, et al. Flashlamp pulsed dye laser (PDL) suppression of keloid proliferation through down-regulation of TGF-beta1 expression and extracellular matrix expression. Lasers in surgery and medicine. 2004;34(2):104-8.
79. Qu L, Liu A, Zhou L, He C, Grossman PH, Moy RL, et al. Clinical and molecular effects on mature burn scars after treatment with a fractional CO(2) laser. Lasers in surgery and medicine. 2012;44(7):517-24.
80. Ozog DM, Liu A, Chaffins ML, Ormsby AH, Fincher EF, Chipps LK, et al. Evaluation of clinical results, histological architecture, and collagen expression following treatment of mature burn scars with a fractional carbon dioxide laser. JAMA dermatology. 2013;149(1):50-7.
81. Singh A, Yadav S. Microneedling: Advances and widening horizons. Indian Dermatology Online Journal. 2016;7(4):244-54.
82. Donnelly RF, Raj Singh TR, Woolfson AD. Microneedle-based drug delivery systems: Microfabrication, drug delivery, and safety. Drug delivery. 2010;17(4):187-207.
83. Aust MC, Knobloch K, Reimers K, Redeker J, Ipaktchi R, Altintas MA, et al. Percutaneous collagen induction therapy: an alternative treatment for burn scars. Burns. 2010;36(6):836-43.

84. Xiao Z, Zhang M. Botulinum toxin type A affects cell cycle distribution of fibroblasts derived from hypertrophic scar. Journal of Plastic, Reconstructive & Aesthetic Surgery. 2008;61(9):1128-9.
85. Xiao Z, Zhang M, Liu Y, Ren L. Botulinum toxin type a inhibits connective tissue growth factor expression in fibroblasts derived from hypertrophic scar. Aesthetic Plast Surg. 2011;35(5):802-7.
86. Haubner F, Leyh M, Ohmann E, Sadick H, Gassner HG. Effects of botulinum toxin A on patient-specific keloid fibroblasts in vitro. The Laryngoscope. 2014;124(6):1344-51.
87. Haubner F, Ohmann E, Muller-Vogt U, Kummer P, Strutz J, Gassner HG. Effects of botulinum toxin a on cytokine synthesis in a cell culture model of cutaneous scarring. Archives of Facial Plastic Surgery. 2012;14(2):122-6.
88. Wilson AM. Use of botulinum toxin type A to prevent widening of facial scars. Plastic & Reconstructive Surgery. 2006;117(6):1758-66; discussion 67-8.
89. Wilson AM. Eradication of keloids: Surgical excision followed by a single injection of intralesional 5-fluorouracil and botulinum toxin. The Canadian journal of plastic surgery = Journal canadien de chirurgie plastique. 2013;21(2):87-91.
90. Gauglitz GG, Bureik D, Dombrowski Y, Pavicic T, Ruzicka T, Schauber J. Botulinum toxin A for the treatment of keloids. Skin pharmacology and physiology. 2012;25(6):313-8.
91. Prodromidou A, Frountzas M, Vlachos D-EG, Vlachos GD, Bakoyiannis I, Perrea D, et al. Botulinum toxin for the prevention and healing of wound scars: A systematic review of the literature. Plastic Surgery. 2015;23(4):260-4.
92. Xu SJ, Teng JY, Xie J, Shen MQ, Chen DM. Comparison of the mechanisms of intralesional steroid, interferon or verapamil injection in the treatment of proliferative scars. [Chinese]. Zhonghua zheng xing wai ke za zhi = Zhonghua zhengxing waike zazhi = Chinese journal of plastic surgery. 2009;25(1):37-40.
93. Tredget EE, Wang R, Shen Q, Scott PG, Ghahary A. Transforming growth factor-beta mRNA and protein in hypertrophic scar tissues and fibroblasts: antagonism by IFN-alpha and IFN-gamma in vitro and in vivo. J Interf Cytokine Res. 2000;20.
94. Tredget EE, Shankowsky HA, Pannu R, Nedelec B, Iwashina T, Ghahary A. Transforming growth factor-beta in thermally injured patients with hypertrophic scars: effects of interferon alpha-2b. Plastic and reconstructive surgery. 1998;102.
95. Sleijfer S, Bannink M, Van Gool AR, Kruit WH, Stoter G. Side effects of interferon-alpha therapy. Pharmacy world & science : PWS. 2005;27(6):423-31.
96. Giugliano G, Pasquali D, Notaro A, Brongo S, Nicoletti G, D'Andrea F, et al. Verapamil inhibits interleukin-6 and vascular endothelial growth factor production in primary cultures of keloid fibroblasts. British journal of plastic surgery. 2003;56(8):804-9.
97. Ahuja RB, Chatterjee P. Comparative efficacy of intralesional verapamil hydrochloride and triamcinolone acetonide in hypertrophic scars and keloids. Burns. 2014;40(4):583-8.
98. Neuber G. Fat transplantation. Verh Dtsch Ges Chir. 1893;22:66.
99. Coleman SR. Long-term survival of fat transplants: controlled demonstrations. Aesthetic Plast Surg. 1995;19(5):421-5.
100. Covarrubias P, Cardenas-Camarena L, Guerrerosantos J, Valenzuela L, Espejo I, Robles JA, et al. Evaluation of the histologic changes in the fat-grafted facial skin: clinical trial. Aesthetic Plast Surg. 2013;37(4):778-83.
101. Lisa A, Summo V, Bandi V, Maione L, Murolo M, Klinger F, et al. Autologous Fat Grafting in the Treatment of Painful Postsurgical Scar of the Oral Mucosa. Case Reports in Medicine. 2015;2015:4.
102. Caviggioli F, Maione L, Klinger F, Lisa A, Klinger M. Autologous Fat Grafting Reduces Pain in Irradiated Breast: A Review of Our Experience. Stem cells international. 2016;2016:2527349.
103. Frese L, Dijkman PE, Hoerstrup SP. Adipose Tissue-Derived Stem Cells in Regenerative Medicine. Transfusion Medicine and Hemotherapy. 2016;43(4):268-74.
104. Wallukat G. The beta-adrenergic receptors. Herz. 2002;27(7):683-90.

105. Nagatsu T, Stjarne L. Catecholamine synthesis and release. Overview. Advances in pharmacology (San Diego, Calif). 1998;42:1-14.
106. Pullar CE, Isseroff RR. Cyclic AMP mediates keratinocyte directional migration in an electric field. Journal of Cell Science. 2005;118(9):2023-34.
107. Pullar CE, Chen J, Isseroff RR. PP2A Activation by β2-Adrenergic Receptor Agonists: Novel Regulatory Mechanism of Keratinocyte Migration. Journal of Biological Chemistry. 2003;278(25):22555-62.
108. Steinkraus V, Mak JC, Pichlmeier U, Mensing H, Ring J, Barnes PJ. Autoradiographic mapping of beta-adrenoceptors in human skin. Archives of dermatological research. 1996;288(9):549-53.
109. McSwigan JD, Hanson DR, Lubiniecki A, Heston LL, Sheppard JR. Down syndrome fibroblasts are hyperresponsive to beta-adrenergic stimulation. Proceedings of the National Academy of Sciences. 1981;78(12):7670-3.
110. Gillbro JM, Marles LK, Hibberts NA, Schallreuter KU. Autocrine catecholamine biosynthesis and the beta-adrenoceptor signal promote pigmentation in human epidermal melanocytes. J Invest Dermatol. 2004;123(2):346-53.
111. Pullar CE, Manabat-Hidalgo CG, Bolaji RS, Isseroff RR. beta-Adrenergic receptor modulation of wound repair. Pharmacological research. 2008;58(2):158-64.
112. Pullar CE, Rizzo A, Isseroff RR. beta-Adrenergic receptor antagonists accelerate skin wound healing: evidence for a catecholamine synthesis network in the epidermis. J Biol Chem. 2006;281(30):21225-35.
113. Sivamani RK, Pullar CE, Manabat-Hidalgo CG, Rocke DM, Carlsen RC, Greenhalgh DG, et al. Stress-mediated increases in systemic and local epinephrine impair skin wound healing: potential new indication for beta blockers. PLoS medicine. 2009;6(1):e12.
114. Arbabi S, Ahrns KS, Wahl WL, Hemmila MR, Wang SC, Brandt MM, et al. Beta-blocker use is associated with improved outcomes in adult burn patients. The Journal of trauma. 2004;56(2):265-9; discussion 9-71.
115. Pullar CE, Grahn JC, Liu W, Isseroff RR. β2-Adrenergic receptor activation delays wound healing. The FASEB Journal. 2006;20(1):76-86.
116. Le Provost GS, Pullar CE. β2-Adrenoceptor Activation Modulates Skin Wound Healing Processes to Reduce Scarring. The Journal of Investigative Dermatology. 2015;135(1):279-88.
117. Pullar CE. The development of topical Salbutamol to prevent human skin scarring and hyperpigmentation Gateway to Research 2015 [cited 2017 09/11/2017]. Available from: http://gtr.rcuk.ac.uk/projects?ref=MR%2FM024679%2F1.
118. Logan A, Baird A, Berry M. Decorin attenuates gliotic scar formation in the rat cerebral hemisphere. Experimental neurology. 1999;159(2):504-10.
119. Baghy K, Dezso K, Laszlo V, Fullar A, Peterfia B, Paku S, et al. Ablation of the decorin gene enhances experimental hepatic fibrosis and impairs hepatic healing in mice. Laboratory investigation; a journal of technical methods and pathology. 2011;91(3):439-51.
120. Ma R, He S, Liang X, Yu H, Liang Y, Cai X. Decorin prevents the development of CCl(4)-induced liver fibrosis in mice. Chinese medical journal. 2014;127(6):1100-4.
121. Schaefer L, Macakova K, Raslik I, Micegova M, Grone HJ, Schonherr E, et al. Absence of decorin adversely influences tubulointerstitial fibrosis of the obstructed kidney by enhanced apoptosis and increased inflammatory reaction. Am J Pathol. 2002;160(3):1181-91.
122. Kolb M, Margetts PJ, Galt T, Sime PJ, Xing Z, Schmidt M, et al. Transient transgene expression of decorin in the lung reduces the fibrotic response to bleomycin. American journal of respiratory and critical care medicine. 2001;163(3 Pt 1):770-7.
123. Zheng F, Lu W, Wu F, Li H, Hu X, Zhang F. Recombinant decorin ameliorates the pulmonary structure alterations by down-regulating transforming growth factor-beta1/SMADS signaling in the diabetic rats. Endocrine research. 2010;35(1):35-49.

124. Klass BR, Grobbelaar AO, Rolfe KJ. Transforming growth factor β1 signalling, wound healing and repair: a multifunctional cytokine with clinical implications for wound repair, a delicate balance. Postgraduate Medical Journal. 2009;85(999):9-14.
125. Sato Y, Rifkin DB. Inhibition of endothelial cell movement by pericytes and smooth muscle cells: activation of a latent transforming growth factor-beta 1-like molecule by plasmin during co-culture. The Journal of cell biology. 1989;109(1):309-15.
126. Murphy-Ullrich JE, Poczatek M. Activation of latent TGF-beta by thrombospondin-1: mechanisms and physiology. Cytokine Growth Factor Rev. 2000;11(1-2):59-69.
127. Annes JP, Munger JS, Rifkin DB. Making sense of latent TGFbeta activation. J Cell Sci. 2003;116(Pt 2):217-24.
128. Yu Q, Stamenkovic I. Cell surface-localized matrix metalloproteinase-9 proteolytically activates TGF-beta and promotes tumor invasion and angiogenesis. Genes & development. 2000;14(2):163-76.
129. Lyons RM, Keski-Oja J, Moses HL. Proteolytic activation of latent transforming growth factor-beta from fibroblast-conditioned medium. The Journal of cell biology. 1988;106(5):1659-65.
130. Shah M, Foreman DM, Ferguson MW. Neutralising antibody to TGF-beta 1,2 reduces cutaneous scarring in adult rodents. J Cell Sci. 1994;107.
131. Ferguson MW, Duncan J, Bond J, Bush J, Durani P, So K, et al. Prophylactic administration of avotermin for improvement of skin scarring: three double-blind, placebo-controlled, phase I/II studies. The Lancet. 2009;373(9671):1264-74.
132. Occleston NL, Laverty HG, O'Kane S, Ferguson MW. Prevention and reduction of scarring in the skin by Transforming Growth Factor beta 3 (TGFbeta3): from laboratory discovery to clinical pharmaceutical. Journal of biomaterials science Polymer edition. 2008;19(8):1047-63.
133. Grainger DJ, Wakefield L, Bethell HW, Farndale RW, Metcalfe JC. Release and activation of platelet latent TGF-beta in blood clots during dissolution with plasmin. Nature medicine. 1995;1(9):932-7.
134. Esparza-Lopez J, Montiel JL, Vilchis-Landeros MM, Okadome T, Miyazono K, Lopez-Casillas F. Ligand binding and functional properties of betaglycan, a co-receptor of the transforming growth factor-beta superfamily. Specialized binding regions for transforming growth factor-beta and inhibin A. J Biol Chem. 2001;276(18):14588-96.
135. Penn JW, Grobbelaar AO, Rolfe KJ. The role of the TGF-β family in wound healing, burns and scarring: a review. International Journal of Burns and Trauma. 2012;2(1):18-28.
136. Drake WT, Issekutz AC. Transforming growth factor-beta 1 enhances polymorphonuclear leucocyte accumulation in dermal inflammation and transendothelial migration by a priming action. Immunology. 1993;78(2):197-204.
137. Ashcroft GS. Bidirectional regulation of macrophage function by TGF-beta. Microbes and infection. 1999;1(15):1275-82.
138. Gailit J, Welch MP, Clark RA. TGF-beta 1 stimulates expression of keratinocyte integrins during re-epithelialization of cutaneous wounds. J Invest Dermatol. 1994;103(2):221-7.
139. Yang EY, Moses HL. Transforming growth factor beta 1-induced changes in cell migration, proliferation, and angiogenesis in the chicken chorioallantoic membrane. The Journal of cell biology. 1990;111(2):731-41.
140. Li Y, Liu Y, Xia W, Lei D, Voorhees JJ, Fisher GJ. Age-dependent alterations of decorin glycosaminoglycans in human skin. Sci Rep. 2013;3.
141. Blochberger TC, Cornuet PK, Hassell JR. Isolation and partial characterization of lumican and decorin from adult chicken corneas. A keratan sulfate-containing isoform of decorin is developmentally regulated. J Biol Chem. 1992;267(29):20613-9.
142. Seidler DG, Dreier R. Decorin and its galactosaminoglycan chain: extracellular regulator of cellular function? IUBMB Life. 2008;60(11):729-33.
143. Chen S, Birk DE. The regulatory roles of small leucine-rich proteoglycans in extracellular matrix assembly. The FEBS journal. 2013;280(10):2120-37.

144. Schaefer L, Iozzo RV. Biological Functions of the Small Leucine-rich Proteoglycans: From Genetics to Signal Transduction. The Journal of Biological Chemistry. 2008;283(31):21305-9.
145. Zhu WEI, Robey PG, Boskey AL. CHAPTER 9 - The Regulatory Role of Matrix Proteins in Mineralization of Bone A2 - MARCUS, ROBERT. In: Feldman D, Nelson DA, Rosen CJ, editors. Osteoporosis (Third Edition). San Diego: Academic Press; 2008. p. 191-240.
146. Scott PG, McEwan PA, Dodd CM, Bergmann EM, Bishop PN, Bella J. Crystal structure of the dimeric protein core of decorin, the archetypal small leucine-rich repeat proteoglycan. Proceedings of the National Academy of Sciences of the United States of America. 2004;101(44):15633-8.
147. Weber IT, Harrison RW, Iozzo RV. Model structure of decorin and implications for collagen fibrillogenesis. J Biol Chem. 1996;271(50):31767-70.
148. Scott JE. Supramolecular organization of extracellular matrix glycosaminoglycans, in vitro and in the tissues. FASEB journal : official publication of the Federation of American Societies for Experimental Biology. 1992;6(9):2639-45.
149. Stella M, Calcagni M, Teich-Alasia S, Ramieri G, Cellino G, Panzica G. Sensory endings in skin grafts and scars after extensive burns. Burns. 1994;20(6):491-5.
150. Goldoni S, Owens RT, McQuillan DJ, Shriver Z, Sasisekharan R, Birk DE, et al. Biologically Active Decorin Is a Monomer in Solution. Journal of Biological Chemistry. 2004;279(8):6606-12.
151. Islam M, Gor J, Perkins SJ, Ishikawa Y, Bächinger HP, Hohenester E. The Concave Face of Decorin Mediates Reversible Dimerization and Collagen Binding. Journal of Biological Chemistry. 2013;288(49):35526-33.
152. Takeuchi Y, Kodama Y, Matsumoto T. Bone matrix decorin binds transforming growth factor-beta and enhances its bioactivity. Journal of Biological Chemistry. 1994;269(51):32634-8.
153. Schonherr E, Broszat M, Brandan E, Bruckner P, Kresse H. Decorin core protein fragment Leu155-Val260 interacts with TGF-beta but does not compete for decorin binding to type I collagen. Arch Biochem Biophys. 1998;355(2):241-8.
154. Jarvelainen H, Puolakkainen P, Pakkanen S, Brown EL, Hook M, Iozzo RV, et al. A role for decorin in cutaneous wound healing and angiogenesis. Wound repair and regeneration : official publication of the Wound Healing Society [and] the European Tissue Repair Society. 2006;14(4):443-52.
155. Beanes SR, Dang C, Soo C, Wang Y, Urata M, Ting K, et al. Down-regulation of decorin, a transforming growth factor-beta modulator, is associated with scarless fetal wound healing. Journal of pediatric surgery. 2001;36(11):1666-71.
156. Nakamura N, Hart DA, Boorman RS, Kaneda Y, Shrive NG, Marchuk LL, et al. Decorin antisense gene therapy improves functional healing of early rabbit ligament scar with enhanced collagen fibrillogenesis in vivo. Journal of orthopaedic research : official publication of the Orthopaedic Research Society. 2000;18(4):517-23.
157. Hosaka Y, Kirisawa R, Mafune N, Takehana K. Downregulation of decorin and transforming growth factor-beta1 by decorin gene suppression in tendinocytes. Connective tissue research. 2005;46(1):18-26.
158. al-Tarrah K, Lee KC, Moiemen N. Systemic Levels of Transforming Growth Factor β1, Decorin and Interleukin-1β influence Scar Severity: A Kinetic Overview. British Burns Association Annual meeting; London2017.
159. Abdel MP, Morrey ME, Barlow JD, Grill DE, Kolbert CP, An KN, et al. Intra-articular decorin influences the fibrosis genetic expression profile in a rabbit model of joint contracture. Bone & joint research. 2014;3(3):82-8.
160. Fukushima K, Badlani N, Usas A, Riano F, Fu F, Huard J. The use of an antifibrosis agent to improve muscle recovery after laceration. The American journal of sports medicine. 2001;29(4):394-402.
161. Hill LJ, Blanch RJ, Mead B, Morgan-Warren PJ, Botfield H, Mohamed S, et al. Decorin, an anti-fibrogenic and fibrolytic glycoprotein, reduces established trabecular meshwork scarring and

intraocular pressure and protects retinal function in a rat model of glaucoma. Investigative ophthalmology & visual science. 2014;55(13):562-.
162. Botfield H, Gonzalez AM, Abdullah O, Skjolding AD, Berry M, McAllister JP, 2nd, et al. Decorin prevents the development of juvenile communicating hydrocephalus. Brain : a journal of neurology. 2013;136(Pt 9):2842-58.
163. Khan GA, Girish GV, Lala N, Di Guglielmo GM, Lala PK. Decorin Is a Novel VEGFR-2-Binding Antagonist for the Human Extravillous Trophoblast. Molecular Endocrinology. 2011;25(8):1431-43.
164. Fiedler LR, Schönherr E, Waddington R, Niland S, Seidler DG, Aeschlimann D, et al. Decorin Regulates Endothelial Cell Motility on Collagen I through Activation of Insulin-like Growth Factor I Receptor and Modulation of α2β1 Integrin Activity. Journal of Biological Chemistry. 2008;283(25):17406-15.
165. Jarvinen TA, Ruoslahti E. Target-seeking antifibrotic compound enhances wound healing and suppresses scar formation in mice. Proceedings of the National Academy of Sciences of the United States of America. 2010;107(50):21671-6.
166. Goldoni S, Seidler DG, Heath J, Fassan M, Baffa R, Thakur ML, et al. An antimetastatic role for decorin in breast cancer. Am J Pathol. 2008;173(3):844-55.
167. Mohan RR, Tovey JC, Gupta R, Sharma A, Tandon A. Decorin biology, expression, function and therapy in the cornea. Current molecular medicine. 2011;11(2):110-28.
168. Morais JM, Papadimitrakopoulos F, Burgess DJ. Biomaterials/Tissue Interactions: Possible Solutions to Overcome Foreign Body Response. The AAPS Journal. 2010;12(2):188-96.
169. Headon H, Kasem A, Mokbel K. Capsular Contracture after Breast Augmentation: An Update for Clinical Practice. Archives of Plastic Surgery. 2015;42(5):532-43.
170. Sylvester ML. Engineering a Decorin Surface Coating and Evaluating the Role of Decorin in the Foreign Body Response to Implants: University of Washington; 2012.
171. de Cogan F, Hill LJ, Lynch A, Morgan-Warren PJ, Lechner J, Berwick MR, et al. Topical Delivery of Anti-VEGF Drugs to the Ocular Posterior Segment Using Cell-Penetrating PeptidesCPP Delivery of Anti-VEGF Drugs to the Retina. Investigative ophthalmology & visual science. 2017;58(5):2578-90.
172. Chung CH. The use of Injectable Nonsteroidal Anti-Inflammatory Drugs in Local Accident & Emergency Practice. Hong Kong Journal of Emergency Medicine. 2002;9(2):65-71.
173. Cost comparison charts Newcastle: Regional drug and therapeutics centre (Newcastle); 2019 [cited 2019 26th August 2019]. Available from: http://gmmmg.nhs.uk/docs/cost_comparison_charts.pdf.
174. National Drug Monograph Intravenous Ibuprofen (Caldolor™): VA Pharmacy Benefits Management Services, Medical Advisory Panel, and VISN Pharmacist Executives; 2010 [cited 2019 August]. Available from: https://www.pbm.va.gov/PBM/clinicalguidance/drugmonographs/IntravenousIbuprofenCaldolor.doc.
175. Meller D, Pauklin M, Thomasen H, Westekemper H, Steuhl K-P. Amniotic Membrane Transplantation in the Human Eye. Deutsches Ärzteblatt International. 2011;108(14):243-8.
176. ElHeneidy H, Omran E, Halwagy A, Al-Inany H, Al-Ansary M, Gad A. Amniotic membrane can be a valid source for wound healing. International Journal of Women's Health. 2016;8:225-31.
177. Sedighi A, Mehrabani D, Shirazi R. Histopathological evaluation of the healing effects of human amniotic membrane transplantation in third-degree burn wound injuries. Comp Clin Pathol 2016;25:381–5.
178. Leila G, Saeideh P, Hajar K, Ali Bp, Vahid HS, Ali N, et al. A randomized trial study on the effect of amniotic membrane graft on wound healing process after anal fistulotomy. Journal of Coloproctology. 2017;37(3):187-92.
179. Loeffelbein DJ, Rohleder NH, Eddicks M, Baumann CM, Stoeckelhuber M, Wolff K-D, et al. Evaluation of Human Amniotic Membrane as a Wound Dressing for Split-Thickness Skin-Graft Donor Sites. BioMed Research International. 2014;2014:12.
180. Adds PJ, Hunt C, Hartley S. Bacterial contamination of amniotic membrane. Br J Ophthalmol. 2001;85(2):228-30.

181. Kassem RR, Gawdat GI, Zedan RH. Severe fibrosis of extraocular muscles after the use of lyophilized amniotic membrane in strabismus surgery. Journal of AAPOS : the official publication of the American Association for Pediatric Ophthalmology and Strabismus. 2010;14(6):548-9.
182. Turkoglu E, Dinc C, Tuncer C, Oktay M, Serbes G, Sekerci Z. Use of decorin to prevent epidural fibrosis in a post-laminectomy rat model. European journal of pharmacology. 2014;724:86-91.
183. Kang KS, Veeder GT, Mirrasoul PJ, Kaneko T, Cottrell IW. Agar-Like Polysaccharide Produced by a Pseudomonas Species: Production and Basic Properties. Applied and Environmental Microbiology. 1982;43(5):1086-91.
184. Sigma A. Gellan gum price: Sigma Aldrich; 2019 [cited 2019 23rd August 2019]. Available from: https://www.sigmaaldrich.com/catalog/search?interface=All&term=gellan+gum&N=0&mode=partialmax&focus=product&lang=en&region=global.
185. Jenkins RO. Biotechnological Innovations in Chemical Synthesis. Oxford: Butterworth-Heinemann Limited; 1997.
186. Jansson P-E, Lindberg B, Sandford PA. Structural studies of gellan gum, an extracellular polysaccharide elaborated by Pseudomonas elodea. Carbohydrate research. 1983;124(1):135-9.
187. O'Neill MA, Selvendran RR, Morris VJ. Structure of the acidic extracellular gelling polysaccharide produced by Pseudomonas elodea. Carbohydrate research. 1983;124(1):123-33.
188. Mao R, Tang J, Swanson BG. Texture properties of high and low acyl mixed gellan gels. Carbohydrate Polymers. 2000;41(4):331-8.
189. Lee H, Fisher S, Kallos MS, Hunter CJ. Optimizing gelling parameters of gellan gum for fibrocartilage tissue engineering. Journal of Biomedical Materials Research Part B: Applied Biomaterials. 2011;98B(2):238-45.
190. Morris ER, Nishinari K, Rinaudo M. Gelation of gellan – A review. Food Hydrocolloids. 2012;28(2):373-411.
191. Norton AB, Hancocks RD, Grover LM. Poly (vinyl alcohol) modification of low acyl gellan hydrogels for applications in tissue regeneration. Food Hydrocolloids. 2014;42, Part 3(0):373-7.
192. Miyazaki S, Aoyama H, Kawasaki N, Kubo W, Attwood D. In situ-gelling gellan formulations as vehicles for oral drug delivery. Journal of controlled release : official journal of the Controlled Release Society. 1999;60(2-3):287-95.
193. Gong Y, Wang C, Lai RC, Su K, Zhang F, Wang D-a. An improved injectable polysaccharide hydrogel: modified gellan gum for long-term cartilage regenerationin vitro. Journal of Materials Chemistry. 2009;19(14):1968-77.
194. Osmalek T, Froelich A, Tasarek S. Application of gellan gum in pharmacy and medicine. International journal of pharmaceutics. 2014;466(1-2):328-40.
195. Field FK, Kerstein MD. Overview of wound healing in a moist environment. American journal of surgery. 1994;167(1a):2s-6s.
196. Miyoshi E, Nishinari K. Non-Newtonian flow behaviour of gellan gum aqueous solutions. Colloid and Polymer Science. 1999;277(8):727-34.
197. (FDA) FaDA. Part 172: Food additives permitted for direct addition to food for human consumption. Subpart G: Gums, chewing gum bases and related substances. 2017 [updated April 1, 2017; cited 2017 23/08/2017]. Available from: https://www.accessdata.fda.gov/scripts/cdrh/cfdocs/cfcfr/CFRSearch.cfm?fr=172.665.
198. Anderson DM, Brydon WG, Eastwood MA. The dietary effects of gellan gum in humans. Food additives and contaminants. 1988;5(3):237-49.
199. Cao SL, Zhang QZ, Jiang XG. Preparation of ion-activated in situ gel systems of scopolamine hydrobromide and evaluation of its antimotion sickness efficacy. Acta pharmacologica Sinica. 2007;28(4):584-90.

200. Cao SL, Ren XW, Zhang QZ, Chen E, Xu F, Chen J, et al. In situ gel based on gellan gum as new carrier for nasal administration of mometasone furoate. International journal of pharmaceutics. 2009;365(1-2):109-15.
201. Shedden AH, Laurence J, Barrish A, Olah TV. Plasma timolol concentrations of timolol maleate: timolol gel-forming solution (TIMOPTIC-XE) once daily versus timolol maleate ophthalmic solution twice daily. Documenta ophthalmologica Advances in ophthalmology. 2001;103(1):73-9.
202. Kesavan K, Kant S, Pandit JK. Therapeutic Effectiveness in the Treatment of Experimental Bacterial Keratitis with Ion-activated Mucoadhesive Hydrogel. Ocular immunology and inflammation. 2016;24(5):489-92.
203. Vijan V, Kaity S, Biswas S, Isaac J, Ghosh A. Microwave assisted synthesis and characterization of acrylamide grafted gellan, application in drug delivery. Carbohydrate Polymers. 2012;90(1):496-506.
204. Shiyani BG, Dholakiya RB, Akbari BV, Lodhiya DJ, Ramani GK. Development and evaluation of novel immediate release tablets of Metoclopramide HCl by direct compression using treated gellan gum as a disintegration-accelerating agent. Journal of Pharmacy Research. 2009;2(9):1460-4.
205. Posadowska U, Brzychczy-Wloch M, Drozdz A, Krok-Borkowicz M, Wlodarczyk-Biegun M, Dobrzynski P, et al. Injectable hybrid delivery system composed of gellan gum, nanoparticles and gentamicin for the localized treatment of bone infections. Expert opinion on drug delivery. 2016;13(5):613-20.
206. Sullivan T, Smith J, Kermode J, McIver E, Courtemanche DJ. Rating the burn scar. Journal of Burn Care and Rehabilitation. 1990;11(3):256-60.
207. Draaijers LJ, Tempelman FR, Botman YA, Tuinebreijer WE, Middelkoop E, Kreis RW, et al. The patient and observer scar assessment scale: a reliable and feasible tool for scar evaluation. Plastic and reconstructive surgery. 2004;113(7):1960-5; discussion 6-7.
208. Liu X, Nelemans PJ, Van Winden M, Kelleners-Smeets NW, Mosterd K. Reliability of the Patient and Observer Scar Assessment Scale and a 4-point scale in evaluating linear facial surgical scars. Journal of the European Academy of Dermatology and Venereology : JEADV. 2017;31(2):341-6.
209. Li-Tsang CW, Lau JC, Liu SK. Validation of an objective scar pigmentation measurement by using a spectrocolorimeter. Burns. 2003;29(8):779-84.
210. Draaijers LJ, Tempelman FR, Botman YA, Kreis RW, Middelkoop E, van Zuijlen PP. Colour evaluation in scars: tristimulus colorimeter, narrow-band simple reflectance meter or subjective evaluation? Burns. 2004;30(2):103-7.
211. Boyce ST, Supp AP, Wickett RR, Hoath SB, Warden GD. Assessment with the dermal torque meter of skin pliability after treatment of burns with cultured skin substitutes. The Journal of burn care & rehabilitation. 2000;21(1 Pt 1):55-63.
212. Fong SS, Hung LK, Cheng JC. The cutometer and ultrasonography in the assessment of postburn hypertrophic scar--a preliminary study. Burns. 1997;23 Suppl 1:S12-8.
213. Magliaro A, Romanelli M. Skin hardness measurement in hypertrophic scars. Wounds-a Compendium of Clinical Research and Practice. 2003;15(3):66-70.
214. Van den Kerckhove E, Staes F, Flour M, Stappaerts K, Boeckx W. Reproducibility of repeated measurements on post-burn scars with Dermascan C. Skin research and technology : official journal of International Society for Bioengineering and the Skin (ISBS) [and] International Society for Digital Imaging of Skin (ISDIS) [and] International Society for Skin Imaging (ISSI). 2003;9(1):81-4.
215. FDA. Learn About Drug and Device Approvals 2017 [updated 01/25/2017 cited 2017 23/10/2017]. Available from: https://www.fda.gov/ForPatients/Approvals/default.htm.
216. WHO. World Health Organisation. Disease and injury regional estimates, 2004-2008. .
217. WHO. World Health Organisation. Global Health Estimates: deaths, disability-adjusted life year (DALYs), years of life lost (YLL) and years lost due to disability (YLD) by cause, age and sex, 2000–2012. .

218. Brusselaers N, Hoste EA, Monstrey S, Colpaert KE, De Waele JJ, Vandewoude KH, et al. Outcome and changes over time in survival following severe burns from 1985 to 2004. Intensive care medicine. 2005;31(12):1648-53.
219. Brusselaers N, Pirayesh A, Hoeksema H, Verbelen J, Blot S, Monstrey S. Burn scar assessment: A systematic review of objective scar assessment tools. Burns. 2010;36(8):1157-64.
220. Gankande TU, Duke JM, Danielsen PL, DeJong HM, Wood FM, Wallace HJ. Reliability of scar assessments performed with an integrated skin testing device—the DermaLab Combo®. Burns. 2014;40.
221. Kaartinen IS, Valisuo PO, Alander JT, Kuokkanen HO. Objective scar assessment--a new method using standardized digital imaging and spectral modelling. Burns. 2011;37(1):74-81.
222. Kaartinen IS, Valisuo PO, Bochko V, Alander JT, Kuokkanen HO. How to assess scar hypertrophy--a comparison of subjective scales and Spectrocutometry: a new objective method. Wound repair and regeneration : official publication of the Wound Healing Society [and] the European Tissue Repair Society. 2011;19(3):316-23.
223. Hoogewerf CJ, van Baar ME, Middelkoop E, van Loey NE. Impact of facial burns: relationship between depressive symptoms, self-esteem and scar severity. General hospital psychiatry. 2014;36(3):271-6.
224. Landis JR, Koch GG. The Measurement of Observer Agreement for Categorical Data. Biometrics. 1977;33(1):159-74.
225. Alster TS, Lewis AB, Rosenbach A. Laser scar revision: comparison of CO2 laser vaporization with and without simultaneous pulsed dye laser treatment. Dermatologic surgery : official publication for American Society for Dermatologic Surgery [et al]. 1998;24(12):1299-302.
226. Winkler AD, Spillmann L, Werner JS, Webster MA. Asymmetries in blue–yellow color perception and in the color of 'the dress'. Current Biology. 2015;25(13):R547-R8.
227. Tseng FY, Chao CJ, Feng WY, Hwang SL. Assessment of human color discrimination based on illuminant color, ambient illumination and screen background color for visual display terminal workers. Industrial health. 2010;48(4):438-46.
228. Shuwairi SM, Cronin-Golomb A, McCarley RW, O'Donnell BF. Color discrimination in schizophrenia. Schizophrenia research. 2002;55(1-2):197-204.
229. Davey RB, Sprod RT, Neild TO. Computerised colour: a technique for the assessment of burn scar hypertrophy. A preliminary report. Burns. 1999;25(3):207-13.
230. Li-Tsang CWP, Lau JCM, Liu SKY. Validation of an objective scar pigmentation measurement by using a spectrocolorimeter. Burns. 2003;29(8):779-84.
231. Chan HH, Wong DS, Ho WS, Lam LK, Wei W. The use of pulsed dye laser for the prevention and treatment of hypertrophic scars in chinese persons. Dermatologic surgery : official publication for American Society for Dermatologic Surgery [et al]. 2004;30(7):987-94; discussion 94.
232. Kim MS, Rodney WN, Cooper T, Kite C, Reece GP, Markey MK. Towards quantifying the aesthetic outcomes of breast cancer treatment: comparison of clinical photography and colorimetry. Journal of evaluation in clinical practice. 2009;15(1):20-31.
233. van der Wal M, Bloemen M, Verhaegen P, Tuinebreijer W, de Vet H, van Zuijlen P, et al. Objective color measurements: clinimetric performance of three devices on normal skin and scar tissue. Journal of burn care & research : official publication of the American Burn Association. 2013;34(3):e187-94.
234. Akita S, Akino K, Imaizumi T, Hirano A. A basic fibroblast growth factor improved the quality of skin grafting in burn patients. Burns. 2005;31(7):855-8.
235. Ardigò M, Muzio F, Picardo M, Brazzelli V. Non-invasive methods for vitiligo evaluation. Picardo M, Taïeb A, editors. London, New York: Springer Heidelberg Dordrecht; 2010.
236. Yip C. Re-pigmentation of skin following wounding [Doctor of Medicine]: The University of Manchester; 2012.
237. Barel AO, Clarys P, Alewaeters K, Duez C, Hubinon JL, Mommaerts M. The Visi-Chroma VC-100: a new imaging colorimeter for dermatocosmetic research. Skin research and technology :

official journal of International Society for Bioengineering and the Skin (ISBS) [and] International Society for Digital Imaging of Skin (ISDIS) [and] International Society for Skin Imaging (ISSI). 2001;7(1):24-31.
238. Hallam MJ, McNaught K, Thomas AN, Nduka C. A practical and objective approach to scar colour assessment. Journal of plastic, reconstructive & aesthetic surgery : JPRAS. 2013;66(10):e271-6.
239. van der Wal MB, van Zuijlen PP, van de Ven P, Middelkoop E. Topical silicone gel versus placebo in promoting the maturation of burn scars: a randomized controlled trial. Plastic and reconstructive surgery. 2010;126(2):524-31.
240. Verhaegen PD, Bloemen MC, van der Wal MB, Vloemans AF, Tempelman FR, Beerthuizen GI, et al. Skin stretching for primary closure of acute burn wounds. Burns. 2014;40(8):1727-37.
241. Nedelec B, Correa JA, de Oliveira A, LaSalle L, Perrault I. Longitudinal burn scar quantification. Burns. 2014;40(8):1504-12.
242. Oliveira GV, Chinkes D, Mitchell C, Oliveras G, Hawkins HK, Herndon DN. Objective assessment of burn scar vascularity, erythema, pliability, thickness, and planimetry. Dermatologic surgery : official publication for American Society for Dermatologic Surgery [et al]. 2005;31(1):48-58.
243. Nedelec B, Correa JA, Rachelska G, Armour A, LaSalle L. Quantitative measurement of hypertrophic scar: intrarater reliability, sensitivity, and specificity. Journal of burn care & research : official publication of the American Burn Association. 2008;29(3):489-500.
244. Cheon Y, Lee W, Rah D. Objective analysis of burn scar color by L*a*b* color coordinates. Burns. 2009;35:S33.
245. Cheon YW, Lee WJ, Rah DK. Objective and quantitative evaluation of scar color using the L*a*b* color coordinates. The Journal of craniofacial surgery. 2010;21(3):679-84.
246. Valisuo P, Harju T, Alander J. Reflectance measurement using digital camera and a protecting dome with built in light source. Journal of biophotonics. 2011;4(7-8):559-64.
247. Bae EJ, Seo SH, Kye YC, Ahn HH. A quantitative assessment of the human skin surface using polarized light digital photography and its dermatologic significance. Skin research and technology : official journal of International Society for Bioengineering and the Skin (ISBS) [and] International Society for Digital Imaging of Skin (ISDIS) [and] International Society for Skin Imaging (ISSI). 2010;16(3):270-4.
248. Khorasani H, Zheng Z, Nguyen C, Zara J, Zhang X, Wang J, et al. A Quantitative Approach to Scar Analysis. The American Journal of Pathology. 2011;178(2):621-8.
249. Ferreira T, Rasband W. ImageJ User Guide — IJ 1.46 2010—2012 [2nd September 2015]. imagej.nih.gov/ij/docs/guide/].
250. Burke-Smith A, Collier J, Jones I. A comparison of non-invasive imaging modalities: Infrared thermography, spectrophotometric intracutaneous analysis and laser Doppler imaging for the assessment of adult burns. Burns. 2015.
251. Jones HG. Clinimetrics of tristimulus colourimeters in scar assessment: a review of evidence. Journal of wound care. 2012;21(1):30-5.
252. Moncrieff M, Cotton S, Claridge E, Hall P. Spectrophotometric intracutaneous analysis: a new technique for imaging pigmented skin lesions. Br J Dermatol. 2002;146(3):448-57.
253. Ud-Din S, Perry D, Giddings P, Colthurst J, Zaman K, Whiteside S, et al. Clinical evaluation of the application of electrical stimulation (degenerative wave) in a temporal acute wound biopsy in human volunteers shows enhanced wound healing captured by objective non-invasive devices. Wound Repair and Regeneration. 2011;19 (2):A58.
254. Li ZY, Su HT, Lu SL, Huang LB, Yang XB, Shao TB, et al. [Clinical study on the relationship among the dermis, fat dome and postburn hyperplastic scar formation]. Zhonghua shao shang za zhi = Zhonghua shaoshang zazhi = Chinese journal of burns. 2004;20(6):343-6.
255. Wan BK, Qi HZ, Ming D, Zhang MJ, Wang QF. Chromatic analysis of burn scar based on ANN by using photoelectrical technology. In: Chance B, Chen M, Chiou AET, Luo Q, editors. Optics in

Health Care and Biomedical Optics: Diagnostics and Treatment Ii , Pts 1 and 2. Proceedings of the Society of Photo-Optical Instrumentation Engineers (Spie). 56302005. p. 538-43.
256. Beausang E, Floyd H, Dunn KW, Orton CI, Ferguson MW. A new quantitative scale for clinical scar assessment. Plastic and reconstructive surgery. 1998;102(6):1954-61.
257. Powell MW, Sarkar S, Goldgof DB, Ivanov K. A methodology for extracting objective color from images. IEEE transactions on systems, man, and cybernetics Part B, Cybernetics : a publication of the IEEE Systems, Man, and Cybernetics Society. 2004;34(5):1964-78.
258. Anderson JC, Hallam MJ, Nduka C, Osorio D. The challenge of objective scar colour assessment in a clinical setting: using digital photography. Journal of wound care. 2015;24(8):379-87.
259. Van Zuijlen PPM, Angeles AP, Kreis RW, Bos KE, Middelkoop E. Scar assessment tools: Implications for current research. Plastic and reconstructive surgery. 2002;109(3):1108-22.
260. Valente JH, Jay GD, Schmidt ST, Oh AK, Reinert SE, Zabbo CP. Digital imaging analysis of scar aesthetics. Advances in skin & wound care. 2012;25(3):119-23.
261. Kim DW, Hwang NH, Yoon ES, Dhong ES, Park SH. Outcomes of ablative fractional laser scar treatment. Journal of Plastic Surgery and Hand Surgery. 2015;49(2):88-94.
262. Li-Tsang CW, Lau JC, Chan CC. Prevalence of hypertrophic scar formation and its characteristics among the Chinese population. Burns. 2005;31(5):610-6.
263. Nedelec B, Correa JA, Rachelska G, Armour A, LaSalle L. Quantitative measurement of hypertrophic scar: interrater reliability and concurrent validity. Journal of burn care & research : official publication of the American Burn Association. 2008;29(3):501-11.
264. Gankande TU, Duke JM, Wood FM, Wallace HJ. Interpretation of the DermaLab Combo((R)) pigmentation and vascularity measurements in burn scar assessment: An exploratory analysis. Burns. 2015;41(6):1176-85.
265. Wei Y, Li-Tsang CW, Luk DC, Tan T, Zhang W, Chiu TW. A validation study of scar vascularity and pigmentation assessment using dermoscopy. Burns. 2015;41(8):1717-23.
266. Bray R, Forrester K, Leonard C, McArthur R, Tulip J, Lindsay R. Laser Doppler imaging of burn scars: a comparison of wavelength and scanning methods. Burns. 2003;29(3):199-206.
267. Ehrlich HP, Kelley SF. Hypertrophic scar: an interruption in the remodeling of repair--a laser Doppler blood flow study. Plastic and reconstructive surgery. 1992;90(6):993-8.
268. Hosoda G, Holloway GA, Heimbach DM. Laser Doppler flowmetry for the early detection of hypertrophic burn scars. The Journal of burn care & rehabilitation. 1986;7(6):496-7.
269. Timar-Banu O, Beauregard H, Tousignant J, Lassonde M, Harris P, Viau G, et al. Development of noninvasive and quantitative methodologies for the assessment of chronic ulcers and scars in humans. Wound repair and regeneration : official publication of the Wound Healing Society [and] the European Tissue Repair Society. 2001;9(2):123-32.
270. Page RE, Robertson GA, Pettigrew NM. Microcirculation in hypertrophic burn scars. Burns, including thermal injury. 1983;10(1):64-70.
271. Leung KS, Sher A, Clark JA, Cheng JC, Leung PC. Microcirculation in hypertrophic scars after burn injury. The Journal of burn care & rehabilitation. 1989;10(5):436-44.
272. Clark JA, Leung KS, Cheng JC, Leung PC. The hypertrophic scar and microcirculation properties. Burns. 1996;22(6):447-50.
273. Forrester KR, Tulip J, Leonard C, Stewart C, Bray RC. A laser speckle imaging technique for measuring tissue perfusion. IEEE transactions on bio-medical engineering. 2004;51(11):2074-84.
274. Leung KS, Sher A, Clark JA, Cheng JCY, Leung PC. Microcirculation in hypertrophic scars after burn injury. Journal of Burn Care and Rehabilitation. 1989;10(5):436-44.
275. Clark JA, Leung KS, Cheng JCY, Leung PC. The hypertrophic scar and microcirculation properties. Burns. 1996;22(6):447-50.
276. Wittenberg GP, Fabian BG, Bogomilsky JL, Schultz LR, Rudner EJ, Chaffins ML, et al. Prospective, single-blind, randomized, controlled study to assess the efficacy of the 585-nm flashlamp-pumped pulsed-dye laser and silicone gel sheeting in hypertrophic scar treatment. Arch Dermatol. 1999;135(9):1049-55.

277. Allely RR, Van-Buendia LB, Jeng JC, White P, Wu J, Niszczak J, et al. Laser Doppler imaging of cutaneous blood flow through transparent face masks: a necessary preamble to computer-controlled rapid prototyping fabrication with submillimeter precision. Journal of burn care & research : official publication of the American Burn Association. 2008;29(1):42-8.
278. Stewart CJ, Frank R, Forrester KR, Tulip J, Lindsay R, Bray RC. A comparison of two laser-based methods for determination of burn scar perfusion: laser Doppler versus laser speckle imaging. Burns. 2005;31(6):744-52.
279. moorFLPI-2 (Laser speckle contrast imager) [01/04/2015]. Available from: http://us.moor.co.uk/product/moorflpi-2-/291.
280. Prindeze NJ, Hoffman HA, Ardanuy JG, Zhang J, Carney BC, Moffatt LT, et al. Active Dynamic Thermography is a Sensitive Method for Distinguishing Burn Wound Conversion. Journal of burn care & research : official publication of the American Burn Association. 2015.
281. Monstrey S, Hoeksema H, Verbelen J, Pirayesh A, Blondeel P. Assessment of burn depth and burn wound healing potential. Burns. 2008;34(6):761-9.
282. Hardwicke J, Thomson R, Bamford A, Moiemen N. A pilot evaluation study of high resolution digital thermal imaging in the assessment of burn depth. Burns. 2013;39(1):76-81.
283. Coster A, Klein Baltink H, Zilvold G. Thermographic assessment of healed burn wounds. Rays. 1985;10(3):85-8.
284. Horta R, Nascimento R, Vilas-Boas J, Sousa F, Orvalho V, Silva A, et al. Thermographic analysis of facially burned patients. Burns. 2015.
285. Bhedi A, Saxena AK, Gadani R, Patel R. Digital Photography and Transparency-Based Methods for Measuring Wound Surface Area. The Indian Journal of Surgery. 2013;75(2):111-4.
286. Verhaegen PDHM, Bloemen MCT, Van Der Wal MBA, Vloemans AFPM, Tempelman FRH, Beerthuizen GIJM, et al. Skin stretching for primary closure of acute burn wounds. Burns. 2014;40(8):1727-37.
287. Chang AC, Dearman B, Greenwood JE. A Comparison of Wound Area Measurement Techniques: Visitrak Versus Photography. Eplasty. 2011;11:e18.
288. Cui J, Zhang J, Wang J, Xu M, Pei YH, Wang T, et al. [Effect of topical application with mitomycin C in the management of benign cicatricial airway stenosis]. Chung-Hua Chieh Ho Ho Hu Hsi Tsa Chih Chinese Journal of Tuberculosis & Respiratory Diseases. 2012;35(12):901-6.
289. Sugama J, Matsui Y, Sanada H, Konya C, Okuwa M, Kitagawa A. A study of the efficiency and convenience of an advanced portable Wound Measurement System (VISITRAK). Journal of clinical nursing. 2007;16(7):1265-9.
290. van Zuijlen PP, Angeles AP, Suijker MH, Kreis RW, Middelkoop E. Reliability and accuracy of techniques for surface area measurements of wounds and scars. The international journal of lower extremity wounds. 2004;3(1):7-11.
291. Berman B, Young VL, McAndrews J. Objective Assessment of the Precision, Accuracy, and Reliability of a Measurement Method for Keloid Scar Volume (PARKS Study). Dermatologic surgery : official publication for American Society for Dermatologic Surgery [et al]. 2015.
292. 3dMD static systems [2nd September 2015]. Available from: http://www.3dmd.com/#3dmd-products.
293. Kim JE, Heo YS, Oh TS, Song HJ, Oh CH. The efficacy of cultured autologous fibroblast injection treatment for depressed acne scar and evaluation by stereoimage optical topometer. Journal of Dermatology Conference: 1st Eastern Asia Dermatology Congress, EADC2010 Fukuoka Japan Conference Start. 2010;37(pp 77):77.
294. Stekelenburg CM, van der Wal MB, Knol DL, de Vet HC, van Zuijlen PP. Three-dimensional digital stereophotogrammetry: a reliable and valid technique for measuring scar surface area. Plastic and reconstructive surgery. 2013;132(1):204-11.
295. Lumenta DB, Kitzinger HB, Selig H, Kamolz LP. Objective Quantification of Subjective Parameters in Scars by Use of a Portable Stereophotographic System. Annals of Plastic Surgery. 2011;67(6):641-5.

296. Tanaka Y, Tsunemi Y, Kawashima M, Tatewaki N, Nishida H. Objective assessment of skin tightening in Asians using a water-filtered near-infrared (1,000-1,800 nm) device with contact-cooling and freezer-stored gel. Clinical, cosmetic and investigational dermatology. 2013;6:167-76.
297. Canfield Photography solutions [cited 2015 2nd September]. Available from: http://www.canfieldsci.com/imaging-systems/categories/photography-solutions/.
298. Tanaka Y. Long-term three-dimensional volumetric assessment of skin tightening using a sharply tapered non-insulated microneedle radiofrequency applicator with novel fractionated pulse mode in asians. Lasers in surgery and medicine. 2015;47(8):626-33.
299. Urbanova P, Hejna P, Jurda M. Testing photogrammetry-based techniques for three-dimensional surface documentation in forensic pathology. Forensic science international. 2015;250:77-86.
300. Ardehali B, Nouraei SA, Van Dam H, Dex E, Wood S, Nduka C. Objective assessment of keloid scars with three-dimensional imaging: quantifying response to intralesional steroid therapy. Plastic and reconstructive surgery. 2007;119(2):556-61.
301. Hoeffelin H, Jacquemin D, Defaweux V, Nizet JL. A Methodological Evaluation of Volumetric Measurement Techniques including Three-Dimensional Imaging in Breast Surgery. BioMed Research International. 2014;2014:573249.
302. Gee Kee EL, Kimble RM, Stockton KA. 3D photography is a reliable burn wound area assessment tool compared to digital planimetry in very young children. Burns. 2015.
303. Bowling FL, King L, Fadavi H, Paterson JA, Preece K, Daniel RW, et al. An assessment of the accuracy and usability of a novel optical wound measurement system. Diabetic medicine : a journal of the British Diabetic Association. 2009;26(1):93-6.
304. Bowling FL, King L, Paterson JA, Hu J, Lipsky BA, Matthews DR, et al. Remote assessment of diabetic foot ulcers using a novel wound imaging system. Wound repair and regeneration : official publication of the Wound Healing Society [and] the European Tissue Repair Society. 2011;19(1):25-30.
305. Paterson J. Eykona Medical Imaging FAQ. EYK/AA/021rev02 ed.
306. Lifeviz Mini Technical specifications. Quantificare.
307. Vectra H1 Technical specifications: Canfield Imaging systems Inc. ; [9th December 2015]. Available from: http://www.canfieldsci.com/imaging-systems/vectra-h1-3d-imaging-system/.
308. Raytrix Light field/ Plenoptic 3D cameras [cited 2015 2nd September]. Available from: http://www.raytrix.de/produkte/.
309. Straub J, Kerlin S. Development of a Large, Low-Cost, Instant 3D Scanner. Technologies. 2014;2(2):76.
310. Pilley MJ, Hitchens C, Rose G, Alexander S, Wimpenny DI. The use of non-contact structured light scanning in burns pressure splint construction. Burns. 2011;37(7):1168-73.
311. Kovacs L, Eder M, Hollweck R, Zimmermann A, Settles M, Schneider A, et al. Comparison between breast volume measurement using 3D surface imaging and classical techniques. Breast. 2007;16(2):137-45.
312. Taylor B, McGrouther DA, Bayat A. Use of a non-contact 3D digitiser to measure the volume of keloid scars: a useful tool for scar assessment. Journal of plastic, reconstructive & aesthetic surgery : JPRAS. 2007;60(1):87-94.
313. Powers PS, Sarkar S, Goldgof DB, Cruse CW, Tsap LV. Scar assessment: current problems and future solutions. The Journal of burn care & rehabilitation. 1999;20(1 Pt 1):54-60; discussion 53.
314. Haller HL, Dirnberger J, Giretzlehner M, Rodemund C, Kamolz L. "Understanding burns": Research project BurnCase 3D-Overcome the limits of existing methods in burns documentation. Burns. 2009;35(3):311-7.
315. Thumfart S, Giretzlehner M, Holler J, Ehrenmuller M, Pfurtscheller K, Haller H, et al. Proportionally correct 3D models of infants, children and adolescents for precise burn size measurement. European Burns Association Congress 2015; Hannover, Germany2015.

316. Wurzer P., Giretzlehner M., Klein D. SY, Haller H. L., Branski L. K., Benjamin N., et al. Burncase 3D software validation study: Burn size measurement accuracy, test-retest reliability and inter-rater reliability. European Burns Association Congress 2015; Hannover, Germany: Annals of Burns and Fire Disasters-Supplement EBA; 2015.
317. Tzou CH, Artner NM, Pona I, Hold A, Placheta E, Kropatsch WG, et al. Comparison of three-dimensional surface-imaging systems. Journal of plastic, reconstructive & aesthetic surgery : JPRAS. 2014;67(4):489-97.
318. Cheng W, Saing H, Zhou H, Han Y, Peh W, Tam PK. Ultrasound assessment of scald scars in Asian children receiving pressure garment therapy. Journal of pediatric surgery. 2001;36(3):466-9.
319. Wang ZY, Zhang J, Lu SL. Objective evaluation of burn and post-surgical scars and the accuracy of subjective scar type judgment. Chinese medical journal. 2008;121(24):2517-20.
320. Sawada Y. A method of recording and objective assessment of hypertrophic burn scars. Burns. 1994;20(1):76-8.
321. Hambleton J, Shakespeare PG, Pratt BJ. The progress of hypertrophic scars monitored by ultrasound measurements of thickness. Burns. 1992;18(4):301-7.
322. Lau JC, Li-Tsang CW, Zheng YP. Application of tissue ultrasound palpation system (TUPS) in objective scar evaluation. Burns. 2005;31(4):445-52.
323. Hoi Yan CL. Study of pressure effect on hypertrophic scar tissues: The Hong Kong Polytechnic University; 2010.
324. CM JL. A prospective randomized clinical trial to compare the effectiveness of pressure therapy, silicone gel sheeting and the combined therapy on surgical hypertrophic scar: The Hong Kong Polytechnic University; 2006.
325. Van den Kerckhove E, Colla C, Van Brussel M. Pressure Therapy: Does it work? . Düsseldorf: German Medical Science GMS Publishing House; 2010.
326. Qui L, Jin X, Kingston PA, Luo X, Ding X. [Experimental study on BMSCs transfected by endogene inhibiting hypertrophic scar]. Zhongguo xiu fu chong jian wai ke za zhi = Zhongguo xiufu chongjian waike zazhi = Chinese journal of reparative and reconstructive surgery. 2008;22(2):212-6.
327. Du YC, Lin CM, Chen YF, Chen CL, Chen T. Implementation of a burn scar assessment system by ultrasound techniques. Conference proceedings : Annual International Conference of the IEEE Engineering in Medicine and Biology Society IEEE Engineering in Medicine and Biology Society Annual Conference. 2006;1:2328-31.
328. Danin A, Georgesco G, Le Touze A, Penaud A, Quignon R, Zakine G. Assessment of burned hands reconstructed with Integra (R) by ultrasonography and elastometry. Burns. 2012;38(7):998-1004.
329. Lacarrubba F, Verzi AE, Tedeschi A, Catalfo P, Nasca MR, Micali G. Clinical and ultrasonographic correlation of acne scars. Dermatologic surgery : official publication for American Society for Dermatologic Surgery [et al]. 2013;39(11):1683-8.
330. Li JQ, Li-Tsang CW, Huang YP, Chen Y, Zheng YP. Detection of changes of scar thickness under mechanical loading using ultrasonic measurement. Burns. 2013;39(1):89-97.
331. Zhuang A, Nguyen TA, Naheedy J, Krakowski A. Use of intraoperative highdefinition ultrasound to accurately gauge scar thickness and identify intra-scar anatomy during multimodal revision of a hypertrophic burn scar. Lasers in surgery and medicine. 2015;47:54-5.
332. Katz SM, Frank DH, Leopold GR, Wachtel TL. Objective measurement of hypertrophic burn scar: a preliminary study of tonometry and ultrasonography. Ann Plast Surg. 1985;14(2):121-7.
333. Zmudzinska M, Czarnecka-Operacz M, Silny W. Principles of Dermatologic Ultrasound Diagnostics. Acta Dermatovenerologica Croatica. 2008;16(3):126-9.
334. Wohlrab J, Wohlrab D, Finke R, Fischer M, Marsch WC. Ultrasonographic characterization of burn scars in children. Unfallchirurg. 2000;103(9):754-60.
335. Nedelec B, Shankowsky HA, Tredget EE. Rating the resolving hypertrophic scar: Comparison of the Vancouver Scar Scale and scar volume. Journal of Burn Care and Rehabilitation. 2000;21(3):205-12.

336. Cilip CM, Allaf ME, Fried NM. Application of optical coherence tomography and high-frequency ultrasound imaging during noninvasive laser vasectomy. Journal of biomedical optics. 2012;17(4):046006.
337. Bagatin E, De Vasconcelos Nasser Caetano L, Soares JLM. Ultrasound and dermatology: Basic principles and main applications in dermatologic research. Expert Review of Dermatology. 2013;8(5):463-77.
338. Skin scanner DUB [cited 2015 January]. Available from: http://www.eotech-sa.com/Life-science/Systems/DUBSkin-Scanner/Products/t1/r9/i107.
339. Lau JCM, Li-Tsang CWP, Zheng YP. Application of tissue ultrasound palpation system (TUPS) in objective scar evaluation. Burns. 2005;31(4):445-52.
340. Verhaegen P, van der Wal MBA, Middelkoop E, van Zuijlen PPM. Objective Scar Assessment Tools: A Clinimetric Appraisal. Plastic and reconstructive surgery. 2011;127(4):1561-70.
341. Kautzky F, Dahm MW, Drosner M, Köhler LD, Vogt H-J, Borelli S. Direct profilometry of the skin: its reproducibility and variability. Journal of the European Academy of Dermatology and Venereology. 1995;5(1):15-23.
342. Lagarde JM, Rouvrais C, Black D, Diridollou S, Gall Y. Skin topography measurement by interference fringe projection: a technical validation. Skin research and technology : official journal of International Society for Bioengineering and the Skin (ISBS) [and] International Society for Digital Imaging of Skin (ISDIS) [and] International Society for Skin Imaging (ISSI). 2001;7(2):112-21.
343. Nardin P, Nita D, Mignot J. Automation of a series of cutaneous topography measurements from silicon rubber replicas. Skin research and technology : official journal of International Society for Bioengineering and the Skin (ISBS) [and] International Society for Digital Imaging of Skin (ISDIS) [and] International Society for Skin Imaging (ISSI). 2002;8(2):112-7.
344. Fischer TW, Wigger-Alberti W, Elsner P. Direct and non-direct measurement techniques for analysis of skin surface topography. Skin pharmacology and applied skin physiology. 1999;12(1-2):1-11.
345. De Paepe K, Lagarde JM, Gall Y, Roseeuw D, Rogiers V. Microrelief of the skin using a light transmission method. Archives of dermatological research. 2000;292(10):500-10.
346. Bloemen MC, van Gerven MS, van der Wal MB, Verhaegen PD, Middelkoop E. An objective device for measuring surface roughness of skin and scars. J Am Acad Dermatol. 2011;64(4):706-15.
347. Barolet D, Boucher A. Prophylactic low-level light therapy for the treatment of hypertrophic scars and keloids: a case series. Lasers in surgery and medicine. 2010;42(6):597-601.
348. Kottner J, Schario M, Garcia Bartels N, Pantchechnikova E, Hillmann K, Blume-Peytavi U. Comparison of two in vivo measurements for skin surface topography. Skin research and technology : official journal of International Society for Bioengineering and the Skin (ISBS) [and] International Society for Digital Imaging of Skin (ISDIS) [and] International Society for Skin Imaging (ISSI). 2013;19(2):84-90.
349. Moon J, Yi G, Oh C, Lee M, Lee Y, Kim M. A new technique for three-dimensional measurements of skin surface contours: evaluation of skin surface contours according to the ageing process using a stereo image optical topometer. Physiological measurement. 2002;23(2):247-59.
350. Zhao L, Hung LK, Zhang YT. Electrical properties of normal and scarred skin. In: Chang HK, Zhang YT, editors. Proceedings of the 20th Annual International Conference of the Ieee Engineering in Medicine and Biology Society, Vol 20, Pts 1-6: Biomedical Engineering Towards the Year 2000 and Beyond. Proceedings of Annual International Conference of the Ieee Engineering in Medicine and Biology Society. 201998. p. 2917-20.
351. Moloney EC, Brunner M, Alexander AJ, Clark J. Quantifying fibrosis in head and neck cancer treatment: An overview. Head and Neck-Journal for the Sciences and Specialties of the Head and Neck. 2015;37(8):1225-31.
352. Dematte MF, Gemperli R, Salles AG, Dolhnikoff M, Lancas T, Nascimento Saldiva PH, et al. Mechanical evaluation of the resistance and elastance of post-burn scars after topical treatment with tretinoin. Clinics. 2011;66(11):1949-54.

353. Clark JA, Cheng JC, Leung KS. Mechanical properties of normal skin and hypertrophic scars. Burns. 1996;22(6):443-6.
354. Gunner CW, Hutton WC, Burlin TE. The mechanical properties of skin in vivo--a portable hand-held extensometer. Br J Dermatol. 1979;100(2):161-3.
355. Lim KH, Chew CM, Chen PC, Jeyapalina S, Ho HN, Rappel JK, et al. New extensometer to measure in vivo uniaxial mechanical properties of human skin. Journal of biomechanics. 2008;41(5):931-6.
356. Thacker JG, lachetta FA, Allaire PE. In vivo extensometer for measurement of the biomechanical properties of human skin. The Review of scientific instruments. 1977;48(2):181-5.
357. Clark JA, Cheng JC, Leung KS, Leung PC. Mechanical characterisation of human postburn hypertrophic skin during pressure therapy. Journal of biomechanics. 1987;20(4):397-406.
358. Chu BM, Brody G. Nondestructive measurements of the properties of healing burn scars. Medical instrumentation. 1975;9(3):139-42.
359. Bartell TH, Monafo WW, Mustoe TA. A new instrument for serial measurements of elasticity in hypertrophic scar. The Journal of burn care & rehabilitation. 1988;9(6):657-60.
360. Rennekampff HO, Rabbels J, Reinhard V, Becker ST, Schaller HE. Comparing the Vancouver Scar Scale with the cutometer in the assessment of donor site wounds treated with various dressings in a randomized trial. Journal of burn care & research : official publication of the American Burn Association. 2006;27(3):345-51.
361. Klosova H, Stetinsky J, Bryjova I, Hledik S, Klein L. Objective evaluation of the effect of autologous platelet concentrate on post-operative scarring in deep burns. Burns. 2013;39(6):1263-76.
362. Nguyen DQ, Potokar T, Price P. A review of current objective and subjective scar assessment tools. Journal of wound care. 2008;17(3):101-2, 4-6.
363. Rahmanian-Schwarz A, Beiderwieden A, Willkomm LM, Amr A, Schaller HE, Lotter O. A clinical evaluation of Biobrane((R)) and Suprathel((R)) in acute burns and reconstructive surgery. Burns. 2011;37(8):1343-8.
364. Draaijers LJ, Botman YAM, Tempelman FRH, Kreis RW, Middelkoop E, van Zuijlen PPM. Skin elasticity meter or subjective evaluation in scars: a reliability assessment. Burns. 2004;30(2):109-14.
365. Selig HF, Keck M, Lumenta DB, Mittlbock M, Kamolz LP. The use of a polylactide-based copolymer as a temporary skin substitute in deep dermal burns: 1-year follow-up results of a prospective clinical noninferiority trial. Wound repair and regeneration : official publication of the Wound Healing Society [and] the European Tissue Repair Society. 2013;21(3):402-9.
366. Sin P, Stupka I, Brychta P. Evaluation and comparison of composite and split-thickness skin grafts using cutometer mpa 580. Annals of burns and fire disasters. 2010;23(4):208-13.
367. Van Zuijlen PPM, Vloemans JFPM, Van Trier AJM, Suijker MH, Van Unen E, Groenevelt F, et al. Dermal substitution in acute burns and reconstructive surgery: A subjective and objective long-term follow-up. Plastic and reconstructive surgery. 2001;108(7):1938-46.
368. Fournier R, Pierard GE. Skin tensile strength modulation by compressive garments in burn patients. A pilot study. Journal of medical engineering & technology. 2000;24(6):277-80.
369. Krusche T, Worret WI. Mechanical properties of keloids in vivo during treatment with intralesional triamcinolone acetonide. Archives of Dermatological Research. 1995;287(3-4):289-93.
370. Matsuzaki K, Kumagai N, Fukushi S, Ohshima H, Tanabe M, Ishida H. Cultured epithelial autografting on meshed skin graft scars: evaluation of skin elasticity. The Journal of burn care & rehabilitation. 1995;16(5):496-502.
371. Nguyen NT, Roberge D, Freeman CR, Wong C, Hines J, Turcotte RE. Skin Elasticity as a Measure of Radiation Fibrosis: Is it Reproducible and Does it Correlate with Patient and Physician-reported Measures? Technology in cancer research & treatment. 2013.
372. Rennekampff HO, Rabbels J, Pfau M, Schaller HE. [Evaluating scar development with objective computer-assisted viscoelastic measurement]. Kongressband / Deutsche Gesellschaft fur Chirurgie Deutsche Gesellschaft fur Chirurgie Kongress. 2002;119:749-55.

373. Dobrev H. Application of Cutometer area parameters for the study of human skin fatigue. Skin research and technology : official journal of International Society for Bioengineering and the Skin (ISBS) [and] International Society for Digital Imaging of Skin (ISDIS) [and] International Society for Skin Imaging (ISSI). 2005;11(2):120-2.
374. Anthonissen M, Daly D, Fieuws S, Massage P, Van Brussel M, Vranckx J, et al. Measurement of elasticity and transepidermal water loss rate of burn scars with the Dermalab((R)). Burns. 2013;39(3):420-8.
375. Spann K, Mileski WJ, Atiles L, Purdue G, Hunt J. The 1996 Clinical Research award. Use of a pneumatonometer in burn scar assessment. The Journal of burn care & rehabilitation. 1996;17(6 Pt 1):515-7.
376. Lye I, Edgar DW, Wood FM, Carroll S. Tissue tonometry is a simple, objective measure for pliability of burn scar: is it reliable? Journal of burn care & research : official publication of the American Burn Association. 2006;27(1):82-5.
377. Merkel PA, Silliman NP, Denton CP, Furst DE, Khanna D, Emery P, et al. Validity, reliability, and feasibility of durometer measurements of scleroderma skin disease in a multicenter treatment trial. Arthritis and rheumatism. 2008;59(5):699-705.
378. Esposito G, Ziccardi P, Di Caprio G, Scioli M. Objective measurement of hypertrophic scars. [Italian]. Giornale di Chirurgia Plastica Ricostruttiva ed Estetica. 1990;5(1):21-9.
379. Wernicke AG, Greenwood EA, Coplowitz S, Parashar B, Kulidzhanov F, Christos PJ, et al. Tissue compliance meter is a more reproducible method of measuring radiation-induced fibrosis than late effects of normal tissue-subjective objective management analytical in patients treated with intracavitary brachytherapy accelerated partial breast irradiation: results of a prospective trial. The breast journal. 2013;19(3):250-8.
380. Corica GF, Wigger NC, Edgar DW, Wood FM, Carroll S. Objective measurement of scarring by multiple assessors: is the tissue tonometer a reliable option? Journal of burn care & research : official publication of the American Burn Association. 2006;27(4):520-3.
381. McHugh AA, Fowlkes BJ, Maevsky EI, Smith DJ, Jr., Rodriguez JL, Garner WL. Biomechanical alterations in normal skin and hypertrophic scar after thermal injury. The Journal of burn care & rehabilitation. 1997;18(2):104-8.
382. Popovic G, Sarvazyan A, Ponomarjev V, Vucelic D. Method and device for noninvasive acoustic testing of elasticity of soft biological tissues. Google Patents; 1992.
383. Verhaegen PD, Res EM, van Engelen A, Middelkoop E, van Zuijlen PP. A reliable, non-invasive measurement tool for anisotropy in normal skin and scar tissue. Skin research and technology : official journal of International Society for Bioengineering and the Skin (ISBS) [and] International Society for Digital Imaging of Skin (ISDIS) [and] International Society for Skin Imaging (ISSI). 2010;16(3):325-31.
384. Ferriero G, Vercelli S, Salgovic L, Stissi V, Sartorio F. Validation of a new device to measure postsurgical scar adherence. Physical therapy. 2010;90(5):776-83.
385. Tsap LV, Goldgof DB, Sarkar S, Powers PS. A vision-based technique for objective assessment of burn scars. IEEE transactions on medical imaging. 1998;17(4):620-33.
386. Zhang Y, Goldgof DB, Sarkar S, Tsap LV. A modeling approach for burn scar assessment using natural features and elastic property. IEEE transactions on medical imaging. 2004;23(10):1325-9.
387. Larrabee WF, Jr. A finite element model of skin deformation. I. Biomechanics of skin and soft tissue: a review. The Laryngoscope. 1986;96(4):399-405.
388. Zhang Y, Goldgof DB, Sarkar S, Tsap LV. Model-based nonrigid motion analysis using natural feature adaptive mesh. In: Sanfeliu A, Villanueva JJ, Vanrell M, Alquezar R, Huang T, Serra J, editors. 15th International Conference on Pattern Recognition, Vol 3, Proceedings: Image, Speech and Signal Processing. International Conference on Pattern Recognition2000. p. 831-5.
389. Palmieri TL, Petuskey K, Bagley A, Takashiba S, Greenhalgh DG, Rab GT. Alterations in functional movement after axillary burn scar contracture: a motion analysis study. The Journal of burn care & rehabilitation. 2003;24(2):104-8.

390. Parry I, Walker K, Niszczak J, Palmieri T, Greenhalgh D. Methods and tools used for the measurement of burn scar contracture. Journal of burn care & research : official publication of the American Burn Association. 2010;31(6):888-903.
391. Rab G, Petuskey K, Bagley A. A method for determination of upper extremity kinematics. Gait & posture. 2002;15(2):113-9.
392. van der Helm FC, Pronk GM. Three-dimensional recording and description of motions of the shoulder mechanism. Journal of biomechanical engineering. 1995;117(1):27-40.
393. Koller R, Kargul G, Giovanoli P, Meissl G, Frey M. Quantification of functional results after facial burns by the faciometer. Burns : journal of the International Society for Burn Injuries. 2000;26(8):716-23.
394. Draaijers LJ, Botman YA, Tempelman FR, Kreis RW, Middelkoop E, van Zuijlen PP. Skin elasticity meter or subjective evaluation in scars: a reliability assessment. Burns. 2004;30(2):109-14.
395. Niyaz A, Matsumura H, Watanabe K, Hamamoto T, Matsusawa T. Quantification of the physical properties of keloid and hypertrophic scars using the Vesmeter novel sensing device. International wound journal. 2012;9(6):643-9.
396. Berry RB, Tan OT, Cooke ED, Gaylarde PM, Bowcock SA, Lamberty BG, et al. Transcutaneous oxygen tension as an index of maturity in hypertrophic scars treated by compression. British journal of plastic surgery. 1985;38(2):163-73.
397. Ichioka S, Ando T, Shibata M, Sekiya N, Nakatsuka T. Oxygen consumption of keloids and hypertrophic scars. Ann Plast Surg. 2008;60(2):194-7.
398. Rodrigues LM, Roberto MA. Characterization strategies for the functional assessment of the cutaneous lesion. Burns. 2006;32(7):797-801.
399. Fluhr JW, Feingold KR, Elias PM. Transepidermal water loss reflects permeability barrier status: validation in human and rodent in vivo and ex vivo models. Exp Dermatol. 2006;15(7):483-92.
400. Rosado C, Pinto P, Rodrigues LM. Comparative assessment of the performance of two generations of Tewameter: TM210 and TM300. International journal of cosmetic science. 2005;27(4):237-41.
401. De Paepe K, Houben E, Adam R, Wiesemann F, Rogiers V. Validation of the VapoMeter, a closed unventilated chamber system to assess transepidermal water loss vs. the open chamber Tewameter. Skin research and technology : official journal of International Society for Bioengineering and the Skin (ISBS) [and] International Society for Digital Imaging of Skin (ISDIS) [and] International Society for Skin Imaging (ISSI). 2005;11(1):61-9.
402. Clarys P, Clijsen R, Taeymans J, Barel AO. Hydration measurements of the stratum corneum: comparison between the capacitance method (digital version of the Corneometer CM 825(R)) and the impedance method (Skicon-200EX(R)). Skin research and technology : official journal of International Society for Bioengineering and the Skin (ISBS) [and] International Society for Digital Imaging of Skin (ISDIS) [and] International Society for Skin Imaging (ISSI). 2012;18(3):316-23.
403. O'Goshi K, Serup J. Skin conductance; validation of Skicon-200EX compared to the original model, Skicon-100. Skin research and technology : official journal of International Society for Bioengineering and the Skin (ISBS) [and] International Society for Digital Imaging of Skin (ISDIS) [and] International Society for Skin Imaging (ISSI). 2007;13(1):13-8.
404. Magnusson M, Papini RP, Rea SM, Reed CC, Wood FM. Cultured autologous keratinocytes in suspension accelerate epithelial maturation in an in vivo wound model as measured by surface electrical capacitance. Plastic and reconstructive surgery. 2007;119(2):495-9.
405. Anthonissen M, Daly D, Peeters R, Van Brussel M, Fieuws S, Moortgat P, et al. Reliability of Repeated Measurements on Post-Burn Scars with Corneometer CM 825. Skin research and technology : official journal of International Society for Bioengineering and the Skin (ISBS) [and] International Society for Digital Imaging of Skin (ISDIS) [and] International Society for Skin Imaging (ISSI). 2014.

406. Nuutinen. J. Skin dielectric constant at high radiofrequency with special emphasis on radiation-induced late skin reaction [Ph.D. thesis]. Kuopio University Publications C. Natural and Environmental Sciences 55, Kuopio, Finland; 1997.
407. Lahtinen T, Nuutinen J, Alanen E, Turunen M, Nuortio L, Usenius T, et al. Quantitative assessment of protein content in irradiated human skin. International journal of radiation oncology, biology, physics. 1999;43(3):635-8.
408. Suetake T, Sasai S, Zhen YX, Ohi T, Tagami H. Functional analyses of the stratum corneum in scars. Sequential studies after injury and comparison among keloids, hypertrophic scars, and atrophic scars. Arch Dermatol. 1996;132(12):1453-8.
409. Ghassemi P, Travis TE, Moffatt LT, Shupp JW, Ramella-Roman JC. A polarized multispectral imaging system for quantitative assessment of hypertrophic scars. Biomedical optics express. 2014;5(10):3337-54.
410. Ghassemi P, Shupp JW, Moffatt LT, Ramella-Roman JC. A Novel Spectral Imaging System for Quantitative Analysis of Hypertrophic Scar. In: Kollias N, Choi B, Zeng H, Kang HW, Knudsen BE, Wong BJF, et al., editors. Photonic Therapeutics and Diagnostics Ix. Proceedings of SPIE. 85652013.
411. Drexler W, Fujimoto JG. State-of-the-art retinal optical coherence tomography. Progress in retinal and eye research. 2008;27(1):45-88.
412. Alex A, Povazay B, Hofer B, Popov S, Glittenberg C, Binder S, et al. Multispectral in vivo three-dimensional optical coherence tomography of human skin. Journal of biomedical optics. 2010;15(2):026025.
413. Welzel J. Optical coherence tomography in dermatology: a review. Skin research and technology : official journal of International Society for Bioengineering and the Skin (ISBS) [and] International Society for Digital Imaging of Skin (ISDIS) [and] International Society for Skin Imaging (ISSI). 2001;7(1):1-9.
414. Gambichler T, Moussa G, Sand M, Sand D, Altmeyer P, Hoffmann K. Applications of optical coherence tomography in dermatology. J Dermatol Sci. 2005;40(2):85-94.
415. Welzel J, Lankenau E, Birngruber R, Engelhardt R. Optical coherence tomography of the human skin. J Am Acad Dermatol. 1997;37(6):958-63.
416. Steiner R, Kunzi-Rapp K, Scharffetter-Kochanek K. Optical Coherence Tomography: Clinical Applications in Dermatology. Medical Laser Application. 2003;18(3):249-59.
417. Liew YM, McLaughlin RA, Gong P, Wood FM, Sampson DD. In vivo assessment of human burn scars through automated quantification of vascularity using optical coherence tomography. Journal of biomedical optics. 2013;18(6):061213.
418. Gong P, Chin L, Es'haghian S, Liew YM, Wood FM, Sampson DD, et al. Imaging of skin birefringence for human scar assessment using polarization-sensitive optical coherence tomography aided by vascular masking. Journal of biomedical optics. 2014;19(12):126014.
419. Gong P, McLaughlin RA, Liew YM, Munro PR, Wood FM, Sampson DD. Assessment of human burn scars with optical coherence tomography by imaging the attenuation coefficient of tissue after vascular masking. Journal of biomedical optics. 2014;19(2):21111.
420. Babalola O, Mamalis A, Lev-Tov H, Jagdeo J. Optical coherence tomography (OCT) of collagen in normal skin and skin fibrosis. Archives of dermatological research. 2014;306(1):1-9.
421. Choi WJ, Reif R, Yousefi S, Wang RK. Improved microcirculation imaging of human skin in vivo using optical microangiography with a correlation mapping mask. Journal of biomedical optics. 2014;19(3):36010.
422. Wang XQ, Mill J, Kravchuk O, Kimble RM. Ultrasound assessed thickness of burn scars in association with laser Doppler imaging determined depth of burns in paediatric patients. Burns. 2010;36(8):1254-62.
423. Lo WC, Villiger M, Golberg A, Broelsch GF, Khan S, Lian CG, et al. Longitudinal, 3D In Vivo Imaging of Collagen Remodeling in Murine Hypertrophic Scars using Polarization-sensitive Optical Frequency Domain Imaging. J Invest Dermatol. 2015.

424. Eraud J, Gonnelli D, Carmassi M, Bruzzese L, Andrac-Meyer L, Casanova D, et al. [Differential diagnosis between keloid and hypertrophic scars: a new approach by full-field optical coherence tomography]. Annales de chirurgie plastique et esthetique. 2014;59(4):253-60.
425. Moshref SS, Mufti ST. Keloid and hypertrophic scars: comparative histopathological and immunohistochemical study. Med Sci. 2010;17:3–22.
426. Chen G, Chen J, Zhuo S, Xiong S, Zeng H, Jiang X, et al. Nonlinear spectral imaging of human hypertrophic scar based on two-photon excited fluorescence and second-harmonic generation. Br J Dermatol. 2009;161(1):48-55.
427. Chen J, Zhuo S, Jiang X, Zhu X, Zheng L, Xie S, et al. Multiphoton microscopy study of the morphological and quantity changes of collagen and elastic fiber components in keloid disease. Journal of biomedical optics. 2011;16(5):051305.
428. Brewer MB, Yeh A, Torkian B, Sun CH, Tromberg BJ, Wong BJ. Multiphoton imaging of excised normal skin and keloid scar: preliminary investigations. In: Bartels KE, Bass LS, DeRiese WTW, Gregory KW, Hirschberg H, Katzir A, et al., editors. Lasers in Surgery: Advanced Characterization, Therapeutics, and Systems Xiv. Proceedings of the Society of Photo-Optical Instrumentation Engineers (Spie). 53122004. p. 204-8.
429. Chen A, Liu PY, McNeilly C, Cuttle L, Kempf M, Kendall M, et al. Collagen deposition assessment in burn scar tissue using second harmonic generation and multi-photon microscopy. Journal of Investigative Dermatology. 2010;130:S16-S.
430. Stoller P, Celliers PM, Reiser KM, Rubenchik AM. Imaging collagen orientation using polarization-modulated second harmonic generation. In: Periasamy A, So PTC, editors. Multiphoton Microscopy in the Biomedical Sciences Ii. Proceedings of the Society of Photo-Optical Instrumentation Engineers (Spie). 46202002. p. 157-65.
431. Kelf TA, Gosnell M, Sandnes B, Guller AE, Shekhter AB, Zvyagin AV. Scar tissue classification using nonlinear optical microscopy and discriminant analysis. Journal of biophotonics. 2012;5(2):159-67.
432. Da Costa V, Wei R, Lim R, Sun CH, Brown JJ, Wong BJ. Nondestructive imaging of live human keloid and facial tissue using multiphoton microscopy. Arch Facial Plast Surg. 2008;10(1):38-43.
433. Zhu XQ, Zhuo SM, Zheng LQ, Lu KC, Jiang XS, Chen JX, et al. Quantified characterization of human cutaneous normal scar using multiphoton microscopy. Journal of Biophotonics. 2010;3(1-2):108-16.
434. de Vries HJ, Enomoto DN, van Marle J, van Zuijlen PP, Mekkes JR, Bos JD. Dermal organization in scleroderma: the fast Fourier transform and the laser scatter method objectify fibrosis in nonlesional as well as lesional skin. Laboratory investigation; a journal of technical methods and pathology. 2000;80(8):1281-9.
435. Konig K, Riemann I. High-resolution multiphoton tomography of human skin with subcellular spatial resolution and picosecond time resolution. Journal of biomedical optics. 2003;8(3):432-9.
436. Chen ACH, McNeilly C, Liu APY, Flaim CJ, Cuttle L, Kendall M, et al. Second harmonic generation and multiphoton microscopic detection of collagen without the need for species specific antibodies. Burns : journal of the International Society for Burn Injuries. 2011;37(6):1001-9.
437. Jiang Y, Tong Y, Xiao T, Lu S. Phase-contrast microtomography with synchrotron radiation technology: a new noninvasive technique to analyze the three-dimensional structure of dermal tissues. Dermatology (Basel, Switzerland). 2012;225(1):75-80.
438. Theer P, Hasan MT, Denk W. Two-photon imaging to a depth of 1000 microm in living brains by use of a Ti:Al2O3 regenerative amplifier. Optics letters. 2003;28(12):1022-4.
439. Tseng SH, Hsu CK, Yu-Yun Lee J, Tzeng SY, Chen WR, Liaw YK. Noninvasive evaluation of collagen and hemoglobin contents and scattering property of in vivo keloid scars and normal skin using diffuse reflectance spectroscopy: pilot study. Journal of biomedical optics. 2012;17(7):077005.
440. Rajadhyaksha M, Gonzalez S, Zavislan JM, Anderson RR, Webb RH. In vivo confocal scanning laser microscopy of human skin II: advances in instrumentation and comparison with histology. J Invest Dermatol. 1999;113(3):293-303.

441. Rolfe H, Wurm E, Gilmore S. An investigation of striae distensae using reflectance confocal microscopy. The Australasian journal of dermatology. 2012;53(3):181-5.
442. Nehal KS, Gareau D, Rajadhyaksha M. Skin imaging with reflectance confocal microscopy. Seminars in cutaneous medicine and surgery. 2008;27(1):37-43.
443. Chang SK, Mirabal YN, Atkinson EN, Cox D, Malpica A, Follen M, et al. Combined reflectance and fluorescence spectroscopy for in vivo detection of cervical pre-cancer. Journal of biomedical optics. 2005;10(2):024031.
444. Gisquet H, Liu H, Blondel WC, Leroux A, Latarche C, Merlin JL, et al. Intradermal tacrolimus prevent scar hypertrophy in a rabbit ear model: a clinical, histological and spectroscopical analysis. Skin research and technology : official journal of International Society for Bioengineering and the Skin (ISBS) [and] International Society for Digital Imaging of Skin (ISDIS) [and] International Society for Skin Imaging (ISSI). 2011;17(2):160-6.
445. Liu HH, Gisquet H, Guillemin F, Blondel W. Bimodal spectroscopy for in vivo characterization of hypertrophic skin tissue: pre-clinical experimentation, spectral data selection and classification. In: Ramanujam N, Popp J, editors. Clinical and Biomedical Spectroscopy and Imaging Ii. Proceedings of SPIE. 80872011.
446. Hsu CK, Tzeng SY, Yang CC, Lee JY, Huang LL, Chen WR, et al. Non-invasive evaluation of therapeutic response in keloid scar using diffuse reflectance spectroscopy. Biomedical optics express. 2015;6(2):390-404.
447. Bessonart MN, Macedo N, Carmona C. High resolution B-scan ultrasound of hypertrophic scars. Skin research and technology : official journal of International Society for Bioengineering and the Skin (ISBS) [and] International Society for Digital Imaging of Skin (ISDIS) [and] International Society for Skin Imaging (ISSI). 2005;11(3):185-8.
448. Gangemi EN, Carnino R, Stella M. Videocapillaroscopy in postburn scars: in vivo analysis of the microcirculation. Burns. 2010;36(6):799-805.
449. Campanati A, Savelli A, Sandroni L, Marconi B, Giuliano A, Giuliodori K, et al. Effect of allium cepa-allantoin-pentaglycan gel on skin hypertrophic scars: clinical and video-capillaroscopic results of an open-label, controlled, nonrandomized clinical trial. Dermatologic surgery : official publication for American Society for Dermatologic Surgery [et al]. 2010;36(9):1439-44.
450. Pasqui AL, Pastorelli M, Puccetti L, Beerman U, Biagi F, Camarri A, et al. Microvascular assessment in Behcet disease: videocapillaroscopic study. International journal of tissue reactions. 2003;25(3):105-15.
451. Hern S, Mortimer PS. In vivo quantification of microvessels in clinically uninvolved psoriatic skin and in normal skin. Br J Dermatol. 2007;156(6):1224-9.
452. Lamah M, Chaudhry H, Mortimer PS, Dormandy JA. Repeatability of intravital capillaroscopic measurement of capillary density. International journal of microcirculation, clinical and experimental / sponsored by the European Society for Microcirculation. 1996;16(1):23-9.
453. Yoo MG, Kim IH. Keloids and Hypertrophic Scars: Characteristic Vascular Structures Visualized by Using Dermoscopy. Annals of Dermatology. 2014;26(5):603-9.
454. Malenfant A, Forget R, Papillon J, Amsel R, Frigon JY, Choiniere M. Prevalence and characteristics of chronic sensory problems in burn patients. Pain. 1996;67(2-3):493-500.
455. Brown JE, Chatterjee N, Younger J, Mackey S. Towards a physiology-based measure of pain: patterns of human brain activity distinguish painful from non-painful thermal stimulation. PloS one. 2011;6(9):e24124.
456. Meirte J, Moortgat P, Truijen S, Maertens K, Lafaire C, De Cuyper L, et al. Interrater and intrarater reliability of the Semmes Weinstein aesthesiometer to assess touch pressure threshold in burn scars. Burns. 2015;41(6):1261-7.
457. Tena B. Evaluación y prevención de la cronificación del dolor postoperatorio tras toracotomía: Universitat de Barcelona; 2014.
458. Tena B, Escobar B, Arguis MJ, Cantero C, Rios J, Gomar C. Reproducibility of Electronic Von Frey and Von Frey monofilaments testing. The Clinical journal of pain. 2012;28(4):318-23.

459. Perry DM, McGrouther DA, Bayat A. Current tools for noninvasive objective assessment of skin scars. Plastic and reconstructive surgery. 2010;126(3):912-23.
460. Brandt MG, Moore CC, Micomonaco D, Fung K, Franklin JH, Yoo J, et al. A Prospective Randomized Evaluation of Scar Assessment Measures. The Laryngoscope. 2009;119(5):841-5.
461. Gankande U, Duke J, Wood F, Danielsen PL, Wallace H. Evidence based recommedations for burn scar assessment. Wound Repair and Regeneration. 2015;23(4):A8-A9.
462. Singer AJ, Thode HC, Jr., McClain SA. Development of a histomorphologic scale to quantify cutaneous scars after burns. Academic emergency medicine : official journal of the Society for Academic Emergency Medicine. 2000;7(10):1083-8.
463. Beausang E, Floyd H, Dunn KW, Orton CI, Ferguson MWJ. A new quantitative scale for clinical scar assessment. Plastic and reconstructive surgery. 1998;102(6):1954-61.
464. de Rigal J, Abella ML, Giron F, Caisey L, Lefebvre MA. Development and validation of a new Skin Color Chart. Skin research and technology : official journal of International Society for Bioengineering and the Skin (ISBS) [and] International Society for Digital Imaging of Skin (ISDIS) [and] International Society for Skin Imaging (ISSI). 2007;13(1):101-9.
465. Bloemen MC, van Leeuwen MC, van Vucht NE, van Zuijlen PP, Middelkoop E. Dermal substitution in acute burns and reconstructive surgery: a 12-year follow-up. Plastic and reconstructive surgery. 2010;125(5):1450-9.
466. Blome-Eberwein SA, Roarabaugh C, Gogal C, Eid S. Exploration of nonsurgical scar modification options: can the irregular surface of matured mesh graft scars be smoothed with microdermabrasion? Journal of burn care & research : official publication of the American Burn Association. 2012;33(3):e133-40.
467. Atiyeh BS, Gunn SW, Hayek SN. State of the art in burn treatment. World Journal of Surgery. 2005;29(2):131-48.
468. Hoeksema H, Van de Sijpe K, Tondu T, Hamdi M, Van Landuyt K, Blondeel P, et al. Accuracy of early burn depth assessment by laser Doppler imaging on different days post burn. Burns. 2009;35(1):36-45.
469. Miller RH, Sim I. Physicians' use of electronic medical records: barriers and solutions. Health affairs (Project Hope). 2004;23(2):116-26.
470. Tyack Z, Wasiak J, Spinks A, Kimble R, Simons M. A guide to choosing a burn scar rating scale for clinical or research use. Burns.39(7):1341-50.
471. Fearmonti R, Bond J, Erdmann D, Levinson H. A Review of Scar Scales and Scar Measuring Devices. Eplasty. 2010;10:e43.
472. Parnell LK, Nedelec B, Rachelska G, LaSalle L. Assessment of pruritus characteristics and impact on burn survivors. Journal of burn care & research : official publication of the American Burn Association. 2012;33(3):407-18.
473. Shahid F, Ismail M, Khan S. Assessment of quality of life in post burn survivors: A cross-sectional single-center first validation study from Pakistan. Burns Open. 2018;2(1):35-42.
474. Lee KC, Dretzke J, Grover L, Logan A, Moiemen N. A systematic review of objective burn scar measurements. Burns Trauma. 2016;4:14.
475. Tan A, Pedrini FA, Oni G, Frew Q, Philp B, Barnes D, et al. Spectrophotometric intracutaneous analysis for the assessment of burn wounds: A service evaluation of its clinical application in 50 burn wounds. Burns. 2017;43(3):549-54.
476. Wang M, Xiao K, Luo MR, Pointer M, Cheung V, Wuerger S. An investigation into the variability of skin colour measurements. Color Research & Application. 2018;43(4):458-70.
477. Ehrlich HP, Desmouliere A, Diegelmann RF, Cohen IK, Compton CC, Garner WL. Morphological and immunochemical differences between keloid and hypertrophic scar. Am J Pathol. 1994;145.
478. van der Wal MB, Tuinebreijer WE, Bloemen MC, Verhaegen PD, Middelkoop E, van Zuijlen PP. Rasch analysis of the Patient and Observer Scar Assessment Scale (POSAS) in burn scars. Quality

of life research : an international journal of quality of life aspects of treatment, care and rehabilitation. 2012;21(1):13-23.
479. Fitzpatrick TB. The validity and practicality of sun-reactive skin types I through VI. Arch Dermatol. 1988;124(6):869-71.
480. Smalls LK, Randall Wickett R, Visscher MO. Effect of dermal thickness, tissue composition, and body site on skin biomechanical properties. Skin research and technology : official journal of International Society for Bioengineering and the Skin (ISBS) [and] International Society for Digital Imaging of Skin (ISDIS) [and] International Society for Skin Imaging (ISSI). 2006;12(1):43-9.
481. Pierard GE, Nikkels-Tassoudji N, Pierard-Franchimont C. Influence of the test area on the mechanical properties of skin. Dermatology (Basel, Switzerland). 1995;191(1):9-15.
482. Roten SV, Bhat S, Bhawan J. Elastic fibers in scar tissue. Journal of cutaneous pathology. 1996;23(1):37-42.
483. Billings PC, Sanzari JK, Kennedy AR, Cengel KA, Seykora JT. Comparative analysis of colorimetric staining in skin using open-source software. Experimental dermatology. 2015;24(2):157-9.
484. Shoukri MM, Asyali MH, Donner A. Sample size requirements for the design of reliability study: review and new results. Statistical Methods in Medical Research. 2004;13(4):251-71.
485. Shrout PE, Fleiss JL. Intraclass correlations: uses in assessing rater reliability. Psychological bulletin. 1979;86(2):420-8.
486. Nichols D. STATS FLEISS KAPPA 4ed. SPSS, IBMJuly 24, 2015.
487. Streiner DL, GR N. Health measurement scales: a practical guide to their development and use. . Oxford, NY: Oxford University Press; 2003.
488. McHugh ML. Interrater reliability: the kappa statistic. Biochemia Medica. 2012;22(3):276-82.
489. Holavanahalli RK, Helm PA, Kowalske KJ. Long-term outcomes in patients surviving large burns: the skin. Journal of burn care & research : official publication of the American Burn Association. 2010;31(4):631-9.
490. Xie B, Xiao SC, Zhu SH, Xia ZF. Evaluation of long term health-related quality of life in extensive burns: a 12-year experience in a burn center. Burns. 2012;38(3):348-55.
491. Jaspers MEH, Stekelenburg CM, Simons JM, Brouwer KM, Vlig M, van den Kerckhove E, et al. Assessing blood flow, microvasculature, erythema and redness in hypertrophic scars: A cross sectional study showing different features that require precise definitions. Burns. 2017;43(5):1044-50.
492. Bond JS, Duncan JA, Mason T, Sattar A, Boanas A, O'Kane S, et al. Scar redness in humans: how long does it persist after incisional and excisional wounding? Plastic and reconstructive surgery. 2008;121(2):487-96.
493. Dai NT, Chang HI, Wang YW, Fu KY, Huang TC, Huang NC, et al. Restoration of skin pigmentation after deep partial or full-thickness burn injury. Advanced drug delivery reviews. 2018;123:155-64.
494. Agabalyan NA, Su S, Sinha S, Gabriel V. Comparison between high-frequency ultrasonography and histological assessment reveals weak correlation for measurements of scar tissue thickness. Burns. 2017;43(3):531-8.
495. Olsen LO, Takiwaki H, Serup J. High-frequency ultrasound characterization of normal skin. Skin thickness and echographic density of 22 anatomical sites. Skin Research and Technology. 1995;1(2):74-80.
496. Herbig LE, Kohler L, Eule JC. High resolution imaging of the equine cornea using the DUB(R)-SkinScanner v3.9. Tierarztliche Praxis Ausgabe G, Grosstiere/Nutztiere. 2016;44(6):360-7.
497. Järvinen TAH, Prince S. Decorin: A Growth Factor Antagonist for Tumor Growth Inhibition. BioMed Research International. 2015;2015:654765.
498. Zhang Z, Li XJ, Liu Y, Zhang X, Li YY, Xu WS. Recombinant human decorin inhibits cell proliferation and downregulates TGF-beta1 production in hypertrophic scar fibroblasts. Burns. 2007;33(5):634-41.

499. Wu H, Wang S, Xue A, Liu Y, Liu Y, Wang H, et al. Overexpression of decorin induces apoptosis and cell growth arrest in cultured rat mesangial cells in vitro. Nephrology (Carlton, Vic). 2008;13(7):607-15.
500. Honardoust D, Ding J, Varkey M, Shankowsky HA, Tredget EE. Deep dermal fibroblasts refractory to migration and decorin-induced apoptosis contribute to hypertrophic scarring. Journal of burn care & research : official publication of the American Burn Association. 2012;33(5):668-77.
501. Seidler DG, Goldoni S, Agnew C, Cardi C, Thakur ML, Owens RT, et al. Decorin protein core inhibits in vivo cancer growth and metabolism by hindering epidermal growth factor receptor function and triggering apoptosis via caspase-3 activation. J Biol Chem. 2006;281(36):26408-18.
502. Nash MA, Loercher AE, Freedman RS. In vitro growth inhibition of ovarian cancer cells by decorin: synergism of action between decorin and carboplatin. Cancer Res. 1999;59(24):6192-6.
503. Vigneswara V, Berry M, Logan A, Ahmed Z. Caspase-2 is upregulated after sciatic nerve transection and its inhibition protects dorsal root ganglion neurons from apoptosis after serum withdrawal. PloS one. 2013;8(2):e57861.
504. Kishioka Y, Thomas M, Wakamatsu J, Hattori A, Sharma M, Kambadur R, et al. Decorin enhances the proliferation and differentiation of myogenic cells through suppressing myostatin activity. J Cell Physiol. 2008;215(3):856-67.
505. Kishioka Y, Thomas M, Wakamatsu J-i, Hattori A, Sharma M, Kambadur R, et al. Decorin enhances the proliferation and differentiation of myogenic cells through suppressing myostatin activity. Journal of Cellular Physiology. 2008;215(3):856-67.
506. Mietz H, Chevez-Barrios P, Lieberman MW, Wendt M, Gross R, Basinger SF. Decorin and suramin inhibit ocular fibroblast collagen production. Graefe's archive for clinical and experimental ophthalmology = Albrecht von Graefes Archiv fur klinische und experimentelle Ophthalmologie. 1997;235(6):399-403.
507. Nakatani T, Honda E, Hayakawa S, Sato M, Satoh K, Kudo M, et al. Effects of decorin on the expression of alpha-smooth muscle actin in a human myofibroblast cell line. Molecular and cellular biochemistry. 2008;308(1-2):201-7.
508. Border WA, Noble NA, Yamamoto T, Harper JR, Yamaguchi Y, Pierschbacher MD, et al. Natural inhibitor of transforming growth factor-beta protects against scarring in experimental kidney disease. Nature. 1992;360(6402):361-4.
509. Harper JR, Spiro RC, Gaarde WA, Tamura RN, Pierschbacher MD, Noble NA, et al. [12] Role of transforming growth factor β and decorin in controlling fibrosis. Methods in Enzymology. 1994;245:241-54.
510. Isaka Y, Brees DK, Ikegaya K, Kaneda Y, Imai E, Noble NA, et al. Gene therapy by skeletal muscle expression of decorin prevents fibrotic disease in rat kidney. Nature medicine. 1996;2(4):418-23.
511. Yamaguchi Y, Mann DM, Ruoslahti E. Negative regulation of transforming growth factor-beta by the proteoglycan decorin. Nature. 1990;346(6281):281-4.
512. Brown DC, Vogel KG. Characteristics of the in vitro interaction of a small proteoglycan (PG II) of bovine tendon with type I collagen. Matrix (Stuttgart, Germany). 1989;9(6):468-78.
513. Winnemoller M, Schmidt G, Kresse H. Influence of decorin on fibroblast adhesion to fibronectin. European journal of cell biology. 1991;54(1):10-7.
514. Winnemoller M, Schon P, Vischer P, Kresse H. Interactions between thrombospondin and the small proteoglycan decorin: interference with cell attachment. European journal of cell biology. 1992;59(1):47-55.
515. Ruhland C, Schonherr E, Robenek H, Hansen U, Iozzo RV, Bruckner P, et al. The glycosaminoglycan chain of decorin plays an important role in collagen fibril formation at the early stages of fibrillogenesis. The FEBS journal. 2007;274(16):4246-55.
516. Bhide VM, Laschinger CA, Arora PD, Lee W, Hakkinen L, Larjava H, et al. Collagen phagocytosis by fibroblasts is regulated by decorin. J Biol Chem. 2005;280(24):23103-13.

517. Puchtler H, Waldrop FS, Valentine LS. Polarization Microscopic Studies of Connective Tissue Stained with Picro-Sirius Red FBA. Beiträge zur Pathologie. 1973;150(2):174-87.
518. Junqueira LC, Bignolas G, Brentani RR. Picrosirius staining plus polarization microscopy, a specific method for collagen detection in tissue sections. The Histochemical journal. 1979;11(4):447-55.
519. Tullberg-Reinert H, Jundt G. In situ measurement of collagen synthesis by human bone cells with a sirius red-based colorimetric microassay: effects of transforming growth factor beta2 and ascorbic acid 2-phosphate. Histochemistry and cell biology. 1999;112(4):271-6.
520. Walsh BJ, Thornton SC, Penny R, Breit SN. Microplate reader-based quantitation of collagens. Analytical Biochemistry. 1992;203(2):187-90.
521. Scott PG, Dodd CM, Bergmann EM, Sheehan JK, Bishop PN. Crystal structure of the biglycan dimer and evidence that dimerization is essential for folding and stability of class I small leucine-rich repeat proteoglycans. J Biol Chem. 2006;281(19):13324-32.
522. Krishnan P, Hocking AM, Scholtz JM, Pace CN, Holik KK, McQuillan DJ. Distinct secondary structures of the leucine-rich repeat proteoglycans decorin and biglycan. Glycosylation-dependent conformational stability. J Biol Chem. 1999;274(16):10945-50.
523. Scott PG, Grossmann JG, Dodd CM, Sheehan JK, Bishop PN. Light and X-ray scattering show decorin to be a dimer in solution. J Biol Chem. 2003;278(20):18353-9.
524. Scott PG, Winterbottom N, Dodd CM, Edwards E, Harold Pearson C. A role for disulphide bridges in the protein core in the interaction of proteodermatan sulphate and collagen. Biochemical and Biophysical Research Communications. 1986;138(3):1348-54.
525. Hausser H, Groning A, Hasilik A, Schonherr E, Kresse H. Selective inactivity of TGF-beta/decorin complexes. FEBS letters. 1994;353(3):243-5.
526. ISO. Biological evaluation of medical devices. Part 10: Tests for irritation and skin sensitization: International Organization for Standardization; 2010 (reviewed in 2016).
527. Foti C, Bonamonte D, Conserva A, Angelini G. Allergic contact dermatitis to regenerated oxidized cellulose contained in a matrix employed for wound therapy. Contact dermatitis. 2007;57(1):47-8.
528. Pereira TM, Flour M, Goossens A. Allergic contact dermatitis from modified colophonium in wound dressings. Contact dermatitis. 2007;56(1):5-9.
529. Sasseville D, Tennstedt D, Lachapelle JM. Allergic contact dermatitis from hydrocolloid dressings. American journal of contact dermatitis : official journal of the American Contact Dermatitis Society. 1997;8(4):236-8.
530. Suhng EA, Byun JY, Choi YW, Myung KB, Choi HY. A Case of Allergic Contact Dermatitis Due to DuoDERM Extrathin®. Ann Dermatol. 2011;23(Suppl 3):S387-S9.
531. Timmer-de Mik L, Toonstra J. Allergy to hydrocolloid dressings. Contact dermatitis. 2008;58(2):124-5.
532. Grange-Prunier A, Couilliet D, Grange F, Guillaume JC. [Allergic contact dermatitis to the Comfeel hydrocolloid dressing]. Annales de dermatologie et de venereologie. 2002;129(5 Pt 1):725-7.
533. Lee JE, Kim SC. Allergic contact dermatitis from a hydrogel dressing (Intrasite Gel) in a patient with scleroderma. Contact dermatitis. 2004;50(6):376-7.
534. Renner R, Simon JC, Treudler R. Contact sensitization to modern wound dressings in 70 patients with chronic leg ulcers. Dermatitis : contact, atopic, occupational, drug. 2013;24(2):60-3.
535. Sheldon JM, Hensel HM, Blumenthal F. Studies in Adhesive Tape Irritation11From the Allergy Clinic, Department of Internal Medicine, and the Department of Dermatology, University of Michigan Medical School, Ann Arbor. Journal of Investigative Dermatology. 1941;4(4):295-315.
536. Zeng LA, Lie SA, Chong SY. Comparison of Medical Adhesive Tapes in Patients at Risk of Facial Skin Trauma under Anesthesia. Anesthesiology Research and Practice. 2016;2016:4878246.

537. Konya C, Sanada H, Sugama J, Okuwa M, Kamatani Y, Nakagami G, et al. Skin injuries caused by medical adhesive tape in older people and associated factors. Journal of clinical nursing. 2010;19(9-10):1236-42.
538. Tokumura F, Ohyama K, Fujisawa H, Matsuda T, Kitazaki Y. Conformability and irritancy of adhesive tapes on the skin. Contact dermatitis. 1997;37(4):173-8.
539. Gibson W, Sanderson GR. Gellan gum. In: Imeson AP, editor. Thickening and Gelling Agents for Food. Boston, MA: Springer US; 1997. p. 119-43.
540. Prajapati VD, Jani GK, Zala BS, Khutliwala TA. An insight into the emerging exopolysaccharide gellan gum as a novel polymer. Carbohydrate Polymers. 2013;93(2):670-8.
541. Mahdi MH, Conway BR, Mills T, Smith AM. Gellan gum fluid gels for topical administration of diclofenac. International journal of pharmaceutics. 2016;515(1):535-42.
542. Mahdi MH, Conway BR, Smith AM. Development of mucoadhesive sprayable gellan gum fluid gels. International journal of pharmaceutics. 2015;488(1):12-9.
543. Lee MW, Chen HJ, Tsao SW. Preparation, characterization and biological properties of Gellan gum films with 1-ethyl-3-(3-dimethylaminopropyl)carbodiimide cross-linker. Carbohydrate Polymers. 2010;82(3):920-6.
544. Lee MW, Tsai HF, Wen SM, Huang CH. Photocrosslinkable gellan gum film as an anti-adhesion barrier. Carbohydrate Polymers. 2012;90(2):1132-8.
545. Mazmanian SK, Round JL, Kasper DL. A microbial symbiosis factor prevents intestinal inflammatory disease. Nature. 2008;453(7195):620-5.
546. Lazzarini R, Duarte I, Ferreira AL. Patch tests. Anais brasileiros de dermatologia. 2013;88(6):879-88.
547. Held E, Lorentzen H, Agner T, Menne T. Comparison between visual score and erythema index (DermaSpectrometer) in evaluation of allergic patch tests. Skin research and technology : official journal of International Society for Bioengineering and the Skin (ISBS) [and] International Society for Digital Imaging of Skin (ISDIS) [and] International Society for Skin Imaging (ISSI). 1998;4(4):188-91.
548. Gawkrodger DJ, McDonagh AJ, Wright AL. Quantification of allergic and irritant patch test reactions using laser-Doppler flowmetry and erythema index. Contact dermatitis. 1991;24(3):172-7.
549. Orgel JPRO, Eid A, Antipova O, Bella J, Scott JE. Decorin Core Protein (Decoron) Shape Complements Collagen Fibril Surface Structure and Mediates Its Binding. PloS one. 2009;4(9):e7028.

Appendix

Appendix A

Lee et al. Burns & Trauma (2016) 4:14
DOI 10.1186/s41038-016-0036-x

Burns & Trauma

RESEARCH ARTICLE Open Access

A systematic review of objective burn scar measurements

Kwang Chear Lee[1,4*], Janine Dretzke[2], Liam Grover[3], Ann Logan[4] and Naiem Moiemen[1]

Abstract

Background: Problematic scarring remains a challenging aspect to address in the treatment of burns and can significantly affect the quality of life of the burn survivor. At present, there are few treatments available in the clinic to control adverse scarring, but experimental pharmacological anti-scarring strategies are now beginning to emerge. Their comparative success must be based on objective measurements of scarring, yet currently the clinical assessment of scars is not carried out systematically and is mostly based on subjective review of patients. However, several techniques and devices are being introduced that allow objective analysis of the burn scar. The aim of this article is to evaluate various objective measurement tools currently available and recommend a useful panel that is suitable for use in clinical trials of anti-scarring therapies.

Methods: A systematic literature search was done using the Web of Science, PubMed and Cochrane databases. The identified devices were then classified and grouped according to the parameters they measured.
The tools were then compared and assessed in terms of inter- and intra-rater reproducibility, ease of use and cost.

Results: After duplicates were removed, 5062 articles were obtained in the search. After further screening, 157 articles which utilised objective burn scar measurement systems or tools were obtained. The scar measurement devices can be broadly classified into those measuring colour, metric variables, texture, biomechanical properties and pathophysiological disturbances.

Conclusions: Objective scar measurement tools allow the accurate and reproducible evaluation of scars, which is important for both clinical and scientific use. However, studies to evaluate their relative performance and merits of these tools are scarce, and there remain factors, such as itch and pain, which cannot be measured objectively. On reviewing the available evidence, a panel of devices for objective scar measurement is recommended consisting of the 3D cameras (Eykona/Lifeviz/Vectra H1) for surface area and volume, DSM II colorimeter for colour, Dermascan high-frequency ultrasound for scar thickness and Cutometer for skin elasticity and pliability.

Keywords: Scar measurement, Burn, Objective measurement, 3D camera, Laser imaging, High-frequency ultrasound image, Colorimeter, Cutometer

Background

Burn injury is one of the most common type of traumatic injuries in the world with an estimated incidence of 1.1 per 100,000 population [1] and remains one of the leading causes of deaths, accounting for 5.2 % of 5.1 million deaths due to injuries and violence in 2012 [2]. In the last few decades, major advances in burn care have greatly improved survival rates [3] and an increased number of patients are surviving large burns. Non-fatal burns however is a leading cause of morbidity, as many of these patients develop hypertrophic scars that may lead to significant disfigurement and disability (e.g. contractures).

In order to assess and track the evolution of scars over time, subjective rating scales have been introduced into clinical practice. These scales in general are free or low cost and require minimal training to utilise. Several such scar scales have been developed and are used widely, including the commonly used Vancouver Scar Scale (VSS) and the Patient and Observer Scar Assessment Scale (POSAS) [4]. However, these scar scales are considered to be subjective and the resulting scores can vary between different assessors (inter-assessor variation) [5], different scar severities [6] and age of the scar [7], and some studies have suggested

* Correspondence: kwangchear@hotmail.com
Ann Logan and Naiem Moiemen are joint last authors.
[1]The Healing Foundation Burn Research Centre, University Hospital Birmingham Foundation Trust, Birmingham B15 2TH, UK
[4]School of Clinical and Experimental Medicine, College of Medical and Dental Sciences, University of Birmingham, Birmingham B15 2TT, UK
Full list of author information is available at the end of the article

that more than one rater (sometimes as many as five), and utilising the average, is required in order to produce reliable ratings [7, 8]. The POSAS attempts to improve the method of rating scars by including the patients' perspective; however, patients' perception and subjective evaluation of their scars have been shown to be influenced by depressive symptoms [9]. The physical characteristics of scars further add to the complexity of rating as changes in both the vascularity and pigmentation can occur simultaneously, and scars are also rarely homogenous in both colour and texture, which makes estimation of mean values difficult and inaccurate for a human observer.

Standardised, quantifiable, reliable (reproducible) and valid assessment tools that provide a more objective evaluation of scars are essential for monitoring the changes in scar quality over time and also to determine the effectiveness of scar treatments.

The various objective measures that relate to scar severity can be divided into the following categories:

- *Colour*: erythema and pigmentation contribute significantly to the appearance of a scar.
- *Dimensions*: it includes planimetry (surface area), thickness and volume.
- *Texture*: surface texture or scar roughness has a significant effect on the patient's and observer's opinion of the scar.
- *Biomechanical properties*: it includes pliability and elasticity. Stiffness and hardening of scars are due to increased collagen synthesis and lack of elastin in the dermal layer and can lead to impairment of skin function, especially when the scar is located around joints.
- *Pathophysiological disturbances*: it includes transcutaneous oxygen tension and transepidermal water loss and moisture content.
- *Tissue microstructure*: new non-invasive in vivo imaging techniques analyse the morphological tissue architecture of the scar, providing measurements previously only possible by histopathological analysis of biopsy samples.
- *Pain/sensation*: pain is a commonly measured parameter in many subjective scales however objective methods to measure it are yet to be available. However the measurement of altered sensation may be useful.

In this article, we describe and compare the underlying principles and performance of various currently available objective measurement devices in order to inform clinicians and researchers about their clinical utility for scar assessment. In addition, we discuss innovative technologies that may be applicable to burn scar assessment in the near future.

Methods

Criteria for considering articles for inclusion

Published articles that describe non-invasive burn scar measurements were included in this systematic review. Studies that used scar scales which utilise subjective scoring systems were excluded, as studies that made histopathological evaluations of scars via biopsies had no potential to be used in vivo (i.e. requiring the use of ex vivo processing and staining). We chose to include studies comparing the outcomes of wound or scar treatments as well as animal studies and in some cases non-burn scars if appropriate, as excluding these studies may prevent us from identifying new or emerging technologies.

Search methods

A computerised literature search (until October 2015) was performed using the web-based Web of Science (http://wok.mimas.ac.uk/; years 1900–2015) and PubMed services (www.ncbi.nlm.nih.gov/pubmed/; years 1950–2015) and utilising the Web of Science Core collection and Medline databases. No language limit was set.

The following search strategies were used:

1) (Skin OR derma* OR dermis OR epidermis OR epiderma*) AND (scar OR cicatrix OR fibrosis) AND (objective OR quantitative) AND (burn OR burn$ OR hypertrophic).
2) (Skin OR derma* OR dermis OR epidermis OR epiderma*) AND (scar OR cicatrix OR fibrosis) AND (evaluation OR assessment) AND scale
3) ((burn$ or burn) and hypertrophy)
4) ((burn$ or burn) and (scar or cicatrix))
5) ((scar or cicatrix or fibrosis) and hypertrophy)
6) ((Objective assess* or objective evaluat* or objective measure* or assess$ instrument or assess$ tool or device or measurement system or objective) adj3 assess$)
7) (objective evaluat* or objective measur* or assess$ instrument or assess$ tool or (device or scale or measurement system))
8) NOT (uterus or cardio* or neoplasm or cancer or metastas$ or malignancy)

Web of Science core collection results were further refined by the following terms: surgery or dermatology or critical care medicine or emergency medicine or medicine research experimental or computer science interdisciplinary applications or computer science artificial intelligence or imaging science photographic technology or rehabilitation or medical laboratory technology or engineering biomedical or medicine legal or medical informatics or biophysics or anatomy morphology.

This search produced 5062 articles after duplicates ($n = 2334$) were removed. After filtering by review of titles and abstracts, 151 suitable articles were chosen.

A separate search was also conducted using the PubMed database (www.ncbi.nlm.nih.gov/pubmed) using the following keywords/terms (including MeSH [Medical Subject Headings] terms): skin AND (scar OR cicatrix OR fibrosis) AND (evaluation OR assessment OR assess OR measure OR measurement) AND (objective OR quantitative) AND (burn OR burns OR hypertrophic). A further broader search was conducted using the following keywords and MeSH terms: skin AND (scar OR cicatrix OR fibrosis) AND (evaluation OR assessment) AND scale. No language limit was set. This search retrieved 613 articles, and after filtering by review of titles and abstracts and removal of duplicates, a further 27 articles were included. The reference lists of the selected articles were also searched for suitable studies, and an additional 12 articles were included.

A search of the Cochrane database retrieved no suitable articles.

A grey literature search was performed using the Bielefeld Academic Search Engine (BASE) database with the term "objective measurement of scarring". This search included books, reports, papers, lectures, theses, reviews, and primary data document types and excluded article, journals, audio, videos, images, maps, software and sheet music document types. This search produced 180 hits (after 50 duplicates removed), and after review, 6 articles were deemed suitable for inclusion into the review.

Full text articles were obtained for the articles where possible, and a further 28 records were removed after evaluating the full text. Articles which were only available in abstract form and had no extractable data were also excluded.

Thus, the total number of articles selected for review was 157. This includes 9 review articles.

The selection process for the eligible articles is outlined in Fig. 1 below.

Quality assessment

The validity and reproducibility of the devices were evaluated when statistical data were available especially in terms of reproducibility of the assessments. Where available, the additional value of the device compared with subjective scar scales and/or other tools is discussed.

In terms of interpreting the intra-class correlation coefficients (ICC), some guidelines have been provided by Landis and Koch [10] for Kappa coefficients (which are also reasonable for the ICC) suggesting that:

- Kappa of <0.00 indicates "poor" agreement
- Kappas from 0.00 to 0.20 indicate "slight" agreement
- Kappas from 0.21 to 0.40 indicate "fair" agreement
- Kappas from 0.41 to 0.60 indicate "moderate" agreement
- Kappas from 0.61 to 0.80 indicate "substantial" agreement
- Kappas from 0.81 to 1.00 indicate "almost prefect" agreement

However, it should be noted that these guidelines are subjective.

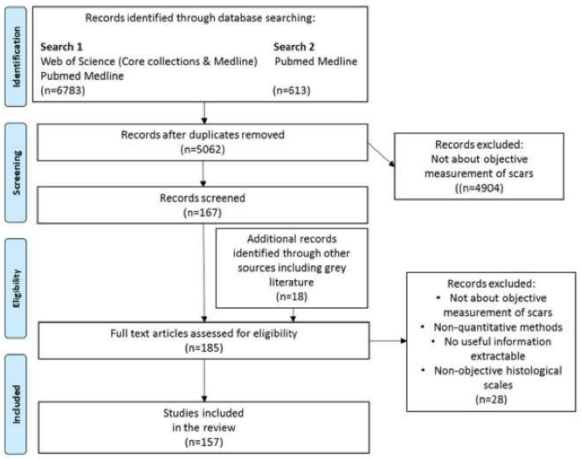

Fig. 1 Preferred Reporting Items for Systematic Reviews and Meta-Analyses flowchart

Feasibility of devices was assessed via the commercial availability, portability and cost of the devices.

An economical assessment of the devices based on the literature was not possible due to the lack of such data in the articles; however, several of the companies with commercially available devices were contacted to provide quotes, and although it was not possible to publish the exact prices due to confidentiality issues, the devices are categorised into price ranges (<£5000, £5000–10,000, >£10,000, >£30,000).

Results

Articles, reviews and editorials that described objective burn scar assessments were retained. These were then classified into six categories based on the assessed variables: (1) colour, (2) scar dimensions (e.g. thickness or height, surface area), (3) texture, (4) biomechanical properties (e.g. elasticity, pliability), (5) physiological disturbances (e.g. hydration) and (6) non-invasive morphological imaging techniques.

Colour

Colour is a major factor that affects the aesthetics of a scar and is mainly composed of two components: melanin (the brown pigment made by activated cutaneous melanocytes) and erythema (the redness that is caused by haemoglobin in the dilated/congested remodelled cutaneous vasculature). Other pigments that localise in scars, such as bile and carotene, may also contribute to the overall appearance of the scar. Colour measurements can be used to gauge the effectiveness of anti-scarring treatments since they reflect abnormal skin architecture/composition [11]. Measurement of the scar colour can be complicated by several factors, such as skin layer thickness, reflection from the skin surface and environmental factors including light and temperature. The measurement of erythema is further influenced by patient-related factors such as activity and positioning of affected areas as such movements may affect the blood circulation and hence the erythema of the skin.

Although visual assessment of colour has been incorporated into various scar scales, it is a subjective evaluation method that provides relative rating systems. Even in normal circumstances, the human brain cannot accurately quantify colour or its intensity. A famous recent example of this is the "blue and black dress" which shows that human colour discrimination may be affected by the illuminant colours, level of ambient illumination and the background colours of a visual display terminal [12, 13]. Neuropsychiatric conditions have also been shown to affect colour discrimination [14]. In scars, changes in vascularity and pigmentation occur simultaneously and overlap each other which make colour observation and reporting even more difficult for a human observer, e.g. it is difficult to assess the pigmentation of a scar in a highly vascularised scar as the erythema would obscure the increase or lack of pigment. Additionally, as scars often have an uneven colour distribution, human observers cannot easily or accurately provide a mean value for a certain area.

More recently, several objective and reproducible methods of colour evaluation have been developed and they can be broadly classified as follows:

- *Reflectance spectroscopy*: tristimulus reflectance colorimetry and narrow-band spectrophotometry
- *Laser imaging*: it measures the microcirculation in the scar which influences the erythema of the scar.
- *Computerised analysis of digital photographs*: it can include two-dimensional (2D) and three-dimensional (3D) images which are then digitally analysed to quantify colour values.

Reflectance spectroscopy

Reflectance spectroscopy is a well-established technique of more than 50 years [7] and currently one of the most commonly used methods for measuring colour. Techniques that utilise reflectance spectroscopy quantitatively measure the colour and intensity of reflected light. For example in Fig. 2, when light consisting of red, blue and green is shone upon a surface, if the material absorbs red and green light, then only the blue light is reflected which will make us perceive the material as blue. A biological example is the detection of the oxygenation of haemoglobin. When haemoglobin is illuminated with white light, oxygenated haemoglobin will absorb a higher proportion of blue light and reflect back red light whereas de-oxygenated haemoglobin absorbs more red light and thus appears bluer. In reality, the process is more complicated as the light that is shone (termed incident light) onto biological tissues can be reflected in many different trajectories, and this scattering also influences our perception of the colour of an object.

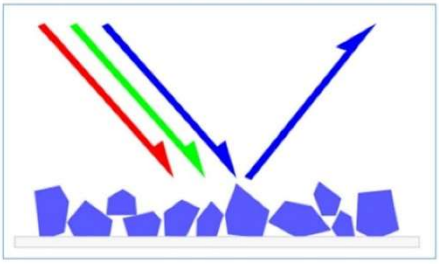

Fig. 2 Graphical illustration of the concept of reflectance spectroscopy. (Source: http://commons.wikimedia.org/wiki/File:Simple_reflectance.svg)

Tristimulus reflectance colorimetry and narrow-band simple reflectance (or spectrophotometry) are both based on the principle of reflectance spectroscopy.

Tristimulus reflectance colorimetry [15] describes colour by three values: L* (clarity, lightness or brightness); a*, the amount of red or green (erythema); and b*, the amount of yellow or blue (pigmentation) (see Fig. 3). For example, a white coloured object would have a higher L* value compared to a darker coloured object and a scar that it is redder than normal skin would give a higher a* value than normal skin. Additionally, another approach to quantify colour is by using the saturation or chroma of colour (C*) which is a vector magnitude in the chromatic plane calculated from a* and b* values [16, 17].

There are currently several spectrocolorimeter devices that utilise the principle of tristimulus reflectance colorimetry, including the Minolta Chromameter [15, 18, 19] (Minolta Camera Co., Osaka, Japan), the Labscan XE [17] (Hunter Associates Laboratory, Inc., Reston, VA), DSM II Colormeter [20], NF-333 [21] (Nippon Denshoku Co. Ltd, Japan), Micro Color (Dr. Bruno Lange GmBH, Dusseldorf, Germany) [22], X-Rite SP64 Spectrophotometer (X-rite Inc, Michigan, USA) [23] and the Visi-Chroma VC-100 (Biophotonics, Belgium) [22, 24]. Camera systems such as the Eykona 3D camera can also be calibrated to report colour values using the L*a*b* system [25]. However, a drawback of the Eykona 3D camera is that although its cost is low, it currently requires consumables in the form of one-use targets (about £70 for 25 targets) that have to be placed next to the area of interest when taking an image, although there are plans to introduce reusable targets in the coming months according to the company.

A study by Li-Tsang et al. [17] showed that the intra- and inter-rater reliability for the Labscan XE device for hypertrophic scars was satisfactory, with an intra-class correlation coefficient (ICC) ranging from 0.95 to 0.99 for intra-rater reliability, and 0.50 to 0.99 for inter-rater reliability in all the three colour parameters (L*, a* and b*). A strong positive correlation was also found between VSS scores and the readings obtained from the Labscan XE device. The device that was utilised in the literature was not portable; however, newer portable versions are currently available. A study by Draaijers et al. showed that the overall evaluations of scar colour with both the Dermaspectrometer and the Minolta Chromameter are more reliable than the visual evaluation and scoring of scar colour carried out by observers using a 10-step score, whereby a score of 1 reflects normal skin and a score of 10 reflects the worst scar imaginable [15]. However, devices that rely solely on tristimulus colorimetery have been shown to have poor correlation scores with patient scar scales when measuring pigmented or hypo-pigmented scars due to the scar scales scoring hyper- and hypo-pigmented scars higher as deviations from normal skin.

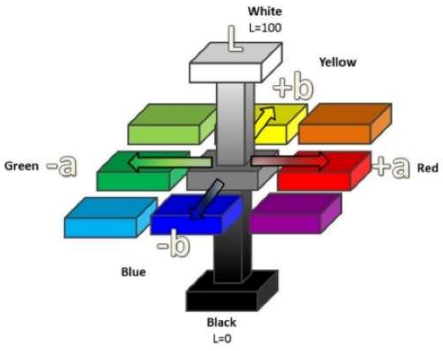

Fig. 3 Graphical representation of the L*a*b* colour measurement system. (Source: Kwang Chear Lee)

Narrow-band spectrophotometry [15] devices on the other hand measures the vascularisation and pigmentation of the scar based on differences in red and green light absorption by haemoglobin and melanin, respectively. The Dermatospectrometer (or the newer version, DSM II Colormeter) [20, 26, 27] (Cortex Technology, Hadsund, Denmark) and Mexameter [20, 28] (Courage + Khazaka, Germany) are examples of a device that uses this principle. In comparison with the Minolta Chromameter and Labscan XE, the Dermaspectrometer is a smaller and hence a more portable device and the use of the erythema and melanin indexes is less complicated to understand and analyse compared to the L*, a* and b* of the Minolta Chromameter. It has also been shown to have a slightly better correlation with clinical scores when compared with the Chromameter [29]. Unfortunately, the Dermatospectrometer has been withdrawn from the market but it has been replaced with a newer model, the DSM II Colormeter. The DSM II Colormeter [20] (Cortex Technology, Denmark) is a small, fully hand-held device that utilises both tristimulus colorimetry and narrow-band spectrophotometry technology and produces reliable readings [20]. It has an improved utility, in terms of cost and assessment time as it utilises one instrument instead of two to obtain both tristimulus colorimetry readings as well as narrow-band spectroscopy readings. The Mexameter also has good intra-observer and inter-observer reliability in scar assessments [20].

Caution however must be used when using erythema to grade the severity of scars. This is because scars can often be very vascular initially but this does not mean that they will become hypertrophic, e.g. in the study by Nedelec et al. [30], the Mexameter was unable to differentiate hypertrophic scars from normal scars as donor

sites were very erythematous, but we know that donor sites rarely progress to become hypertrophic scars.

A common disadvantage of all of the aforementioned devices is that they employ a small measuring area, e.g. the measuring area for the Minolta Chromameter is only 3 mm [18] and the other devices range from 5 to 8 mm [7]. Therefore, multiple measurements, especially in larger scars, need to be performed to provide accurate scores, but these increase the risk of observational bias. Additionally, these devices also require contact with the skin which can change the colour if too much pressure is applied. Environmental lighting may also affect the readings obtained, although many of the companies of these devices (e.g. DSM II Colormeter) claim that the flash that is utilised by these devices is strong enough to overcome and compensate for any differences in colour caused by indoor lighting.

Large area spectrophotometry

Some investigators have attempted to overcome the problem of small measurement areas by utilising camera systems to allow the imaging of larger areas. Cheon et al. utilised digital photographs taken with a digital camera (Nikon D70s, Tokyo, Japan) under the same light source and obtained L*a*b* values for the regions of interest (whole scar lesions when possible) using Adobe Photoshop (Adobe systems Incorporated, San Jose, CA). The test–retest consistency (or intra-rater reliability) of the L*a*b* as determined by the intra-class coefficient ranged from 0.95 to 0.99 and the inter-rater reliability was also good with values ranging from 0.94 to 0.98 [31, 32].

Another method of spectral modelling developed by Kaartinen et al. utilises standardised digital imaging (SDI) with computer controlled lighting to quantify colour changes [7, 8, 33]. This system allows a larger area of the skin to be analysed with an only slightly weaker accuracy compared to the previously mentioned spectroscopy-based systems [33]. This method, however, is yet to become commercially available, but a similar system, Scanoskin (Leniomed Ltd, London, UK), is available. The Scanoskin system utilises polarised light, which has the advantage of blocking the reflectance from the skin which allows better analysis of the epidermal and superficial dermal layers [34]. The system is currently used only to assess burn depth via the imaging of haemoglobin (erythema/vascularisation) and haemosiderin or melanin. Images which are taken (with a modified SLR camera with polarised lenses) are processed by the provided software which splits them into separate erythema and melanin components. Quantification of erythema and pigmentation (melanin) has to be performed on the exported images using software such as ImageJ [35–37].

The evidence for using objective measures in measuring colour is encouraging and is based on a relatively small number of studies, and more research is needed [38].

Spectrophotometric intra-cutaneous analysis (SIA)

Analysis of colour information purely in the visible spectrum is insufficient to provide information relating to a lesion's deeper structures, and it was this realisation that prompted research at the University of Birmingham to extend the spectrum of light used into the infrared region (700–1000 nm). Spectrophotometric intra-cutaneous analysis via the clinical device, SIAscope, utilises a probe (12×12 mm or 24×24 mm) that utilises radiation ranging from 400–1000 nm and produces 8 narrow-band spectrally filtered images of the skin which are then processed by software algorithms and allows the visualisation and quantification of melanin, collagen and blood [39]. Although developed for diagnosing skin cancers, it can and has been used to monitor the changes in scar tissue in response to treatment [40].

Computerised analysis of digital photographs

Digital photographs can be taken with any standard digital camera, e.g. the Nikon 8400 [19].

Photos are then downloaded for analysis by proprietary software packages such as KS400 (Kontron Electronic GMB, Carl Zeiss Micro-Imaging, Inc., Thornwood, NY, USA) [41] or the freely available ImageJ. One study utilised an artificial neural network to perform chromatic analysis of the digital image of a burn scar [42]. Colour measurements using ImageJ have been shown to be equivalent to those obtained using a colorimeter (Chromameter, Konica-Minolta) [19]. Several studies have attempted to improve the objectivity of photograph analysis of scars by standardising factors such as distance and lighting [19] or using computerised image capturing systems [43–45]. However, even this method fails to allow scars to be compared objectively as humans vary in terms of how we set the measurement criteria for and analyse colour [29, 46] and the photographs have been shown to have limited utility when assessed using computer-based subjective scales [47]. Improved computer programmes may overcome the limitations of the human brain and provide objective analysis of the digital photographs. However, computer programmes cannot properly "see" colour and thus have to convert colour information into digital data, thereby losing valuable information.

Computer programmes utilise two methods to analyse colour. The hue-saturation-value (HSV) method analyses colour by separating it into three main components: hue (dominant wavelength), saturation (amount of white) and value (amount of black). The other method utilises colour models of which there are two main ones: the Red, Green and Blue (RGB) model and the Cyan, Magenta, Yellow and Black (CMYK) model. Measurement techniques using other systems such as the L*a*b* system have also been described [48].

To remove the influence of light and camera settings, generally a card carrying standard colours (e.g. Pantone colour chart [Pantone Inc, USA] [16], Macbeth Digital Colorchecker SG colour chart [Munsell Colour services Laboratory, X-Rite Inc, Michigan, USA] [25, 44]) is recommended to be placed beside the scar being photographed so that every photo taken would include areas of known colour properties, allowing an objective colour evaluation [16].

Table 1 summarises the colour measurement devices in terms of parameter measured, reliability, correlation with clinical score and cost.

Laser imaging

The amount of haemoglobin or erythema present in a scar can be measured indirectly via laser imaging [49, 50] that measures the blood flow in a scar. Immature scars show a significantly increased blood flow due to their higher vascularity compared to mature scars. Increased microcirculatory blood flow (as measured by Laser Doppler Flowmetry (LDF)) has also been shown to be a potential indicator for the occurrence of hypertrophic scarring [51]. Hypertrophic scars will typically generate readings that are two to three times greater than that made in normal skin [50, 52, 53] and four times greater than that in a non-hypertrophic scar [50]. Laser-based methods have the advantage of being fast, reproducible and having a good correlation with the VSS; however, they are subject to structural changes in the skin and environmental and body temperature fluctuations [54–56].

Laser-based methods can be divided into three techniques: LDF, Laser Doppler Imaging (LDI) and Laser Speckle Imaging (LSI)/Laser Speckle Perfusion Imaging (LSPI). With the older Laser Doppler Flowmeter, the fibre optic probe is in contact with the tissue surface and is a single-point measure [49, 57]. Laser Doppler Flowmeter [29, 52, 55, 56] systems, such as the DRT4 [53] (Moor instruments, Devon, UK) or the LaserfloBPM [58] (Vasamedics Corp, St Paul, Minnesota, USA), the fibre optic probe is in contact with the tissue surface and provides a single-point measure of an indirect evaluation of scar colour by measuring the cutaneous bloodflow present in a scar [49, 57]. LDF systems are more limited compared to the other laser-based methods (see below) as they measure flow within a small area and, thus, are unsuitable for use with larger, heterogeneous scars.

In contrast, Laser Doppler Imaging (LDI) devices, such as the Lisca PIM1.0 imager (Lisca Development AB, Linköpen, Sweden) and The Moor LDI (Moor Instruments, Devon, UK) [49], utilise a laser beam to scan several points across a tissue surface and generates a 2D colour-coded image that is correlated to the blood flow [49]. They are primarily used for burn depth assessment but have been utilised for scar evaluation [49, 59]. The method is, however, hampered by long measurement times and low resolution [57]. LSI and LSPI are alternative perfusion monitoring techniques that generate rapid, high-resolution images of tissue. As red blood cells move during circulation, dynamic interference patterns that change with time are created. Blood flow maps can then be created from the coherent light that is reflected from stationary tissue, generating a high contrasted speckle pattern that remains static in time. As indicated previously, high measurements reflect high blood flow and immature/hypertrophic scars. LSI devices compare favourably with the more established LDI instruments, but offer advantages in terms of a faster scan time, higher resolutions and the ability to zoom in with increased resolution of a smaller field of view, a feature that is not possible with LDI [57, 60].

A major disadvantage common to all laser imaging systems are that they are not very portable (with the exception of a new commercially available laser speckle imaging device developed by Moor instruments [61]) due to their size and are often very expensive, with costs of >£30,000.

Table 2 summarises the comparison of laser devices in terms of parameter measured, reliability, correlation with clinical score and cost.

Thermographic analysis of burn scars

Thermographic cameras detect radiation in the long-infrared range of the electromagnetic spectrum (9–14 μm) and can be used to produce images or videos of that radiation. Thermography can be divided into passive (where the object can be imaged directly as it has a higher or lower temperature than the background) and active thermography (where an energy source is required to produce a thermal contrast between the imaged object and the background). Several studies have looked at using thermography to assess the depth of burn wounds [37, 62–64].

Our literature search however has only been able to identify one small study done in 1985 ($n = 12$) which utilised thermographic analysis of the scar temperature in an attempt to differentiate hypertrophic and non-hypertrophic scars [65]. No relationship between scar temperature and hypertrophic scar formation was found.

A more recent case report by Horta et al. [66] which utilised a thermography camera (FLIR SC7000 thermography camera; FLIR Systems, Wilsonville, OR, USA) showed that factors such as muscle activity or the lack of mucosa, cartilage and bone can influence the thermographic reading of scars rather than the degree of hypertrophy itself. This further complicates the use of thermography to objectively quantify scars.

Table 1 Comparison of colour measurement devices in terms of parameter measured, reliability, correlation with clinical score and cost

Device	Company	Parameter	Intra-rater Reliability	Inter-rater reliability	Correlation with clinical score	Cost	Portability	References
Computerised colour analysis	Sony Hi-8 Handycam CCD-TR 705E video camera recorder and Adobe Photoshop	Hue, saturation, value	No data	No data	VSS Vascularity score significantly correlated with hue ($r = 0.311$) and saturation ($r = 0.35$) ($p < 0.051$), index with hue and saturation combined correlated even better ($r = 0.42$).	£5000–10,000	Yes	Davey et al. 1999 [16].
Computerised colour analysis	Nikon D70 camera and Adobe photoshop	Tristimulus colorimetry ($L^*a^*b^*$)	0.95–0.99	0.94–0.95	L* and a* values are more important than b* values in distinguishing colour features between normal skin and scars.	No data	Yes	Cheon et al. 2010 [32]
Labscan XE (non-portable version)	Hunterlab	Tristimulus colorimetry (L*a*b*), chroma and hue.	Good (0.95–0.99)	Acceptable to good (0.50–0.99, outlier low value of 0.50 for a* [ranged from 0.01 to 0.77])	L*, a*, b* and hue had moderate to strong correlation with VSS pigmentation and vascularity scores. Chroma had low correlation with pigmentation and vascularity ($r = -0.40$ and -0.17)	>£10,000	Poor	Li-Tsang et al. 2003 [17]
Labscan XE (portable version)	Hunterlab	Tristimulus colorimetry (L*a*b*)	No data	No data	No data	£5000–10,000	Yes	Li-Tsang et al. 2005 [102]
Chromameter	Konica-Minolta	Tristimulus colorimetry (L*a*b*)	Acceptable (0.73–0.89)	Good (0.91–0.97)	Unable to differentiate between hypo- and hyperpigmented scars and normal and 'red' skin (On Seattle, Hamilton and Vancouver scar scales)	£5000–10,000	Yes	Draaijers et al. 2004 [15], Oliveira et al. 2005 [29],
Eykona 3D camera	Fuel 3D	Tristimulus colorimetry ($L^*a^*b^*$)	No data	No data	Good correlation (Manchester scar scale)	<£5000 (not including targets)	Yes	Hallam et al 2013 [25]
Colorimeter	Courage + Khazaka	Tristimulus colorimetry ($L^*a^*b^*$) and ITA (Individual Typology Angle)	No data	Good (0.91–98)	No data	£5000–10,000 (including cost of hub)	Yes	van der Wal et al. 2013 [20].
Mexameter	Courage + Khazaka	Narrow-band spectrophotometry (melanin and erythema)	Good for melanin (0.89–0.97) and acceptable for erythema (0.74–0.90)	Good for melanin (0.95) and erythema (0.82–0.85)	No data	<£5000	Yes	Nedelec et al. 2008 (I) [30], Nedelec et al. 2008 (II) [106], van der Wal et al. 2013 [20].
Dermaspectrometer/ DSM II Colorimeter	Cortex	Both tristimulus colorimetry and narrow-band spectrophotometry	Erythema: 0.29–0.94 Melanin: 0.72–0.87 L*a*b*: no data.	Erythema: 0.68–0.91 Melanin: 0.91–0.94 L*a*b*: no data.	Erythema: Moderate but significant $r = 0.50$ (<0.001) Melanin: weak but significant $r = 0.32$ (0.02)–0.63 (<0.001)	<£5000	Yes	Gankande et al. 2014 [6], Gankande et al. 2015 [248], van der Wal et al. 2013 [20], Oliveira et al. 2005 [29].

Table 1 Comparison of colour measurement devices in terms of parameter measured, reliability, correlation with clinical score and cost *(Continued)*

Standardised digital imaging (SDI) + Spectral modelling (SpM)	Custom made	Estimated concentration change of haemoglobin and melanin	Good for haemoglobin (0.875) and melanin (0.886)	Good for haemoglobin (0.955) and melanin (0.959)	Acceptable correlation with POSAS (0.63 for haemoglobin, 0.60 for melanin) and VSS (0.74 for haemoglobin, 0.53 for melanin)	<£5000 (but not commercially available)	Yes	Kaartinen et al. 2011 [7, 8].
Dermoscopy	Hong Kong Productivity Council	RGB values: lightness and redness	Redness: 0.980 Lightness: 0.965	Redness: 0.93 Lightness: 0.871	Strong correlation between the VSS scores of vascularity and the RGB values of redness obtained from the dermoscope ($r = 0.625$, $p < 0.01$). Strong correlation also found between transformed VSS scores of pigmentation and the lightness of the dermoscope pictures when vascularity was blanched out (i.e. when measuring pure pigmentation) ($r = 0.783$, $p < 0.01$).	No data	Yes	Wei et al. 2015 [238].

RGB = red, green and blue

Table 2 Comparison of laser devices in terms of parameter measured, reliability, correlation with clinical score and cost

Device	Company	Parameter	Intra-rater reliability	Inter-rater reliability	Correlation with clinical score	Cost	Portability	References
Laser Doppler Flowmeter	Moor	Blood flow	No data	No data	LDF showed significant difference in blood flow within hypertrophic and keloid scars and normal skin (2.6–2.8-fold higher).	>£30,000	Poor	Clark et al. 1996 [56], Timar-Banu et al. 2001 [53].
Laser Doppler Imaging	Lisca, Moor	Blood flow (red and near infrared wavelengths)	No data	No data	Correlations with clinically assessed grades (VSS) of pigment, vascularity, pliability, and height ranged from $r^2 = 0.63$ to 0.95.	>£30,000	Poor	Stewart et al. 2005 [60] Bray et al. 2003 [49].
Laser Speckle Perfusion Imaging	Moor	Blood flow	No data	No data	Correlations with clinically assessed grades (VSS) of pigment, vascularity, pliability, and height ranged from $r^2 = 0.73$ to 0.94.	>£30,000	Poor	Stewart et al. 2005 [60]

LDF = Laser Doppler Flowmetry; *VSS* = Vancouver Scar Scale

Scar dimensions

Surface area and volume

Planimetry is the measure of the surface area of a scar and, when done over time, can be used to assess the contraction or expansion of a scar.

The most basic method of planimetry, that does not require specialist equipment or trained personnel, is the linear method where the maximum length and width of the wound is measured directly on the patient and the surface area is then calculated by multiplying the maximum length and width. As can be expected, this technique is inaccurate as scars are rarely rectangular or square in shape and will produce results that are significantly different from those obtained with tracing and photography methods [67].

The second method involves the tracing of scar margins either on sheets of paper, clear plastic film or any transparent non-stretchable material [27, 46]. The surface area traced on these sheets can then be calculated by outlining wound margin with the tip of a planimeter (Koizuni Sokk Manufacturing Ltd., Nagoaka-shi, Japan) [67] or by digitising the tracings on these sheets and using software such as NIS-Elements (Nikon, Amstelveen, The Netherlands) [27] , ImageJ [68] or Digimizer software [69] to calculate the surface area. Dedicated systems have also been developed such as the Visitrak (Smith & Nephew) which have been shown to have high intra- and inter-rater reliability and high validity in the measurement of the surface area of ulcers [70] although the maximum size of the area that can be measured at a time is limited by the disposable tracing grid used (14 cm × 14 cm).

The third method uses digital photography combined with image analysing programmes such as ImageJ, Image Tool (C.D. Wilcox and colleagues, San Antonio, TX, USA) [29] or Adobe Photoshop (Adobe Systems Inc., San Jose, California, USA) [71] to measure the surface area. A significant problem with 2D photography is that it is subject to parallax errors and projecting a three-dimensional object onto a two-dimensional image. Due to this, the 2D surface area (or planimetric area) calculated does not take into account the wound surface topography and will nearly always underestimate the true three-dimensional surface area (see Fig. 4).

With smaller scars, this error would be small but will increase as the size increases. A study by van Zuijlen et al. compared the direct and indirect (through 2D photography) tracing methods [71]. It found that both techniques were reliable ($r \geq 0.82$, $p < .001$) for surface lesions with a scar surface area of 25 cm^2, but planimetry by photography was superior to planimetry by direct tracing in respect to inter-observer reliability for surface lesions of 50 and 75 cm^2, with increasing scar size resulting in decreasing inter-observer reliability. However, planimetry by direct tracing was more accurate on curved surfaces (e.g. forearm), with a statistically significant reduction of the surface area obtained when compared to results with planimetry after photography. The use of photography [29, 43] to measure surface area, although useful, is subject to variance caused by lighting conditions, distance and camera settings and does not provide any information on volume.

Three-dimensional (3D) measurement systems can overcome the limitation of 2D photograph, and in addition to

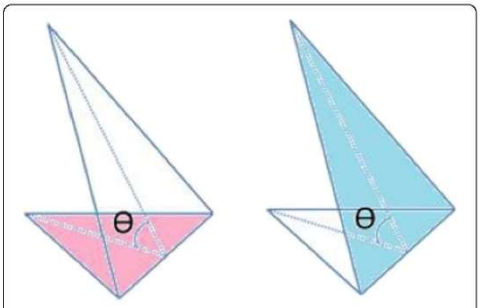

Fig. 4 The 2D or planimetric area (in *pink*) is always smaller than the 3D area (in *blue*). (Source: Kwang Chear Lee)

surface area measurements, the 3D camera systems are also able to measure the volume of scars much more quickly and easily compared to traditional moulage and moulding [72] methods.

A 3D image can be achieved via various methods. A method that is commonly used in the medical is stereophotogrammetry. These systems are non-contact and involve taking two or more pictures using either one or multiple cameras which can be on the same device (e.g. Eykona wound measurement system, Fuel 3D, UK [25]) or separate devices (e.g. 3D MD static systems, 3dMD, USA [73]). Some authors have even developed their own systems with standard cameras (e.g. Stereoimage optical topometer (Korea University, Seoul, South Korea) with PC vision plus (AES, Sydney, Australia)) [74]. Other devices utilise mirrors to achieve a similar effect for, e.g. LifeViz I, II, Mini or Micro (Quantificare S.A., Sophia Antipolis, France) [75, 76] and Vectra H1 3D imaging system (Canfield Scientific Inc, Fairfield, NJ, USA) [77–80]. Other systems utilise the projection of a complex speckled pattern in combination with a colour camera to produce the 3D images [81].

These software are able to provide information about the surface area [82] and tissue volume above the skin [83] (including correction for curved surfaces) as well as geometry, texture and, as mentioned above, the colour of scars for which the performance of the Eykona device has been shown to compare favourably with the subjective Manchester Scar Scale (MSS) [25]. These devices share a few common drawbacks. Firstly, none of them have been validated in scar studies, but their ability to measure the area [83–85] and volume of wounds and tissue (e.g. breasts [82]) has been shown in other non-scar related studies. Additionally, the maximum area that can be imaged is limited to the size of about an A4 size sheet of paper which is not ideal for large burns scars. Furthermore, although stitching of images is possible, this really only applies to the face as it is easy to identify anchor points such as the eyes and nose, but to do so for other highly curved surfaces such as the forearm or the whole body would be technically challenging and time consuming and requires high-end hardware and thus a true 360° view would not be easily possible [80]. Hairy areas of the body can also pose a problem [80].

The Lifeviz and Vectra H1 systems have an advantage over the Eykona in that they have adjustable light-beam pointers to aid positioning and do not require one-use disposable targets which the Eykona system does but they are also significantly more expensive. Furthermore, the Eykona is no longer being developed by the company and has not been updated recently, thus its resolution is significantly lower (250 micron sampling via two 5 MP sensors) [86] compared to the Lifeviz Mini (13.5–24 MP, 0.5–2 mm geometry resolution) [87] or Vectra H1 cameras (18 MP, 0.8 mm geometry resolution) [88].

More recently, light field or plenoptic technology has been introduced. Cameras utilising this technology (Raytrix 3D camera systems, Raytrix, Germany [89]) capture information about the intensity and also direction of the light rays utilising an array of micro-lenses [89]. The images or data are then processed and merged using dedicated image analysis software into a single 3D image. Additionally, other commonly used 3D imaging techniques include structured light scanner systems (or coherence scanning interferometery) such as the Artec [90] (Artec Group,USA/Luxemborg/Russia) and ATOS series of scanners [91], and laser scanning devices such as the Minolta Vivid 900 or 910 3D linear laser scanner (Konica-Minolta, Osaka, Japan) [92, 93]. Whole body scanners such as the Cyberware Whole Body Color 3D Scanner (Model WBX, Cyberware Inc, Monterey, California) [94] are also available. These other systems have the ability to scan much larger areas (up to the size of a car with some systems) compared to the Eykona, Lifeviz and Vectra; however, they have not been specifically manufactured or optimised for medical use. For example with the Artec Eva system, the software supplied is able to calculate the surface area and volume of an object on a flat surface but not on curved surfaces. Specialised 3D analysis software such as Rapidform (Inus technology, Seoul, South Korea) [93] is required to measure and quantify surface area and volume information obtained from these scans. The authors are not aware of any published studies that have validated the surface area and volume measurements produced by these devices or software.

A different approach to calculating the surface area of scars is through the use of a combination of 2D photography and 3D models. The Burncase 3D (RISC Software GmbH, Austria) software has been developed for the estimation of burn surface areas primarily but it theoretically can be adapted to measure the surface area of scars. With the Burncase 3D programme, 2D photographs of the lesions are superimposed onto a 3D model that can be adjusted according to the height, weight, age and gender of the patient. The outline of the lesion is then traced onto the 3D model from the photographs (which can be multiple and is aided by an automated alignment algorithm that uses corresponding landmarks to allow quick matching [95]) and the software then estimates the surface area. The areas can also be classified into different categories if needed (e.g. normal and hypertrophic scar areas) and thus useful to track the progression of the wounds from time of burn through to scar formation. As it uses standardised 3D models to estimate surface area, much work is still required to validate the accuracy and precision especially in small children (currently in

progress [96, 97]) and obese patients [95]. In a study which utilised mannequins, the inter-class correlation between the single raters of the mean percentage of artificially created burn areas was 0.988 with relative underestimations of burn wound areas of 0.4 % in the child mannequin, and overestimations of 2.8 and 1.5 % for the female and male mannequins when compared to areas as measured with 2D planimetry imaging [97].

Table 3 below summarises the comparison of 3D measurement devices in terms of parameter measured, reliability, correlation with clinical score and cost.

Thickness

The accuracy of subjective estimation of scar thickness has been shown to be quite low, 67 % (when measured against ultrasound measured thickness) [98] and thus unreliable.

Objective thickness or height of a scar can be evaluated by measurement by 3D photography (see above) or the use of negative–positive moulage [99]. A negative–positive moulage is performed by firstly making a negative impression cast (negative moulage) of the scar using materials such as alginate, silicon, siloxane [58, 72], dental impression material [100] or plaster of paris. A positive impression cast (positive moulage) is then made by pouring a material that will harden (e.g. plaster of paris, wax) into the negative moulage. Once hardened, this positive moulage can then be measured. These techniques have some limitations and are inaccurate as the portion of the scar below the surface of the skin is not included in the measurement [101].

This limitation can be overcomed by using high-frequency (5–20 MHz) ultrasound systems such as the Tissue Ultrasound Palpation System (TUPS; Biomedical Ultrasonic Solutions, Hong Kong) [102–105] , the Dermascan C [30, 53, 106, 107] (Cortex, Hadsund, Denmark) devices, Acuson Sequoia 512 [108] (Siemens, Germany; highest frequency probe available is 10 MHz), HDI 5000 (Philips, Amsterdam, Netherlands) [109], and the Dermcup 2020 (Atys Medica, Soucieu-en-Jarret, France) [110]. High-frequency ultrasound systems have previously been used in many dermatological applications [111].

Ultrasound skin imaging is performed by firing an acoustic pulse into the skin and measuring the acoustic response from the skin which is picked up by an ultrasound transducer. The signals are then processed, and a cross-sectional image is produced which represents an intensity/amplitude analysis of these returned signals. Areas with small changes in density between structures such as scar tissue and fat will produce a low reflection and be visualised as dark colours, whereas areas with significant changes in density between structures (e.g. healthy dermis) will be visualised as bright areas (Fig. 5).

An advantage of ultrasound systems are that they allow real-time measurement on changes of scar thickness upon pressure loading [112]. Additionally, high-frequency ultrasound systems will also allow the identification of aberrant structures within the scars which may affect treatment [113].

The frequency of the ultrasound determines the resolution and penetrance of the measurement. A low frequency will allow deeper penetration but lower resolution images, whereas a higher frequency will have a shallower penetrance but produce higher resolution images (Fig. 6). High-frequency ultrasound systems utilise a frequency above 18 MHz to obtain images of the skin structure with acceptable resolution. In earlier studies, 7.5-MHz probes have been used to measure and track the change in thickness of healing burn scars [101, 114]. These lower frequency systems allow evaluation of deeper tissues (penetration of >15 mm) but have a low resolution of 2–3 mm which may not be sufficient for the evaluation of superficial skin structures [115]. More recently, higher frequency ultrasound probes (20 MHz) have been used to allow more detailed images of the structures of the skin to be visualised, producing higher resolutions of at least 50 μm [115–117]. Probes with frequencies below 50 MHz are advised as systems with higher frequencies and will not be able to penetrate to the average depth of hypertrophic scars which is around 4–5 mm.

It is advisable to always check with the manufacturer the actual penetrance of the systems as cheaper portable ultrasound systems (e.g. Dermalab USB Ultrasound, Cortex, Hadsund, Denmark) only penetrate a maximum of 3.4 mm despite being a 20-MHz system [6].

These high-frequency ultrasound devices both show good inter-observer reliability and moderately correlate with the modified VSS [118] (modified version of the Vancouver Scar Scale by Nedelec et al.), with the Dermascan C system having the better correlation of the two (0.41–0.50 versus 0.34). It has to be noted that the VSS measures clinical scar thickness (i.e. the thickness of the scar that is above the surface of the skin), whereas the two ultrasound systems measure histological thickness (i.e. the whole thickness of the scar above and below the surface of the skin). The Dermascan system would thus be preferred, although it is more expensive than the TUPS (however at the time of writing, there was no method to purchase the TUPS from their website). Other ultrasound systems that are commercially available include the Acuson Sequoia 512 (Siemens, Germany) [119], Episcan(Longport, USA) [120, 121] and the DUB®SkinScanner (EOTech, France) [122], although at present there are no published studies that have utilised these for scar measurement.

Ultrasound systems that can capture a 3D image of a scar have now become commercially available, albeit

Table 3 Comparison of 3D measurement devices in terms of parameter measured, reliability, correlation with clinical score and cost

Device	Company	Parameter	Intra-rater Reliability	Inter-rater reliability	Correlation with clinical score	Cost	Portability	References
Eykona 3D camera	Fuel 3D	Surface area and volume	Intra-operator variability: area: 0.9 %; volume: 4.0 %	Intra-operator variability: area: 1.7 %; volume: 4.0 %	No data	<£5000 for the camera unit. ~£3 for each disposable target but device can now be configured to use reusable targets.	Yes	Paterson et al. (Eykona Medical Imaging FAQ) [86].
Lifeviz I, II, Micro	Quantificare	Surface area and volume	No data	Surface area: ICC = 0.99 (Coefficient of variation 5.9–6.8 %) Volume: no data	Surface area: Excellent level of agreement with Visitrak (ICC 0.96, 95 % CI 0.93, 0.97); however greater level of variability in larger wounds especially circumferential wounds. Volume: $r^2 = 0.9678$ when correlated with actual volumes of model scars	£10,000–£15,000	Yes	Lumenta et al. 2011 [76], Stekelenburg et al. 2013 [75].
Vectra H1	Canfield Imaging Systems Inc.	Surface area and volume	No data	No data	No data	£10,000–£15,000	Yes	Tzou et al. 2014 [256], Urbanova et al. 2015 [80].
Artec Eva	Artec	Surface area and volume	No data	No data	No data	<£10,000 (depends on package)	Yes	N/a
Minolta Vivid 910 3D linear laser scanner	Konica-Minolta	Surface area and volume	No data	No data	No data	>£15,000	Yes	Taylor et al. 2007 [93].
Moulding (positive–negative moulage)	N/a	Volume	ICC = 0.921–0.995	ICC = 0.759–0.977	No data	Dependent on moulding material and measurement techniques used	Yes	Berman et al. 2015 [72].

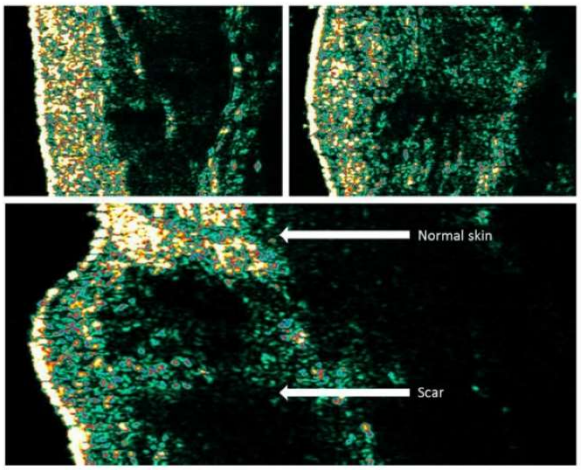

Fig. 5 High-frequency ultrasound image of normal skin (*top left*, site: forearm). High-frequency ultrasound image of hypertrophic scar (*top right*, site: shoulder). High-frequency ultrasound image of normal skin (*top*) and adjacent scar tissue (*bottom*) (*bottom*, site: shoulder). Note that the scars appear more hypo-echoic as it is more homogenic and thus appears darker. Colours represent the intensity of the acoustic signal with bright colours (*yellow*) representing high-intensity and darker colours (e.g. *green*, *black*) representing low-intensity areas. (Source: Kwang Chear Lee, taken with Dermascan C)

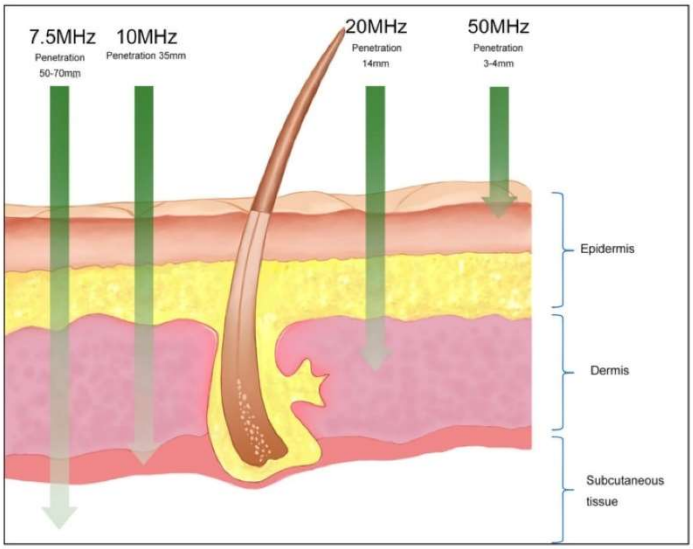

Fig. 6 Different frequencies of ultrasounds and their penetrance into the skin. (Source: Kwang Chear Lee, adapted from image from http://www.eotech.fr/Fiches/produits/107_DUB_Brochure_English_DB10_2012_O.pdf)

only from one company (Cortex, Hadsund, Denmark). However, this system has not been trialled on scars, is limited to a small measurement area (22 × 22 mm) and costs significantly more compared to the 2D system (Table 4).

A summary of the different ultrasound systems is given in Table 4.

Texture

Skin topography

Scar roughness has a significant effect on the patient's and observer's opinion of the scar [4]. Indirect methods of measuring skin topography that involve creating a negative replica of the skin using materials such as polymers (e.g. Silflo silicon polymer; Flexico Developments Ltd., Hertfordshire, UK [123]) and then further analysing this with devices (e.g. mechanical, optical, laser or interference fringe projection profilometry [123–125]), although accurate can be very time consuming and not appropriate for clinical use [126]. Transparency profilometry (using the Visiometer; Courage + Khazaka, Germany) uses the Silflo silicon polymer but analysis is much easier and quicker [127, 128]. However, these indirect measurement techniques have been clinimetrically evaluated [123].

The Phaseshift Rapid In Vivo Measurement Of the Skin [129] (PRIMOS; Omniscan, GFMesstechnik GmbH; Germany) and the Visioscan VC 98 (Courage + Khazaka, Germany) are the only devices currently on the market that can be used to measure skin topography directly, but only the PRIMOS system has published studies in scars.

Three parameters were used for the evaluation of the PRIMOS system by Bloemen et al [129]. These were the peak count (PC, number of peaks per unit length), arithmetic mean of surface area roughness (Sa, in micrometers) and the mean of five highest peaks and five deepest valleys form entire measurement (Sz, in milimeters).

The PRIMOS has been shown to have excellent intra-observer and inter-observer reliability on both normal skin and scars and a high correlation with the relief score of the Patient and Observer Scar Assessment Scale (POSAS) on scar (The relief score in the POSAS questionnaire is the rating given by patients and clinicians on the surface irregularity of their scar compared to normal skin).

An added advantage of the PRIMOS system is that it can also be used to measure scar height [130].

The Visioscan VC 98 is a UVA-light video camera with high resolution that utilises the Surface Evaluation for Living Skin (SELS) method to evaluate the roughness of skin [131]. This method analyses the grey level distribution of the image captures and allows the calculation of four clinical parameters to quantitatively and qualitatively describe the skin surface as an index: skin smoothness (Sesm), skin roughness (Ser), scaliness (Sesc), wrinkles (Sew). As mentioned previously, this system has not been used to evaluate scars but has shown a high reliability for the measure of in vivo skin roughness in normal skin [131]. However, the Visioscan only measures an area of 6 × 8 mm at a time which is probably too small for the analysis of the irregularity of a burn scar.

The aforementioned 3D camera systems can potentially also be used for skin topography analysis. However, these systems are already becoming the preferred devices in the clinic for scar surface area measurement as they are significantly more portable than the PRIMOS system although portable versions of the PRIMOS system are now commercially available (PRIMOS lite, GFMesstechnik GmbH; Germany). Lumenta et al. showed that the Lifeviz Micro 3D camera system (Quantificare S.A., Sophia Antipolis, France) was able to detect surface irregularities (SI) much better than subjective visual assessment which failed to detect at least half of the broader changes in SI of ≥34 % [76]. Kim et al. utilised a self-developed 3D camera system (Stereoimage Optical Topometer, Korea University, Seoul, Korea) to calculate the mean surface area roughness (Sa) and root mean square roughness (Sq) for acne scars which were found to have a positive correlation with visual gradings (Spearman correlation coefficient $\rho = 0.463$ and 0.438 respectively, $p < 0.001$). Table 5 below summarises the surface topography devices.

Biomechanical properties

Pliability, elasticity or stiffness

The biomechanical properties of skin can be measured with a variety of methods including suction, tonometry, torsion, adherence and reviscometry. Other methods include elastometry, ballistometry, quantitative electrical methods (dielectric measurements and bio-impedance) [132] as well as ultrasound and MRI techniques [133].

Non-suction extension methods Older methods of measuring skin elasticity relied on extension methods (i.e. physical stretching) to measure the viscoelastic properties of skin tissue using ex vivo [134] or in vivo extensometers [135–140] or elastometers [58], which utilises a constant-tension spring and a strain gauge to distract two points on the skin [58, 141]. The majority of these devices suffer from an unwanted peripheral force contribution due to the deformation of surrounding tissues during measurement which can lead to reduced accuracy and reproducibility of results, although newer designs have sought to improve their accuracy [137].

Suction extension methods Extension of the skin by suction is the method used by devices such as the Cutometer [18, 28, 106, 142–153] (Courage + Khazaka, Germany) and the DermaLab elasticity probe [144, 154]

Table 4 Comparison of ultrasound devices in terms of parameter measured, reliability, correlation with clinical score and cost

Device	Company	Parameter	Intra-rater reliability	Inter-rater reliability	Correlation with clinical score	Cost	Portability	References
Dermascan C (2D)	Cortex	Thickness (2D)	ICC = 0.91–0.93	ICC = 0.90–0.91	Modified VSS and ultrasound thickness: Spearman's $r = 0.41–0.50$	£15,000–20,000	Yes	Nedelec et al. 2008 [30, 106].
Dermalab USB (2D)	Cortex	Thickness (2D)	ICC = 0.92–0.97	ICC = 0.86–0.98	No data	<£10,000	Yes	Gankande et al. 2014 [6].
Dermascan C (3D)	Cortex	Thickness (3D)	No data	No data	No data	£30,000–40,000	Yes	N/a
Tissue ultrasound palpation system	Biomedical Ultrasonic Solutions	Thickness (2D)	ICC = 0.98	ICC = 0.84	Spearman Correlation of 0.42 between VSS thickness score and TUPS measurement ($p < 0.01$), and $r = 0.34$ ($p < 0.01$) between VSS total score and TUPS.	Not currently commercially available.	Yes	Lau et al. 2005 [103].

2D = two-dimensional; *3D* = three-dimensional; *ICC* = intra-class correlation coefficient; *VSS* = Vancouver Scar Scale; *TUPS* = Tissue Ultrasound Palpation System

Lee et al. Burns & Trauma (2016) 4:14

Table 5 Comparison of surface topography measuring devices in terms of parameter measured, reliability, correlation with clinical score and cost

Device	Company	Parameter	Intra-rater reliability	Inter-rater reliability	Correlation with clinical score	Cost	Portability	References
PRIMOS	GFMesstechnik	Surface roughness (PC, Sa, Sz)	ICC of PC = 0.97, Sa = 0.99, Sz = 0.98	ICC of PC = 0.9, Sa = 0.96, Sz = 0.94	Correlation with POSAS: $r = 0.617$ ($p < 0.001$)	£17,000–£14,000	Yes	Bloemen et al. 2011 [129].
Visioscan VC 98	Courage + Khazaka	Skin parameters (Sesm, Ser, Sesc, Sewi)	Not been used in scars	Not been used in scars	Not been used in scars	£5000–£10,000	Yes	N/a
Eykona 3D camera	Fuel 3D	Not been used in scars	Not been used in scars	Not been used in scars	Not been used in scars	<£5000	Yes	N/a
Lifeviz Micro	Quantificare	Surface Irregularity	No data	No data	Performed better than subjective visual assessment	£10,000–£15,000	Yes	Lumenta et al. 2011 [76].

PRIMOS = Phaseshift Rapid In Vivo Measurement Of the Skin; *ICC* = intra-class correlation coefficient; *PC* = peak count; *Sa* = mean surface area roughness; *Sz* = mean of five highest peaks and five deepest valleys; *POSAS* = Patient and Observer Scar Assessment Scale

(Cortex Technology, Hadsund, Denmark). With the Cutometer, negative pressure is created in the device by vacuum and the skin is drawn into the aperture of the probe and after a defined time is released again. Inside the probe, height of skin that is drawn up is determined by a non-contact optical measuring system which consists of a light source and a light receptor, as well as two prisms facing each other, which project the light from transmitter to receptor (Fig. 7). The resistance of the skin to the negative pressure (firmness) and its ability to return into its original position (elasticity) are displayed as curves (penetration depth in mm/time) in real time during the measurement (Fig. 8). This measurement principle allows getting information about the elastic and mechanical properties of the skin surface.

The Cutometer is reliable for measurement of the elastic and mechanical properties in scars and normal skin; however, its measurements only have a weak to moderate correlation with the pliability score of the POSAS and the subjective pliability assessment of the VSS [142]. Rennekampff et al. also suggested that the Cutometer may not be sensitive enough to pick up small changes in pliability as he found no correlation was found between subscale VSS pliability rating and Cutometer readings [155].

It was also found to be unreliable for severe scars due to a ceiling effect when rigid tissue is encountered [106]. However, the low ICC values have more to do with difficulty in relocating device to same measurement spot and the high sensitivity of the device [30, 106].

The mechanical parameters of the skin can be divided into absolute and relative parameters:

- Absolute (in milimeters): Ue (immediate deformation), Uv (delayed deformation), Uf (maximal deformation), Uf (immediate retraction), Ua (final detraction), R (residual deformation), R8 (visco part).
- Relative (in percentage): Ua/Uf (gross elasticity), Ur/Uf (biological elasticity), Ur/Ue (net elasticity), Uv/Ue (viscoelastic to elastic ratio), H (hysteresis).

Absolute parameters are likely to be influenced by skin thickness which in turn is dependent on various factors such as age, gender, anatomical region thus to compare values you will need to standardise them for skin thickness using an ultrasound and this is not always possible thus the relative parameters are more useful as it can be assumed to be independent of skin thickness which allows the values in different subjects, anatomical regions and times to be compared.

Various different opinions regarding the value that should be used (Table 6); however, Draaijers et al. concluded that either Ue or Uf is sufficient for the evaluation

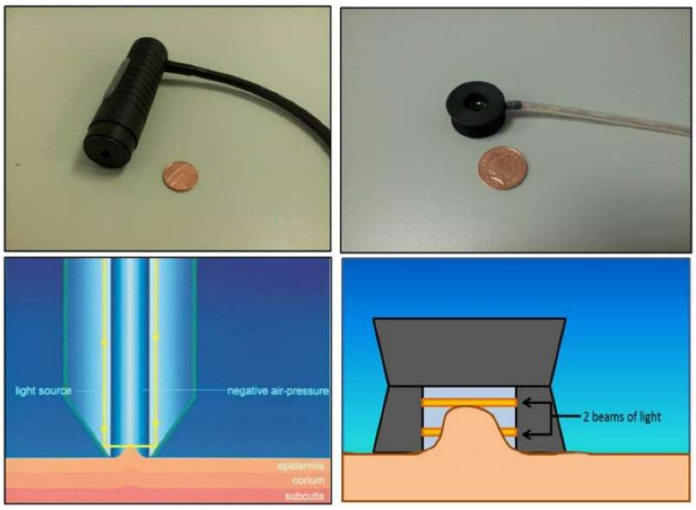

Fig. 7 The Cutometer (*top left*) and Dermalab elasticity probe (*top right*), one penny coin to provide an idea of the size of the probes. Illustration of the mechanism of the Cutometer and Dermalab elasticity probe (*bottom left* and *right*, respectively). (Source: photographs and diagram of elasticity probe by Kwang Chear Lee; Cutometer image source: Courage + Khazaka Electronic GmbH, http://www.courage-khazaka.de/index.php/en/products/scientific/140-cutometer, reprinted with permission)

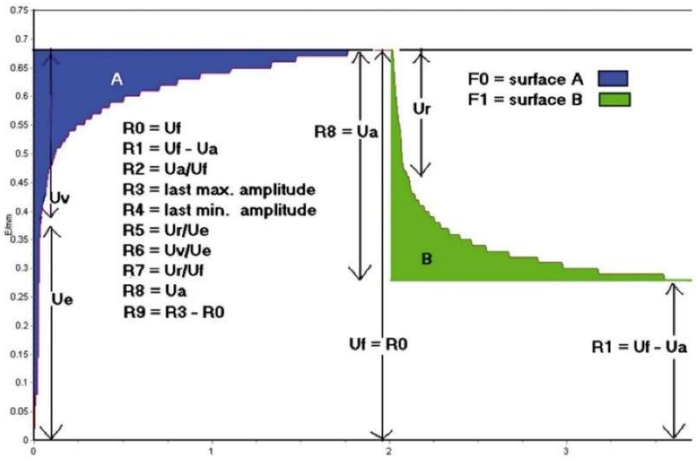

Fig. 8 Example of skin deformation curve obtained with the Cutometer. (Source: Courage + Khazaka Electronic GmbH, reprinted with permission)

of scar as they found a high correlation between the parameters Ua, Ue, Uf, Ur and Uv, and that Ue and Uf were found to have the highest reliability. Nedelec et al. agreed with this and also found Uf to have a higher reliability (but not for severe scars) but concluded that as Uf is more convenient to record (automatically calculated by computer software, whereas Ue requires manual calculations), it should be used instead.

Other studies have also utilised the R (dimensionless parameters derived from the U values) and Q (maximum recovery, elastic recovery and viscous recovery areas) values [143].

The Dermalab elasticity probe [6, 156] consists of a light plastic probe that is much smaller than that of the Cutometer (Fig. 5). This probe is attached to the skin using double-sided adhesive rings to form a closed chamber. Within this chamber, two narrow beams of light run at different heights parallel to the skin surface and serve as elevation detectors [154] (Fig. 5). A computer controlled vacuum pump connected to the probe is then used to increase the suction within this closed chamber over 30–60 s. In contrast to the Cutometer where a set pressure is applied and the skin deformation is measured, the Dermalab elasticity probe measures the amount of suction (in kilopascals, kPa) that is required to lift the skin to pass the height of the two light beams. This may cause problems when the measured skin is too stiff to be stretched enough to reach the level of the detectors [154]. The stiffness of the skin (or Young's modulus, E) is then calculated and expressed in millimeter per kilopascal. Skin that is firm, e.g. scar tissue will have a higher stiffness index compared to normal skin.

Table 6 Comparison of used and recommended parameters for the cutometer in different papers

Authors and papers	Parameter used/recommended
Fong et al. 1997 [146].	Uf, Ur/Uf, Ur/Ue, R8
Draaijers et al. 2004 [147].	Recommends Ue or Uf
Dobrev et al. 2005. [257]	Recommends Ue and Uf (distensibility), Ua/Uf and Ur/Uf (elasticity) and Uv and Uv/Ue (viscoelasticity)
Nedelec et al. 2008 [30, 106].	Recommends using only Uf
Rennekampff et al. 2002 [155] and 2006 [142].	Uf, Ua, Ur, Ue, Ur/Ue and Ur/Uf

A study by Gankande et al. with the Dermalab elasticity probe showed that the test–retest reliability for pliability was "excellent" (ICC 0.76–0.91) in scar areas but only "good" (ICC 0.45, 95 % CI 0.30–0.76) in contralateral normal skin areas [6]. It should be noted that significant difficulties were encountered by the researchers in the study in obtaining elasticity measurements and they failed to obtain matched measurements for test–retest analysis in 31–52 % of the subjects [6].

Both devices have the advantage of being a "hub" to which other measuring devices can be attached. For example, the Dermalab combo device provides additional probes that can be fitted to provide spectrophotometry data (melanin and erythema) and ultrasound measurement of dermal thickness [6].

Tonometry

Tonometry measures the firmness and flexibility of skin and scars by exerting pressure either via an airflow

system that is blocked at a certain pressure (e.g. Pneumatometer [157] (Medtronic Solan Model 30 Classic, Jacksonville, FL, USA), Cicatrometer [114], Tissue Tonometer [158] (Flinders Medical Centre Biomedical Engineering, Australia) or an indentional load in a vertical direction, e.g. durometer [114, 158–161] (Rex model H 1000, Rex Gauge company, IL, USA), Schiotz tonometer [162], and Tissue Compliance Meter [163] (Model and company not stated by author). In the study by Lye et al., the Tissue Tonometer showed good intra-observer reliability and a moderate correlation with the pliability score of the VSS scale, but the measure is a relative one as it requires a contralateral reference point [158]. A study by Corica et al. [164], utilising a modified Tissue Tonometer, showed that the intra-class correlation coefficient for averaged measures between measurers (inter-rater reliability) was 0.957, and the standard error of measurement was 0.025 mm. A significant difference ($p = .0000$) between scar (2.64 ± 0.5 mm) and normal tissue (3.23 ± 0.46 mm) measurements was also demonstrated in the study. Tonometry devices are, however, less suitable for skin locations with hard bony structures underneath—as the hard underlying structures limit the degree in which the skin can be compressed. At the time of writing, the mechanical tonometer is no longer commercially available but a digital version is in the experimental phase. Other shortcomings with the mechanical design include the need to place the device accurately (must be within 5° of upright to measure correctly).

The durometer also showed good reliability and validity in one study but this was performed on sclerodermal skin [160] which demonstrates symmetrical skin thickening compared to scars where thickening can vary from area to area depending on the initial injury.

Torsional force and adherence measurement methods

Torsional force can be used to measure the elasticity of skin (Dermal Torque Meter; Dia-Stron, UK) [165] and the device is able to differentiate between native skin, autographs and cultured skin substitutes; however, rigorous clinical appraisals of the device have not yet been performed.

Acoustic methods

The Shear Velocity Device (SVD) is a portable tool that can be used to analyse soft biologic tissue by measuring the propagation of an auditory shear wave through the skin surface [166, 167]. The device works on the principal that an acoustic shear wave will have a higher velocity in a hard material (e.g. scar tissue) compared to softer material (e.g. normal skin). Experimental validation of the SVD by McHugh et al. claims that it provides similar results to the Shore Type A durometer; however, this data has yet to be published [166]. The coefficient of variation (CV) for the device in measurements of 254 hypertrophic scar locations was ±4.8 % whilst on 210 normal skin sites this was ±4.4 %. Unfortunately, the authors have not been able to locate any subsequent publications on this device and it is not currently commercially available.

Revisometry [168] (Reviscometer; Dermaviduals and Courage + Khazaka, Germany) is another portable tool that measures the elastic and viscoelastic features of skin and scars by utilising an acoustic shock wave and reports this as resonance running time (RRT). Scars have a significantly lower mean RRT compared with normal skin (52.3 versus 91.6). It has been shown to be reliable with inter-rater observer reliability of more than 0.86 on scars but more studies are required to establish its validity and comparative performance.

Electrical of bio-impedance methods

Utilising an impedance device, the capacitance of scar tissue has been shown to be stronger than that of normal skin and the resistance of scar tissue is lower than that of normal skin. The impedance of scar tissue however varies according to the depth and density of scar tissue [132]. This electrical property of scar tissue could be utilised to quantify scars; however, no method has been developed as of yet.

Modelling and other techniques

All of the methods that have been discussed thus far rely on measurements in a small area of the scar which may not be representative of the scar as a whole.

The Adheremeter [169] (Fondazione Salvatore Maugeri, Italy) uses an entirely different approach and measures the restriction of scar mobility with respect to the underlying tissue at the worst adherent point when stretched in 4 orthogonal directions using a transparent film print-out of 9 concentric rings with varying radii. It is a relatively new device and has only been tested in one study [169] but it showed an adequate level of reliability and validity when compared to the VSS. However, it has a degree of subjectivity in operation as the measurement is based on the rater's evaluation of the force required to stretch the skin and on the patient's judgement of comfort. It is also not suitable for use on highly concave surfaces.

A different approach to measuring the elasticity of skin is to use computerised models of skin motion analysis [170, 171]. These experimental methods are able to detect and measure the differences in elasticity between normal and scar tissue by comparing images taken at two time instances before and after deformation. Regular 2D images, combined with 3D data, can offer a method of estimating scar pliability in a more global manner [94]. In simple terms, these methods utilise a grid painted onto the skin which will then deform according to the elasticity

of the skin. Grid portions that are less pliable (scar tissue) will deform less than areas which are more pliable (normal skin). A technique called Finite element modelling (FEM) can then be used to analyse this information [170–173]. This technique is still experimental and yet to be commercially available. Some devices that may be commercially available soon that utilise this technique include CutiScan CS 100 (Courage + Khazaka, Germany) which is still under development.

Other methods include the measurement of ranges of movement to determine the severity of burn contractures and thus indirectly the viscoelasticity of the scars. The current standard involves the measurement of the passive and active range of motion of an extremity in a single plane or functional movements (which are better related to activities of daily living) [174] using conventional measurements [175] (e.g. goniometry, tape measures, inclinometer) or 3D motion analysis [174, 176, 177]. The Faciometer (University of Vienna) measures the ranges of mimic movements, e.g. the distance between the tragus and the mouth using calipers and an electronic display [178]. A survey by Parry et al. however showed that there is a lack of consensus in the methods and tools used clinically for the measurement of burn contracture and these methods are also rarely checked for reliability or performance competency [175].

Table 7 gives a summary of the comparison of viscoelasticity devices in terms of parameter measured, reliability, correlation with clinical score and cost.

Comparing the devices that measure biomechanical properties of scars, the Cutometer seems to be the best choice at present as it is reliable (in normal, non-hypertrophic scars), shows a reasonable validity and can be used over bony areas. Additionally, the Cutometer is the most often used device for skin viscoelasticity measurements with more publications than most of the other devices reviewed in this paper.

Pathophysiological disturbances

Pathophysiological disturbances are defined as functional changes in the skin associated with, or resulting from, disease or injury, with measurable parameters including gas perfusion and moisture content.

Transcutaneous oxygen tension

Transcutaneous oxygen tension ($tcpO_2$) is perturbed in injured tissues and can be used as an index of maturity in hypertrophic scars. The $tcpO_2$ in scar tissue is lower compared to healthy skin, and an increase in $tcpO_2$ is correlated with a reduction in scar thickness assessed both clinically and by ultrasound [179]. This is thought to be due to low oxygen diffusibility through scar tissue. A study by Ichioka et al. [180] has also shown in animal and human tissues that immature repairing tissues consumed more oxygen than mature tissues and that the oxygen consumption rate in keloid and hypertrophic scars were significantly higher when compared to mature scars which may also explain the lower $tcpO_2$ in scar tissues. The method for measuring transcutaneous oxygen tension exploits the redox reactions that occur in a modified Clark electrode that measures the oxygen ($tcpO_2$) and carbon dioxide ($tcpCO_2$) tension on the surface of the skin. The $tcpCO_2$ is considered non-specific and highly dependent of external factors, whilst the $tcpO_2$ is a much more precise indicator of local perfusion [181]. This technique seems to have been recently abandoned from clinical practice.

Transepidermal water loss and moisture content

The water content of the skin is an important factor that influences the softness and smoothness of the skin, and transepidermal water loss and skin hydration are key indicators of skin function. Transepidermal water loss (TEWL) and moisture content can be measured by open and closed chamber systems. Open systems such as the Dermalab TEWL module [182] and Tewameter [183] (Courage + Khazaka, Germany) are the most frequently used (Fig 9). Closed systems such as the Vapometer (Delphin Technologies, Finland) are also available, but one study has shown that the Tewameter is able to detect significantly smaller differences in TEWL when compared to the Vapometer [184]. Anthonissen et al. showed a significant difference in mean TEWL values between normal skin and spontaneously healed scars ($p = 0.036$) and a significant negative relation between mean TEWL values and time after burn ($p = 0.008$); however, high SEM values were reported [156, 185].

The hydration of the skin layers, specifically the stratum corneum, can also be measured using electrical methods, such as the conductance method (for example, the Skicon-200 conductance meter [186, 187], IBS Co, Hamamatsu, Japan, Location, and the NOVA Dermal phase Meter [188], Nova, Technology Corp., Gloucester, Mass.) and impedance method (for example, the Corneometer [186], Courage + Khazaka, Germany). One study has shown that the Corneometer is suitable for use in clinical trials, with useful intra-class correlation coefficient (ICC) values (ICCintra = 0.985; ICCinter = 0.984), but only under very strict conditions with a standardised test protocol [189]. Another method for measuring hydration (and protein content) is to measure the dielectric properties of the skin. This is based on the interaction of high-frequency electromagnetic (EM) waves and biological material [190, 191]. The EM waves are generated using a network analyser (HP8753B, Agilent, USA).

A study by Suetake et al. found that TEWL was a better parameter for the functional evaluation of scars than

Table 7 Comparison of viscoelasticity devices in terms of parameter measured, reliability, correlation with clinical score and cost

Device	Company	Parameter	Intra-rater Reliability	Inter-rater reliability	Correlation with clinical score	Cost	Portability	References
Cutometer	Courage + Khazaka	Viscoelastic parameters	Ranges from unacceptable to good (0.12–0.76)*; poor in severe firm scars	Ranges from unacceptable to good (0.11–0.93)*, poor in severe firm scars	Low to moderate, but significant (Spearman's $r = -0.29$ to -0.53). Rennekampf et al. could not find any significant correlation between objective viscoelastic measurements and the subjective pliability assessment of the VSS.	£5000–£10,000 (with hub)	Yes	Nedelec et al. 2008 [30, 106], Draaijers et al. 2004 [147], Rennekampf et al. 2006 [142].
Dermalab Elasticity probe	Cortex	Viscoelastic parameters	ICC = 0.90–0.93; limited ability to measure rigid scars	ICC = 0.86–0.93; limited ability to measure rigid scars	No data	£5000–£10,000 (with hub)	Yes	Gankande et al. 2014 [6].
Tonometer	Flinders Medical Centre Biomedical Engineering	Viscoelastic parameters	ICC = 0.90–0.94	ICC = 0.948	Negative correlation between VSS pliability scores and tonometer readings: −0.457 and −0.442 respectively for 3 and 6 second readings.	No longer commercially available	Yes	Corica et al. 2006 [164], Lye et al. 2006 [158].
Durometer	Rex Gauge company	Viscoelastic parameters	No data	No data for scars but ICC = 0.82–0.92 for sclerodermal skin	Good correlation with modified Rodnan skin score (0.70) for sclerodermal skin	<£1000	Yes	Merkel et al. 2008 [160].
Dermal Torque meter	Dias-tron	Viscoelastic parameters	No data	No data	No data	N/a	Yes	Boyce et al. 2000 [165].
Adheremeter	Fondazione Salvatore Maugeri	Viscoelastic parameters	Good (0.96)	Good (0.87–0.99)	Moderate correlation with VSS and Pliability subscale of VSS ($rs = -0.58$ to -0.66)	Free	Yes	Ferriero et al. 2010 [169].
Reviscometer	Courage + Khazaka	Resonance running time	Good (>0.86)	No data	No data	£10,000–15,000 (with hub)	Yes	Verhaegen et al. 2010 [168].
Vesmeter	Wave Cyber Co. Ltd.	No data	No data	No data	No data	N/a	Yes	Niyaz et al. 2012 [246].
Shear Velocity Device	N/a	Shear wave propagation velocity	No data for ICC. (CV for scars is ±4.8 %)	No data	No data	Not commercially available	Yes	McHugh et al. 1997 [166].

*Low ICC values for Cutometer may also be attributed to the difficulty in relocating device to same measurement spot and the high sensitivity of the device [30]
ICC = intra-class correlation coefficients; *CV* = coefficient of variation; *VSS* = Vancouver Scar Scale

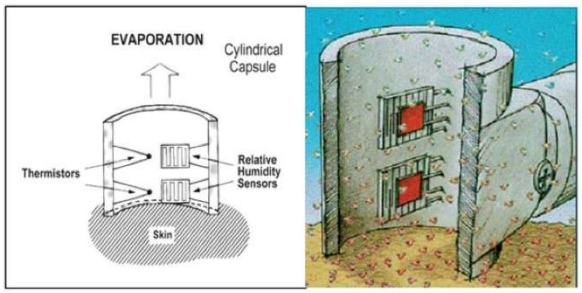

Fig. 9 Open chamber transepidermal water loss system. (Source: Courage + Khazaka Electronic GmbH and Cortex Technology, reprinted with permission)

was the hydration state of the skin surface measured by high-frequency conductometry [192].

Multispectral imaging systems

A novel polarised multispectral imaging system that combines out-of-plane Stokes polarimetry and Spatial Frequency Domain Imaging has been developed by Ghassemi et al. and allows the colour (haemoglobin, melanin), pathophysiology (blood oxygenation, hydration) as well as structural features (cellularity and roughness) of hypertrophic scars to be analysed in vivo [193, 194]. The results obtained with this multi-modal system showed a good agreement with the VSS and with histological examinations [193]. Although still in experimental stages, it could potentially simplify the scar measuring process due to its multi-modal measurements.

Non-invasive morphological imaging techniques

Previously, histopathological analysis of biopsy samples was the only method of morphological investigation of damaged biological tissues. Now, recent advances in imaging techniques have made non-invasive in vivo morphological investigation of tissue microstructure possible.

Optical coherence tomography

With the advances in fibre optics and other technologies such as ultra-broadband light sources and frequency domain techniques, optical coherence tomography (OCT) imaging that is capable of generating 3D images of tissue microstructure is now possible. OCT is most frequently used in ophthalmology [195] but can be adapted to be used to analyse the skin [196–203]. OCT can be utilised in various different modes for the assessment of scars [202, 203]. The layered arrangement of normal skin is perturbed in scarred skin so that OCT can be used to provide information about microstructure as well as depth and volume [196]. Scar tissue imaged by OCT appears dense and bright due to the increased collagen content, and this parameter can be used to measure the collagen status of scars [204]. Scar microvasculature density has been quantified using an automated OCT system and found to be increased in hypertrophic scar tissues (38 %) when compared against normal, unscarred skin (22 %) [201]. Vessels in scars have also been shown to be much larger compared to normal skin on OCT [205]. However, due to the strong scattering and absorption of light by skin, current OCT methods are only capable of imaging to a depth of 1 to 2 mm, whereas scar thickness is usually greater than 2 mm (as determined by ultrasound) [6, 103, 206]. Nevertheless, in areas where scar tissue is thinner (e.g. in fingers), OCT (utilising the 1300-nm wavelength region) may still be useful [196]. Another way of differentiating scar tissue from normal tissue using OCT is the use of the attenuation rate, which is defined as the rate at which the OCT signal decreases with depth in the tissue [203]. Lower attenuation coefficients are seen in scarred tissue compared with normal skin tissue [203]. This method bypasses the problem of penetration depth but yields less detailed morphological data when compared to standard OCT methods. A form of OCT (termed "Polarization-sensitive Optical Frequency Domain Imaging") can also be used to image collagen remodelling [207].

OCT imaging has been demonstrated to be feasible for use in the clinical monitoring of scar progression automated quantification of vascularity in cutaneous burn scars [195]. OCT imaging for scarring and fibrosis is currently still in its infancy and further development in the technology is required. In a study by Eraud et al. [208], although OCT was able to detect dermal nodules (which are present in hypertrophic but not keloid scars [209]) in 100 % of the specimens, it was not helpful in identifying hyalinised collagen (which is present in keloids) and cells. The technology however has the potential for tremendous growth [204].

Other in vivo tomography/microscopy techniques

Imaging techniques utilising specialised optical microscopes have been used to image scar tissue.

Nonlinear spectral imaging, such as multi-photon tomography based on both two-photon excited fluorescence (TPEF) and second harmonic generation (SHG), can be utilised to demonstrate the morphological structure and spectral characteristics of collagen (with SHG) and elastin fibres (with TPEF) and thus can be used to potentially distinguish hypertrophic scar tissues from normal skin and to evaluate the effects of treatments [210–216]. Information on the orientation of collagen fibres can also be investigated and analysed from these images using fast Fourier transform methods [217, 218]. Advantages these techniques have are that several extracellular matrix components and endogenous biomolecules such as collagen, keratin, melanin and elastin can be visualised in living tissue without the need for specialised processing or staining [219, 220] and high-resolution, high-contrast three-dimensional images can be obtained [220, 221].

These techniques however have similar drawbacks to OCT. The maximum depth of two-photon imaging has been reported to reach up to 1 mm in living brains [222] and thus is comparable to OCT imaging but clinical use in the skin is typically only up to 200 μm, thereby limiting its potential utility for deep scar assessment. In addition, advances in the miniaturisation of spectral imaging apparatus need to be made before it can become of practical use in a clinical setting. The multi-photon technique also has high overall system costs, a long measurement times and the inability to quantify skin redness [223]. Other non-invasive in vivo imaging techniques which currently being developed, such as confocal laser microscopy (CLM) [224, 225], also have a limited imaging depth (~300 μm) due to tissue-related aberrations and light scattering [226].

Other similar microscopy techniques include phase-contrast microtomography with synchrotron radiation technology to detect the 3D structure of dermal tissues [221].

Spectroscopy techniques

Another imaging method that holds future promise is the use of optical spectroscopy methods in the UV-visible-near-infrared wavelength range, including diffuse reflectance (DR) and autofluorescence (AF) spectroscopies. DR spectroscopy is based on the scattering of photons (350–800 nm) inside biological tissues due to the differences in the refractive indices and morphology of the constituents of skin such as collagen fibres. AF spectroscopy, on the other hand, is based on the fluorescence emissions from endogenous fluorophores such as collagen and elastin when excited by light in the 350–459 nm wavelength range. A combination of both spectroscopy methods increases its accuracy [227] and has been used successfully in a rabbit hypertrophic scar model with high sensitivity and specificity [228, 229]. DR spectroscopy on its own has also been shown to be able to differentiate keloids from normal skin in terms of collagen concentration, haemoglobin oxygen saturation and scattering coefficient in an in vivo human study [217] and can potentially be used to evaluate keloid scar severity [230].

High-frequency ultrasound systems

High-frequency ultrasound systems (such as the Dermascan and Dermalab systems [6], Cortex, Denmark) are able to provide a much greater depth of imaging (~8 mm at 20 MHz) but the resolution is inferior to OCT, CLM and MPT [196]. Pathological scars appear as easily identified echo-poor areas that are clearly distinguishable from normal skin and with densitometry analysis with dedicated software, scars are also shown to have significantly reduced densitometric values compared with normal skin (7.6 ± 4.7 versus 31.79 ± 10.8) [231]. More detailed architectural information such as collagen arrangement and cell structure cannot currently be visualised with 2D nor 3D ultrasound techniques.

Intravital video-capillaroscopy

Intravital video-capillaroscopy [232] is a technique that utilises an optic contact probe microscope that is attached to a computerised video microscope (e.g. Microwatcher Model VS-901, Mitsubishi Kasei Corp, Tokyo, Japan [232]) which allows photographic images of skin capillaries to be taken. Scarred skin has a deranged capillary organisation. The pictures are then scored either subjectively and/or objectively. Subjective methods score images according to angiogenic markers [232, 233] such as enlarged or tortuous loops, architectural derangement, neoangiogenesis and quantitative changes of capillary lesions. These scoring systems can be modified to allow objective quantification [234, 235]; for example, the methods used in a study by Hern et al. allowed for both non-stereological measurements (microvessel density and vessel image width) and stereological measurements (image area fraction and microvessel length density) [235]. Intravital capillaroscopic measurement of capillary density (CD) has been shown to be reliable and reproducible with a mean coefficient of intra-observer variation of CD estimate of 5.6 % and the inter-observer correlation coefficient of 0.94 [236].

A similar technique, dermoscopy, and its use in the examination of vascular structures can be a clinically

useful diagnostic tool for differentiating between keloids and hypertrophic scars [237].

The dermoscopy can be used to visualise capillaries and pigmentation in the epidermal and dermal layers of the skin. An added advantage is that since dermascopes have their own light source, it is not likely to be affected by differences in environmental lighting which has been shown by Wei et al [238].

Wei et al. [238] showed that the L* (or lightness reading) from the Dermoscope (Hong Kong Productivity Council) had a significant correlation (0.448–0.536, $p < 0.01$) with the readings from the MiniScan XE Plus spectrocolorimeter (HunterLab, Reston, VA, USA) and VSS scores of pigmentation (when the skin was blanched with pressure; $r = 0.783$, $p < 0.01$). The RGB values of redness also showed a strong correlation with the VSS scores of vascularity ($r = 0.625$, $p < 0.01$). Both the intra-rater and inter-rater reliability of the dermoscope were found to be excellent (0.965–0.98 and 0.871 to 0.930, respectively).

Measurement of sensory change

A majority of patients with burn scars experience a change in sensation of the scarred skin such as pruritis, pain and hyper- or hypo-sensitivity is common in scars and this can often last for years after the initial injury [239]. However, the objective measurement of such sensory deficits is challenging task and the only gold standard for pain assessment available currently is self-report.

Functional MRI (fMRI) scans have shown promise in assessing pain in the absence of self-report however it is far from ready for regular clinical use [240]. However, skin sensitivity/touch and (indirectly) pain can be examined in an objective manner with the touch pressure threshold method (TPT) using for example Semmes Weinstein monofilaments, which have been shown to have good intra- and inter-rater reliability (ICC = 0.822 and 0.908, respectively) in patients with scars [241].

More recently, an electronic version of the von Frey filaments is also available and showed better reproducibility compared to the traditional von Frey with good to almost perfect intra-observer reliability (ICC ranges from 0.61 to >0.8) (study done on normal skin, not scars) [242, 243].

Discussion

There have been significant advances in many aspects of burn treatment, but hypertrophic scarring remains as one of the major chronic problems after severe burns with few therapeutic options currently available. The accurate assessment of scarring is an important aspect of research into better treatments for this condition. Despite this, scar assessment is still mostly subjective and there is still little consensus regarding the ideal scar measurement tool [244].

Most if not all currently used subjective scales used in evaluating skin scars assume that scar dimensions conform to linear models and thus employ equal appearing interval (EAI) scales. However, a study by Brandt et al. showed that whilst pliability, thickness and surface area were defined well using linear models, the dimensions of vascularity and pigmentation were more accurately described using curvilinear functions [245].

Tools for scar measurement are often modified from tools developed for other industries, e.g. dermatological use in the cosmetic industry, such as the Cutometer; colour probes for measuring the colours of materials in the food and building industries and durometers such as the Vesmeter for testing the hardness of materials in the manufacturing industry [246]. As such, their utility for burns patients is mostly unproven. Accordingly, trials on these tools to evaluate their accuracy and reliability are scarce and few trials have compared the different devices.

The ideal assessment of scars should include the objective and subjective aspects of scars as well as an assessment of the functional limitations that are caused by the scar tissues [94]. The different physical aspects of scars can all change independently of each other during the course of scar evolution and as such a hybrid method of scar assessment which incorporates the most reliable and feasible methods should be used [247]. Combination systems such as the Dermalab combo which incorporate multiple scar measurement tools (e.g. colour, thickness and pliability [6, 248]) are now available [248] to facilitate this although improvement in the clinical interpretation of the measurements is required [247].

A problem with validating objective scar measurement tools is the lack of an ideal gold standard.

Biopsies and standard histological analysis whilst proven to be accurate mostly rely on subjective scoring systems [249] unless quantitative measurement techniques are used [43]. Furthermore, Singer et al. showed that histomorphologic scales have been shown to only correlate fairly with gross macroscopic scores [249]. Beausang et al. also found that the clinical scar appearance correlated better with the upper portion of the skin (epidermis and papillary dermis) compared to the deeper parts of the scar [43]. Therefore, the lack of correlation of objective measurement techniques with clinical subjective scores should be considered carefully and not used to dismiss the objective methods.

Future validation studies of pigmentation and vascularity may be possible with standard colour reference cards developed for the cosmetic industry [250].

Objective scar measurement tools are important, especially for interventional clinical studies, as scars and the effect of therapies can be described, analysed and compared more accurately than is possible with

subjective scar scales. Subjective scar scales however should still be incorporated into studies as they can provide a more global assessment of the scar and allow the measurement of variables that are currently not possible with objective measurement devices, such as pain and itch. Indeed, several published studies have incorporated both subjective and objective scar measuring tools [251, 252].

The implementation of objective measurement devices into standard clinical practice still faces many obstacles and there are multiple reasons why potentially great technologies are struggling to get incorporated into the health care system.

As mentioned previously, many new technologies (including all if not most of the devices mentioned in this review) have been developed for non-medical uses and very little if any input has been sought from clinicians or patients during the design process, and thus these devices may have limited practical clinical use. The lack of data security features is also a factor although this issue probably applies more to mobile apps rather than physical devices.

Some clinicians also view the use of new technologies in clinical practice as a crutch to the development of clinical acumen even though many studies have shown that clinical judgement to perform poorer, e.g. in determining surface area [253] or burn depth [254].

Another main issue is the high cost of these devices. Even the simplest of devices, e.g. colour probe, costs at least >£3000 not including annual servicing costs. Without solid research evidence of clinical and patient benefit, it is difficult to justify the costs and use of these devices outside of research.

Despite many of these devices being fairly simple to use, a certain level of technical expertise and additional clinical time to collect and analyse the data generated is still required. To take an example, electronic health records have been used more frequently in hospitals nowadays but it takes longer for an average clinician to input data into the electronic system than onto a paper record for months, even years, after they have started using them [255]. This has been anecdotally quoted as one of the main reasons why some burn clinicians have been slow to adopt new technologies such as LDI in determining burn depth even though there is strong evidence for its accuracy compared to clinical judgement. Staff specially trained in the use of these devices and who are responsible for training of other staff and championing their use in regular clinical practice may be the way forward [255].

Lastly, the scope of this review largely did not include journals or articles in physical sciences or engineering which may have unearthed more potentially useful objective scar measurement devices.

Conclusions

In this review, we aimed to recommend a panel of objective scar measurement tools for burn scars to be used in conjunction with subjective scar scales, that were reliable, patient friendly, and easy to use (feasibility in terms of cost and portability have now been commented on in the tables in the various sections); generated simple data; and were appropriate for use in a clinical (bedside) environment (i.e. portable). We included in the panel the least number of devices that could measure surface area, colour, thickness, pliability, texture or topography and pathophysiological skin disturbances in order to reduce measurement time and cost. All of the devices considered for inclusion have to be commercially available. As such, the recommended device panel for burn scar assessment is as follows:

- *3D wound measurement camera systems (Eykona/Lifeviz/Vectra H1)*: for surface area, texture, volume (including clinical thickness) and colour.
- *Dermascan*: for histological thickness measurements (the TUPS is an alternative but not commercially available).
- *DSM II Colormeter*: for colour measurements (both Tristimulus reflectance colorimetry and narrow-band simple spectrophotometry).
- *Cutometer system*: for viscoelastic measurements of the skin.
- *Tewameter (optional probe for the Cutometer system)*: for the measurement of transepidermal water loss.

Further studies are needed to validate the performance and utility of this scar panel and to compare them with the commonly used subjective scar scales, such as the POSAS.

It is recommended that new technologies to be utilised in objective measurement should ideally be evaluated in terms of intra- and inter-rater reliability (with at least two observers) before being used in trials; however, this could be time and resource consuming. Collaborations should be established between the industry, clinical research and patient groups to streamline and refine this process and encourage the testing and introduction of improved devices.

Although there is a greater emphasis now compared to previous decades on developing and evaluating devices that measure physical scar parameters, scarce attention has been given to measure the physiological characteristics of scars. It is essential to develop tools that can be used to measure and quantify metabolic and cellular activity in scars so that treatments can be tailored to the individual.

Competing interests
The authors declare that they have no competing interests.

Authors' contributions
KL conceived and designed the review, collected the data (including searches, screening and extracting data from the papers) and wrote the manuscript. KL and JD designed the search methodology. LG, AL and NM provided general advice on the review and reviewed the manuscript drafts before submission. All authors read and approved the final manuscript.

Author details
[1]The Healing Foundation Burn Research Centre, University Hospital Birmingham Foundation Trust, Birmingham B15 2TH, UK. [2]Public Health, Epidemiology and Biostatistics, Institute of Applied Health Research, College of Medical and Dental Sciences, University of Birmingham, Birmingham B15 2TT, UK. [3]School of Chemical Engineering, University of Birmingham, Birmingham B15 2TT, UK. [4]School of Clinical and Experimental Medicine, College of Medical and Dental Sciences, University of Birmingham, Birmingham B15 2TT, UK.

Received: 14 January 2016 Accepted: 29 March 2016
Published online: 27 April 2016

References

1. World Health Organisation. Disease and injury regional estimates, 2004-2008. [19th Apr 2016] Available from: http://www.who.int/healthinfo/global_burden_disease/estimates_regional_2004_2008/en/
2. Global Health Estimates: deaths, disability-adjusted life year (DALYs), years of life lost (YLL) and years lost due to disability (YLD) by cause, age and sex, 2000–2012. Geneva: World Health Organization. [29 Feb 2016]. Available from: http://www.who.int/healthinfo/global_burden_disease/estimates/en/.
3. Brusselaers N, Hoste EA, Monstrey S, Colpaert KE, De Waele JJ, Vandewoude KH, et al. Outcome and changes over time in survival following severe burns from 1985 to 2004. Intensive Care Med. 2005;31(12):1648–53.
4. Draaijers LJ, Tempelman FR, Botman YA, Tuinebreijer WE, Middelkoop E, Kreis RW, et al. The patient and observer scar assessment scale: a reliable and feasible tool for scar evaluation. Plast Reconstr Surg. 2004;113(7):1960–5. discussion 6-7.
5. Brusselaers N, Pirayesh A, Hoeksema H, Verbelen J, Blot S, Monstrey S. Burn scar assessment: a systematic review of different scar scales. The Journal of surgical research. 2010;164(1):e115–23.
6. Gankande TU, Duke JM, Danielsen PL, DeJong HM, Wood FM, Wallace HJ. Reliability of scar assessments performed with an integrated skin testing device - The DermaLab Combo((R)). Burns : journal of the International Society for Burn Injuries. 2014;40(8):1521–9.
7. Kaartinen IS, Valisuo PO, Alander JT, Kuokkanen HO. Objective scar assessment–a new method using standardized digital imaging and spectral modelling. Burns : journal of the International Society for Burn Injuries. 2011;37(1):74–81.
8. Kaartinen IS, Valisuo PO, Bochko V, Alander JT, Kuokkanen HO. How to assess scar hypertrophy--a comparison of subjective scales and Spectrocutometry: a new objective method. Wound repair and regeneration : official publication of the Wound Healing Society [and] the European Tissue Repair. Society. 2011;19(3):316–23.
9. Hoogewerf CJ, van Baar ME, Middelkoop E, van Loey NE. Impact of facial burns: Relationship between depressive symptoms, self-esteem and scar severity. Gen Hosp Psychiatry. 2014;36(3):271–6.
10. Landis JR, Koch GG. The measurement of observer agreement for categorical data. Biometrics. 1977;33(1):159–74.
11. Alster TS, Lewis AB, Rosenbach A, et al. Laser scar revision: comparison of CO2 laser vaporization with and without simultaneous pulsed dye laser treatment. Dermatologic surgery : official publication for American Society for Dermatologic Surgery. 1998;24(12):1299–302.
12. Winkler AD, Spillmann L, Werner JS, Webster MA. Asymmetries in blue-yellow color perception and in the color of 'the dress'. Current biology: CB. 2015.
13. Tseng FY, Chao CJ, Feng WY, Hwang SL. Assessment of human color discrimination based on illuminant color, ambient illumination and screen background color for visual display terminal workers. Ind Health. 2010;48(4):438–46.
14. Shuwairi SM, Cronin-Golomb A, McCarley RW, O'Donnell BF. Color discrimination in schizophrenia. Schizophr Res. 2002;55(1-2):197–204.
15. Draaijers LJ, Tempelman FR, Botman YA, Kreis RW, Middelkoop E, van Zuijlen PP. Colour evaluation in scars: tristimulus colorimeter, narrow-band simple reflectance meter or subjective evaluation? Burns : journal of the International Society for Burn Injuries. 2004;30(2):103–7.
16. Davey RB, Sprod RT, Neild TO. Computerised colour: a technique for the assessment of burn scar hypertrophy. A preliminary report. Burns : journal of the International Society for Burn Injuries. 1999;25(3):207–13.
17. Li-Tsang CW, Lau JC, Liu SK. Validation of an objective scar pigmentation measurement by using a spectrocolorimeter. Burns : journal of the International Society for Burn Injuries. 2003;29(8):779–84.
18. Chan HH, Wong DS, Ho WS, Lam LK, Wei W, et al. The use of pulsed dye laser for the prevention and treatment of hypertrophic scars in chinese persons. Dermatologic surgery : official publication for American Society for Dermatologic Surgery. 2004;30(7):987–94. discussion 94.
19. Kim MS, Rodney WN, Cooper T, Kite C, Reece GP, Markey MK. Towards quantifying the aesthetic outcomes of breast cancer treatment: comparison of clinical photography and colorimetry. J Eval Clin Pract. 2009;15(1):20–31.
20. van der Wal M, Bloemen M, Verhaegen P, Tuinebreijer W, de Vet H, van Zuijlen P, et al. Objective color measurements: clinimetric performance of three devices on normal skin and scar tissue. Journal of burn care & research : official publication of the American Burn Association. 2013;34(3):e187–94.
21. Akita S, Akino K, Imaizumi T, Hirano A. A basic fibroblast growth factor improved the quality of skin grafting in burn patients. Burns : journal of the International Society for Burn Injuries. 2005;31(7):855–8.
22. Ardigò M, Muzio F, Picardo M, Brazzelli V. In: Picardo M, Taïeb A, editors. Non-invasive methods for vitiligo evaluation. London, New York: Springer Heidelberg Dordrecht; 2010.
23. Yip C. Re-pigmentation of skin following wounding. Manchester, UK: The University of Manchester; 2013.
24. Barel AO, Clarys P, Alewaeters K, Duez C, Hubinon JL, Mommaerts M. The Visi-Chroma VC-100: a new imaging colorimeter for dermatocosmetic research. Skin research and technology : official journal of International Society for Bioengineering and the Skin (ISBS) [and] International Society for Digital Imaging of Skin (ISDIS) [and] International Society for Skin Imaging (ISSI). 2001;7(1):24–31.
25. Hallam MJ, McNaught K, Thomas AN, Nduka C. A practical and objective approach to scar colour assessment. Journal of plastic, reconstructive & aesthetic surgery : JPRAS. 2013;66(10):e271–6.
26. van der Wal MB, van Zuijlen PP, van de Ven P, Middelkoop E. Topical silicone gel versus placebo in promoting the maturation of burn scars: a randomized controlled trial. Plast Reconstr Surg. 2010;126(2):524–31.
27. Verhaegen PD, Bloemen MC, van der Wal MB, Vloemans AF, Tempelman FR, Beerthuizen GI, et al. Skin stretching for primary closure of acute burn wounds. Burns: journal of the International Society for Burn Injuries. 2014;40(8):1727–37.
28. Nedelec B, Correa JA, de Oliveira A, LaSalle L, Perrault I. Longitudinal burn scar quantification. Burns : journal of the International Society for Burn Injuries. 2014;40(8):1504–12.
29. Oliveira GV, Chinkes D, Mitchell C, Oliveras G, Hawkins HK, Herndon DN, et al. Objective assessment of burn scar vascularity, erythema, pliability, thickness, and planimetry. Dermatologic surgery : official publication for American Society for Dermatologic Surgery. 2005;31(1):48–58.
30. Nedelec B, Correa JA, Rachelska G, Armour A, LaSalle L. Quantitative measurement of hypertrophic scar: intrarater reliability, sensitivity, and specificity. Journal of burn care & research : official publication of the American Burn Association. 2008;29(3):489–500.
31. Cheon Y, Lee W, Rah D. Objective analysis of burn scar color by L*a*b* color coordinates. Burns : journal of the International Society for Burn Injuries. 2009;35:S33.
32. Cheon YW, Lee WJ, Rah DK. Objective and quantitative evaluation of scar color using the L*a*b* color coordinates. The Journal of craniofacial surgery. 2010;21(3):679–84.
33. Valisuo P, Harju T, Alander J. Reflectance measurement using digital camera and a protecting dome with built in light source. J Biophotonics. 2011;4(7-8):559–64.
34. Bae EJ, Seo SH, Kye YC, Ahn HH. A quantitative assessment of the human skin surface using polarized light digital photography and its dermatologic significance. Skin research and technology : official journal of International Society for Bioengineering and the Skin (ISBS) [and] International Society for Digital Imaging of Skin (ISDIS) [and] International Society for Skin Imaging (ISSI). 2010;16(3):270–4.

35. Khorasani H, Zheng Z, Nguyen C, Zara J, Zhang X, Wang J, et al. A quantitative approach to scar analysis. Am J Pathol. 2011;178(2):621–8.
36. Ferreira T, Rasband W. ImageJ User Guide — IJ 1.46 2010—2012 [2nd September 2015]. imagej.nih.gov/ij/docs/guide/].
37. Burke-Smith A, Collier J, Jones I. A comparison of non-invasive imaging modalities: Infrared thermography, spectrophotometric intracutaneous analysis and laser Doppler imaging for the assessment of adult burns. Burns : journal of the International Society for Burn Injuries. 2015.
38. Jones HG. Clinimetrics of tristimulus colourimeters in scar assessment: a review of evidence. J Wound Care. 2012;21(1):30–5.
39. Moncrieff M, Cotton S, Claridge E, Hall P. Spectrophotometric intracutaneous analysis: a new technique for imaging pigmented skin lesions. The British journal of dermatology. 2002;146(3):448–57.
40. Ud-Din S, Perry D, Giddings P, Colthurst J, Zaman K, Cotton S, et al. Electrical stimulation increases blood flow and haemoglobin levels in acute cutaneous wounds without affecting wound closure time: Evidenced by non-invasive assessment of temporal biopsy wounds in human volunteers. Exp Dermatol. 2012;21(10):758–64.
41. Li ZY, Su HT, Lu SL, Huang LB, Yang XB, Shao TB, et al. [Clinical study on the relationship among the dermis, fat dome and postburn hyperplastic scar formation]. Zhonghua shao shang za zhi = Zhonghua shaoshang zazhi =. Chinese journal of burns. 2004;20(6):343–6.
42. Wan BK, Qi HZ, Ming D, Zhang MJ, Wang QF. Chromatic analysis of burn scar based on ANN by using photoelectrical technology. In: Chance B, Chen M, Chiou AET, Luo Q, editors. Optics in Health Care and Biomedical Optics: Diagnostics and Treatment Ii, Pts 1 and 2. Proceedings of the Society of Photo-Optical Instrumentation Engineers (Spie). 56302005. 538-43.
43. Beausang E, Floyd H, Dunn KW, Orton CI, Ferguson MW. A new quantitative scale for clinical scar assessment. Plast Reconstr Surg. 1998;102(6):1954–61.
44. Powell MW, Sarkar S, Goldgof DB, Ivanov K. A methodology for extracting objective color from images. IEEE transactions on systems, man, and cybernetics Part B, Cybernetics : a publication of the IEEE Systems, Man, and Cybernetics Society. 2004;34(5):1964–78.
45. Anderson JC, Hallam MJ, Nduka C, Osorio D. The challenge of objective scar colour assessment in a clinical setting: using digital photography. J Wound Care. 2015;24(8):379–87.
46. van Zuijlen PP, Angeles AP, Kreis RW, Bos KE, Middelkoop E. Scar assessment tools: implications for current research. Plast Reconstr Surg. 2002;109(3):1108–22.
47. Valente JH, Jay GD, Schmidt ST, Oh AK, Reinert SE, Zabbo CP. Digital imaging analysis of scar aesthetics. Adv Skin Wound Care. 2012;25(3):119–23.
48. Kim DW, Hwang NH, Yoon ES, Dhong ES, Park SH. Outcomes of ablative fractional laser scar treatment. Journal of plastic surgery and hand surgery. 2015;49(2):88–94.
49. Bray R, Forrester K, Leonard C, McArthur R, Tulip J, Lindsay R. Laser Doppler imaging of burn scars: a comparison of wavelength and scanning methods. Burns : journal of the International Society for Burn Injuries. 2003;29(3):199–206.
50. Ehrlich HP, Kelley SF. Hypertrophic scar: an interruption in the remodeling of repair–a laser Doppler blood flow study. Plast Reconstr Surg. 1992;90(6):993–8.
51. Hosoda G, Holloway GA, Heimbach DM. Laser Doppler flowmetry for the early detection of hypertrophic burn scars. The Journal of burn care & rehabilitation. 1986;7(6):496–7.
52. Musgrave MA, Umraw N, Fish JS, Gomez M, Cartotto RC. The effect of silicone gel sheets on perfusion of hypertrophic burn scars. The Journal of burn care & rehabilitation. 2002;23(3):208–14.
53. Timar-Banu O, Beauregard H, Tousignant J, Lassonde M, Harris P, Viau G, et al. Development of noninvasive and quantitative methodologies for the assessment of chronic ulcers and scars in humans. Wound repair and regeneration : official publication of the Wound Healing Society [and] the European Tissue Repair. Society. 2001;9(2):123–32.
54. Page RE, Robertson GA, Pettigrew NM. Microcirculation in hypertrophic burn scars. Burns, including thermal injury. 1983;10(1):64–70.
55. Leung KS, Sher A, Clark JA, Cheng JC, Leung PC. Microcirculation in hypertrophic scars after burn injury. The Journal of burn care & rehabilitation. 1989;10(5):436–44.
56. Clark JA, Leung KS, Cheng JC, Leung PC. The hypertrophic scar and microcirculation properties. Burns : journal of the International Society for Burn Injuries. 1996;22(6):447–50.
57. Forrester KR, Tulip J, Leonard C, Stewart C, Bray RC. A laser speckle imaging technique for measuring tissue perfusion. IEEE transactions on bio-medical engineering. 2004;51(11):2074–84.
58. Wittenberg GP, Fabian BG, Bogomilsky JL, Schultz LR, Rudner EJ, Chaffins ML, et al. Prospective, single-blind, randomized, controlled study to assess the efficacy of the 585-nm flashlamp-pumped pulsed-dye laser and silicone gel sheeting in hypertrophic scar treatment. Arch Dermatol. 1999;135(9):1049–55.
59. Allely RR, Van-Buendia LB, Jeng JC, White P, Wu J, Niszczak J, et al. Laser Doppler imaging of cutaneous blood flow through transparent face masks: a necessary preamble to computer-controlled rapid prototyping fabrication with submillimeter precision. Journal of burn care & research : official publication of the American Burn Association. 2008;29(1):42–8.
60. Stewart CJ, Frank R, Forrester KR, Tulip J, Lindsay R, Bray RC. A comparison of two laser-based methods for determination of burn scar perfusion: laser Doppler versus laser speckle imaging. Burns : journal of the International Society for Burn Injuries. 2005;31(6):744–52.
61. moorFLPI-2 (Laser speckle contrast imager) [01/04/2015]. Available from: http://us.moor.co.uk/product/moorflpi-2-/291.
62. Prindeze NJ, Hoffman HA, Ardanuy JG, Zhang J, Carney BC, Moffatt LT, et al. Active Dynamic Thermography is a Sensitive Method for Distinguishing Burn Wound Conversion. Journal of burn care & research : official publication of the American Burn Association. 2015.
63. Monstrey S, Hoeksema H, Verbelen J, Pirayesh A, Blondeel P. Assessment of burn depth and burn wound healing potential. Burns : journal of the International Society for Burn Injuries. 2008;34(6):761–9.
64. Hardwicke J, Thomson R, Bamford A, Moiemen N. A pilot evaluation study of high resolution digital thermal imaging in the assessment of burn depth. Burns : journal of the International Society for Burn Injuries. 2013;39(1):76–81.
65. Coster A, Klein Baltink H, Zilvold G. Thermographic assessment of healed burn wounds. Rays. 1985;10(3):85–8.
66. Horta R, Nascimento R, Vilas-Boas J, Sousa F, Orvalho V, Silva A, et al. Thermographic analysis of facially burned patients. Burns : journal of the International Society for Burn Injuries. 2015.
67. Bhedi A, Saxena AK, Gadani R, Patel R. Digital Photography and Transparency-Based Methods for Measuring Wound Surface Area. The Indian Journal of Surgery. 2013;75(2):111–4.
68. Chang AC, Dearman B, Greenwood JE. A Comparison of Wound Area Measurement Techniques: Visitrak Versus Photography. Eplasty. 2011;11:e18.
69. Cui J, Zhang J, Wang J, Xu M, Pei YH, Wang T, et al. Effect of topical application with mitomycin C in the management of benign cicatricial airway stenosis. Chung-Hua Chieh Ho Ho Hu Hsi Tsa Chih Chinese Journal of Tuberculosis & Respiratory Diseases. 2012;35(12):901–6.
70. Sugama J, Matsui Y, Sanada H, Konya C, Okuwa M, Kitagawa A. A study of the efficiency and convenience of an advanced portable Wound Measurement System (VISITRAK). J Clin Nurs. 2007;16(7):1265–9.
71. van Zuijlen PP, Angeles AP, Suijker MH, Kreis RW, Middelkoop E. Reliability and accuracy of techniques for surface area measurements of wounds and scars. The international journal of lower extremity wounds. 2004;3(1):7–11.
72. Berman B, Young VL, McAndrews J, et al. Objective Assessment of the Precision, Accuracy, and Reliability of a Measurement Method for Keloid Scar Volume (PARKS Study). Dermatologic surgery: official publication for American Society for Dermatologic Surgery. 2015.
73. 3dMD static systems [2nd September 2015]. Available from: http://www.3dmd.com/#3dmd-products.
74. Kim JE, Heo YS, Oh TS, Song HJ, Oh CH. The efficacy of cultured autologous fibroblast injection treatment for depressed acne scar and evaluation by stereoimage optical topometer. Journal of Dermatology Conference: 1st Eastern Asia Dermatology Congress, EADC2010 Fukuoka Japan Conference Start. 2010;37:77.
75. Stekelenburg CM, van der Wal MB, Knol DL, de Vet HC, van Zuijlen PP. Three-dimensional digital stereophotogrammetry: a reliable and valid technique for measuring scar surface area. Plast Reconstr Surg. 2013;132(1):204–11.
76. Lumenta DB, Kitzinger HB, Selig H, Kamolz LP. Objective quantification of subjective parameters in scars by use of a portable stereophotographic system. Ann Plast Surg. 2011;67(6):641–5.
77. Tanaka Y, Tsunemi Y, Kawashima M, Tatewaki N, Nishida H. Objective assessment of skin tightening in Asians using a water-filtered near-infrared (1,000-1,800 nm) device with contact-cooling and freezer-stored gel. Clin Cosmet Investig Dermatol. 2013;6:167–76.
78. Canfield Photography solutions [cited 2015 2nd September]. Available from: http://www.canfieldsci.com/imaging-systems/categories/photography-solutions/.
79. Tanaka Y. Long-term three-dimensional volumetric assessment of skin tightening using a sharply tapered non-insulated microneedle

radiofrequency applicator with novel fractionated pulse mode in asians. Lasers Surg Med. 2015;47(8):626–33.
80. Urbanová P, Hejna P, Jurda M. Testing photogrammetry-based techniques for three-dimensional surface documentation in forensic pathology. Forensic Sci Int. 2015;250:77–86.
81. Ardehali B, Nouraei SA, Van Dam H, Dex E, Wood S, Nduka C. Objective assessment of keloid scars with three-dimensional imaging: quantifying response to intralesional steroid therapy. Plastic & Reconstructive Surgery. 2007;119(2):556–61.
82. Hoeffelin H, Jacquemin D, Defaweux V, Nizet JL. A Methodological Evaluation of Volumetric Measurement Techniques including Three-Dimensional Imaging in Breast Surgery. BioMed Research International. 2014;2014:573249.
83. Gee Kee EL, Kimble RM, Stockton KA. 3D photography is a reliable burn wound area assessment tool compared to digital planimetry in very young children. Burns : journal of the International Society for Burn Injuries. 2015.
84. Bowling FL, King L, Fadavi H, Paterson JA, Preece K, Daniel RW, et al. An assessment of the accuracy and usability of a novel optical wound measurement system. Diabetic medicine : a journal of the British Diabetic Association. 2009;26(1):93–6.
85. Bowling FL, King L, Paterson JA, Hu J, Lipsky BA, Matthews DR, et al. Remote assessment of diabetic foot ulcers using a novel wound imaging system. Wound repair and regeneration : official publication of the Wound Healing Society [and] the European Tissue Repair. Society. 2011;19(1):25–30.
86. Paterson J. Eykona Medical Imaging FAQ. EYK/AA/021rev02 ed.
87. Lifeviz Mini Technical specifications. Quantificare.
88. Vectra H1 Technical specifications: Canfield Imaging systems Inc. ; [9th December 2015]. Available from: http://www.canfieldsci.com/imaging-systems/vectra-h1-3d-imaging-system/.
89. Raytrix Light field/ Plenoptic 3D cameras [cited 2015 2nd September]. Available from: http://www.raytrix.de/produkte/.
90. Straub J, Kerlin S. Development of a Large, Low-Cost, Instant 3D Scanner. Technologies. 2014;2(2):76.
91. Pilley MJ, Hitchens C, Rose G, Alexander S, Wimpenny DI. The use of non-contact structured light scanning in burns pressure splint construction. Burns : journal of the International Society for Burn Injuries. 2011;37(7):1168–73.
92. Kovacs L, Eder M, Hollweck R, Zimmermann A, Settles M, Schneider A, et al. Comparison between breast volume measurement using 3D surface imaging and classical techniques. Breast. 2007;16(2):137–45.
93. Taylor B, McGrouther DA, Bayat A. Use of a non-contact 3D digitiser to measure the volume of keloid scars: a useful tool for scar assessment. Journal of plastic, reconstructive & aesthetic surgery : JPRAS. 2007;60(1):87–94.
94. Powers PS, Sarkar S, Goldgof DB, Cruse CW, Tsap LV. Scar assessment: current problems and future solutions. Journal of Burn Care & Rehabilitation. 1999;20(1 Pt 1):54–60. discussion 53.
95. Haller HL, Dirnberger J, Giretzlehner M, Rodemund C, Kamolz L. "Understanding burns": Research project BurnCase 3D-Overcome the limits of existing methods in burns documentation. Burns : journal of the International Society for Burn Injuries. 2009;35(3):311–7.
96. Thumfart S, Giretzlehner M, Holler J, Ehrenmuller M, Pfurtscheller K, Haller H, et al. Proportionally correct 3D models of infants, children and adolescents for precise burn size measurement. Hannover, Germany: European Burns Association Congress; 2015.
97. Wurzer P, Giretzlehner M, Klein D. SY, Haller H. L., Branski L. K., Benjamin N., et al. Burncase 3D software validation study: Burn size measurement accuracy, test-retest reliability and inter-rater reliability. European Burns Association Congress 2015. Hannover, Germany: Annals of Burns and Fire Disasters-Supplement EBA; 2015.
98. Cheng W, Saing H, Zhou H, Han Y, Peh W, Tam PK. Ultrasound assessment of scald scars in Asian children receiving pressure garment therapy. J Pediatr Surg. 2001;36(3):466–9.
99. Wang ZY, Zhang J, Lu SL. Objective evaluation of burn and post-surgical scars and the accuracy of subjective scar type judgment. Chin Med J. 2008;121(24):2517–20.
100. Sawada Y. A method of recording and objective assessment of hypertrophic burn scars. Burns : journal of the International Society for Burn Injuries. 1994;20(1):76–8.
101. Hambleton J, Shakespeare PG, Pratt BJ. The progress of hypertrophic scars monitored by ultrasound measurements of thickness. Burns : journal of the International Society for Burn Injuries. 1992;18(4):301–7.
102. Li-Tsang CW, Lau JC, Chan CC. Prevalence of hypertrophic scar formation and its characteristics among the Chinese population. Burns : journal of the International Society for Burn Injuries. 2005;31(5):610–6.
103. Lau JC, Li-Tsang CW, Zheng YP. Application of tissue ultrasound palpation system (TUPS) in objective scar evaluation. Burns : journal of the International Society for Burn Injuries. 2005;31(4):445–52.
104. Lai H-yC. Study of pressure effect on hypertrophic scar tissues: The Hong Kong Polytechnic University. 2010.
105. Lau C-mJ. A prospective randomized clinical trial to compare the effectiveness of pressure therapy, silicone gel sheeting and the combined therapy on post-surgical hypertrophic scar: The Hong Kong Polytechnic University. 2006.
106. Nedelec B, Correa JA, Rachelska G, Armour A, LaSalle L. Quantitative measurement of hypertrophic scar: interrater reliability and concurrent validity. Journal of burn care & research : official publication of the American Burn Association. 2008;29(3):501–11.
107. Van den Kerckhove E, Colla C, Van Brussel M. Pressure Therapy: Does it work? Düsseldorf: German Medical Science GMS Publishing House; 2010.
108. Qui L, Jin X, Kingston PA, Luo X, Ding X. Experimental study on BMSCs transfected by endogene inhibiting hypertrophic scar. Chung-Kuo Hsiu Fu Chung Chien Wai Ko Tsa Chih/Chinese Journal of Reparative & Reconstructive Surgery. 2008;22(2):212–6.
109. Du YC, Lin CM, Chen YF, Chen CL, Chen T. Implementation of a burn scar assessment system by ultrasound techniques. Conference proceedings : Annual International Conference of the IEEE Engineering in Medicine and Biology Society IEEE Engineering in Medicine and Biology Society Annual Conference. 2006;1:2328–31.
110. Danin A, Georgesco G, Le Touze A, Penaud A, Quignon R, Zakine G. Assessment of burned hands reconstructed with Integra by ultrasonography and elastometry. Burns : journal of the International Society for Burn Injuries. 2012;38(7):998–1004.
111. Lacarrubba F, Verzi AE, Tedeschi A, Catalfo P, Nasca MR, Micali G. Clinical and ultrasonographic correlation of acne scars. Dermatol Surg. 2013;39(11):1683–8.
112. Li JQ, Li-Tsang CW, Huang YP, Chen Y, Zheng YP. Detection of changes of scar thickness under mechanical loading using ultrasonic measurement. Burns : journal of the International Society for Burn Injuries. 2013;39(1):89–97.
113. Zhuang A, Nguyen TA, Naheedy J, Krakowski A. Use of intraoperative high-definition ultrasound to accurately gauge scar thickness and identify intra-scar anatomy during multimodal revision of a hypertrophic burn scar. Lasers Surg Med. 2015;47:54–5.
114. Katz SM, Frank DH, Leopold GR, Wachtel TL. Objective measurement of hypertrophic burn scar: a preliminary study of tonometry and ultrasonography. Ann Plast Surg. 1985;14(2):121–7.
115. Zmudzinska M, Czarnecka-Operacz M, Silny W. Principles of dermatologic ultrasound diagnostics. Acta Dermatovenerol Croat. 2008;16(3):126–9.
116. Wohlrab J, Wohlrab D, Finke R, Fischer M, Marsch WC. Ultrasonographic characterization of burn scars in children. Unfallchirurg. 2000;103(9):754–60.
117. Van den Kerckhove E, Staes F, Flour M, Stappaerts K, Boeckx W. Reproducibility of repeated measurements on post-burn scars with Dermascan C. Skin research and technology : official journal of International Society for Bioengineering and the Skin (ISBS) [and] International Society for Digital Imaging of Skin (ISDIS) [and] International Society for Skin Imaging (ISSI). 2003;9(1):81–4.
118. Nedelec B, Shankowsky HA, Tredget EE. Rating the resolving hypertrophic scar: Comparison of the Vancouver Scar Scale and scar volume. J Burn Care Rehabil. 2000;21(3):205–12.
119. Qui L, Jin X, Kingston PA, Luo X, Ding X. [Experimental study on BMSCs transfected by endogene inhibiting hypertrophic scar]. Zhongguo xiu fu chong jian wai ke za zhi = Zhongguo xiufu chongjian waike zazhi = Chinese journal of reparative and reconstructive surgery. 2008;22(2):212–6.
120. Cilip CM, Allaf ME, Fried NM. Application of optical coherence tomography and high-frequency ultrasound imaging during noninvasive laser vasectomy. J Biomed Opt. 2012;17(4):046006.
121. Episcan [cited 2015 January]. Available from: http://www.longportinc.com/about/episcan.html.
122. Skin scanner DUB [cited 2015 January]. Available from: http://www.eotech-sa.com/Life-science/Systems/DUBSkin-Scanner/Products/t1/r9/i107.
123. Verhaegen PD, van der Wal MB, Middelkoop E, van Zuijlen PP. Objective scar assessment tools: a clinimetric appraisal. Plast Reconstr Surg. 2011;127(4):1561–70.
124. Kautzky F, Dahm MW, Drosner M, Köhler LD, Vogt H-J, Borelli S. Direct profilometry of the skin: its reproducibility and variability. J Eur Acad Dermatol Venereol. 1995;5(1):15–23.

125. Lagarde JM, Rouvrais C, Black D, Diridollou S, Gall Y. Skin topography measurement by interference fringe projection: a technical validation. Skin research and technology : official journal of International Society for Bioengineering and the Skin (ISBS) [and] International Society for Digital Imaging of Skin (ISDIS) [and] International Society for Skin Imaging (ISSI). 2001;7(2):112–21.
126. Nardin P, Nita D, Mignot J. Automation of a series of cutaneous topography measurements from silicon rubber replicas. Skin research and technology : official journal of International Society for Bioengineering and the Skin (ISBS) [and] International Society for Digital Imaging of Skin (ISDIS) [and] International Society for Skin Imaging (ISSI). 2002;8(2):112–7.
127. Fischer TW, Wigger-Alberti W, Elsner P. Direct and non-direct measurement techniques for analysis of skin surface topography. Skin Pharmacol Appl Ski Physiol. 1999;12(1-2):1–11.
128. De Paepe K, Lagarde JM, Gall Y, Roseeuw D, Rogiers V. Microrelief of the skin using a light transmission method. Arch Dermatol Res. 2000; 292(10):500–10.
129. Bloemen MC, van Gerven MS, van der Wal MB, Verhaegen PD, Middelkoop E. An objective device for measuring surface roughness of skin and scars. J Am Acad Dermatol. 2011;64(4):706–15.
130. Barolet D, Boucher A. Prophylactic low-level light therapy for the treatment of hypertrophic scars and keloids: a case series. Lasers Surg Med. 2010;42(6):597–601.
131. Kottner J, Schario M, Garcia Bartels N, Pantchechnikova E, Hillmann K, Blume-Peytavi U. Comparison of two in vivo measurements for skin surface topography. Skin research and technology : official journal of International Society for Bioengineering and the Skin (ISBS) [and] International Society for Digital Imaging of Skin (ISDIS) [and] International Society for Skin Imaging (ISSI). 2013;19(2):84–90.
132. Zhao L, Hung LK, Zhang YT. Electrical properties of normal and scarred skin. In: Chang HK, Zhang YT, editors. Proceedings of the 20th Annual International Conference of the Ieee Engineering in Medicine and Biology Society, Vol 20, Pts 1-6: Biomedical Engineering Towards the Year 2000 and Beyond. Proceedings of Annual International Conference of the Ieee Engineering in Medicine and Biology Society. 201998. p. 2917-20.
133. Moloney EC, Brunner M, Alexander AJ, Clark J. Quantifying fibrosis in head and neck cancer treatment: An overview. Head and Neck-Journal for the Sciences and Specialties of the Head and Neck. 2015;37(8):1225–31.
134. Dematte MF, Gemperli R, Salles AG, Dolhnikoff M, Lancas T, Nascimento Saldiva PH, et al. Mechanical evaluation of the resistance and elastance of post-burn scars after topical treatment with tretinoin. Clinics. 2011;66(11): 1949–54.
135. Clark JA, Cheng JC, Leung KS. Mechanical properties of normal skin and hypertrophic scars. Burns : journal of the International Society for Burn Injuries. 1996;22(6):443–6.
136. Gunner CW, Hutton WC, Burlin TE. The mechanical properties of skin in vivo–a portable hand-held extensometer. The British journal of dermatology. 1979;100(2):161–3.
137. Lim KH, Chew CM, Chen PC, Jeyapalina S, Ho HN, Rappel JK, et al. New extensometer to measure in vivo uniaxial mechanical properties of human skin. J Biomech. 2008;41(5):931–6.
138. Thacker JG. Iachetta FA, Allaire PE. In vivo extensometer for measurement of the biomechanical properties of human skin. The Review of scientific instruments. 1977;48(2):181–5.
139. Clark JA, Cheng JC, Leung KS, Leung PC. Mechanical characterisation of human postburn hypertrophic skin during pressure therapy. J Biomech. 1987;20(4):397–406.
140. Chu BM, Brody G. Nondestructive measurements of the properties of healing burn scars. Medical instrumentation. 1975;9(3):139–42.
141. Bartell TH, Monafo WW, Mustoe TA. A new instrument for serial measurements of elasticity in hypertrophic scar. J Burn Care Rehabil. 1988; 9(6):657–60.
142. Rennekampff HO, Rabbels J, Reinhard V, Becker ST, Schaller HE. Comparing the Vancouver Scar Scale with the cutometer in the assessment of donor site wounds treated with various dressings in a randomized trial. Journal of burn care & research : official publication of the American Burn Association. 2006;27(3):345–51.
143. Klosova H, Stetinsky J, Bryjova I, Hledik S, Klein L. Objective evaluation of the effect of autologous platelet concentrate on post-operative scarring in deep burns. Burns : journal of the International Society for Burn Injuries. 2013; 39(6):1263–76.
144. Nguyen DQ, Potokar TS, Price P. An objective long-term evaluation of Integra (a dermal skin substitute) and split thickness skin grafts, in acute burns and reconstructive surgery. Burns : journal of the International Society for Burn Injuries. 2010;36(1):23–8.
145. Rahmanian-Schwarz A, Beiderwieden A, Willkomm LM, Amr A, Schaller HE, Lotter O. A clinical evaluation of Biobrane((R)) and Suprathel((R)) in acute burns and reconstructive surgery. Burns : journal of the International Society for Burn Injuries. 2011;37(8):1343–8.
146. Fong SS, Hung LK, Cheng JC. The cutometer and ultrasonography in the assessment of postburn hypertrophic scar–a preliminary study. Burns : journal of the International Society for Burn Injuries. 1997;23 Suppl 1:S12–8.
147. Draaijers LJ, Botman YA, Tempelman FR, Kreis RW, Middelkoop E, van Zuijlen PP. Skin elasticity meter or subjective evaluation in scars: a reliability assessment. Burns : journal of the International Society for Burn Injuries. 2004;30(2):109–14.
148. Selig HF, Keck M, Lumenta DB, Mittlbock M, Kamolz LP. The use of a polylactide-based copolymer as a temporary skin substitute in deep dermal burns: 1-year follow-up results of a prospective clinical noninferiority trial. Wound repair and regeneration : official publication of the Wound Healing Society [and] the European Tissue Repair Society. 2013;21(3):402–9.
149. Sin P, Stupka I, Brychta P. Evaluation and comparison of composite and split-thickness skin grafts using cutometer mpa 580. Annals of burns and fire disasters. 2010;23(4):208–13.
150. van Zuijlen PP, Vloemans JF, van Trier AJ, Suijker MH, van Unen E, Groenevelt F, et al. Dermal substitution in acute burns and reconstructive surgery: a subjective and objective long-term follow-up. Plast Reconstr Surg. 2001;108(7):1938–46.
151. Fournier R, Pierard GE. Skin tensile strength modulation by compressive garments in burn patients. A pilot study. Journal of medical engineering & technology. 2000;24(6):277–80.
152. Krusche T, Worret WI. Mechanical properties of keloids in vivo during treatment with intralesional triamcinolone acetonide. Arch Dermatol Res. 1995;287(3-4):289–93.
153. Matsuzaki K, Kumagai N, Fukushi S, Ohshima H, Tanabe M, Ishida H. Cultured epithelial autografting on meshed skin graft scars: evaluation of skin elasticity. The Journal of burn care & rehabilitation. 1995;16(5):496–502.
154. Nguyen NT, Roberge D, Freeman CR, Wong C, Hines J, Turcotte RE. Skin Elasticity as a Measure of Radiation Fibrosis: Is it Reproducible and Does it Correlate with Patient and Physician-reported Measures? Technology in cancer research & treatment. 2013.
155. Rennekampff HO, Rabbels J, Pfau M, Schaller HE. Kongressband / Deutsche Gesellschaft fur Chirurgie Deutsche Gesellschaft fur Chirurgie Kongress. 2002;119:749–55. Evaluating scar development with objective computer-assisted viscoelastic measurement.
156. Anthonissen M, Daly D, Fieuws S, Massage P, Van Brussel M, Vranckx J, et al. Measurement of elasticity and transepidermal water loss rate of burn scars with the Dermalab((R)). Burns : journal of the International Society for Burn Injuries. 2013;39(3):420–8.
157. Spann K, Mileski WJ, Atiles L, Purdue G, Hunt J. The 1996 Clinical Research award. Use of a pneumatonometer in burn scar assessment. The Journal of burn care & rehabilitation. 1996;17(6 Pt 1):515–7.
158. Lye I, Edgar DW, Wood FM, Carroll S. Tissue tonometry is a simple, objective measure for pliability of burn scar: is it reliable? Journal of burn care & research : official publication of the American Burn Association. 2006;27(1):82–5.
159. Akita S, Akino K, Yakabe A, Imaizumi T, Tanaka K, Anraku K, et al. Combined surgical excision and radiation therapy for keloid treatment. The Journal of craniofacial surgery. 2007;18(5):1164–9.
160. Merkel PA, Silliman NP, Denton CP, Furst DE, Khanna D, Emery P, et al. Validity, reliability, and feasibility of durometer measurements of scleroderma skin disease in a multicenter treatment trial. Arthritis Rheum. 2008;59(5):699–705.
161. Magliaro A, Romanelli M. Skin hardness measurement in hypertrophic scars. Wounds-a Compendium of Clinical Research and Practice. 2003;15(3):66–70.
162. Esposito G, Ziccardi P, Scioli M, Pappone N, Scuderi N. The use of a modified tonometer in burn scar therapy. The Journal of burn care & rehabilitation. 1990;11(1):86–90.
163. Wernicke AG, Greenwood EA, Coplowitz S, Parashar B, Kulidzhanov F, Christos PJ, et al. Tissue compliance meter is a more reproducible method of measuring radiation-induced fibrosis than late effects of normal tissue-subjective objective management analytical in patients treated with intracavitary brachytherapy accelerated partial breast irradiation: results of a prospective trial. Breast J. 2013;19(3):250–8.

164. Corica GF, Wigger NC, Edgar DW, Wood FM, Carroll S. Objective measurement of scarring by multiple assessors: is the tissue tonometer a reliable option? Journal of burn care & research : official publication of the American Burn Association. 2006;27(4):520–3.
165. Boyce ST, Supp AP, Wickett RR, Hoath SB, Warden GD. Assessment with the dermal torque meter of skin pliability after treatment of burns with cultured skin substitutes. The Journal of burn care & rehabilitation. 2000;21(1 Pt 1):55–63.
166. McHugh AA, Fowlkes BJ, Maevsky EI, Smith Jr DJ, Rodriguez JL, Garner WL. Biomechanical alterations in normal skin and hypertrophic scar after thermal injury. The Journal of burn care & rehabilitation. 1997;18(2):104–8.
167. Popovic G, Sarvazyan A, Ponomarjev V, Vucelic D. Method and device for noninvasive acoustic testing of elasticity of soft biological tissues. Google Patents. 1992.
168. Verhaegen PD, Res EM, van Engelen A, Middelkoop E, van Zuijlen PP. A reliable, non-invasive measurement tool for anisotropy in normal skin and scar tissue. Skin research and technology : official journal of International Society for Bioengineering and the Skin (ISBS) [and] International Society for Digital Imaging of Skin (ISDIS) [and] International Society for Skin Imaging (ISSI). 2010;16(3):325–31.
169. Ferriero G, Vercelli S, Salgovic L, Stissi V, Sartorio F. Validation of a new device to measure postsurgical scar adherence. Phys Ther. 2010;90(5): 776–83.
170. Tsap LV, Goldgof DB, Sarkar S, Powers PS. A vision-based technique for objective assessment of burn scars. IEEE Trans Med Imaging. 1998; 17(4):620–33.
171. Zhang Y, Goldgof DB, Sarkar S, Tsap LV. A modeling approach for burn scar assessment using natural features and elastic property. IEEE Trans Med Imaging. 2004;23(10):1325–9.
172. Larrabee Jr WF. A finite element model of skin deformation. I. Biomechanics of skin and soft tissue: a review. Laryngoscope. 1986;96(4):399–405.
173. Zhang Y, Goldgof DB, Sarkar S, Tsap LV. Model-based nonrigid motion analysis using natural feature adaptive mesh. In: Sanfeliu A, Villanueva JJ, Vanrell M, Alquezar R, Huang T, Serra J, editors. 15th International Conference on Pattern Recognition, Vol 3, Proceedings: Image, Speech and Signal Processing. International Conference on Pattern Recognition. 2000. p. 831–5.
174. Palmieri TL, Petuskey K, Bagley A, Takashiba S, Greenhalgh DG, Rab GT. Alterations in functional movement after axillary burn scar contracture: a motion analysis study. The Journal of burn care & rehabilitation. 2003;24(2): 104–8.
175. Parry I, Walker K, Niszczak J, Palmieri T, Greenhalgh D. Methods and tools used for the measurement of burn scar contracture. Journal of burn care & research : official publication of the American Burn Association. 2010;31(6):888–903.
176. Rab G, Petuskey K, Bagley A. A method for determination of upper extremity kinematics. Gait & posture. 2002;15(2):113–9.
177. van der Helm FC, Pronk GM. Three-dimensional recording and description of motions of the shoulder mechanism. J Biomech Eng. 1995;117(1):27–40.
178. Koller R, Kargul G, Giovanoli P, Meissl G, Frey M. Quantification of functional results after facial burns by the faciometer. Burns : journal of the International Society for Burn Injuries. 2000;26(8):716–23.
179. Berry RB, Tan OT, Cooke ED, Gaylarde PM, Bowcock SA, Lamberty BG, et al. Transcutaneous oxygen tension as an index of maturity in hypertrophic scars treated by compression. Br J Plast Surg. 1985;38(2):163–73.
180. Ichioka S, Ando T, Shibata M, Sekiya N, Nakatsuka T. Oxygen consumption of keloids and hypertrophic scars. Ann Plast Surg. 2008;60(2):194–7.
181. Rodrigues LM, Roberto MA. Characterization strategies for the functional assessment of the cutaneous lesion. Burns : journal of the International Society for Burn Injuries. 2006;32(7):797–801.
182. Fluhr JW, Feingold KR, Elias PM. Transepidermal water loss reflects permeability barrier status: validation in human and rodent in vivo and ex vivo models. Exp Dermatol. 2006;15(7):483–92.
183. Rosado C, Pinto P, Rodrigues LM. Comparative assessment of the performance of two generations of Tewameter: TM210 and TM300. Int J Cosmet Sci. 2005;27(4):237–41.
184. De Paepe K, Houben E, Adam R, Wiesemann F, Rogiers V. Validation of the VapoMeter, a closed unventilated chamber system to assess transepidermal water loss vs. the open chamber Tewameter. Skin research and technology : official journal of International Society for Bioengineering and the Skin (ISBS) [and] International Society for Digital Imaging of Skin (ISDIS) [and] International Society for Skin Imaging (ISSI). 2005;11(1):61–9.
185. Anthonissen M. Assessment and conservative treatments of burn scars; Evaluatie en conservatieve behandeling van littekens na brandwonden. 2015.
186. Clarys P, Clijsen R, Taeymans J, Barel AO. Hydration measurements of the stratum corneum: comparison between the capacitance method (digital version of the Corneometer CM 825(R)) and the impedance method (Skicon-200EX(R)). Skin research and technology : official journal of International Society for Bioengineering and the Skin (ISBS) [and] International Society for Digital Imaging of Skin (ISDIS) [and] International Society for Skin Imaging (ISSI). 2012;18(3):316–23.
187. O'Goshi K, Serup J. Skin conductance; validation of Skicon-200EX compared to the original model, Skicon-100. Skin research and technology : official journal of International Society for Bioengineering and the Skin (ISBS) [and] International Society for Digital Imaging of Skin (ISDIS) [and] International Society for Skin Imaging (ISSI). 2007;13(1):13–8.
188. Magnusson M, Papini RP, Rea SM, Reed CC, Wood FM. Cultured autologous keratinocytes in suspension accelerate epithelial maturation in an in vivo wound model as measured by surface electrical capacitance. Plast Reconstr Surg. 2007;119(2):495–9.
189. Anthonissen M, Daly D, Peeters R, Van Brussel M, Fieuws S, Moortgat P, et al. Reliability of Repeated Measurements on Post-Burn Scars with Corneometer CM 825. Skin research and technology : official journal of International Society for Bioengineering and the Skin (ISBS) [and] International Society for Digital Imaging of Skin (ISDIS) [and] International Society for Skin Imaging (ISSI). 2014.
190. Nuutinen J. Skin dielectric constant at high radiofrequency with special emphasis on radiation-induced late skin reaction [Ph.D. thesis]. Kuopio, Finland: Kuopio University Publications C. Natural and Environmental Sciences 55; 1997.
191. Lahtinen T, Nuutinen J, Alanen E, Turunen M, Nuortio L, Usenius T, et al. Quantitative assessment of protein content in irradiated human skin. Int J Radiat Oncol Biol Phys. 1999;43(3):635–8.
192. Suetake T, Sasai S, Zhen YX, Ohi T, Tagami H. Functional analyses of the stratum corneum in scars. Sequential studies after injury and comparison among keloids, hypertrophic scars, and atrophic scars. Arch Dermatol. 1996; 132(12):1453–8.
193. Ghassemi P, Travis TE, Moffatt LT, Shupp JW, Ramella-Roman JC. A polarized multispectral imaging system for quantitative assessment of hypertrophic scars. Biomedical optics express. 2014;5(10):3337–54.
194. Ghassemi P, Shupp JW, Moffatt LT, Ramella-Roman JC. A Novel Spectral Imaging System for Quantitative Analysis of Hypertrophic Scar. In: Kollias N, Choi B, Zeng H, Kang HW, Knudsen BE, Wong BJF, et al., editors. Photonic Therapeutics and Diagnostics Ix. Proceedings of SPIE. 85652013.
195. Drexler W, Fujimoto JG. State-of-the-art retinal optical coherence tomography. Prog Retin Eye Res. 2008;27(1):45–88.
196. Alex A, Povazay B, Hofer B, Popov S, Glittenberg C, Binder S, et al. Multispectral in vivo three-dimensional optical coherence tomography of human skin. J Biomed Opt. 2010;15(2):026025.
197. Welzel J, Lankenau E, Birngruber R, Engelhardt R. Optical coherence tomography of the human skin. J Am Acad Dermatol. 1997;37(6):958–63.
198. Gambichler T, Moussa G, Sand M, Sand D, Altmeyer P, Hoffmann K. Applications of optical coherence tomography in dermatology. J Dermatol Sci. 2005;40(2):85–94.
199. Welzel J. Optical coherence tomography in dermatology: a review. Skin research and technology: official journal of International Society for Bioengineering and the Skin (ISBS) [and] International Society for Digital Imaging of Skin (ISDIS) [and] International Society for Skin Imaging (ISSI). 2001;7(1):1–9.
200. Steiner R, Kunzi-Rapp K, Scharffetter-Kochanek K. Optical Coherence Tomography: Clinical Applications in Dermatology. Medical Laser Application. 2003;18(3):249–59.
201. Liew YM, McLaughlin RA, Gong P, Wood FM, Sampson DD. In vivo assessment of human burn scars through automated quantification of vascularity using optical coherence tomography. J Biomed Opt. 2013;18(6):061213.
202. Gong P, Chin L, Es'haghian S, Liew YM, Wood FM, Sampson DD, et al. Imaging of skin birefringence for human scar assessment using polarization-sensitive optical coherence tomography aided by vascular masking. J Biomed Opt. 2014;19(12):126014.
203. Gong P, McLaughlin RA, Liew YM, Munro PR, Wood FM, Sampson DD. Assessment of human burn scars with optical coherence tomography by imaging the attenuation coefficient of tissue after vascular masking. J Biomed Opt. 2014;19(2):21111.

204. Babalola O, Mamalis A, Lev-Tov H, Jagdeo J. Optical coherence tomography (OCT) of collagen in normal skin and skin fibrosis. Arch Dermatol Res. 2014;306(1):1–9.
205. Choi WJ, Reif R, Yousefi S, Wang RK. Improved microcirculation imaging of human skin in vivo using optical microangiography with a correlation mapping mask. J Biomed Opt. 2014;19(3):36010.
206. Wang XQ, Mill J, Kravchuk O, Kimble RM. Ultrasound assessed thickness of burn scars in association with laser Doppler imaging determined depth of burns in paediatric patients. Burns : journal of the International Society for Burn Injuries. 2010;36(8):1254–62.
207. Lo WC, Villiger M, Golberg A, Broelsch GF, Khan S, Lian CG, et al. Longitudinal, 3D In Vivo Imaging of Collagen Remodeling in Murine Hypertrophic Scars using Polarization-sensitive Optical Frequency Domain Imaging. The Journal of investigative dermatology. 2015.
208. Eraud J, Gonnelli D, Carmassi M, Bruzzese L, Andrac-Meyer L, Casanova D, et al. Differential diagnosis between keloid and hypertrophic scars: a new approach by full-field optical coherence tomography. Ann Chir Plast Esthet. 2014;59(4):253–60.
209. Moshref SS, Mufti ST. Keloid and hypertrophic scars: comparative histopathological and immunohistochemical study. Med Sci. 2010;17:3–22.
210. Chen G, Chen J, Zhuo S, Xiong S, Zeng H, Jiang X, et al. Nonlinear spectral imaging of human hypertrophic scar based on two-photon excited fluorescence and second-harmonic generation. The British journal of dermatology. 2009;161(1):48–55.
211. Chen J, Zhuo S, Jiang X, Zhu X, Zheng L, Xie S, et al. Multiphoton microscopy study of the morphological and quantity changes of collagen and elastic fiber components in keloid disease. J Biomed Opt. 2011;16(5):051305.
212. Brewer MB, Yeh A, Torkian B, Sun CH, Tromberg BJ, Wong BJ. Multiphoton imaging of excised normal skin and keloid scar: preliminary investigations. In: Bartels KE, Bass LS, DeRiese WTW, Gregory KW, Hirschberg H, Katzir A, et al., editors. Lasers in Surgery: Advanced Characterization, Therapeutics, and Systems Xiv. Proceedings of the Society of Photo-Optical Instrumentation Engineers (Spie). 53122004. p. 204-8.
213. Chen A, Liu PY, McNeilly C, Cuttle L, Kempf M, Kendall M, et al. Collagen deposition assessment in burn scar tissue using second harmonic generation and multi-photon microscopy. J Investig Dermatol. 2010;130:S16–S.
214. Stoller P, Celliers PM, Reiser KM, Rubenchik AM. Imaging collagen orientation using polarization-modulated second harmonic generation. In: Periasamy A, So PTC, editors. Multiphoton Microscopy in the Biomedical Sciences Ii. Proceedings of the Society of Photo-Optical Instrumentation Engineers (Spie). 46202002. p. 157-65.
215. Kelf TA, Gosnell M, Sandnes B, Guller AE, Shekhter AB, Zvyagin AV. Scar tissue classification using nonlinear optical microscopy and discriminant analysis. J Biophotonics. 2012;5(2):159–67.
216. Da Costa V, Wei R, Lim R, Sun CH, Brown JJ, Wong BJ. Nondestructive imaging of live human keloid and facial tissue using multiphoton microscopy. Arch Facial Plast Surg. 2008;10(1):38–43.
217. Zhu XQ, Zhuo SM, Zheng LQ, Lu KC, Jiang XS, Chen JX, et al. Quantified characterization of human cutaneous normal scar using multiphoton microscopy. J Biophotonics. 2010;3(1-2):108–16.
218. de Vries HJ, Enomoto DN, van Marle J, van Zuijlen PP, Mekkes JR, Bos JD. Dermal organization in scleroderma: the fast Fourier transform and the laser scatter method objectify fibrosis in nonlesional as well as lesional skin. Laboratory investigation; a journal of technical methods and pathology. 2000;80(8):1281–9.
219. Konig K, Riemann I. High-resolution multiphoton tomography of human skin with subcellular spatial resolution and picosecond time resolution. J Biomed Opt. 2003;8(3):432–9.
220. Chen ACH, McNeilly C, Liu APY, Flaim CJ, Cuttle L, Kendall M, et al. Second harmonic generation and multiphoton microscopic detection of collagen without the need for species specific antibodies. Burns : journal of the International Society for Burn Injuries. 2011;37(6):1001–9.
221. Jiang Y, Tong Y, Xiao T, Lu S. Phase-contrast microtomography with synchrotron radiation technology: a new noninvasive technique to analyze the three-dimensional structure of dermal tissues. Dermatology. 2012;225(1):75–80.
222. Theer P, Hasan MT, Denk W. Two-photon imaging to a depth of 1000 microm in living brains by use of a Ti:Al2O3 regenerative amplifier. Opt Lett. 2003;28(12):1022–4.
223. Tseng SH, Hsu CK, Yu-Yun Lee J, Tzeng SY, Chen WR, Liaw YK. Noninvasive evaluation of collagen and hemoglobin contents and scattering property of in vivo keloid scars and normal skin using diffuse reflectance spectroscopy: pilot study. J Biomed Opt. 2012;17(7):077005.
224. Rajadhyaksha M, Gonzalez S, Zavislan JM, Anderson RR, Webb RH. In vivo confocal scanning laser microscopy of human skin II: advances in instrumentation and comparison with histology. The Journal of investigative dermatology. 1999;113(3):293–303.
225. Rolfe H, Wurm E, Gilmore S. An investigation of striae distensae using reflectance confocal microscopy. The Australasian journal of dermatology. 2012;53(3):181–5.
226. Nehal KS, Gareau D, Rajadhyaksha M. Skin imaging with reflectance confocal microscopy. Seminars in cutaneous medicine and surgery. 2008;27(1):37–43.
227. Chang SK, Mirabal YN, Atkinson EN, Cox D, Malpica A, Follen M, et al. Combined reflectance and fluorescence spectroscopy for in vivo detection of cervical pre-cancer. J Biomed Opt. 2005;10(2):024031.
228. Gisquet H, Liu H, Blondel WC, Leroux A, Latarche C, Merlin JL, et al. Intradermal tacrolimus prevent scar hypertrophy in a rabbit ear model: a clinical, histological and spectroscopical analysis. Skin research and technology : official journal of International Society for Bioengineering and the Skin (ISBS) [and] International Society for Digital Imaging of Skin (ISDIS) [and] International Society for Skin Imaging (ISSI). 2011; 17(2):160–6.
229. Liu HH, Gisquet H, Guillemin F, Blondel W. Bimodal spectroscopy for in vivo characterization of hypertrophic skin tissue: pre-clinical experimentation, spectral data selection and classification. In: Ramanujam N, Popp J, editors. Clinical and Biomedical Spectroscopy and Imaging Ii. Proceedings of SPIE. 80872011.
230. Hsu CK, Tzeng SY, Yang CC, Lee JY, Huang LL, Chen WR, et al. Non-invasive evaluation of therapeutic response in keloid scar using diffuse reflectance spectroscopy. Biomedical optics express. 2015;6(2):390–404.
231. Bessonart MN, Macedo N, Carmona C. High resolution B-scan ultrasound of hypertrophic scars. Skin research and technology : official journal of International Society for Bioengineering and the Skin (ISBS) [and] International Society for Digital Imaging of Skin (ISDIS) [and] International Society for Skin Imaging (ISSI). 2005;11(3):185–8.
232. Gangemi EN, Carnino R, Stella M. Videocapillaroscopy in postburn scars: in vivo analysis of the microcirculation. Burns : journal of the International Society for Burn Injuries. 2010;36(6):799–805.
233. Campanati A, Savelli A, Sandroni L, Marconi B, Giuliano A, Giuliodori K, et al. Effect of allium cepa-allantoin-pentaglycan gel on skin hypertrophic scars: clinical and video-capillaroscopic results of an open-label, controlled, nonrandomized clinical trial. Dermatologic surgery : official publication for American Society for Dermatologic Surgery. 2010;36(9):1439–44.
234. Pasqui AL, Pastorelli M, Puccetti L, Beerman U, Biagi F, Camarri A, et al. Microvascular assessment in Behcet disease: videocapillaroscopic study. Int J Tissue React. 2003;25(3):105–15.
235. Hern S, Mortimer PS. In vivo quantification of microvessels in clinically uninvolved psoriatic skin and in normal skin. The British journal of dermatology. 2007;156(6):1224–9.
236. Lamah M, Chaudhry H, Mortimer PS, Dormandy JA. Repeatability of intravital capillaroscopic measurement of capillary density. International journal of microcirculation, clinical and experimental / sponsored by the European Society for Microcirculation. 1996;16(1):23–9.
237. Yoo MG, Kim IH. Keloids and hypertrophic scars: characteristic vascular structures visualized by using dermoscopy. Ann. 2014;26(5):603–9.
238. Wei Y, Li-Tsang CW, Luk DC, Tan T, Zhang W, Chiu TW. A validation study of scar vascularity and pigmentation assessment using dermoscopy. Burns : journal of the International Society for Burn Injuries. 2015;41(8):1717–23.
239. Malenfant A, Forget R, Papillon J, Amsel R, Frigon JY, Choiniere M. Prevalence and characteristics of chronic sensory problems in burn patients. Pain. 1996;67(2-3):493–500.
240. Brown JE, Chatterjee N, Younger J, Mackey S. Towards a physiology-based measure of pain: patterns of human brain activity distinguish painful from non-painful thermal stimulation. PLoS One. 2011;6(9):e24124.
241. Meirte J, Moortgat P, Truijen S, Maertens K, Lafaire C, De Cuyper L, et al. Interrater and intrarater reliability of the Semmes Weinstein aesthesiometer to assess touch pressure threshold in burn scars. Burns : journal of the International Society for Burn Injuries. 2015.
242. Tena BB. Evaluación y prevención de la cronificación del dolor postoperatorio tras toracotomía: Universitat de Barcelona. 2014.
243. Tena B, Escobar B, Arguis MJ, Cantero C, Rios J, Gomar C. Reproducibility of Electronic Von Frey and Von Frey monofilaments testing. The Clinical journal of pain. 2012;28(4):318–23.

244. Perry DM, McGrouther DA, Bayat A. Current tools for noninvasive objective assessment of skin scars. Plast Reconstr Surg. 2010;126(3):912–23.
245. Brandt MG, Moore CC, Micomonaco D, Fung K, Franklin JH, Yoo J, et al. A Prospective randomized evaluation of scar assessment measures. Laryngoscope. 2009;119(5):841–5.
246. Niyaz A, Matsumura H, Watanabe K, Hamamoto T, Matsusawa T. Quantification of the physical properties of keloid and hypertrophic scars using the Vesmeter novel sensing device. Int Wound J. 2012;9(6):643–9.
247. Gankande U, Duke J, Wood F, Danielsen PL, Wallace HEVIDENCE-BASEDRECOMMENDATIONSFORBURNSCARASSESSMENT. Wound Repair Regen. 2015;23(4):A8–9.
248. Gankande TU, Duke JM, Wood FM, Wallace HJ. Interpretation of the DermaLab Combo((R)) pigmentation and vascularity measurements in burn scar assessment: An exploratory analysis. Burns : journal of the International Society for Burn Injuries. 2015;41(6):1176–85.
249. Singer AJ, Thode Jr HC, McClain SA. Development of a histomorphologic scale to quantify cutaneous scars after burns. Acad Emerg Med. 2000;7(10):1083–8.
250. de Rigal J, Abella ML, Giron F, Caisey L, Lefebvre MA. Development and validation of a new Skin Color Chart. Skin research and technology : official journal of International Society for Bioengineering and the Skin (ISBS) [and] International Society for Digital Imaging of Skin (ISDIS) [and] International Society for Skin Imaging (ISSI). 2007;13(1):101–9.
251. Bloemen MC, van Leeuwen MC, van Vucht NE, van Zuijlen PP, Middelkoop E. Dermal substitution in acute burns and reconstructive surgery: a 12-year follow-up. Plast Reconstr Surg. 2010;125(5):1450–9.
252. Blome-Eberwein SA, Roarabaugh C, Gogal C, Eid S. Exploration of nonsurgical scar modification options: can the irregular surface of matured mesh graft scars be smoothed with microdermabrasion? Journal of burn care & research : official publication of the American Burn Association. 2012; 33(3):e133–40.
253. Atiyeh BS, Gunn SW, Hayek SN. State of the art in burn treatment. World J Surg. 2005;29(2):131–48.
254. Hoeksema H, Van de Sijpe K, Tondu T, Hamdi M, Van Landuyt K, Blondeel P, et al. Accuracy of early burn depth assessment by laser Doppler imaging on different days post burn. Burns : journal of the International Society for Burn Injuries. 2009;35(1):36–45.
255. Miller RH, Sim I. Physicians' use of electronic medical records: barriers and solutions. Health affairs (Project Hope). 2004;23(2):116–26.
256. Tzou CH, Artner NM, Pona I, Hold A, Placheta E, Kropatsch WG, et al. Comparison of three-dimensional surface-imaging systems. Journal of plastic, reconstructive & aesthetic surgery : JPRAS. 2014;67(4):489–97.
257. Dobrev H. Application of Cutometer area parameters for the study of human skin fatigue. Skin research and technology : official journal of International Society for Bioengineering and the Skin (ISBS) [and] International Society for Digital Imaging of Skin (ISDIS) [and] International Society for Skin Imaging (ISSI). 2005;11(2):120–2.

Appendix B

Gellan Contact Study Scoring reference guide (Version 6.0):

Erythema

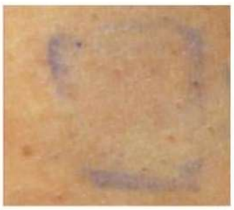

0 = No evidence of erythema

0.5 = Minimal or doubtful erythema

1 = Slight redness, spotty and diffuse

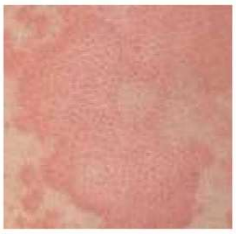

2 = Moderate uniform redness

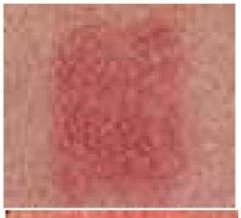

3 = Strong uniform redness

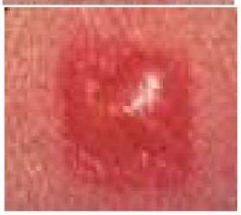

4 = Fiery redness

Dryness (scaling)

0 = No evidence of scaling

0.5 = Dry without scaling, appears smooth and taut

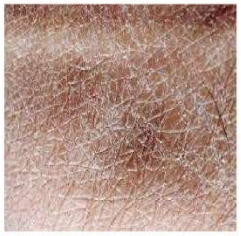

1 = Fine or mild scaling

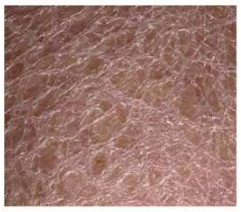

2 = Moderate scaling

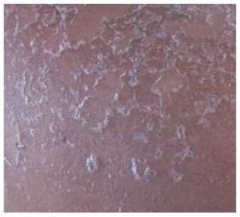

3 = Severe scaling with large flakes

Oedema/ swelling

0 = Absence of oedema/swelling

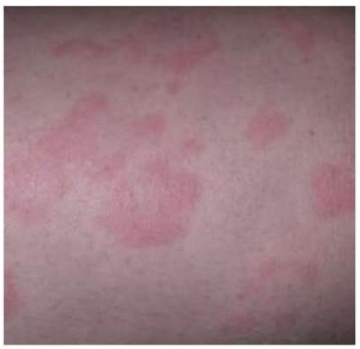

0.5= Mild, localised swelling/urticaria +/- mild itching

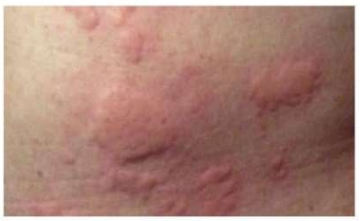

1 = Presence of severe oedema (or generalised discrete weals) with severe itching